Transcriptional Elongation is Important for Neural Crest Development

Victoria Hatch

Thesis submitted for the degree of
Doctor of Philosophy

University of East Anglia
School of Biological Sciences
Norwich
United Kingdom
September 2013

Word count: 50268

Table of Contents

List of figures

List of tables

Abbreviations

AF9: ALL1-fused gene from chromosome 9

AFF1: AF4/FMR2 family, member 1

AIDS: Acquired immunodeficiency syndrome

AP: anterior-posterior

BCIP: 5-Bromo-4-chloro-3-indolyl phosphate

BMP: Bone morphogenic protein

BSA: Bovine serum albumin

Cdk9: Cyclin dependent kinase 9

CHiP: Chromatin immuneprecipitation

Chorulon: Human chorionic gonadotrophin

DEPC: Diethylpyrocarbonate

DNA: Deoxyribonucleic acid

DSIF: 5,6-dichloro-1-beta-D-ribofuranosylbenzimidazole sensitivity inducing factor

EDTA: Ethylenediamine tetraacetate

EGR: Early growth response

ELL: Eleven-nineteen lysine-rich leukemia

ES: Embryonic stem

EtOH: Ethanol

FGF: Fibroblast growth factor

Fig: Figure

GSK3β: Glycogen synthase kinase 3

HEXIM: Hexamethylene bisacetamideinducible

HIV: Human immunodeficiency virus

Hsp: Heat shock protein

ISH: *in situ* hybridisation

MAB: Maleic acid buffer

Med26: Mediator 26

Min: Minutes

MML: Mixed lineage leukaemia

MMR: Marc's modified ringer's

MO: Morpholino

µl: microliter

NBT: nitroblue tetrazolium

NC: Neural crest

NELF: Negative elongation factor complex

ng: nanograms

GS: Goat serum

O/N: Overnight

OD: Optical density

SDS-PAGE: Sodium dodecyl sulphate polyacridamide gel electrophoresis

PBS: Phosphate buffered saline

PCR: Polymerase chain reaction

pg: Picograms

Pol II: Polymerase II

PSMG: Pregnant mare serumgonadotrophin

P-TEFb: Positive transcriptional elongation factor b complex

RT: Room temperature

RNA: Ribonucleic acid

RT-PCR: Reverse transcriptase polymerase chain reaction

SDS: Sodium dodecyl sulphate

SEC: Super elongation complex

Sec: Seconds

Ser2: Serine 2

Ser5: Serine 5

St: Stage

TAE: Tris-acetate-EDTA

TFIIS: Transcription factor II S

TGFβ: Transforming growth factor β

TTF: Transcription termination factor

UV: Ultraviolet

WE: Whole embryo

WT: Wild type

Acknowledgements

The following people have helped in the making of this thesis;

Grant Wheeler. Thank you for being a super awesome supervisor. I've loved doing my PhD and for this I have you to thank.
Andrea Munsterberg and Ian Clarke. For being my secondary supervisors and having some really useful ideas for my project.
Adam Hendry. Thanks for being my best friend everyday. My PhD would have been a lot less fun without you.
Christina Stratford. For being my sassy latino rock.
Simon Moxon. Thank you for being a computer wizard and doing an amazing job analysing my RNA sequencing.
Andy Loveday. Thank you for knowing where everything is even when you don't work for us.
Ruth Williams. Thanks for teaching me everything.
Dominique McCormick, Timothy Grocott and Kasia Whysall. Thank you for knowing everything about everything.
James McColl. Thanks for being all over graphs and scale bars. They're your bag.
Kim Hanson, Niki Kennerley and Ayisha Ahmed. Thanks for the girly times and all your help in the lab
Amanda Barber and Chris Ford. Thanks for working on my project with me. You guys rock.
The rest of the lab. For being such a friendly bunch of people.
Tom Martin. Thank you for putting up with me everyday. I can be a real bag of crazy.
My mum. Because she would cry if I didn't mention her! And for all her support for the last 25 years.

Abstract

Neural crest cells are a multipotent cell population, which migrate from the dorsal neural tube in early vertebrate development throughout the embryo to form a variety of cell types including pigment cells, cranio-facial cartilage and sensory neurons [1, 2]. Here I show that the small molecule compound leflunomide is able to inhibit neural crest specification genes. Leflunomide exerts its actions by inhibiting pyrimidine synthesis and therefore RNA transcription [4]. Neural crest genes are thought to be actively transcribed and like many embryonic stem cell genes may undergo an increased level of transcriptional pausing and subsequent elongation rendering them more sensitive to the effect of leflunomide [3, 5]. I have gone on to show that components of the transcriptional elongation regulatory machinery, Cdk9 and CyclinT1 of the P-TEFb complex are also able to regulate neural crest specification. In particular the expression of the protooncogene c-Myc and c-Myc responsive genes are affected. c-Myc has been previously implicated in embryonic stem cell transcriptional elongation and also is well characterised to play a role in neural crest specification [6]. We postulate that regulation of c-Myc expression at the level of transcriptional elongation is important for the correct temporal and spatial development of the neural crest.

Key words: Neural crest cells, multipotent, leflunomide, transcriptional elongation, c-Myc, P-TEFb, Cdk9, CyclinT1

Chapter I

Introduction

1. Introduction

1.1 Using Xenopus as an animal model

Xenopus laevis and *Xenopus tropicalis* are two species of African clawed frog commonly used as vertebrate animal models for studying early development. *Xenopus* are used because they can lay hundreds of eggs at once which will develop together in synchronicity to allow for experiments to be planned and regulated accordingly [7]. *Xenopus laevis* eggs are large (1.2-1.4mm in diameter) allowing for them to be easily manipulated. They are also robust and easily withstand micro-injection into targeted blastomeres. *Xenopus tropicalis* embryos are more commonly used today for genetic studies as they have a well sequenced diploid genome unlike the *laevis* tetraploid genome [7].

The *Xenopus* life cycle (**figure 1.1**) is separated into key developmental stages using the Nieuwkoop and Faber fate map as a standard example of *Xenopus* stages. The stage 1 *Xenopus* embryo (or a fertilised egg) is separated into two regions, the animal pole, which is dark in colour and the vegetal pole, which appears lighter in colour [8]. Sperm will usually enter the unfertilised egg in the region of the animal pole. The embryo will undergo cleavage around two hours after fertilisation giving the embryo two blastomeres of equal size. Further cleavages occur every half an hour after this until the embryo consists of several thousand cells and reaches the blastula stage. This stage embryo will also contain a fluid filled cavity known as the blastocoel [8].

After reaching blastula stage the embryos will undergo gastrulation, which involves rearrangement of the three germ layers (mesoderm, endoderm and ectoderm). At first a blastopore opens in the surface of the embryo at the position of the Spemann organiser, a crucial organiser for dorsal ventral patterning. Mesoderm and endoderm start to involute at the blastopore and the ectoderm will cover the surface of the embryo by a movement known as epiboly [8].

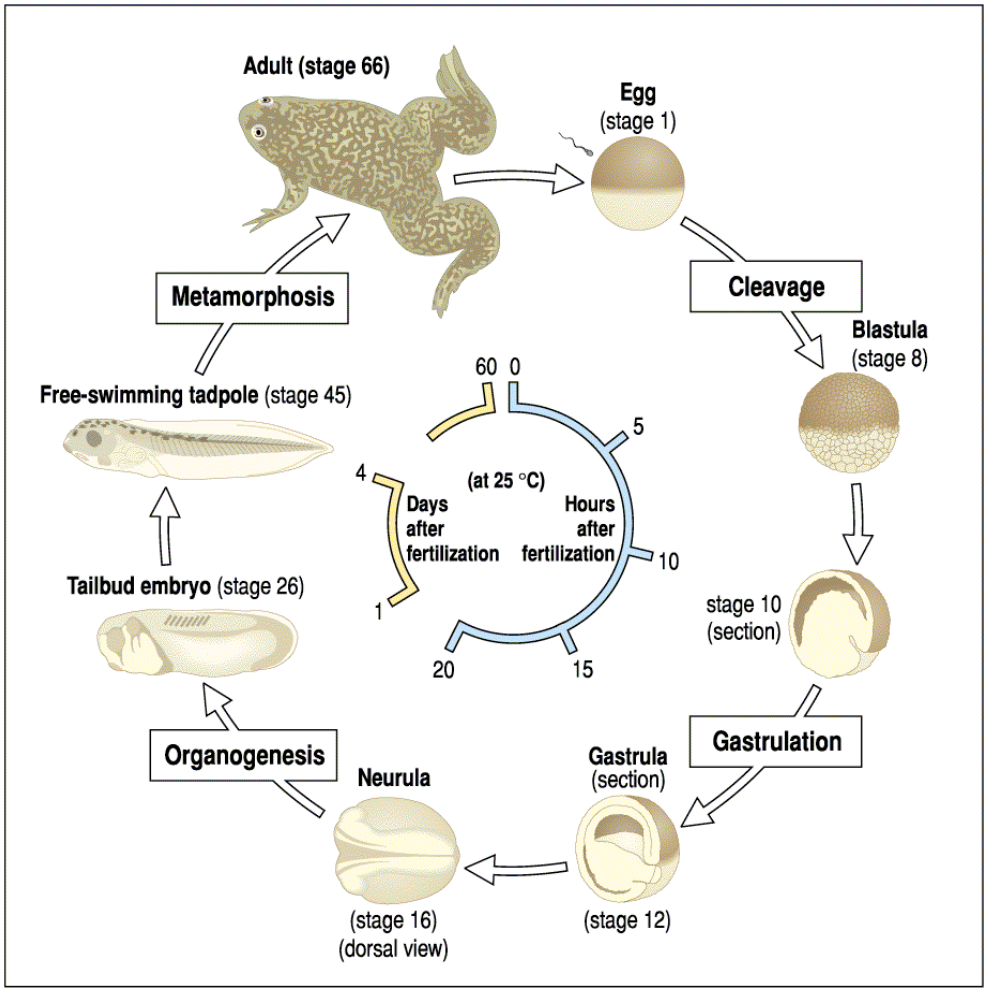

Figure 1.1: The *Xenopus* life cycle. The embryos are staged here based on the standard Niewkoop and Faber fate map. The main stage types of the *Xenopus* are blastula, gastrula, neurula, tailbud and tadpole. After this the tadpole will undergo metamorphosis into the adult froglet. Timing of *Xenopus* development is temperature dependent. Retrieved from [8].

After gastrulation the embryos will undergo neurulation to form neurula stage embryos. During neurulation the neural plate will rise and fold along the midline to form the neural tube. Neural crest cells will format the border of the ectoderm and neuroectoderm. After neurulation the neural tube closes and the NCCs undergo epithelial to mesenchymal transition (EMT) and migrate away. The embryo then undergoes convergent extension movements to elongate into a tailbud stage embryo. At this stage organogenesis occurs and the embryo will further develop its neural tube, notochord and somites (muscle precursors) [8]. The embryo will continue to develop facial features such as the ear, eye, mouth and branchial arches. Finally it develops the heart, kidney, liver and blood to form a fully feeding tadpole [8].

1.2 The neural crest

1.2.1 Neural crest induction

The neural crest is a transient embryonic cell population found exclusively in vertebrates. They migrate from the dorsal neural tube to various parts of the embryo where they differentiate to give rise to a variety of cell types due to their stem-cell-like multipotent potential [2, 6]. These include enteric ganglia, neuroendocrine cells, melanophores, neurons, craniofacial, skeletal and connective tissue. The induction and specification of neural crest cells (NCCs) occurs during gastrulation all the way up to organogenesis due to a multimodule gene regulatory network acting between the neural plate, nonneural ectoderm and the paraxial mesoderm (**figure 1.2**) [2, 9]. During neurulation the NCCs can be found within the neural folds and at the dorsal neural tube. A loss of cell-cell adhesion and the morphological changes which occur promotes the delamination and migration of these multipotent cells which will arrive at their correct destination and subsequently differentiate. Specific gene regulatory networks consisting of multiple signals and transcription factors are responsible for neural crest properties such as multipotency, induction, specification, migration and differentiation [2].

Wnt, fibroblast growth factor (FGF) and bone morphogenic protein BMP are the three important signalling pathways implicated in neural crest induction. The current model for neural crest induction at the neural plate border in *Xenopus* and zebrafish suggests that a dorso-ventral gradient of BMP4 and 7 activity regulated by BMP antagonists such as Chordin, Noggin and Follistatin found in the underlying paraxial mesoderm initiates the induction [10, 11]. However, this BMP gradient alone is not sufficient and so it is thought that this attenuated BMP signal must act in cooperation with Wnt signals to successfully induce neural crest [12-14]. The FGFs specifically involved in neural crest induction have been shown to be FGF2 and FGF8 secreted from the paraxial mesoderm [15]. Notch signalling acts upstream of BMP signals to refine the induced neural crest to the neural plate border. Overexpression of

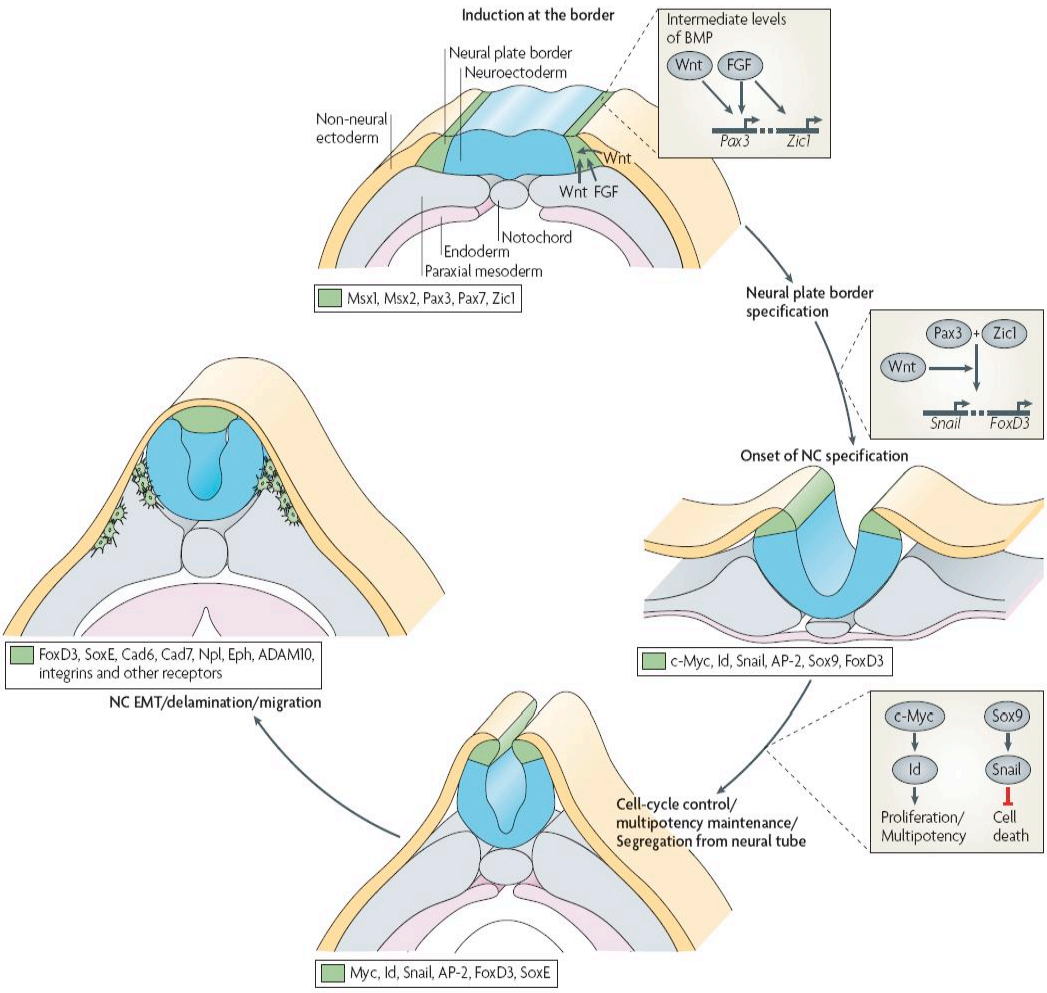

Figure 1.2: Neural crest induction, specification, survival and migration. Neural crest formation is regulated by a network of genes. Top image shows neural crest induction. This involves Wnt signals from the non-neural ectoderm and Wnt and FGF signals from the paraxial mesoderm acting in a BMP dependent fashion on the neural plate border to induce neural crest. The right image shows neural crest specification. This occurs due to the upregulation of neural crest specifiers such as c-Myc, Id3, Snail1/2, Sox10 and FoxD3. The bottom image shows genes involved in neural crest survival after neural tube closure. These include Id, Myc, FoxD3, Snail1/2 and members of the SoxE family. The left image shows neural crest migration. This occurs due to the upregulation of intrinsic matrix metalloproteinases and a change from typeI to typeII cadherins. Retrieved from [2]

Notch or Hairy2 (which acts downstream of Notch) results in neural crest expansion at the neural plate border [16, 17]. BMP signalling has also been shown to play a role in the maintenance of NCCs at neurula stages of development. Active rather than inhibited BMP4 signals in combination with Wnt signals from mesoderm adjacent the neural crest is required for this maintenance step [18]. The Zic factors (Zic1 and Zic3) and Pax3/7 play a role in neural crest induction at the neural plate border. They are

thought of as neural plate border specifiers and will be upregulated in in this region by the attenuated BMP signal. They are thought to upregulate neural crest specifiers such as Slug and FoxD3 by mediating the Wnt, BMP and FGF signals which influence their expression levels[19].

Gain of function and loss of function experiments in *Xenopus* and Zebrafish have been used to show that the canonical Wnt pathway is important for induction and neural crest lineage specification [20, 21]. Specifically Wnt8 has been implicated in *Xenopus* and Zebrafish neural crest induction and Wnt6 in avian neural crest induction [15, 20, 22]. In addition to Wnt8, Wnt1, Wnt3a and Wnt7b have been implicated in *Xenopus* neural crest induction [12, 23, 24]. The downstream Frizzled receptors through which these Wnts are signalling in the *Xenopus* to induce neural crest have been characterised as being Frizzleds 3 and 7 [25, 26].

1.2.2. Neural crest specification and survival

Once the neural plate border is fully specified and the NC has been induced, NCCs will undergo specification by certain transcription factors known as neural crest specifiers (**figure 1.2**). These have been characterised as Snail1, Slug (Snail2), Sox8, Sox9, Sox10, FoxD3, AP-2, Twist, c-Myc and Id3 [2]. Specification occurs due to morphological changes to the neural crest cells including changes to shape, adhesion and cell motility to allow the cells to migrate from the dorsal neural tube (**figure 1.2**). These neural crest specifiers act cooperatively to regulate their expression [2]. The expression of both Slug and FoxD3 is regulated by Fgf8 from the paraxial mesoderm where it is regulated itself by Msx1. Also required for Slug and FoxD3 expression are Pax3 and Zic1 which act together in a Wnt dependent manner [27, 28]. Wnt-dependent Pax3 regulation is also responsible for Sox10 expression which in turn is able to positively feedback on itself to maintain its own regulation [29]. Wnt signalling is also thought to directly activate the recently described neural crest specifier Gbx2. Gbx2 is considered to be the earliest factor in the

specifying cascade as it acts upstream of both Pax3 and Msx1. It functions in the posteriorization of the neural folds indicating a novel but essential role for this in neural crest specification [30]. Sox9 expression has recently been shown to be controlled by the binding of chromo-domain helicase DNA binding domain 7 (CHD7) and polybromo-and BRG1 associated factor containing complex (PBAF) with a neural crest specific enchancer [31].

Neural crest specifiers can be separated into two groups; early NC specifiers and late NC specifiers. The expression of early neural crest specifiers is first identified at the neural plate border. These include c-Myc, Id3 and Snail. The expression of late neural crest specifiers is first seen in pre-migrating neural crest and is maintained throughout migration. These include Slug, FoxD3 and members of the SoxE family such as Sox10 [32]. It has been suggested that early neural crest specifiers such as c-Myc and Id3 may have a role in maintaining neural crest cell multipotency and proliferation through control of the cell cycle by maintaining a balance between cell death and proliferation during neural crest cell fate determination [33-35]. Id3 functions downstream of c-Myc and so loss of function experiments involving either of these genes results in a loss of NC progenitor cells. Overexpression of Id3 has been shown to promote the maintenance of the NCCs multipotent potential and so it is implicated to act as a switch in the cell cycle which will decide whether the NCC proliferates or dies [33-36]. Prohibitin1 has also recently been shown to act downstream of c-Myc to inhibit the transcription factor E2F1 and in doing so promotes the expression of FoxD3, Slug and Twist [1].

Neural crest progenitors are also thought to be held in their multipotent stem cell-like state due to the active influence of epigenetic factors. These epigenetic influences occurring at the chromatin level include histone modifications such as methylation and demethylation. Such modifications are thought to keep the neural crest genes in a poised state ready for transcription. Trimethylation of histone H3 on lysines 4 and 36 (H3K4me3 and H3K36me3) is associated with transcriptionally active genes. Conversely trimethylation of histone H3 on

lysines 9 and 27 (H3K9me3 and H3K27me3) is associated with transcriptionally repressed genes. The histone demethylase JumonjiD2A (JmjD2A) is capable of removing H3K9me3 and H3K27me3 to control neural crest genes including Slug and Sox10 in vertebrates [37]. Recently the Polycomb repressive complex 2 (PRC2) have been shown to repress trimethylation of H3K27me3. Interactions of Polycomb with the Jumonji and ARID-domain containing protein (JARID2) promotes the interaction of PRC2 with H3K27me3. This interaction has been shown to be crucial in the correct differentiation of embryonic stem cells [38]. Similar interactions of polycomb associated proteins have been implicated in neural crest cell specification [39, 40].

1.2.3 Neural crest cell migration

Once NCCs have been specified they undergo an EMT in order to migrate away from the dorsal neural tube and reach their destinations where they will differentiate (**figure 1.3**). Neural crest will migrate in four main streams; those of the enteric neural crest which will migrate into the gut, the cardiac neural crest which migrate to the heart loops, the cephalic neural crest which migrate anteriorly and the trunk neural crest which migrate down the trunk of the embryo [41]. It is still unclear as to whether neural crest cells lose their multipotency before or after they start to migrate. Recent data have shown that most neural crest cells differentiate after migration however there are some, which do not [42]. However, other recent studies have disputed this, claiming that all NC cells are still multipotent before migration occurs [43].

EMT involves cytoskeletal, adhesive and cell junction modifications orchestrated by a network of transcription factors such as Snail, FoxD3 and Slug [44]. Slug plays a crucial role in EMT as it is responsible for changing cell adhesion molecules and cell junctions to a more migratory phenotype [45, 46]. In order for EMT to occur, NCCs must lose their apical-basal polarity and tight-junctions to allow them to detach from the neuroepithelium [44]. The type of cadherin expressed on the surface of NCCs is important during EMT. The cells will undergo a

switch from type I to type II cadherins to reduce the cells adhesiveness and increase motility [47]. E-cadherin expressed in neural crest cells is downregulated by direct binding of Snail to the promoter [48]. Similarly, type I cadherins N-cadherin and cadherin-6b are downregulated by FoxD3 and Slug [46]. Conversely type II cadherin-7 is upregulated by Sox10 and FoxD3 activity [47]. Snail is also responsible for regulating the repression of claudins resulting in the loss of tight junctions in NCCs. The loss of tight junctions allows NCCs to migrate from the dorsal neural tube and is associated with an upregulation of gap junctions [49, 50].

In order for neural crest cells to migrate effectively they must remodel and invade the extracellular matrix. NCCs are able to migrate through a combination of collagen, fibronectin, proteoglycans and laminin due to the activity of intrinsic matrix metalloproteases (MMPs) both secreted and membrane bound. NCCs can tightly regulate MMP activity themselves by the release of tissue inhibitors of MMPs (TIMPs) [51]. MMPs recorded to be involved in NCC migration include MMP2 in cardiac NCC migration and a disintegrin and metalloprotease-10 (ADAM10) in cornea development [52, 53]. In *Xenopus*, ADAM13 has also been shown to play an important role in NCC detachment from the neuroepithelium and subsequent migration [54]. Membrane bound MMP-14 and 15 have been identified in migrating cranial and trunk neural crest cells [55].

Whilst the NCCs are migrating they also undergo a large amount of cell division, which must be tightly regulated. NCCs are held in the G1 phase of the cell cycle until they migrate and undergo the transition to S phase controlled by BMP dependent Wnt signals orchestrating cyclin levels [56]. It is thought that the decrease in Snail expression after delamination allows cyclin levels to increase and therefore promotes cell cycle progression. Pre-migratory cells which still have high Snail expression levels also show a reduced level of cyclin D1 and D2, important for cell cycle progression from G1 to S. These cells also have high levels of p21, an inhibitor of cyclin dependent kinases (CDKs) [57].

In order for neural crest cells to migrate effectively there is a type of cross talk between the neural crest cells and other surrounding cells. If one neural crest cell comes into contact with another it will repolarise due

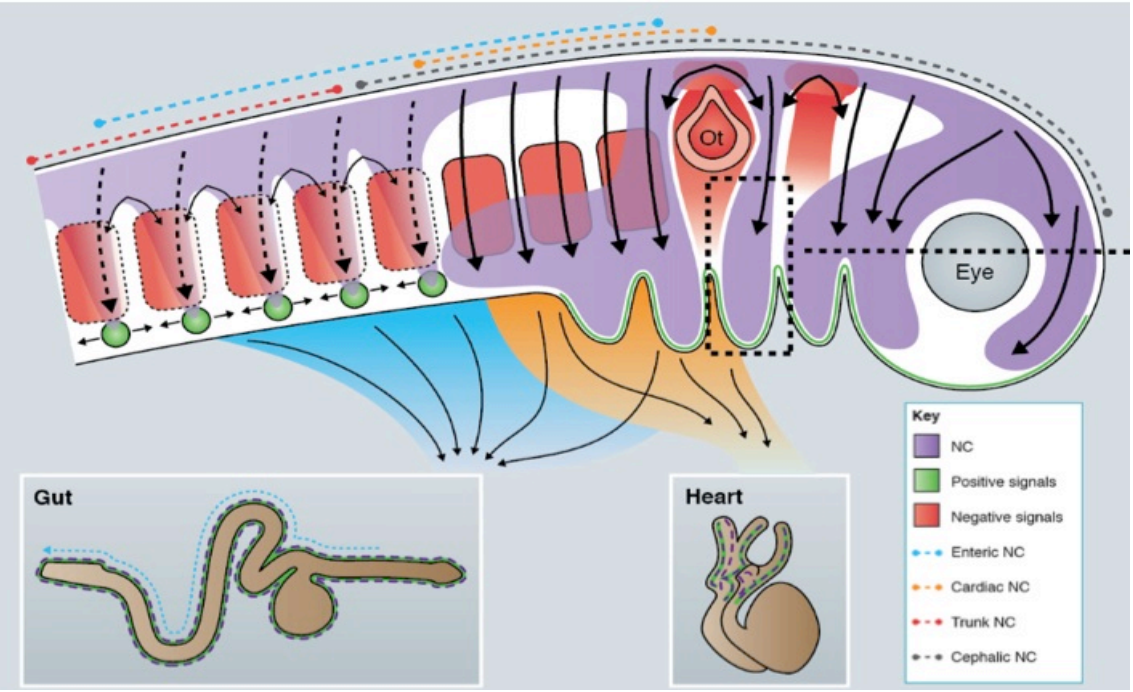

Figure 1.3: Neural crest migration. Neural crest migrate after undergoing EMT which occurs due to a switch from tight junctions to gap junctions. Neural crest streams shown here in purple, migrate into four areas. Enteric neural crest will migrate into the gut. Cardiac neural crest into the heart loops. Trunk nural crest migrate past the somites and Cephalic neural crest into the head to form neural crest cranial structures such as the branchial arches. Retrieved from [41]

to activation of the non-canonical Wnt pathway and migrate in a different direction. This is known as contact inhibition locomotion (CIL) [58, 59]. Despite this, large numbers of neural crest cells manage to migrate alongside each other in a continuous direction. This is because repulsive forces of CIL are balanced with attractive forces between neural crest cells due to the expression of chemoattractant C3a and the C3a receptor on their cell surface [60].

1.2.4 Neural crest differentiation

Neural crest terminal differentiation occurs due to specific groups of neural crest specifying transcription factors regulating specific effector genes which will in turn give the cell its fully differentiated properties and characteristics (**figure 1.4**). NCC differentiation is thought to be both spatial and temporally regulated. If a neural crest specifier i.e. Sox10 plays a role in the cell's differentiation it will continue to be expressed past NC specification in the migrating NCC. Sox10 is seen to be expressed in premigratory NC fated to become melanophores and

neurons but continues to be expressed in these differentiated cell types to upregulate the appropriate effector genes [2]. Taking NCC differentiation into melanophores as an example, SOX10 will act to upregulate microphtalmia-associated transcription factor (MITF) which in turn will regulate dopachrome tautomerase (Dct) expression. Dct is an enzyme which is used by melanophores to synthesise melanin [61, 62].

Conversely certain factors are responsible for repressing the expression of genes specific to NC lineages to promote cells going down a different lineage. For example FoxD3 can repress MITF expressed in melanophores to cause a lineage switch to glial cells [63]. The differentiation of other cell types is due to a similar temporal regulation by genetic hierarchies shown in **figure 1.4**. Neural crest determination also requires the presence of specific ligands. In order for melanophores to maintain their cell fate and survive they require interaction of receptors on their cell surface with specific ligands. In mammalian melanophores these include the c-kit receptor and Endothelin receptor B signalling [64].

There are two main streams of NCCs; those migrating cranially and those migrating in the trunk. Cephalic NCCs give rise to many cranial structures including bone, cartlilage, tendons and tissues of the ear, eye and teeth. They will also give rise to cranial melanophores and neurons. Trunk NCCs follow one of three paths, which in turn determines their cell

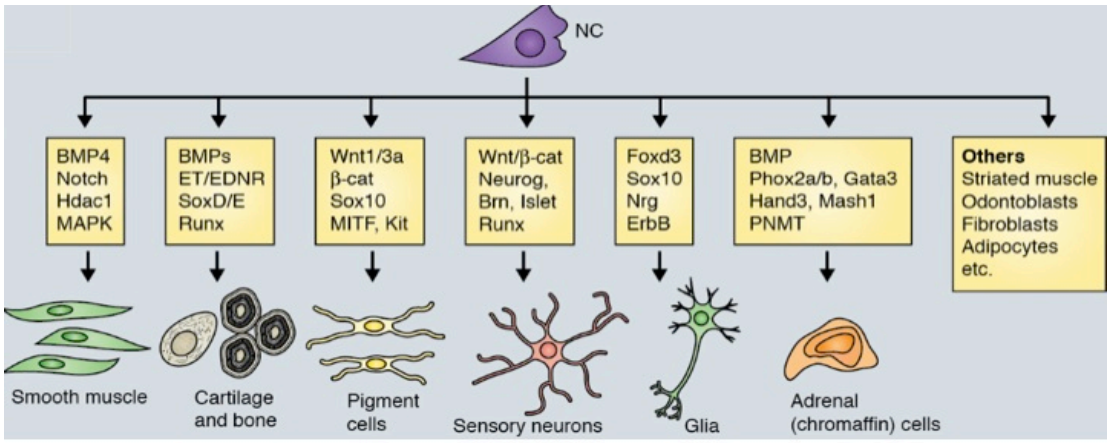

Figure 1.4: Neural crest differentiation. Neural crest cell differentiation is regulated by a network of specifying genes such as members of the SoxE family which will in turn promote the expression of effector genes able to induce the cells to undergo terminal differentiation. This terminal differentiation leads to cell types including smooth muscle, cartilage, bone, pigment cells, sensory neurons, glia and adrenal cells. Retrieved from [41]

fate [41]. The first wave of NCCs will move ventrally to form sympathetic neuron progenitors. The intermediate wave will migrate to the anterior sclerotome to form peripheral neuron progenitors and the final wave will migrate beneath the epidermis to form melanophores [65].

1.2.5. Melanophores

Melanophores are a neural crest derived cell type which function critically to protect organisms from damage caused to DNA by ultraviolet light [66]. They are capable of producing and transferring melanin to surrounding cells to give varying pigmentation patterns in vertebrates. Amphibians and fish contain melanophores which can rapidly change in pigmentation to allow the organism to adapt to its surrounds, evade predation and encourage sexual selection [66]. Mitf plays a key role in melanogenesis and is often referred to as the master regulator of the process. Its expression can be detected in the melanoblasts during their migration from the neural tube indicating that it plays a role in

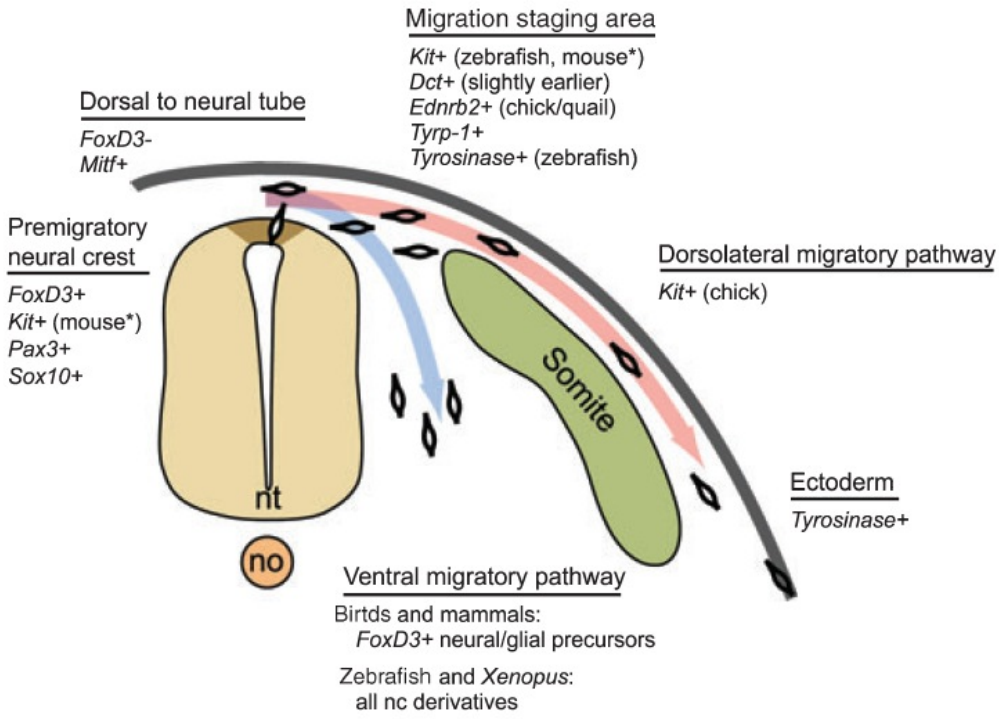

Figure 1.5: Melanophore development. Neural crests migrating along ventral (blue) and dorsolateral (red) pathways are specified by various transcription factors. Melanophores are formed from neural crests migrating along the dorsolateral pathway and are specified by transcription factors shown here. Retrieved from [68]

melanophore specification and survival (**figure 1.5**) [67]. Mitf mutants have been shown in mice and chicks to result in pigmentation defects. It has been determined to upregulate many genes involved in melanogenesis including tyrosinase and tyrosinase related protein 1 (Tyrp-1) [68]. Mitf itself is upregulated in melanophores by Wnt3a which is expressed in the dorsal neural tube during neural crest migration. Another important signal in melanophore development is that of the Kit receptor and its ligand KitL. Mutations in these have been identified to cause pigmentation disorders [68]. Heterozygous Kit mutations in humans is the cause of the disorder piebaldism. Kit receptor activation by KitL results in a signal cascade which results in the phosphorylation of Mitf, increasing its transcriptional activity [68].

Endothelin signalling also plays a role melanophore development and migration. It is currently thought that Edn-3 signalling interacts with the Kit receptor signal cascade in mammals to promote melanoblast differentiation [68]. In chick EdnrB1 has been shown to be expressed in early neural crest [69]. When these differentiate into melanophores this EdnrB1 expression is replaced by EdnrB2 expression. It has also been demonstrated that the Edn3 ligand which binds specifically to EdnrB2 is expressed in the ectoderm at the same stage of pigment cell development [69, 70]. Additionally, experiments in chick have shown that knocking down EdnrB2 significantly reduces the number of melanophores present [71].

1.2.6. Neural crest and melanoma

Melanomas are considered to be extremely aggressive malignant tumours which arise from the neural crest derived melanophores predominantly found in the epidermal basal layer. Mortality rate due to melanoma tends to be high due to the cancer's ability to resist most chemotherapies. Melanoma is often fatal if diagnosed too late and may arise due to all manners of genetic and environmental factors but are most commonly associated with increased ultraviolet light exposure.

Many of the genes which are seen to promote neural crest and melanophore development are also often misregulated in melanoma[72]. Fully developed melanomas are able to grow vertically invading the basement membrane where they can metastasise and spread throughout the body [72, 73]. The most common mutation found in melanomas are those of the BRAF oncogene. 60% of melanoma cases have mutations in this gene. The most common mutation results in a V600E substitution causing a 700-fold increase in BRAF kinase activity [72]. Melanomas resembling those found in humans can be induced in p53 loss of function zebrafish by expressing the $BRAF^{V600E}$ mutation using a Mitf promoter. This gives evidence for the role of this mutation in melanoma formation [74].

Several genes involved in neural crest development are implicated in melanoma formation. These include Mitf which may be overexpressed in melanoma to promote tumour cell survival and cell cycle progression [75]. C-Kit may be overactive in rare acral and mucosal melanomas [76]. Slug is thought to play a role in melanoma tumour cell metastasis as Slug knockdown in melanoma cells has shown decreased cell migration associated with only moderate primary tumour formation [72, 77]. Endothelin receptor B (ENDRB) is found to be overexpressed in many human melanomas. This may act to increase Snail expression and therefore the tumours invasive potential [78]. It is also thought that ENDRB overexpression leads to increased BRAF activity [72]. Neural crest specifiers Sox9 and Sox10 have similarly been shown to be expressed in advanced melanoma and are considered prognostic markers of melanoma aggressiveness [79].

1.2.7. Cranial cartilage development

Vertebrates are able to form facial structures such as the jaw and pharynx due to the differentiation of cranial neural crest cells into branchial arch cartilage. Cranial neural crest cells form at the anterior dorsal neural tube and migrate into the branchial arches where they are

able to form cranio-facial cartilage. These neural crest migrate in three streams; the mandibular, hyoid and branchial streams (**figure 1.6**) [80, 81]. NCCs migrating into the mandibular arch will form Meckel's and palatoquadrate cartilage which gives rise to the jaw [82]. The hyoid arch will go on to form skeletal structures able to support the jaw and tongue. Finally the branchial arches will form skeletal support for the gills and throat [81]. Neural crest are patterned into these three tissue types due to Hox gene expression such as Hoxa2 which is thought to be expressed in the crest of the branchial regions [83].

Cranial neural crest differentiate into cartilage derivatives due to expression of Sox9. This SoxE family member will bind to the chondrocyte enhancer of the collagen type 2 (Col2a1) to promote cartilage production. Mutations in the Sox9 gene result in a loss of branchial cartilage and are associated with congenital jaw defects [84]. A hierarchy of Runx gene expression (Runx1, 2 and 3) is then required for chondrocyte maturation into cartilage [85]. Endothelin-1 and endothelin receptor a (Ednra) signalling is also known to be important for pharyngeal arch dorso-ventral patterning. The receptor is expressed in the migrating crest of the pharyngeal arches and the ligand is produced by the

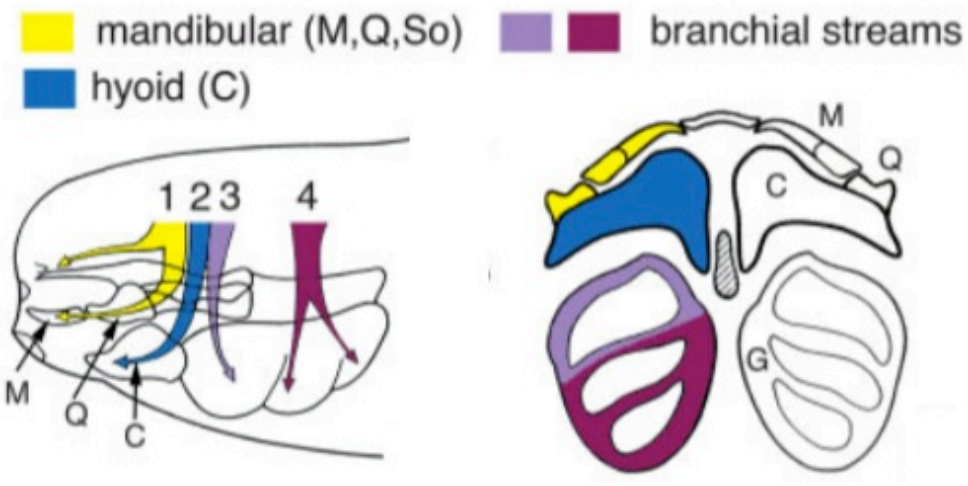

Figure 1.6: Cranial neural crest migration and differentiation. Cranial neural crest cells will migrate into 3 regions of the embryonic face. The mandibular region (yellow) which will go on to form the meckel's cartilage (M) and palatoquadrate cartilage (Q). The hyoid region (blue) will form ceratohyal cartilage (C). The branchial region (pink and purple) will give rise to the ceratobranchial cartilages (G) Retrieved from reference [81]

surrounding mesoderm. Endothelin-1/Ednra signalling is known to further regulate the transcription factor Dlx6 which is also important for pharyngeal arch patterning [86, 87].

1.2.8. Sensory neuron development

Sensory neurons are the neurons of the peripheral nervous system, which respond to external stimuli such as touch or heat. They are known as the dorsal root ganglia in the trunk of the embryo and the trigeminal ganglia in the head. NCCs of the trunk will migrate between the somites to form the dorsal root ganglia [88]. Sensory neurogenesis is thought to be stimulated by Wnt signalling. Treating NCCs with Wnt1 can induce sensory neuron differentiation [89]. Transcription factor signalling also plays a key role in sensory neuron differentiation. The first factors involved are those of the neurogenin family. Neurog1 and 2 are expressed in the migrating cranial and trunk neural crest fated to form sensory neurons and drive sensory neurogenesis [90-92].

Brn3a and Islet1 are transcription factors, which are also thought to regulate sensory neurogenesis. Loss of either of these leads to a reduction in sensory function [93, 94]. They are able to promote sensory neuron differentiation by their binding and upregulation of other genes expressed in differentiated sensory neurons. These genes are the Runx family genes, which regulate the final maturation of sensory neurons [95]. Runx1 promotes the differentiation of nociceptors, the class of neuron, which respond to external stimulus leading to pain. Runx3 will promote the differentiation of proprioceptors, the class of sensory neuron responsible for tactile stimulus and the space in which you are occupying [96, 97].

1.2.9. Cranial sensory placode development and neural crest

Cranial placodes develop alongside neural crest (**figure 1.7A**) to give rise to sensory organs such as the nose, lens of the eye, ear and sensory neurons of the cranial region. Placodes form from thickenings of the ectoderm and are patterned based on their anterior-posterior position. These placodes are the adenohypophyseal, olfactory, lens, trigeminal, profundal, otic and lateral line placodes [98-101]. Both neural crest and placodes develop at the neural plate border and have a multipotent potential to differentiate into various cell types. Placodes will form from a multipotent precursor region known as the preplacodal region and from here they will undergo morphogenesis or invaginate to produce the different placode types [102, 103]. By the end of neurulation (stage 21) *Xenopus* embryos will have 3 placodal regions. The most anterior placode region contains the adenohypophyseal and olfactory placodes. The next region at the edge of the presumptive eye contains the trigeminal and profundal placodes. The most posterior region contains the otic and lateral line placodes (**Figure 1.7B**). These placodes along with the lens placode continue to develop into tailbud stages of *Xenopus* development (**Figure 1.7C**) [104, 105].

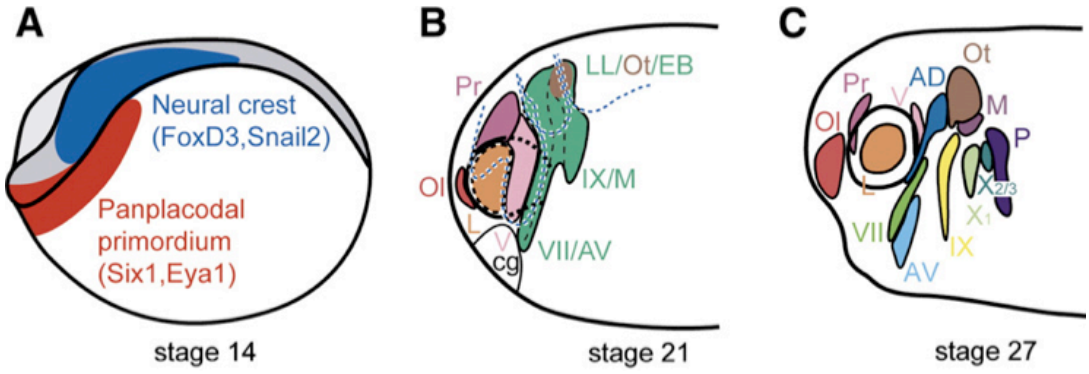

Figure 1.7: Placode development in Xenopus. (A) At stage 14 the presumptive neural crest and placodes develop alongside each other at the neural plate border. (B) At stage 21 placodes develop close together but are separated into the different placode types. Neural crest are shown as dashed lines. (C) At stage 27 placodes are spread out and defined by their anterior posterior position. VII facial epibranchial placode, IX glossopharyngeal epibranchial placode, X1 first vagal epibranchial placode, X2/3 second and third vagal epibranchial placodes, AD anterodorsal lateral line placode, AV anteroventral lateral line placode, L lens placode, LL lateral line, Ot otic, EB epibranchial, M middle lateral line placode, Ot otic placode, Ol olfactory placode, P posterior lateral line placode, Pr profundal placode, V trigeminal placode. Retrieved from reference [98]

The adenohypophyseal placode will invaginate to form the anterior lobe of the pituitary gland, important for hormone secretion in most vertebrates [106-109]. The olfactory placode will invaginate to form supporting, mucus secreting cells and chemoreceptive axons, which respond to odorants of the nasal cavity [110, 111]. The lens placode will form the crystallin producing cells of the eye [112-114]. Trigeminal and profundal placodes form the sensory cranial ganglia along with neural crest cells. These ganglia will respond to somatosensory stimulis such as heat or touch [115-117]. The otic placode will differentiate into the vestibulocochlear ganglia of the inner ear, which will innervate mechanosensory hair cells [118, 119]. Lateral line placodes will form lateral line sensory neurons, which can respond to electrical currents or mechanosensory stimulus [120-122]. Finally, epibranchial and hypobranchial placodes give rise to facial and vagal sensory neurons, which ennervate receptors such as taste bud [123, 124].

Many transcription factors have been shown to be important for placode development, some overlapping with those important for neural crest development [103]. Six1/2, Six4/5 and Eya genes are panplacodally expressed in the pre-placodal ectoderm. Mutations in these genes are associated with placode defects [104, 125]. As development proceeds other transcription factors are upregulated based on the anterior-posterior postion of the placode to define specific placode types. These include Otx2, expressed in the adenohypophyseal, olfactory, and lens placodes [126, 127]. Emx genes are restricted to the olfactory and otic placodes where they promote proliferation and differentiation [128, 129]. Six3/6 are expressed in the anterior neural plate where they inhibit Wnt and BMP to promote the development of adenohypophyseal, olfactory, and lens placodes [130-133]. Tbx genes are placode specific, Tbx1 is expressed in the pharyngeal pouches, pharyngeal arches the otic placode. Tbx2 is expressed in the trigeminal and profundal placodes and also the posterior placodes forming dorsal root ganglia [104]. Finally Pitx genes play an important role in lens and adenohypophyseal development [134, 135].

As mentioned, neural crest and placodes develop alongside each other and have similar evolutionary origins. This has resulted in some overlap in the transcription factors required for the development of these two cell types. Msx genes are expressed in the early neural crest and the preplacodal areas of the anterior neural plate border where they act to pattern the anterior ectoderm [136, 137]. Pax3 and Pax7 are both expressed in the neural plate border and are important for the development of both neural crest and the profundal placodes which both form cranial senory ganglia [104, 138]. Interestingly, c-Myc is implicated to not only regulate the expression of neural crest markers such as Sox10 but it has also been shown to be important for placode development [139]. Morpholino knockdown of c-Myc in Xenopus results in a loss of cranial ganglia derived from trigeminal neurons implicating the importance of c-Myc in trigeminal placode development [33, 103]. It has also been shown that Six1 and Eya are able to stimulate c-Myc expression [140].

Both placodes and neural crest will produce migratory cell types, which can form the cranial sensory glia (**figure 1.8**) [141]. There are both similarities and differences in the induction of these two cell types. They both form at the neural plate border however placodes are restricted to the anterior neural plate whilst neural crest can also form in the trunk [141]. It is also known that there is a temporal difference in their specification. Neural crest are thought to be specified at the neural plate border before placodes [142, 143]. As both cell types form in the same region of the embryo it is not unexpected that the inductive signals for both are very similar. Both cell types receive these signals from the adjacent ectoderm and the underlying mesoderm. However slight differences allow for these distinct cell types. Signals from the paraxial mesoderm signal to neural crest whereas signals from the dorsal lateral plate mesoderm signal to presumptive placodes [19, 144]. It is known that the signals from this mesoderm important for neural crest induction are Wnt, FGF and an attenuated BMP signal. The signals important for placode development are similar but not the same. It is unclear whether

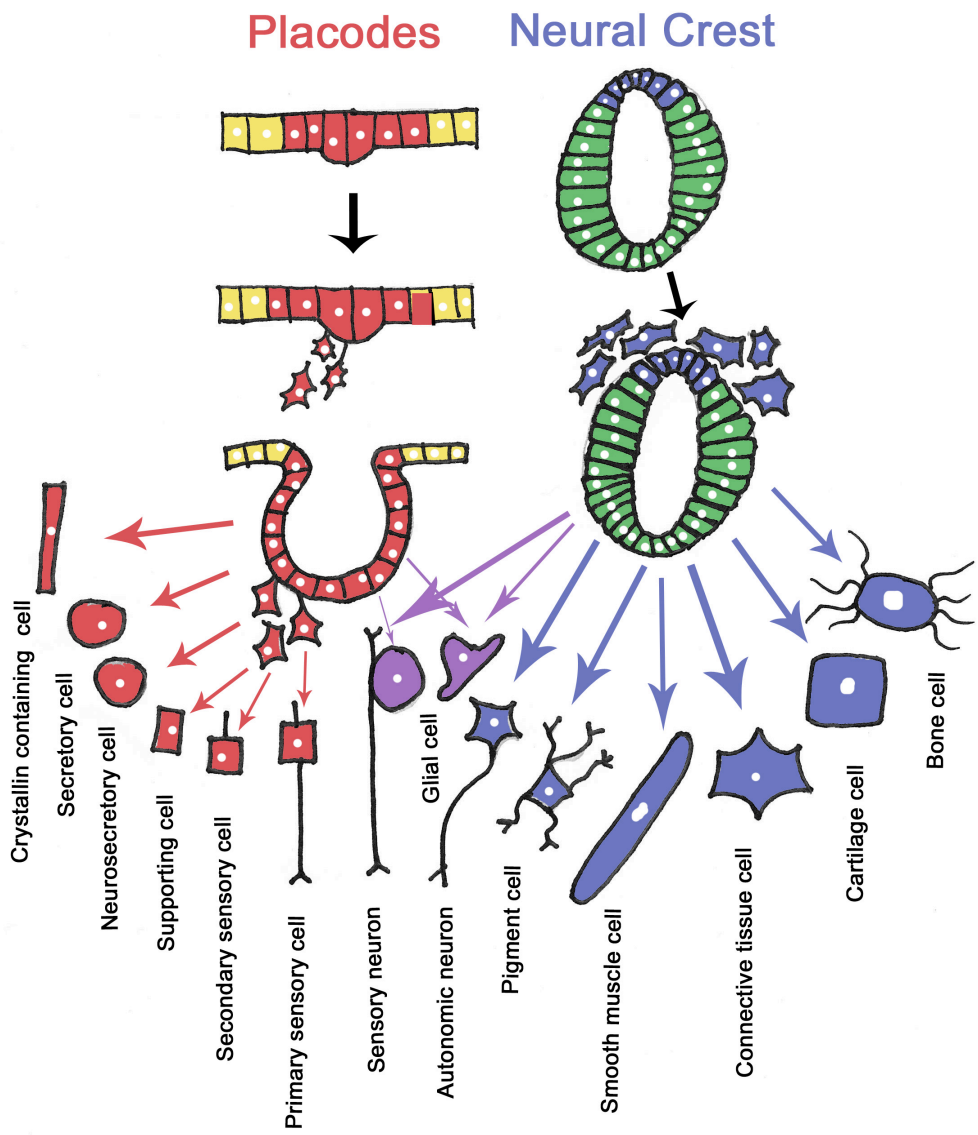

Figure 1.8: Cranial placode and neural crest development. Both placodes and neural crest will form migratory cell types capable of forming many different derivatives. These derivatives even overlap sometimes as both placodes and crest are capable of producing sensory neurons and glial cells. Adapted from reference [141]

BMP signals are important for placode development but studies removing BMP from the area of the presumptive placode have shown that the placodes will still develop indicating that BMP is not important in placode development [144]. FGF signals will switch on the transcription of Msx1, Zic1, Pax3 and Sox9, which are important in the development of both neural crest and placodes. These will upregulate different genes in these different cell types due to the presence of different co-factors present in turn promoting the divergence of the two cell types [141]. Wnt

is important for both placodes and neural crest as it acts to inhibit placode induction and stimulates neural crest development. Placodes are able to form in the anterior most neural folds as Wnt inhibitors are secreted here blocking neural crest induction [22, 27, 144].

1.3. Chemical genetics

1.3.1 Chemical screens

Chemical genetic screens utilise small organic molecules (less than 2000 Da) to alter the function of specific genes and so determine their role in developmental processes. They are easy to set up, cheap to run and can be used to target a specific gene at a specific time point by adding or taking the compound away. Screens can be used for high-throughput phenotype analysis to uncover novel drugs and drug targets with therapeutic potential for a whole manner of diseases. The use of small vertebrates such as the *Xenopus* or Zebrafish is advantageous over the use of mammalian models as they provide a cost effective way to discover new drugs, their targets and test their toxicity levels [145, 146]. Amphibians can be used successfully in chemical screens due to their transparency which makes phenotypic analysis easier, their fast development time and production of thousands of eggs at any one time which makes the process high-throughput and their ability to take up the compounds from their surrounding media [145]. *Xenopus* embryos have been used in chemical screens for these reasons mentioned. The vast number of *Xenopus* embryos which can be collected are also small enough to fit in a 96-well plate. Here the compounds can be added to the salt media the embryos will grow in optimally and can be easily absorbed past the permeable vitelline membrane and through the Embryo epidermis [145, 147].

1.3.2. Leflunomide

Leflunomide is an inhibitor of dihydroorotate dehydrogenase (DHODH), which was shown to be a compound capable of altering

pigment development after a chemical screen carried out in *Xenopus* laevis and Zebrafish. During this screen of 2000 different compounds, NSC210627 was identified to inhibit pigment cell development in *Xenopus* and Zebrafish. The chemoinformatic DiscoveryGate algorithm was used to identify compounds with a high level of structural similarity. This led to the identification of Brequinar, an inhibitor of DHODH. Leflunomide is structurally dissimilar to brequinar but also inhibits DHODH and phenotypically mimics the affect of NSC210627 [3]. As Leflunomide is cheaper, readily available and already FDA approved as an arthritis treatment it was selected for further experiments. DHODH is an enzyme responsible for pyrimidine synthesis and is therefore required for RNA transcription and DNA replication. Leflunomide is therefore thought to act by inhibiting the transcription of genes involved in melanophore development [3, 4].

Recent work in Zebrafish has shown that Leflunomide treatment causes an abrogation of melanophores 36-48h and iridophores 72h post fertilisation (**figure 1.9**). Leflunomide was also shown to reduce the expression of Sox10 and other genes expressed in neural crest and genes such as Dct and Mitf expressed in melanophores (**figure 1.9**) but was shown to have no effect on genes expressed in tissues such as blood or notochord [3]. Leflunomide has also been shown to reduce the number of neural crest cells in cell culture further suggesting this drug specifically affects the self renewal of this multipotent cell type [3]. As melanomas have been documented to adopt a similar genetic signature to that of the neural crest by expressing many of these genes involved in normal neural crest development and melanophore specification, it is thought that Leflunomide may have therapeutic potential for melanoma treatment [3]. Using a combination of leflunomide and a $BRAF^{V600E}$ inhibitor (PLX4720) administered into mouse melanoma xenografts has been shown to block *in vivo* tumour growth [3].

Leflunomide is thought to carry out its function through the inhibition of transcriptional elongation by preventing the synthesis of pyrimidines. Leflunomide treated Zebrafish phenotypically mimic spt5/spt6 Zebrafish mutants. Spt5/spt6 is required for transcriptional

elongation to commence so it is thought that these mutants have increased levels of transcriptional pausing [3, 148]. Spt5 mutants also show an almost complete overlap of genes affected to that of leflunomide treated embryos. This includes a reduction of the expression of neural crest genes Sox10, Crestin and Mitf as shown by microarray. Work carried out in human melanoma cell lines showed leflunomide to specifically inhibit the transcriptional elongation of Myc target genes. This is of particular interest to us as Myc is implicated to play roles in both neural crest specification and transcriptional pause release in embryonic stem cells [6, 33, 36].

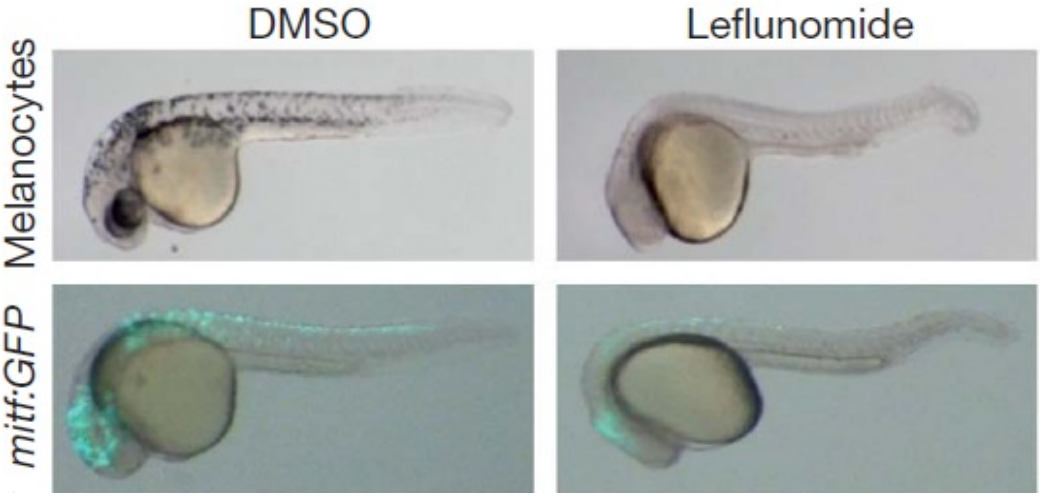

Figure 1.9: The effect of leflunomide on Zebrafish. Top two images show that after leflunomide treatment zebrafish loose melanophores, a neural crest derivative, entirely when compared to the DMSO control. The bottom two images show neural crest progenitors using GFP regulated by a Mitf promoter. After leflunomide treatment there is a loss of these progenitors shown by the loss of GFP expression. Retrieved from [3]

1.4. Transcriptional elongation

1.4.1. The process of RNA polymerase pausing and transcriptional elongation

In order for genes to undergo transcription, RNA polymerase II (Pol II) must be recruited to the promoter region by certain DNA-binding transcription factors [149]. Subsequent to this RNA Pol II may undergo regulation to temporally control the expression of genes in specific cell types. Such regulation includes the promoter proximal pausing of Pol II

(**figure 1.10**). This is the process by which Pol II undergoes stalling or poising at the 5' end of a gene just downstream of the transcription start site [150]. This occurs due to the binding of pause factors DRB-sensitivity inducing factor (DSIF), negative elongation factor (NELF) and transcription factor IIS (TFIIS) [151, 152]. NELF is able to bind to the clamp domain of RNA Pol II through associations with its NELF-A subunit. DSIF is composed of two subunits Spt5 and Spt6, mutations in which have both shown inhibition of transcriptional elongation [148, 153]. In order for transcriptional elongation to commence the positive transcription elongation factor, P-TEFb, must be recruited to the transcription elongation complex. P-TEFb is known to be a complex composed of cyclin dependent kinase 9 (CDK9) and cyclin T1 [154-156].

The poised RNA Pol II is associated in a complex with both DSIF and NELF. To initiate transcriptional elongation, phosphorylation of the serine residues in positions 2 and 5 of the YSPTSPS repeat in the C-terminal domain (CTD) of the large subunit of Pol II must occur. This phosphorylation of Pol II at the CTD and phosphorylation of the Spt5 subunit of DSIF is carried out by P-TEFb to allow for transcription and the production of full length transcripts. After this phosphorylation, NELF dissociates from the complex and DSIF remains bound to RNA Pol II switching roles to promote transcriptional elongation [155]. Other general transcription factors TFIIF and TFIIS contribute to pause release. This pausing and subsequent elongation is known as transcription elongation checkpoint control (TECC) [157].

Transcriptional pausing of subsets of genes has recently been shown to be a crucial step in regulating expression for normal development and also inappropriate regulation arising in diseases such as cancers [3, 158-160]. 30% of genes present in embryonic stem cells will undergo transcriptional pausing with no subsequent elongation. This would suggest the importance of polymerase pausing in maintaining stem-cell pluripotent potential and preventing the transcription of genes involved in differentiation. It is also now known that RNA Pol II can instigate transcription in both a sense and antisense direction. This may also indicate a role for polymerase pausing in the prevention of antisense transcription [6, 161].

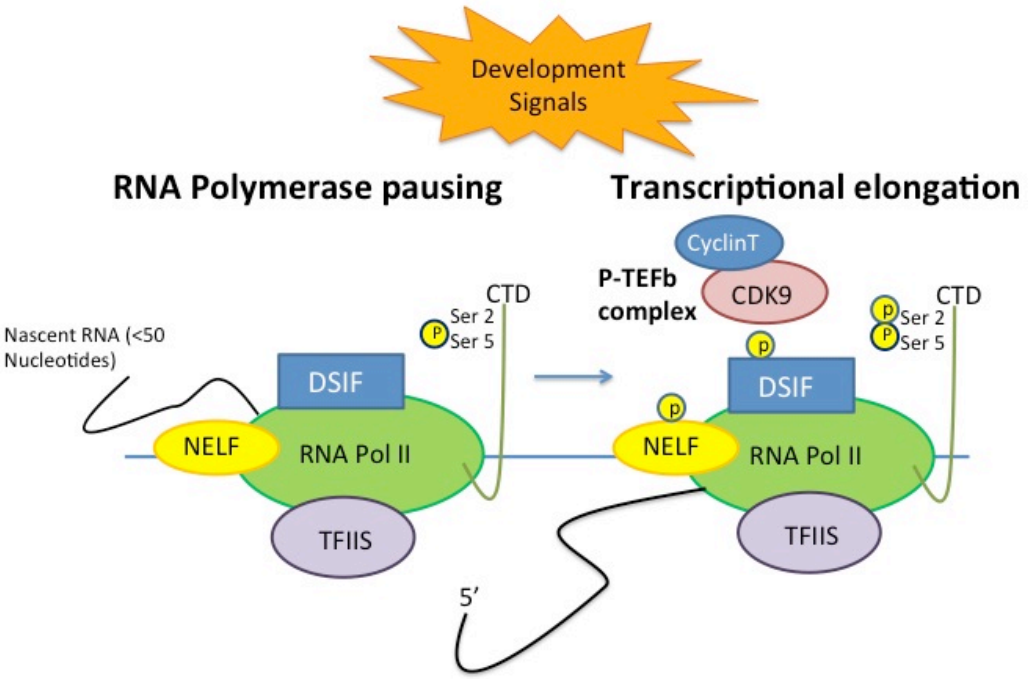

Figure 1.10: RNA polymerase pausing and transcriptional elongation. RNA Pol II is able to stall after transcription initiation 30-50 nucleotides downstream of the start site. Release from polymerase pausing is kick started by developmental and environmental signals. In the paused state Pol II is associated with both DSIF and NELF and the C-termial is phosphorylated only on serine 5. The P-TEFb complex is able to induce pause release by phosphorylating the serine 2 residue and also DSIF and NELF. NELF will dissociate from the complex and transcriptional elongation will commence.

1.4.2. The PTEF-b complex

In order for productive transcription to occur after polymerase pausing, the positive transcription elongation factor complex (P-TEFb) must be recruited. This complex is highly conserved from yeast all the way up to humans and localised in the cell nucleus. Like most cyclin dependent kinase arrangements it consists of a CDK acting as the enzymatic functional subunit and a cyclin subunit which will undergo a conformational change to promote the activation of the kinase[162]. The CDK common to all P-TEFb complexes is CDK9. This itself must be phosphorylated at the Thr186 of the T-loop region of CDK9 before kinase activity is fully activated[163].

It is crucial that the enzymatic activity of P-TEFb is tightly regulated to control the transcription of poised genes at the specific time they are required. P-TEFb has its own unique mechanism of doing this through its reversible binding with the 7SK small nuclear ribonucleoprotein particle (snRNP) (**figure 1.11**). P-TEFb can be found simultaneously in either an active or inactive state in the cell nucleus. It is inactive if bound to 7SK snRNP and will become active when rapid transcription is needed to occur by its recruitment into the super elongation complex (SEC) [162, 164].

Inactive P-TEFb is bound to the inhibitory domain of RNA binding proteins HEXIM1 or HEXIM2 (hexamethylene bisacetamide inducible proteins), which are in turn bound to 7SK snRNP. HEXIM1 and HEXIM2 have been shown to be able to compensate for each other both *in vitro* and *in vivo.* They act by inhibiting the P-TEFb function and so are considered to be entirely novel CDK inhibitors (CDKI) as no other CDKIs interact with RNA to mediate inhibition[165-170]. La-related protein 7 (LARP7) and methyl phosphate capping enzyme (MePCE) bind to the 7SK snRNP complex to help stabilise its binding to P-TEFb [171-173].

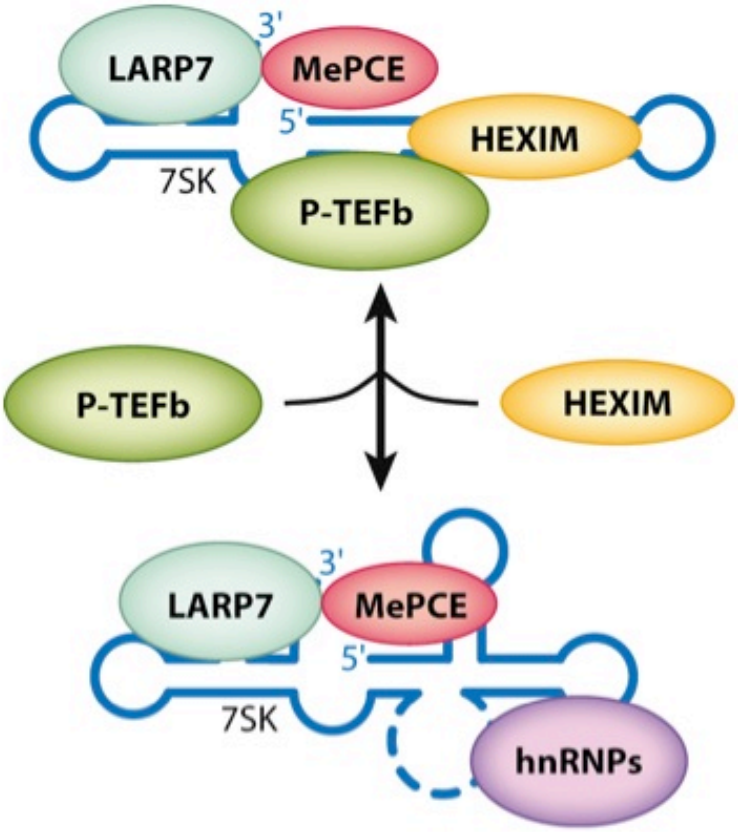

Figure 1.11: Inhibition of P-TEFb by binding to 7SK snRNP. 7SK snRNP is found bound in a complex with LARP7 and MePCE. PTEF-b will only bind to this and become inactive if HEXIM is present and bound to the 7SK snRNP. HEXIM bound to 7SK snRNP has its inhibitory domain revealed allowing P-TEFb to bind. Retrieved from reference [163]

The inhibitory complex formed between P-TEFb and 7SK snRNP means that P-TEFb activity is carefully regulated and its activity can be pinpointed to precise genes when it is required. This prevents the premature release of other poised genes which are not yet needed [162]. Details of how P-TEFb targets specific genes are still unknown. It is thought that P-TEFb can be directed by the different variety of transcription factors which can bind to it in response to numerous signalling cascades allowing it to incorporate into diverse forms of the super elongation complex increasing the specificity between P-TEFb and its gene targets [157]. Incorporation into the super elongation complex has been shown to enhance P-TEFb's enzymatic activity [174].

1.4.3. Regulation of the productive elongation phase.

Upon activation of P-TEFb, the complex will phosphorylate NELF and DSIF causing NELF to dissociate from RNA Pol II allowing transcription elongation to occur. DSIF is retained in the RNA Pol II complex switching roles from inhibiting the productive elongation phase to promoting it [6]. Once P-TEFb has phosphorylated its targets it is no longer required and can be sequestered in its inactive state. Elongation is then regulated by transcription factor IIS (TFIIS) and the rate of elongation is maintained by transcription factor IIF (TFIIF) [162, 175]. These factors both play a key role in regulating transcription arrest. If RNA Pol II is held in a paused state for too long it will enter into arrest. This can occur if the amount of nucleoside triphosphates available is limited [176].

TFIIS is able to save arrested Pol II by promoting the cleavage of the arrested RNA transcript allowing it to form a new 3' end which is reinserted into the RNA Pol II active site and transcription can continue from here[175]. TFIIS depletion in *Drospophila* by RNAi has shown that there is no effect on global gene expression however it does seem to have an effect on specific actively transcribed genes such as those encoding for heat shock proteins. These will remain in a paused state following TFIIS depletion [177, 178]. TFIIS will then act to sustain the rate of transcription elongation [179]. TFIIF will bind to the paused PolI II altering its conformation to an elongation competent one [162]. TFIIF has been shown to bind to human genes before the transcription initiation start site and also on specific elongating genes downstream of the promoter in the transcribed regions. This suggests a role for TFIIF in both initiation and elongation of RNA transcripts[180].

In order for productive elongation to occur it is also necessary that histone modifications occur. RNA Pol II is found to associate with PAFc (RNA polymerase associated factor c) a protein capable of the methylation of H3K4 and H3K79. This association occurs due to a complex which forms between the SEC and PAFc. H3K4 and H3K79 are positive methylation marks and are associated with actively transcribing

genes[181]. It is also able to remove histone modifications associated with polymerase pausing such as H2B by ubiquitination. PAFc itself is made up of several individual components; Paf1, Ctr9, Cdc73, Rtf1, and Leo1[181, 182]. PAFc itself has no enzymatic activity and so it relies upon recruiting enzymes such as Rad6 for ubiquitination and SET for trimethylation of histones [183-187]. This provides a link between transcriptional elongation and histone modification. PAFc itself only acts as an adaptor complex bridging the gap between methytransferases and RNA Pol II. It has also been shown to be in a complex itself with the SEC, P-TEFb and other Pol II associated factors such as DSIF and TFIIS[188-190]. CHIP-seq experiments have shown that PAFc is found all along the length of genes when in an actively transcribed state. A peak representing PAFc is also found at the 3' end indicating a potential role for PAFc in 3' mRNA bio-genesis [182, 191].

1.4.4. The super elongation complex (SEC)

When P-TEFb is in its active form it is usually within a collective of several proteins known to regulate transcriptional elongation. This combined complex is known as the super elongation complex (SEC) (**Figure 1.12**). In addition to housing the active P-TEFb complex it has also been shown to contain ELL-1 and ELL-2 (eleven-nineteen lysine-rich leukemia 1 and 2), ENL, AF9 (ALL1-fused gene from chromosome 9), AFF1 (AF4/FMR2 family, member 1) and AFF4 (AF4/FMR2 family, member 4)[192, 193]. Each SEC will contain a different combination of these extra proteins depending on the gene upon which they are acting. For example it is known that the different ELL proteins can compensate for each other, as can the AFF proteins [194]. AFF proteins act to hold the complex together, supporting the formation of the SEC[157].

These complexes are recruited to the promoter region of genes when rapid transcription is required in response to specific developmental signals, changes to available nutrition or even acute temperature change. It is because of this that the genes primarily regulated by RNA polymerase pausing are master regulator genes and/or rapid response genes such as heat shock and serum inducible genes [157, 195]. The recruitment of the SEC to paused polymerases has been demonstrated using chromatin immunoprecipitation (CHIP) sequencing in embryonic stem (ES) cells. One experiment showing this very clearly used retinoic acid to induce retinoic acid inducible genes in ES cells and observing the SEC components recruited to the promoters of these genes. It is this recruitment of the SEC which is thought to be responsible for the rapid transcription induction of such genes [196].

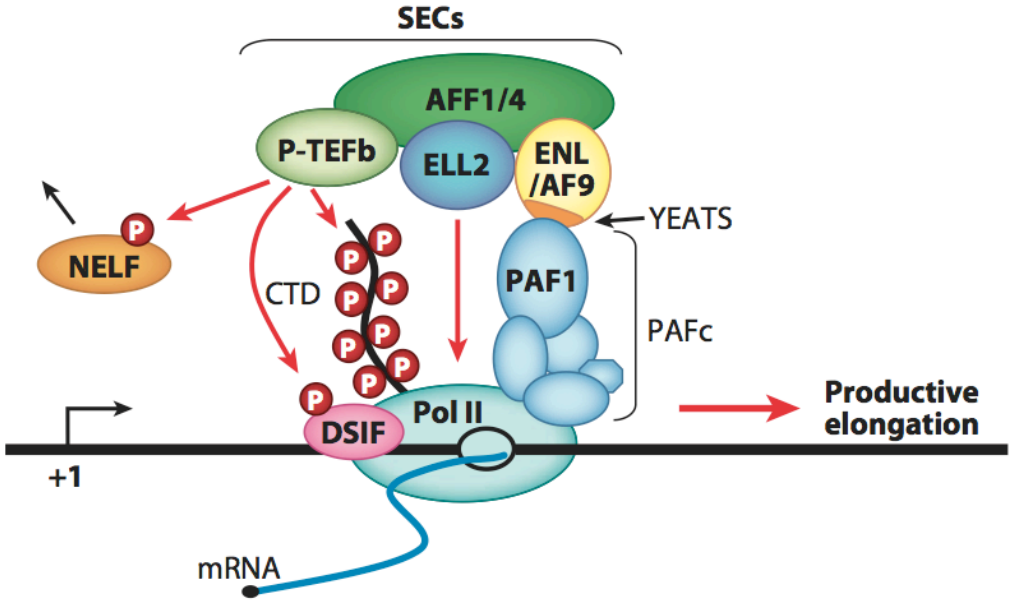

Figure 1.12: The super elongation complex (SEC). In mammals the SEC is comprised of the positive transcription elongation factor b complex (P-TEFb) A member of the AFF family usually either 1 or 4. One of the eleven-nineteen lysine-rich leukemia (ELL) proteins, ENL and AF9. These are also associated with RNA polymerase associated factor c (PAFc) via the YEATS domain of AF9. When associated with the SEC, P-TEFb is active and able to phosphorylate the C terminal domain of RNA Pol II, DSIF and NELF allowing NELF to dissociate and positive transcription elongation to occur. Retrieved from reference [163].

It has also been suggested that the main function of SEC recruitment to paused genes is not necessarily to allow rapid induction but also to increase the amount of synchronicity between genes in

development. Work using *Drosophila* has shown that during embryonic development some genes termed 'synchronous' genes will have a paused pol II at the promoter. These genes, for example *short gastrulation* (*sog*), tended to be those found in complex gene regulatory networks. Other genes did not show this necessity for paused pol II. These were termed stochastic genes and they demonstrated erratic and unpredictable gene expression, for example *thisbe* (*ths*) (**Figure 1.13**) [197]. Convincing studies have shown that pausing is important and present on rapidly induced genes and also on those considered master regulator genes whose expression is tightly regulated. One study using *Drosophila* has shown that genes known to be rapidly induced such as antibacterial genes do not have a paused pol ll. However genes involved in the careful regulation of the fly's innate immune system, will undergo pausing [198]. It is therefore still unknown exactly which gene types pausing is crucial for the expression of.

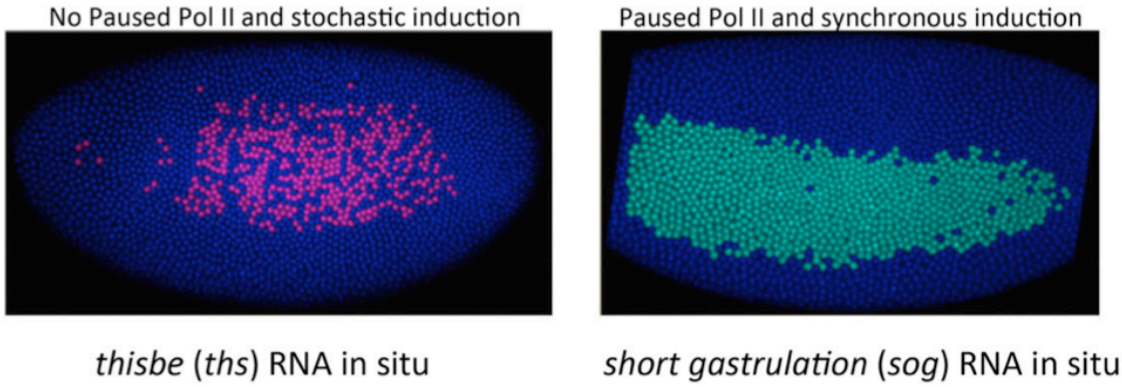

Figure 1.13: Stochastic and synchronous gene expression. In-situ hybridisation experiments in drosophila clearly demonstrate a less organised early expression pattern for genes such as *thisbe* which have no paused Pol ll at the promoter. Conversely, those genes thought of as tightly regulated as they play key roles in complex gene regulatory networks showed a more uniform expression pattern. An example of this is *short gastrulatio*n shown here. Retrieved from [198].

Most evidence for a paused RNA polymerase II has come from ChIP sequencing experiments carried out in embryonic stem cells. Such experiments were the first to show that a paused polymerase associated with the components of the SEC can be recruited consistently to embryonic stem cell genes [196]. Two genes which have specifically been shown to have a paused RNA polymerase associated with them are the c-Myc gene and the heat shock protein hsp70. Recruitment of the SEC to these genes occurs via the N terminal domain of a mediator protein subunit known as Med26 (**figure 1.14**). Knockdown of Med26 leads to a reduction in the amount of SEC associated RNA polymerase II found along the length of the two genes in human cell lines shown using ChIP sequencing. SEC components and the mediator complex can be found at

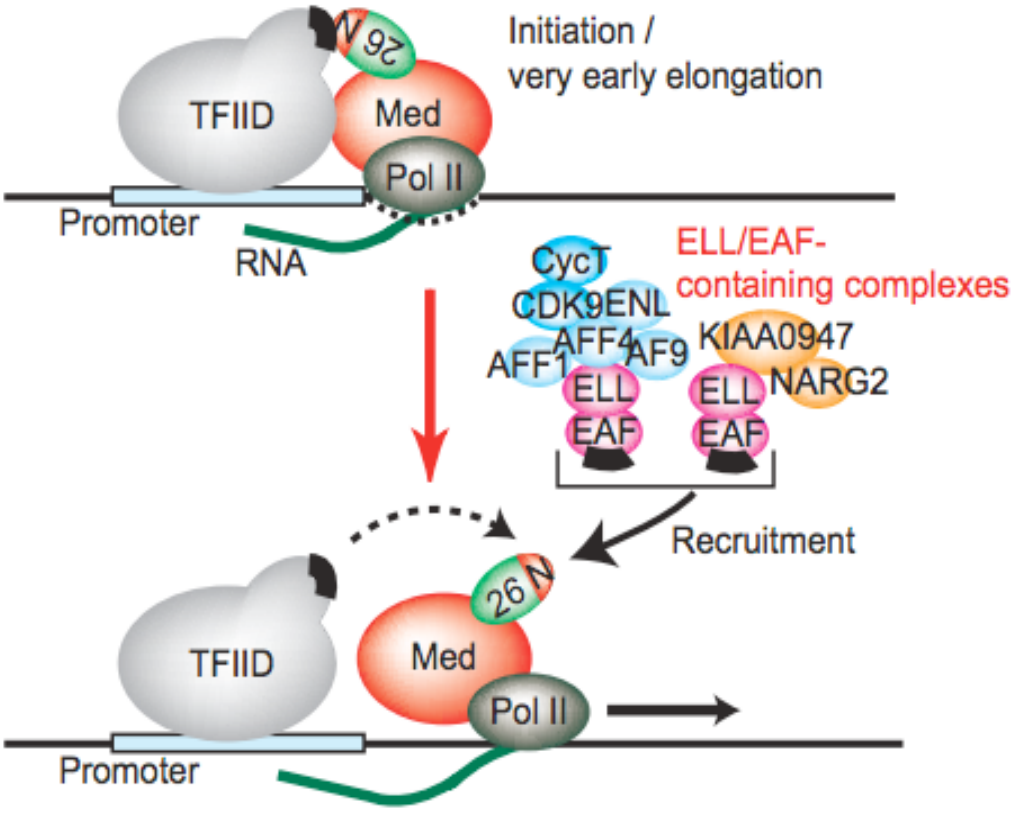

Figure 1.14: Med26 recruits the SEC to RNA polymerase II. The N terminal domain of the mediator subunit Med26 will interact with TFIID associated with paused polymerases at the the promoter region. The induction of certain signals will promote the release of Med26 from TFIID allowing it to associate with the SEC via EAF and allowing positive transcription elongation to occur. Retrieved from reference [200].

the promoter region of hsp70 prior to simulation by heat shock [199]. It was also shown in the same study that the knockdown of Med26 led to a reduction of serine 2 phosphorylation (associated with positive transcription elongation) on both the c-Myc and hsp70 genes indicating that Med26 is necessary not only for the recruitment of the SEC but also the regulation and maintenance of the positive transcription of these genes [199].

The SEC complex combined with the P-TEFb complex is the most common active form of P-TEFb however it is not the only one. P-TEFb can also be found in a complex with bromodomain containing protein 4 (Brd4) capable of directing and promoting the activity of P-TEFb [200, 201]. Brd4 will bind to P-TEFb via its C terminal domain and then will bind to chromatin via the bromodomains found in the N terminal domain. These bromodomains specifically bind to acetylated histone H3 and H4 [202]. This binding will occur at mid-late anaphase before other transcription factors are able to enter the nucleus. These will enter the nucleus at G1 phase of the cell cycle and so this is when transcription of P-TEFb dependent genes will occur [203]. Brd4 is also implicated in the transfer of epigenetic modifications or 'epigenetic memory' due to its ability to bind to chromatin at these early phases of the cell cycle [202].

It is known that both Brd4 and the SEC can associate with P-TEFb to allow it to carry out its function and promote transcription elongation. It is however unclear as to the differences between these two variations in the active form of P-TEFb [204]. Both forms have been shown *in vitro* to be capable of promoting transcription of paused HIV viral genes. The SEC containing P-TEFb in this example is considered the dominant version as the Brd4 containing complex is only capable of promoting a low level of viral gene transcription [201]. Brd4 containing complexes are not always considered as the true active form of P-TEFb. P-TEFb is usually recognized as fully active when it is in a complex with the SEC. It is only in the presence of P-TEFb that rapid induction of transcription can occur. An example of this uses the retinoic acid induced gene Homeobox A1 (HoxA1) [196]. HoxA1 remains in a paused state until retinoic acid is present in the cell. RNAi knockdown of SEC components show a

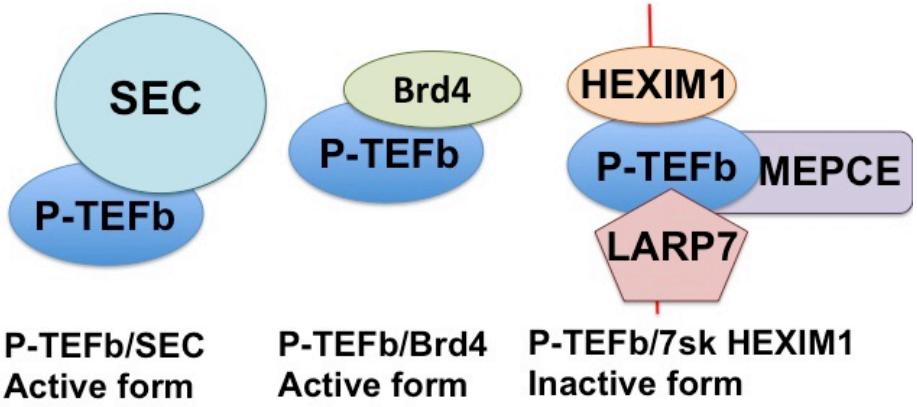

Figure 1.15: The three forms of P-TEFb. All three of the possible forms of P-TEFb shown above can be found at any one time in the cell. On the left is the most commonly found and most active form SEC/P-TEFb. In the middle is another active form which shows less activity, the Brd4/P-TEFb conformation. On the left is the inactive form of P-TEFb found bound to HEXIM and 7SK-snRNP. Retrieved from [205]

dramatic reduction in the transcription of this paused gene however knockdown of Brd4 has very little effect. This gives evidence for the SEC bound to P-TEFb being the dominant form of active P-TEFb [196]. Although it is quite likely that both will cooperate together to provide some redundancy. It is possible to separate out all three of the possible complex combinations associated with P-TEFb from the same cell samples. These complexes are; SEC/P-TEFb, Brd4/P-TEFb and the inactive HEXIM bound 7SK/PTEFb (**Figure 1.15**) [204].

New components of the SEC and other proteins playing a role in polymerase pausing are still being discovered. An example of such proteins includes Gdown1, recently shown by ChIP-seq to associate with paused polymerases across the whole of the human genome. This protein was shown to bind to paused RNA Pol II and stabilize this paused state by promoting the function of negative elongation factors NELF and DSIF [205]. Transcription termination factor TTF2 has recently been shown to associate with exonuclease Xnr2. These two proteins are localized to the start site of paused genes and are thought to promote premature transcription termination. This is because knockdown of these two proteins saw a shift of paused gene transcripts from the start site to the length of the gene body [206].

1.4.5. P-TEFb and the SEC in development and disease

To date P-TEFb has been identified to play a role in many processes including cell differentiation, embryonic development and diseases such as cancer and HIV. The eleven-nineteen lysine-rich leukemia (ELL) component of the SEC is well characterized to associate with the mixed lineage leukaemia (MLL) gene. Mutations in this gene are commonly seen in many childhood leukaemias [207]. These mutations may arise in an MLL fusion protein and it is such fusion proteins which have been found to associate with the SEC [192]. The association of MLL with the SEC allows the misexpression of MLL target genes such as HoxA9 and HoxA10 (**Figure 1.16a**) due to a disruption in regulation of the expression at the transcription elongation checkpoint control (TECC) stage resulting in leukemogenesis [157, 208]. The SEC complex has been implicated in other cancers including ovarian cancer for which, Hexim1 was identified as a possible therapeutic target [209]. Similarly, Hexim1 has been identified as a prognostic marker of breast cancers. Hexim1 is able to bind to the estrogen receptor ERα inhibiting ERα dependent gene expression. Breast cancer patients have been found to have elevated levels of Hexim1 in their breast tissue compared to those with normal breast tissue [210, 211].

One disease model which uses RNA polymerase pausing to regulate gene expression extensively is that caused by the human immunodeficiency virus (HIV). The role of RNA polymerase pausing and transcription elongation in HIV has been well characterized for many years. It was the first system shown to use this transcription regulation and since has proven as a preferred model for further research into polymerase pausing [212, 213]. HIV is a lentivirus, which means that this virus does not rely solely on the host's transcription machinery but will produce its own transcription proteins. In the case of HIV this is the transcriptional transactivator (Tat) protein [212]. Very early experiments were able to show that knockdown of Tat lead to HIV genes stalling close to their promoter region producing only short transcript, representing the phenomena now known as RNA polymerase pausing [213].

It has since been shown that this occurs due to an association of Tat with the P-TEFb component cyclinT1 [214, 215]. Once Tat has associated with P-TEFb, HIV viral genes are transcribed as P-TEFb carries out its normal function of phosphorylating the negative elongation factor and releasing RNA polymerase from its paused state (**Figure 1.16b**) [216]. Brd4, which will normally bind to P-TEFb in the host cell, will compete with Tat for the binding space on cyclinT1. Overexpression of Brd4 in HIV infected cells leads to a reduction in the amount of P-TEFb/Tat complexes and therefore the amount of viral genes transcribed [217]. Affinity purification and mass spectrometry studies have shown that the P-TEFb found bound to Tat is also in a complex with AF4, ELL2, ENL and AF9. From this we can assume that the active P-TEFb used by the HIV is in a complex with the SEC [218, 219].

Paused polymerase II and transcription elongation is not just important for diseases. It is also found in several developmental genes and can therefore be considered to be important in the regulation of transcription coordination of synchronous gene expression during development in certain cell types. So far studies of this have mainly been using embryonic stem cells and *Drosophila* as models [196, 220]. Genome wide studies in embryonic stem cells have revealed that Hoxa genes such as Hoxa1 had paused polymerases at their promoter regions shown using ChIP-seq. This was not seen on other Hox genes such as the Hoxb genes including Hoxb1. The developmental stimulus, retinoic acid caused recruitment of the SEC to the promoter of Hoxa1 and this resulted in rapid transcription. This was not seen for Hoxb1 which underwent relatively slower transcription activation [196].

Both Hoxa1 and Hoxb1 have been shown to regulate the development of cranial neural crest and the hindbrain [221]. Hoxa1 is the most anteriorly expressed Hox gene and its expression appears more rapidly than that of Hoxb1 [222]. Hoxa1 expression is induced in the presence of retinoic acid due to a retinoic acid response element (RARE) found at its 3' end. After its own induction Hoxa1 will bind to the autoregulatory region of the Hoxb1 5' end causing subsequent activation of Hoxb1 transcription [223, 224]. Hoxa1 is therefore a direct target of the

SEC and Hoxb1 expression is a secondary target explaining why a reduction of both genes can be seen after inhibition of Cdk9 in ES cells [196].

This study using retinoic acid stimulation to induce transcription of Hoxa1 also revealed other genes which similarly held a paused pol II at the promoter region and then recruited the SEC to promote rapid transcription. These included the serum inducible genes c-Fos, c-Jun and early growth response gene (EGR), which have previously been implicated to undergo pausing in several studies using mouse and human cell lines [225-227]. c-Fos and c-Jun together form the activator protein-1 (AP-1) complex capable of binding AP-1 sites at the promoter of many genes[228]. In development this has been shown to be important for Spemann organizer gene expression (such as noggin, chordin and goosecoid), hematopoiesis and bone development [229-232].

EGR is a transcription factor, which is important for hematopoiesis [233, 234]. One thing all these developmental genes undergoing pausing have in common is that they are all considered rapidly transcribed genes and are known to be immediate-early transcription factors or primary response genes. These genes are thought to be on the front lines of transcription and will be the first to respond to a given stimulus. It is perhaps because of this paused state, which makes them primed and ready to go within seconds of stimulation [235, 236]. One other gene previously identified to undergo pausing is the transcription factor c-Myc (**figure 1.16c**), which similarly is considered a primary response gene although not due to retinoic acid stimulation like c-Fos, c-Jun and EGR [235]. Rapid c-Myc transcription has been shown to be stimulated by other factors such as the platelet derived growth factor (PDGF) and endothelin [237, 238]. c-Myc is interesting to this study as it has been separately implicated in both RNA polymerase pausing and neural crest development which will be discussed in more detail later [33, 199].

Also as mentioned previously, wild type cells have been shown to have paused polymerases at the promoter regions of heat shock proteins (**figure 15c**) [199]. Heat shock proteins are transcribed in response to stress upon the cell and act to prevent protein denaturation giving the cell

resistance to apoptosis [239-242]. From this it is not surprising that heat shock protein are known to be involved in cancer. HSP27 and HSP70 are highly expressed in many different cancers but are also thought to play a role in promoting tumor cell resistance to many chemotherapeutic drugs [242-244]. Upregulation of these HSPs leads to an upregulation of protooncogene, c-Myc [243]. From a developmental perspective it is also interesting that although upregulated in cancer, heat shock proteins are found to be downregulated in correlation with ageing [245].

Heat shock genes are thought to be held in a paused state due to the presence of a paused polymerase at their promoter region. This pausing is released after stress induction by the recruitment of the SEC with P-TEFb. Studies in ES cells and *Drosophila* have shown that heat shock proteins such as HSP70, HSP26 and HSP27 are all capable of undergoing polymerase pausing [220, 246, 247]. Like other genes found to undergo pausing such as c-Myc and c-fos, heat shock proteins are considered rapidly induced genes [248]. After heat shock stimulation, the heat shock factor 1 (HSF1) transcription factor will recruit P-TEFb to the promoter region by directly interacting with mediator of the SEC. This promotes the phosphorylation of NELF and the CTD of RNA pol II and allows heat shock transcription to occur [249, 250].

Inhibiting the process of transcription elongation by knockdown of the positive transcription components such as cdk9 by molecular methods or by small molecule compound treatment leads to a reduction in transcription of the genes described here to undergo polymerase pausing. However this knockdown of genes is also coupled with an increase in certain gene transcription due to the feedback loops put in place throughout the transcriptome [251]. One example of this seen when overall transcription is inhibited is an accumulation of p53 due to an

in

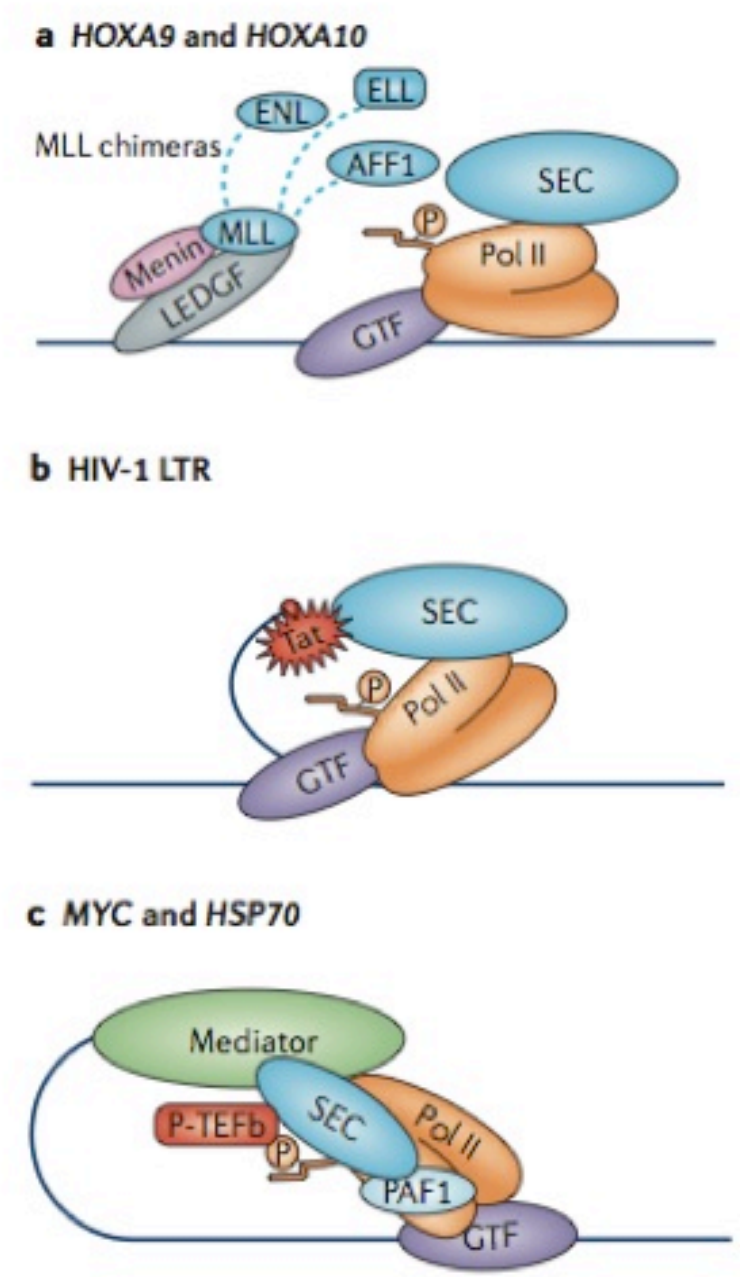

Figure 1.16: Recruitment of the SEC. **a)** In certain leukaemias, chromosomal translocations occur which result in fusion proteins of the mixed lineage leukaemia (MLL) gene and components of the SEC including ENL, ELL and AF1. This results in the release of paused polymerases found on MLL target genes such as HoxA9 and HoxA10 leading to the onset of leukaemia. **b)** The HIV transcriptional transactivator (Tat) protein will bind to the P-TEFb of the SEC found in infected host cells. This promotes the transcription of viral genes. c) Certain wild type genes will also undergo pausing such as c-Myc and Hsp70. These are released from pausing due to the SEC containg P-TEFb. Retrieved from reference [158]

increased level of its transcription and inhibition of feedback loops leading to a reduction in the breakdown of the protein [252-254]. Transcription inhibition leads to an increase in ribosomal proteins such as RPL26, which will bind to human double minute-2 (hdm2), an E3 ubiquitin ligase which normally targets p53 for degradation [255].

1.4.6. The role of c-Myc in transcriptional elongation

Very recently the transcription factor c-Myc has been implicated to play a crucial role in proximal pause release in embryonic stem cells [6]. c-Myc had previously been associated with both the self-renewal of embryonic stem cells and multipotent neural crest cells. One study has shown that myc is able to bind to P-TEFb and is therefore involved in RNA polymerase pause release [33, 256, 257]. c-Myc is now thought to regulate pause release in embryonic stem cell genes by recruiting P-TEFb to RNA Pol II. Inhibiting the function of c-Myc reduces the levels of

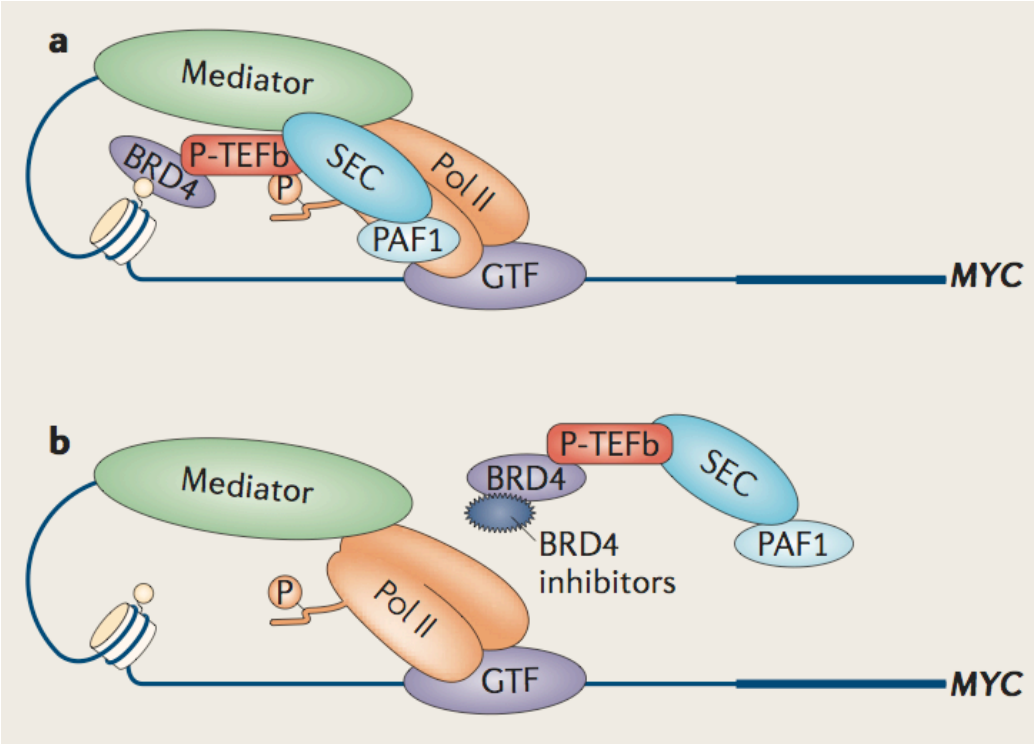

Figure 1.17: Myc undergoes RNA polymerase pausing. (a) In order for the myc gene to be transcribed it must first associate with the active form of P-TEFb in association with the SEC. This occurs as Brd4 will also associate with P-TEFb and attach to the chromatin at the myc promoter region. (b) Possible therapeutic targets of myc overexpressing cancers is Brd4. Inhibitors of Brd4 have been shown to downregulate myc gene expression. Retrieved from reference [158]

Ser2-phosphorylated Pol II and therefore levels of elongation. Ser5-phosphorylation associated with initiation is unaltered and therefore there is no change to the amount of RNA Pol II pausing. The genes predominantly regulated by c-Myc are those found to be most actively transcribed which will undergo more pausing and subsequent elongation [6]. It could be assumed from this that c-Myc is playing a key role in transcriptional elongation in other proliferative cell types. Also the increase in proliferative genes seen in many cancers may be due in part to an increase in the expression of c-Myc. Drugs targeting c-Myc or c-Myc target genes such as Leflunomide may therefore make excellent therapeutics' in a range of cancers [3, 6].

c-Myc itself is also thought to undergo RNA polymerase pausing (**figure 1.17a**). Studies using human ES cells have knocked down the SEC subunit Med26 and Paf1 to show a loss of SEC components along the gene body of both c-Myc and other paused gene Hsp70. RNA pol ll is shown to accumulate at the promoter region of these genes by ChIP-Seq and this results in a reduction of their transcription and therefore their overall mRNA level present in the cells. It also results in a reduction of Ser2 phosphorylation, which is associated with positive transcription elongation. From this study it is hypothesised that c-Myc transcription requires the transcription co-activators Med26 and Paf1 to recruit the SEC to its promoter region [199].

Interestingly, it has been shown that knockdown of Brd4 also leads to a reduction of c-Myc expression. Brd4 is present in the other P-TEFb active complex which is usually associated with basal level transcription. This study was carried out using human acute myeloid leukaemia (AML) cells. It was shown that Brd4 knockdown reduces c-Myc expression and decreases the amount of cancer cell self-renewal [258]. Brd4 was shown to associate with the chromatin at the promoter region of myc. Treatment of the cells with a Brd4 inhibitor (I-BET151) caused a dissociation of Brd4 and the SEC causing a loss of myc expression (**figure 1.17b**) [258]. The same loss of c-Myc after Brd4 knockdown was shown in a separate study using HeLa cells and mouse mammary tumour line, C127. RNAi knockdown of Brd4 reduced c-Myc and c-Jun expression levels (both

early immediate response genes) and reduced the amount of cdk9 present along their gene bodies. These Brd4 knockdown cells were shown to be less proliferative and many cells underwent G_1 cell cycle arrest [203]. These studies suggest that inhibiting myc expression by preventing the function of P-TEFb could be a potential target for cancers overexpressing the myc gene.

1.4.7. CDK9 and cancer; CDK9 as a drug target

Uncontrolled and excessive transcription elongation caused by the abnormal activation of the P-TEFb complex can lead to these diseases described such as leukemia and HIV/AIDS. A greater understanding of the regulation and action of P-TEFb and the SEC will lead to improved therapies for these diseases as very specific variations of the SEC are found in these cell types and therefore targeted therapies could be developed. This also suggests a possibility for the use of CDK9 inhibitors and other inhibitors of transcription elongation in the treatment of cancers including leukemia [157]. Many inhibitors of CDK9 and transcriptional elongation are now in clinical trials for cancer treatment. These include Seliciclib, a cdk9 inhibitor currently in phase II clinical trials for the treatment of non-small cell lung carcinoma [259]. Studies using multiple myeloma cells have shown that CDK9 inhibition by Seliciclib causes a downregulation of anti-apoptotic factor Mcl-1 resulting in an increased amount of apoptotic cancer cells [260, 261].

Another example is the drug Alvocodib also known as flavopiridol. Flavopiridol is commonly used in genetic studies as it is known to inhibit CDK9. It is therefore often used as a tool to inhibit transcriptional elongation [262]. It is currently in human clinical trials for cancers including many B-cell lymphomas and ovarian carcinomas [263, 264]. Similarly to Seliciclib, flavopridol has been shown to down regulate Mcl-1 resulting in tumour cell apoptosis [263]. Since the discovery of flavopiridol many other CDK9 inhibiting compounds have been compared to it. There are now known to be compounds with even greater specificity for cancer cells and lower toxicity than flavopiridol. The compound CDKI-71 is

another CDK9 inhibitor that has been shown to be more specific for leukaemia cell lines and not normal B or T cell lines when compared to flavopiridol [265].

Cancer therapies targeting CDKs are now moving away from those involved in cell cycle and towards those involved in transcription regulation such as CDK9. Cancer cells seem more sensitive to these compounds and will undergo apoptosis more readily than wild type cells. One issue often faced when using compounds, which target CDK9, is the large amount of off target effects that can occur [266]. This often occurs due to the high similarity between the CDK drug target sites. Drugs which target CDK9 are often found to target CDK2 as well which is a CDK functioning solely in the cell cycle making these compounds more toxic to normal as well as cancer cell types. It is now thought that compounds with high specificity for CDK9 alone rather than general CDK inhibitors, will be more useful for cancer therapy [267].

Compounds which limit the available nucleotides present for RNA transcription may also inhibit transcriptional elongation. Genes undergoing polymerase pausing have been shown to be more sensitive to such compounds. One compound previously mentioned to have this effect is Leflunomide. This was shown in Zebrafish and *Xenopus* embryos to decrease the amount of neural crest derivatives such as melanophores and also to decrease the cell viability of the melanoma cell line A375 [3]. Subsequent to these studies Leflunomide is now in clinical trials for human melanoma treatment. Further studies treating A375 cells with leflunomide have identified the aryl hydrocarbon receptor as a target of leflunomide, mediating its anti-proliferative affects on melanoma cells [268]. Following on from the success of using leflunomide to treat melanoma its effects on other cancer types, for example human medullary thyroid cancer, are now being investigated [269].

1.5 Aims

Using leflunomide as a tool to inhibit transcriptional elongation I aim to show the importance of this process during neural crest specification. It has already been shown from the work of our lab and the Zon lab that leflunomide's action inhibits the transcriptional elongation of c-Myc target genes in Zebrafish and melanoma cell lines [3]. It has also been shown that c-Myc plays an important role in initiating the transcription of genes required for neural crest specification [33]. I aim to show that administration of leflunomide on *X.laevis* embryos is capable of preventing expression of various neural crest specifying genes such as Slug, Sox10 and FoxD3 and c-Myc. This will implicate the importance for transcriptional elongation during neural crest development. It is quite likely that this would be the case as transcriptional pausing and subsequent elongation has already been shown to regulate genes associated with embryonic stem cell pluripotency [6]. We would hypothesise that this would also be the case for neural crest cells as these share this same stem-cell like multipotent potential. Genes involved in neural crest cell specification must be tightly regulated to prevent improper differentiation and so transcriptional pausing would prevent the transcription of such genes keeping their multipotent potential. I therefore aim to investigate this process in neural crest cells by inhibiting the function of P-TEFb by morpholino knockdown of components of the P-TEFb complex, Cdk9 and CyclinT1 or the use of inhibitors. Inhibiting P-TEFb function in the *Xenopus* embryo will allow me to investigate the effect of inhibiting transcriptional elongation on neural crest specific genes to show that transcription regulation at this level is important for neural crest specification.

Chapter II

Materials and Methods

2.1 Obtaining Embryos

Females were primed 5-10 days before eggs are required with 100 units of PMSG (pregnant mare serum gonadotrophin). To induce ovulation primed female *Xenopus laevis* were injected with 500 units of human chorionic gonadotrophin (hCG) into their dorsal lymph sac and stored at 18^{o}C. Eggs were then be collected 14-16 hours prior to this. To obtain eggs, the abdomens of the frogs were manually squeezed over a clean petri dish. Testes were isolated from a euthanized male frog and placed in testes buffer. A piece of masticated testes was first swiped gently over the eggs then crushed with 1ml of high salt solution, 1xMMR and distributed over the collected eggs and left for 5 minutes at 18^{o}C. 0.1xMMR was then be added to the eggs and left for 20 minutes at 18^{o}C. After fertilisation, the jelly coat which encases the eggs was removed. For this they were added to a 250ml beaker containing 2% L-cysteine (Sigma, UK) pH 8.0 dissolved in 1XMMR. Swirling the eggs in this solution gently removed the jelly. Eggs were then washed in 1X MMR then 0.1XMMR to remove cysteine. Embryos were then left to develop until they reach the required stage according to Niewkoop and Faber 1967.

Solutions

- 0.1XMMR: 10mM NaCl, 0.2mM KCl, 0.1mM $MgCl_2$,0.2mM $CaCl_2$, 0.5mM HEPES (pH 7.5)
- 1XMMR: 100mM NaCl, 2mM KCl, 1mM $MgCl_2$, 2mM $CaCl_2$, 5mM HEPES (pH 7.5)
- Testis Buffer: 80% fetal calf serum, 20% 1x MMR, gentamycin (Sigma 1:1000u)
- PMSG (Intervet): 100U/ml PMSG prepared in solvent and stored at 4^{o}C
- Chorulon (Intervet): 1000U/ml Chorulon prepared in solvent and stored at 4^{o}C

2.2 Fixing Embryos

Once *Xenopus* embryos or animal caps reached their desired stage (depicted by Nieukoop and Faber 1967) they were fixed. The embryos were fixed using MEMFA (3.7% formaldehyde (Sigma, UK), 1x MEM salts made up with DEPC H_20). They were then left at room temperature for 1 hour or overnight at 4^oC, washed 3 times in PBST and then left at 20^oC for storage in 100% methanol (Sigma UK).

2.3 Preparation of competent cells

A 5ml culture of DH5α *e.coli* was grown overnight in Luria Broth (LB) at 37^oC and shaking at 200 rpm. 1ml of this culture was added to 200ml of LB and grown at 37^oC with shaking until optical density (OD) at 600nm reaches 0.3 to 0.4. At this point the culture was divided into 4x 50ml falcon tubes and put on ice for 15 minutes. The cells were centrifuged at 4^oC for 10 minutes at 2000rpm. The supernatant was discarded and the bacterial pellet was resuspended in 16mls of filter sterilised TB I buffer. Cells were put on ice for 15 minutes then centrifuged at 4^oC and 2000 rpm for 10 minutes. The supernatant is discarded and the pellet was resuspended in 4mls of filter sterilised TB II. Aliquots are stored at -80^oC.

Solutions

- TB I pH 5.8: $RbCl_2$ 0.1M, $MnCl_2H_2O$ 0.068M, $CaCl_2$ 0.01M, 1M KAc pH 7.5, 37.5ml Glycerol adjust to 250ml and pH using 0.2M HAc
- TB II: MOPS 0.5M pH 6.8, $RbCL_2$ 0.01M, $CaCl_2H_2O$ 1.04M, 37.5ml Glycerol adjust to 250ml aliquoted and stored at -80^oC.

2.4 Transformation

1µl of plasmid was added into 100µl of competent E.coli cells and left on ice for 30 minutes. These were heatshocked at 42^oC for 90

seconds to open the cells and allow the plasmid to enter followed by 5 minutes on ice. 300µl of LB media was added and cells are left for 1 hour at 37^{o}C to allow growth. 200µl of ligated cells were plated out onto agar and LB plates containing the correct antibiotic. These were left at 37^{o}C overnight to allow colonies to form. For blue/white selection 40µl Xgal (20mg/ml in DMF) and 4µl IPTG (200mg/ml dH_2O) was added to the agar and LB plate.

2.5 DNA Mini prep

Colonies from the transformation were taken to be incubated in 5ml LB/carbicillin liquid media overnight at 37^{o}C with rocking. The DNA plasmid was then isolated using the Qiagen mini plasmid purification kit (Qiagen, UK) according to manufacturers instructions. 1µl of the final product was run on agarose gel by electrophoresis and analysed using a Nanodrop to determine DNA concentration

2.6 DNA Midi prep

Colonies from the transformation were taken to be incubated in 50ml LB/carbicillin liquid media overnight at 37^{o}C with rocking. The DNA plasmid was then be isolated using the Qiagen Hi-speed plasmid purification kit (Qiagen, UK) according to manufacturers instructions. 1µl of the final product was run on agarose gel by electrophoresis and analysed using a Nanodrop to determine DNA concentration.

2.7 Capped RNA synthesis

10µg of plasmid DNA was digested using 5µl buffer, 2µl restriction enzyme (Xba1 for Wnt and Not1 for Noggin) made up to 50µl with RNAse free water. This was left at 37^{o}C for 2 hours and purified using a Qiagen PCR purification kit according to kit instructions. The linearised DNA was

then analysed using a Nanodrop to determine the concentration. For capped RNA synthesis 1µg linearised DNA, 10µl NTP/CAP, 2µl buffer, 2µl SP6/T7 RNA polymerase and made up to 20µl with RNAse free water. This was left for 2 hours at 37^{o}C. 1µl of Turbo DNAse was added for 15 minutes at 37^{o}C. 1µl of this was run on a gel. The capped RNA then underwent lithium chloride purification and was made into 1ng/10nl stocks used to make 10µl aliquots. The plasmids used are shown in **table 1.1**

Table 2.1 Plasmids used to make capped RNA

Clone name	**Sense RE**	**Sense polymerase**	**Source**
Noggin	Not1	Sp6	Dr Dave Hsu
Wnt1	Xba1	Sp6	Dr Oliver Destree
Lac-Z	Not1	Sp6	Dr Maggie Walmesly
c-Myc	Not1	SP6	Dr Carol Labonne
Cdk9-a Mutant	Asc1	Sp6	Synthesised
Cdk9-b Mutant	Asc1	Sp6	Synthesised
CyclinT1 Mutant	Asc1	Sp6	Synthesised

2.8 Animal cap assay

Embryos were injected at the one cell stage with either Noggin alone to induce neuroectoderm or Noggin and Wnt. Non-injected embryos will give caps with ectodermal cell fate (**figure 2.1**). These were left to develop to stage 9 when animal caps can be cut. Caps are cut in filter-sterile 1XMMR. The vitelline membrane was removed using sharp forceps and the cap was cut from the center of the animal hemisphere. Caps were transferred to 12 well dishes containing 0.7XMMR, 1mg/ml Bovine serum albumin (Fischer, UK) 100µg/ml gentamycin (Sigma, UK) and either DMSO (Sigma, UK) for controls or 60µM leflunomide (Sigma

UK). Caps were kept at a constant temperature until they reach stage 18 when they will either undergo RNA extraction or *in situ* hybridisation.

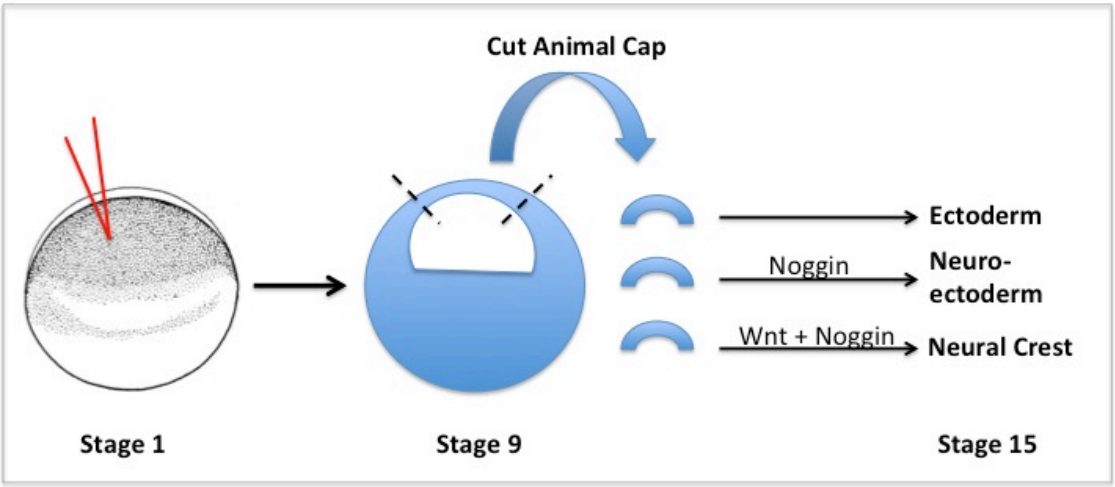

Figure 2.1: Animal cap assay. Embryos are injected at the one cell stage and left to develop to stage 9 when they undergo animal capping. These caps can then be placed in either DMSO or leflunomide and left to develop until stage 18 when they will undergo *in situ* or RNA extraction.

2.9 RNA extaction

Animal tissue was placed in a 1.5ml eppendorf tube and all fluid was removed from animal tissue and then flash frozen on dry ice for 15 minutes. 1ml of TRIzol was then added and left on ice for up to 1 hour. The tissue and TRIzol was then vortexed until all tissue is broken down to leave a homogenous solution. RNA is stable in TRIzol as it deactivates RNases so at this step the solution can be stored in a -80^{o}C freezer until needed. Next, 0.5ml of chloroform was added to the trizol, shaken for 15 seconds and incubated at room temperature for 5 minutes. The tubes were then spun at max speed at 4^{o}C for 20-40 minutes. After this tubes were immediately placed on ice and the aqueous upper phase was put into a new tube. To this 500μl of isopropanol (Fischer, UK), 50μl 5M NaCl and 2μl of glycogen (Roche, UK) was added. This was quickly vortexed and incubated for 10 minutes at room temperature before spinning at max speed for 30 minutes at 4^{o}C. The supernatent was removed and discarded and the RNA pellet was washed with 70% ethanol prepared in RNase free water. This was spun at max speed at 4^{o}C again for 10

minutes and the ethanol was removed and the pellet dissolved in 45μl of RNase free water ready for DNase treatment.

2.10 DNase treatment

10x DNase I buffer (Roche, UK) was added to each RNA sample so final concentration is 1x. 1μl of DNase I (Roche, UK) was then added and incubated at 37^{o}C for 30 minutes. To this 50μl of RNase free water was added so sample final volume is 100μl. 100μl of acidic phenol/chloroform was then added, tubes are inverted for 10 seconds 3 times and then spun at max speed at 4^{o}C for 40 minutes. The aqueous phase was transferred to a clean 1.5ml eppendorf tube. 70μl of isopropanol (Sigma, UK) and 7μl of 5M NaCl was added and tubes are quickly vortexed before spinning at max speed for 30 minutes at 4^{o}C. The supernatant was removed and the pellet washed with 75% ethanol (Sigma, UK). This was centrifuged again at max speed for 10 minutes at 4^{o}C. The pellet was air dried and resuspended in 20μl of RNase free water. Concentration was determined using a Nanodrop.

2.11 cDNA Preparation

To synthesise cDNA for PCR, 1μg of RNA, 0.5μl of oligo-dT (Sigma, UK) was made up to 12.5μl with H_20 and left at 65^{o}C for 10 minutes to denature the RNA structure and then put onto ice to stop renaturing. To this 4μl of 5x RT buffer, 0.5μl of RNAsin (Roche, UK), 2.5μl of 10mM dNTPs and 0.5μl RT (Roche, UK) was added and left for 30 minutes at 65^{o}C. To synthesise cDNA for qRT-PCR, 1μg RNA, 1μl random hexamers (Sigma, UK) were made up to 11μl with RNAse free water and left at 70^{o}C for 10 minutes. 4μl 5x first strand buffer (Sigma, UK), 2μl DTT (Sigma, UK), 1μl dNTP (Roche, UK), 1μl RNAsin (Roche, UK) and 1μl superscript II (Sigma, UK) were added for 1 hour at 42^{o}C. cDNAs were diluted 1:20 to give a final concentration of 10ng/μl.

2.12 PCR

The reaction mixture was as follows; 12.5µl of Bioline Taq mix (Bioline, UK), 1µl cDNA as a template, 2µl of forward primer, 2µl reverse primer made up to 25µl with RNAse free Sigma water. The reaction conditions were 95^{o}C for 3 minutes, 25-35 cycles (specific for each primer set) of 95^{o}C for 30 seconds, 50-60^{o}C temperature gradient for 1 minute, 72^{o}C for 2 minutes and one final 72^{o}C for 10 minutes. 5µl samples were then analysed by agarose gel electrophoresis and visualised using ethidium bromide under UV.

2.13 qRT-PCR

The reaction mixture used was as follows; 10µl cDNA, 0.5µl of each primer (forward and reverse), 8.5µl SyberGreen (Applied biosystems, UK) and 0.5µl RNAse free water. The reaction conditions 50^{o}C for 2 minutes, 95^{o}C for 10 minutes 95^{o}C for 15 seconds cycled 40 times and 60^{o}C for 1 minute. Amplification curves were analysed using 7500 sequence detection software.

2.14 Primers used

Table 2.2 Primers used

Name	Forward primer	Reverse primer
FoxD3	TCTCTGGGGCAATCACACTC	GTACATTTGTTGATAAAGGG
Slug	TCCCGCCACTGAAAATGCCACGATC	CCGTCCTAAAGATGAAGGGTATTCCTG
Sox2	GAGGATGGACACTTATGCCCAC	GGACATGCTGTAGGTAGGCGA
Brachyury	GCTGGAAGTATGTGAATGGAG	TTAAGTGCTGTAATCTCTTCA
Keratin	CACCAGAACACAGAGTAC	CAACCTTCCCATCAACCA
Histone H4	CGGGATAACATTCAGGGTA	TCCATGGCGGTAACTGTC

2.15 Restriction digest

Clones within plasmids were linearised by restriction digest using the appropriate restriction enzyme for each plasmid. 2-10µg of plasmid was added to 2µl of the appropriate enzyme, 5µl of the optimal buffer for the enzyme and then made up to 50µl with sigma H_2O. This is left at 37^{o}C for a minimum of 2 hours or a maximum of overnight. The cut plasmid can be visualised on an agarose gel.

2.16 Ethanol precipitation

Digests were purified by ethanol precipitation. 1:10 volumes of 0.3M sodium acetate and 250µl of absolute ethanol were added to a 50µl digest. This is left overnight at -20^{o}C. This was then centrifuged for 15 minutes at 14000 rpm. The supernatant was removed and the pellet was washed using 400µl of 70% ethanol and spun for 5 minutes at 14000 rpm. The ethanol was then removed and the pellet left to air-dry at room temperature. The pellet was then resuspened in 20µl of sigma H_2O and stored at -20^{o}C.

2.17 Agarose gel electrophoresis

Agarose (Sigma, UK) gels were made at a 2% concentration. 1g of agarose was dissolved in 50mls of 1x TAE buffer by warming. Ethidium bromide (Sigma, UK) was added to the gel at a concentration of 0.5µg/ml to visualize DNA or RNA using a UV trans-illuminator (BiO-RAD) following electrophoresis. Samples were mixed with 1/10 volume of 10x DNA loading dye before loading onto the gel. Electrophoresis was carried out at 70 volts for 65 minutes.

2.18 Probe synthesis

Plasmids containing a gene of interest were linearised using the appropriate restriction enzymes to digest at restriction sites to give antisense and sense RNA probes. Linearised DNA was purified before probe synthesis. For probe synthesis the following reaction mixture was used; 4µl 5x transcription buffer (Sigma, UK), 2µl DTT (Sigma, UK), 1µl digoxygenin (DIG) or Fluorescein labelled UTPs (Roche, UK), 1µl RNAsin, 1µl linearised DNA, 2µl RNA polymerase (Roche, UK) made to a final volume of 20µl with dH_2O. This was incubated at 37^{o}C for 3 hours. Any remaining DNA template was removed by adding 1µl of DNase I (Roche, UK) and incubating for 30 minutes at 37^{o}C. The probe was then run on a 2% agarose gel and visualised in a UV transmitter (BiO-RAD). Plasmids used to make probes are shown in **table 2.3**

Table 2.3 Plasmids used to make probes

Clone name	Sense RE	Antisense RE	Sense Polymerase	Antisense Polymerase	Source
Sox2	Not1	EcoR1	Sp6	T7	Prof Yoshiki Sasai
Slug	Xho1	Bgl2	T7	Sp6	Dr Michael Sargent
Sox10	Xho1	EcoR1	T7	T3	Prof Jean-Pierre Saint-Jeannet
FoxD3	Not1	BamH1	Sp6	T7	Prof Yoshiki Sasai
c-Myc	Not1	EcoRV	Sp6	T7	Image Clone from Source Bioscience
Zic1	NS	EcoR1	NS	T3	Dr Jung Aruga
Zic3	Hind III	BamH1	T7	T3	Dr Jung Aruga

Pax3	NS	NS	Bgl2	Sp6	Dr Michael Sargent
Sox9	Sac1	Nco1	T7	Sp6	Dr Karen Chambers
Cdk9-a	Not1	Sal1	Sp6	T7	Image Clone from Source Bioscience
Cdk9-b	NS	Nde1	NS	T7	Dr Paul Mead
CyclinK	NS	Nco1	NS	Sp6	Dr Paul Mead
CyclinT2	NS	Nde1	NS	T7	Dr Paul Mead
CyclinT1	Not1	EcorR1	Sp6	T7	Image Clone from Source Bioscience
Runx1	Xho1	T3	EcoR1	T7	Prof Jean-Pierre Saint-Jeannet,
Islet-1	Xho1	T3	EcoR1	T7	Prof Jean-Pierre Saint-Jeannet
Ngnr-1	NS	NS	BamH1	T3	Prof Jean-Pierre Saint-Jeannet
Tbx2	NS	NS	BamH1	T7	Prof Jin-Kwan Han
Elrd	NS	NS	Xho1	T3	Dr Michela Ori
NeuroD	NS	NS	Xho1	T3	Dr Michela Ori

NS = Not synthesised

2.19 Purification of probes

Probes were purified by adding 30µl of Sigma H_2O and putting it through an illustra MicroSpin G-50 Column (GE healthcare life sciences) according to manufacturers instructions. 5µl of probe was run on a 2% agarose gel to check probe quality. 5µg of purified probe was added to 5-

10ml of hybridisation buffer depending on probe quality and stored at -20°C.

2.20 Whole mount in situ Hybridisation

Embryos were rehydrated from 100% methanol by using 100%, 75%, 50%, 25% methanol (Sigma, UK) and phosphate buffered saline with 0.1% Tween (PBST) for 5 minutes each followed by 2 PBST washes for the same time, all with rocking at room temperature. Embryos were then treated with 10µg/ml Proteinase K (Sigma, UK) for varying times depending on the embryo stage (e.g. *Xenopus* stage 38-10minutes, stage 25-4minutes and stage 10.5-1minute). *Xenopus* embryos were then washed twice in PBST for 5 minutes and incubated in 3.7% formaldehyde/PBST (Sigma, UK) for 20 minutes with rocking at room temperature after which they were washed 3 times in PBST for 5 minutes and incubated in hybridisation buffer at 60°C for 2-6 hours. After this the embryos were placed in fresh hybridisation buffer and the appropriate probe and incubated overnight at 60°C.

Probes were removed and stored at -20°C and embryos were washed with fresh hybridisation buffer for 10 minutes. *Xenopus* embryos undergo 3 washes in 2x Sodium Chloride and Sodium Citrate solution (SSC) for 20 minutes and 2 washes in 0.2x SSC for 30 minutes, all at 60°C. Embryos were then washed twice in Maleic acid buffer with 0.1% Tween (1xMABT) for 30 minutes at room temperature and then put into a 1xMAB and 2% Boerhinger Mannhein Blocking (BMB) solution (Fischer, UK) for 1 hour at room temperature with rocking. BMB solution was replaced with antibody solution containing anti-deoxygenin (Promega, UK) 1:2000 and incubated overnight at 4°C with rocking.

Antibody solution was removed and embryos are washed in 1xMABT 5 times for 60 minutes each at room temperature with rocking and incubated in a sixth MABT wash overnight at 4°C with rocking. The colour reaction is then carried out by firstly washing the embryos in freshly made alkaline phosphate buffer twice for 5 minutes at room

temperature with rocking. Embryos were then put in NBT/BCIP in alkaline phosphate buffer (67.5µl NBT, 52.5µl BCIP made up to 15ml with alkaline phosphate buffer) until the desired level of colour was seen. Embryos were then put in 5xTBST solution overnight if needed to remove background colour and then photographed.

For double *in situ* hybridisation after TBST washes embryos underwent 2x 5 minute PBST washes then embryos were fixed in MEMFA for 1 hour at room temperature. Embryos then underwent 2 further 5 minute PBST washes at room temperature then a 1 hour wash in MABT at 65^{o}C to deactivate any DIG antibody still present. After this embryos were washed twice in MABT for 5 minutes, for an hour in 2% BMB and then 2 hours in 2% BMB with 20% goat serum (Fischer, UK) all at room temperature. BMB and goat serum solution was replaced with antibody solution containing anti-Flourescin (Promega, UK) 1:1000 and incubated overnight at 4^{o}C with rocking.

Antibody solution was removed and embryos were washed in 1xMABT 5 times for 60 minutes each at room temperature with rocking and incubated in a sixth MABT wash overnight at 4^{o}C with rocking. The embryos were then washed twice for 5 minutes with alkaline phosphate buffer then colour reaction is carried out by adding Fast Red solution (Sigma, UK). When colour reaction is complete the reaction was stopped with a 5 minute MABT wash followed by 2 PBST washes all at room temperature then the embryos were left overnight in TBST. After this embryos were fixed in MEMFA for 1 hour at room temperature.

Solutions

- Alkaline Phosphatase Buffer: 100mM Tris (pH 9.5), 50mM $MgCl_2$, 100mM NaCl, 0.1% Tween 20
- Antibody solution: 2% BMB, 20% goat serum, anti-DIG Fab fragment, (1:2000 dilution) in 1X MAB
- BCIP: 50mg/ml in 100% DMF
- Blocking solution: 2% BMB in 1X MAB

- BMB (Boehringer Mannheim Blocking agent) 10%: 10% (w/v) in BMB preheated (50^{o}C) 1XMAB, stirred until dissolved and then autoclaved, aliquoted and stored at –20^{o}C
- Hybridisation buffer: 50% formamide, 5XSSC, 1mg/ml Torula RNA, 100μg/ml Heparin, 1X Denharts solution, 0.1% Tween 20, 0.1% CHAPS, 10mM EDTA
- MAB 1X (Maleic Acid Buffer): 100mM Maleic acid; 150mM NaCL (pH 7.5)
- MEMFA: 10% MEM salts, 10% formaldehyde
- MEM salts: 0.1M MOPS, 2mM EGTA, 1mM $MgSO_4$, pH7.4
- NBT (Nitro Blue tetrazolium): 75mg/ml in 70% dimethylformamide (DMF)
- PBS 10X: 2.5g $NaH_2PO_4.H_2O$, 11.94g $NaHPO_4.H_2O$, 102.2g NaCl, 400ml DEPC dH_2O. pH adjusted to 7.4 and volume to 1 litre
- PBST: 1XPBS, 0.1%Tween 20
- Proteinase K (10μg/ml): 1μl proteinase K, 1ml PTw
- SSC 20X: 175.3g NaCL, 88.2g Sodium citrate. pH adjusted to 7.0 and volume to 1 litre with DEPC H_2O
- TBST: 125ml 1M Tris pH 7.5 40g NaCl, 1g KCl made up to 450ml with dH_20. Autoclave then add 50ml Tween-20
- Fast Red Solution: SIGMA*FAST*™ Fast Red TR/Naphthol AS-MX Tablets dissolved in 10ml alkaline phosphate buffer

2.21 Bleaching

Some embryos were bleached to effectively observe *in situ* staining. For this embryos were placed in a solution of 8.95ml DEPC H_2O, 300μl 30% H_2O_2 (Sigma, UK), 500μl formamide (Fischer, UK) and 250μl 20xSSC and incubated on a light box for 1 hour. After bleaching the embryos were washed twice for 5 minutes in PBS and fixed in MEMFA overnight at 4^{o}C

2.22 Cryosectioning

Embryos were fixed in MEMFA for 1 hour, washed twice for 5 minutes in PBST and then put in 30% sucrose (Fischer, UK) for 4 hours all at room temperature with rocking. Embryos were then transferred to cryomoulds filled with optimal cutting temperature (OCT) compound and left at 4^{o}C overnight. After this, embryos were positioned appropriately for sectioning and left at -20^{o}C overnight. Embryos were sectioned using the LEICA CM 1950 Cryostat and sections were placed on 5% TESPA slides overnight at 37^{o}C. Slides were then washed for 5 minutes in PBST and for 5 minutes in PBS after which they were covered with a coverslip using hydromount and left overnight to dry before use. Images were taken using a Zeiss CCD upright microscope with colour camera.

2.23 In vitro translation using ^{35}S labelled probe

Carried out using the TNT® Coupled Reticulocyte Lysate System (Promega, UK) following manufacturers instructions. The reaction was incubated at 30^{o}C for 90 minutes. 2.5μl of a 25μl radiolabelled protein reaction was added to 1x SDS loading buffer boiled at 80^{o}C for 3 minutes and run on a 12% SDS-polyacridamide gel by electrophoresis in a Mini-PROTEAM®3cell (BIO-RAD) system containing running buffer. The gel was fixed using a fixing buffer for 30 minutes on a shaker then put into drying buffer for 5 minutes. The gel was then dried for 90 minutes at 80^{o}C onto whatmann paper using a Model 583 gel dryer (BIO RAD) and a HydroTech^{TM} vacuum pump (BIO RAD). This was then exposed onto a phosphoimager screen and visualised on a phosphoimager (BIO-RAD).

Solutions

- Fixing buffer: 50% methanol, 10% glacial acetic acid, 40% dH_20
- Drying buffer: 7% acetic acid, 7% methanol, 1% glycerol, 85% dH_20
- TG buffer: 30g Tris, 144g Glycine make up to 1L with dH_2O pH to 8.3

- Runnning buffer: 100ml TG buffer, 10ml 10% SDS, 890ml dH_2O
- 5x SDS loading buffer: 20.83ml 1.5M Tris pH 6.8, 10g SDS powder, 25ml Glycerol, 750μl 2% Bromophenol blue (in EtoH), 5ml 0.1M DTT, make up to 100ml with dH_20. Dilute with sigma H_20 to 1x concentration when needed.

2.24 Microinjection, morpholinos used and β-galactosidase detection

Embryos undergoing microinjection were placed in 3% Ficoll PM400 (Sigma, UK). One or both blastomeres were injected into the animal pole at the 2-cell stage using a 10nl calibrated needle and oxygen free nitrogen was used with a Harvard apparatus injector (Medical Systems Research products). The injector is set up at P_{out} =90 $P_{balance}$=0.6 and P_{inject}=16. For rescue experiments embryos were injected twice into the animal pole of one blastomere to obtain the correct amounts of morpholino and mRNA injected. 2 hours after injection the Ficoll was removed from the embryos and replaced with 0.1x MMR/gentamycin (1:1000) and left to develop at 18^{o}C.

Antisense morpholino oligonucleotides (MOs) used in these studies were designed and synthesised by Gene Tools. The sequence of the morpholinos are shown in **table 2.4**. Morpholinos underwent in vitro translation before use to confirm activity and specificity.

Table 2.4 Morpholino target sequences

Morpholino name	Target sequence
Standard control (CMO)	5'-CCTCTTACCTCAGTTACAATTTATA-3'
Cdk9-a	5'-ATGGCCAAGAACTACGACTCGGTGG-3'
Cdk9-b	5'-ATGGTAAAGAACTACGACTCTGTTG-3'
CyclinT1	5'-GACATCGTACTTTATGGCAACAAAC-3'

Morpholino stocks and working stocks are stored at room temperature. If frozen they must be heated at 65^{o}C before use for 10 minutes. If lineage tracing is required morpholinos are placed on ice and 1μl Lac-Z capped RNA was added and these samples were stored on ice. MOs were coinjected with 300pg of Lac-Z mRNA. β-galactosidase activity was detected using Red-gal (Sigma, UK) as a substrate. For this embryos were washed 3 times in 1x PBS for 5 minutes then fixed for no more than 1 hour at RT in MEMFA. Embryos were rinsed 3 times in 1x PBS then Red-gal solution is added at 37^{o}C until red staining is seen. When staining is complete embryos were fixed again in MEMFA for 1 hour at room temperature.

Solutions

- 3% Ficoll: 6g Ficoll PM400, 60ml 1xMMR, 140ml dH_2O
- Red-gal: 2.5ml 0.1mM $K_3Fe(CN)_6$, 2.5ml 0.1mM $K_4Fe(CN)_63H_20$, 2.5ml 20mg/ml Red-gal solution, 0.1ml of 1M $MgCl_2$ made up to 50ml with 1x PBS

2.25 RNA sequencing

RNA sequencing was carried out on 6 animal cap samples. RNA was extracted by TRIzol method and DNAse treated as mentioned previously. Each of the 6 samples contained 3 biological replicates tested individually by PCR to detect expected gene expression. Samples contained 2-4μg of RNA in 30μl of RNase free H_20. RNA samples were sent to the High-Throughput Genomics Group at the Wellcome Trust Centre for Human Genetics Oxford, for library preparation.

Total RNA was fragmented before undergoing cDNA library preparation. cDNA was end-repaired, A-tailed and adapter-ligated before amplification and size selection. The prepared libraries undergo quality control by running on a gel and using a bioanalyser to check library fragment size distribution before 100bp paired end sequencing over one lane of a flow cell. Samples were multiplexed 2 x 3 and run on one lane each to yield approximately 25 million paired reads per sample. Data

were aligned to the reference genome of Xenopus laevis to be quality checked.

Samples were aligned to the *Xenopus laevis* transcriptome (xlaevisMRNA.fasta) downloaded from Xenbase. Mapping was carried out with bowtie2 on paired-end samples using default parameters. A custom Perl script was used to parse the bowtie results and count the number of sequences in each sample mapping to every mRNA sequence in the transcriptome file. The table of raw abundances for each mRNA was then read into R and differential expression between untreated and leflunomide treated samples was calculated using the Deseq package. Any mRNA with a p-value of <= 0.05 was classed as being differentially expressed between untreated and leflunomide treated samples.

2.26 Site directed mutagenesis

Mutagenesis primers were designed for Cdk9a, Cdk9b and CyclinT1. The sequences for these are shown in **table 2.5.** Mutations are highlighted in yellow. All primers were FPLC purified.

Table 2.5 Mutagenesis primers

Name	Mutagenesis Primer
Cdk9a Forward	5'-ccccctccttccgccatggccaaaaattatgattcggtggaattcc-3'
Cdk9a Reverse	5'-ggaattccaccgaatcataatttttggccatggcggaaggaggggg-3'
Cdk9b Forward	5'-agccccctccttccgccatggtaaaaaattatgattctgttgaattcccttattg-3'
Cdk9 Reverse	5'-caataagggaattcaacagaatcataatttttaccatggcggaaggaggggct-3'
CyclinT1 Forward	5'-gcaaggacttggcacagacatcatatttcatggcgacaaacagcttacatttgacca-3'
CyclinT1 Reverse	5'-tggtcaaatgtaagctgtttgtcgccatgaaatatgatgtctgtgccaagtccttgc-3'

Mutations marked in yellow

The mutagenesis PCR reaction was set up as follows; 5µl 10 x Pfu polymerase buffer (Agilent technologies, UK), 4µl 10mM dNTPs, 0.2µl forward primer, 0.2µl reverse primer, 10µg plasmid DNA, 2µl Pfu polymerase (Agilent technologies, UK) make up to 50µl with Sigma H_2O. The PCR reaction conditions used were 94^oC for 60 seconds then 12 cycles of 94^oC for 30 seconds, 55^oC for 30 seconds and 68^oC for 12 minutes. The PCR reaction was cooled to room temperature and 1µl of DpnI (Agilent technologies, UK) restriction enzyme was added. This will cut all parental methylated DNA leaving only the PCR reaction. 5µl of the PCR product is transformed (following section 2.4) into competent *E.coli* cells and DNA was obtained using a DNA midi prep (following section 2.5). This DNA was sequenced at the University of Dundee sequencing service

2.27 Alcian blue staining

Embryos were fixed for 1 hour at room temperature, dehydrated with 5 washes of 100% ethanol (Sigma, UK) for 5 minutes each at RT and then left in Alcian blue (Fischer, UK) staining solution for 3 nights. After this they were washed 3 times for 15 minutes in 95% ethanol (Sigma, UK) at RT then rehydrated in 2% KOH. This was done gradually using 10 minute washes of 75% EtoH in 2% KOH, 50% EtoH in 2% KOH, 25% EtoH in 2% KOH then 3 2% KOH washes. Embryos were then stored in glycerol to make embryos more transparent. This was done by 1 hour washes of 20% glycerol in 2%, 40%glycerol in 2% KOH, 60% glycerol in 2% KOH and finally stored in 80% glycerol in 2% KOH. Facial cartilage was then dissected out before imaging.

Solutions

- Alcian Blue solution: 20mg Alcian blue, 15ml acetic acid, 35ml 100% ethanol
- 2% KOH: 1g KOH tablets in 500ml dH_20

2.28 Statistical analysis

All statistical tests were carried out using Graph Pad Prism 6 software. Suitable statistical tests were chosen for each data set to suit the type of data analysed. Tests used in this thesis include Kruskall Wallis, Mann Whitney U and students T-tests.

2.28 Determining pigment loss

Throughout this thesis the neural crest derivative melanophores are phenotypically assayed by eye based on whether the embryos are displaying a reduced number in this cell type. Those embryos displaying this phenotype are termed as having pigment loss. Embryos showing a normal phenotype are described as wild type. Examples of what is considered pigment loss is shown in **figure 2.2A-D** and what is considered wild type is shown in **figure 2.2E-H**. Pigment loss was achieved throught the addition of compounds in a chemical genetic screen. These compunds are leflunomide (Sigma, UK), 5,6-dichloro-1-beta-D-ribofuranosylbenzimidazole (Sigma, UK) and Cdk9 inhibitor II (Merck Millipore).

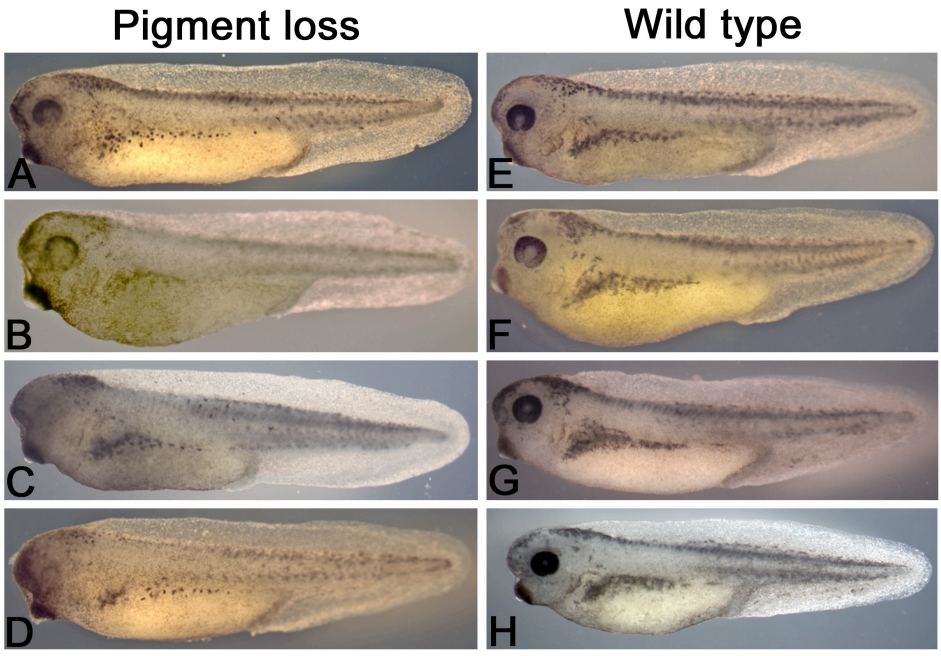

Figure 2.2 Examples of pigment loss and wild type embryos. (A-D) Examples of embryos displaying a pigment loss phenotype. (E-H) Examples of embryos displaying a wild type phenotype.

Chapter III

Using leflunomide as a tool to investigate transcription elongation in neural crest cells

3.1 Introduction

To investigate the role of transcriptional elongation in neural crest cells the drug leflunomide was used to treat *Xenopus* embryos. Leflunomide is a compound identified within our lab in collaboration with the Zon lab, which inhibited pigment cell development. Its mechanism of action was suggested to inhibit transcriptional elongation [3]. We are interested in the role of transcription elongation in neural crest cells so the first experiments carried out here further analyse the leflunomide phenotype. The expected phenotypes would be those showing defects in the neural crest derivatives such as melanophores, cranio-facial cartilage and sensory neurons. One advantage of using a small molecule compound to inhibit transcription elongation is that it can be applied to the embryos at different stages therefore allowing for experiments to be carried out analysing the effect of blocking transcriptional elongation at different stages.

There are many other small molecule compounds readily available which have been commonly used in studies investigating transcriptional elongation. These include 5,6-dichloro-1-beta-D ribofuranosylbenzimidazole (DRB), flavopiridol and many CDK9 inhibitors with varying degrees of specificity. Some of these compounds will also be tested to verify the phenotype given by leflunomide and also to assess the efficiency of leflunomide.

Finally, different genes at various stages of neural crest development will be assayed for their levels of gene expression after leflunomide treatment using in situ hybridisation. Neural crest cells initially undergo induction at the neural plate border and so neural plate border markers should be looked at first. After this they will undergo specification and differentiation and so markers of these phases of crest development will also be looked at. The aims of these experiments are to ascertain whether transcriptional elongation is important for neural crest cell development and if so at what stage of their development.

3.2 The phenotype obtained from leflunomide treatment

3.2.1 The phenotype seen after leflunomide treatment of stage 38 Xenopus laevis

3.2.1.1 Phenotypic analysis

X.laevis embryos were put into 20, 40 and 60µM leflunomide or DMSO as a control, at stage 15. The leflunomide and DMSO were added at the desired concentration to the embryos media, 0.1xMMR. These embryos were left to develop at 18^{o}C until they had reached stage 38. At this stage they were fixed and phenotypically scored for defects in their melanophore formation and migration. Leflunomide acts to inhibit transcriptional elongation and as we are interested in the role this plays in neural crest development we are using the neural crest derivative, melanophores as a read out of the impact inhibiting this process has on neural crest cell specification.

Leflunomide was shown to have a dose-dependent effect on *X.laevis* embryos. A gradual decrease in the number of melanophores present can be seen from the DMSO control to the 20, 40 and 60µM treated samples (**figure 3.1A-D**). A clear loss of melanophore formation can be seen after 60µM leflunomide treatment (**figure 3.1D**) compared to DMSO treated control embryos (**figure 3.1A**). Less melanophores were seen in the head region (**figure 3.1E and F**), the lateral stripe (**figure 3.1G and H**) and the tail region (**figure 3.1I and J**) of 60µM leflunomide treated embryos when compared to DMSO-treated controls. The melanophores in the head region of leflunomide treated embryos (**figure 3.1F**) appear more rounded in shape compared to the dendritic wild type cells seen in the DMSO control (**figure 3.1E**). Melanophores also seem unable to migrate into the underside of the tail after 60µM leflunomide treatment (**figure 3.1J**) when compared to the DMSO control (**figure 3.1I**).

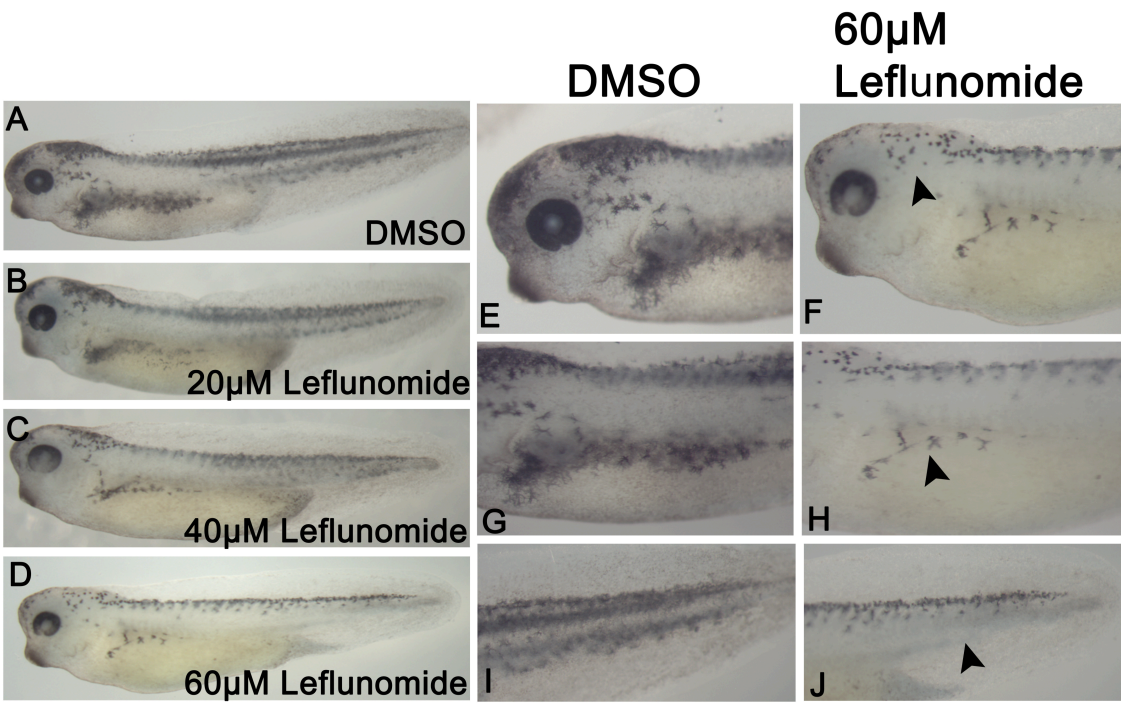

Figure 3.1: The effect of leflunomide on *Xenopus laevis*. (**A-D**) Dose response gradient of leflunomide on stage 38 *X.laevis* embryos. (**A**) DMSO control. (**B**) 20µM leflunomide. (**C**) 40µM leflunomide. (**D**) 60µM leflunomide (**E**) Head region of WT embryo shows normal melanophores. (**F**) Head region of leflunomide treated embryo shows less melanophores which have a rounded morphology (black arrow head). (**G**) Lateral pigment of WT embryo appears normal. (**H**) Lateral pigment of leflunomide treated embryo. Melanophores are much fewer in number (black arrow head). (**I**) Tail of WT embryo shows normal melanophores in the normal position. (**J**) Tail of leflunomide treated embryo has much fewer melanophores none of which have migrated into the underside of the tail (black arrow head).

3.2.1.2 Quantitative analysis

The number of embryos showing wild type and pigment loss phenotypes were counted after both DMSO, 20µM leflunomide, 40µM leflunomide and 60µM leflunomide treatment and plotted as a graph of the percentage of embryos showing these phenotypes (**figure 3.2**). The percentage of embryos showing a pigment loss phenotype gradually increases in a dose dependent manner from 12%, 16%, 24% up to 33% from DMSO up to 60µM leflunomide. This is to be expected as demonstrated in **figure 3.1**, increasing the dose of leflunomide results in a more dramatic phenotype and as shown by the graph is **figure 3.2**, the phenotype is also more commonly seen.

The graph in **figure 3.2** represents the percentage of embryos showing a pigment loss phenotype. There are also other phenotypes commonly seen in *Xenopus* embryos which are considered general developmental defects as they can occur randomly even in control samples as part of poor quality development. These defects include oedemas, stunting of growth (embryos appear shorter than normal) and abnormalities to the eye, which can include retinal pigment loss. The results shown in **table 3.1** demonstrate that a very low percentage (2%) of embryos have developmental defects in the DMSO control sample. This percentage gradually increases from 5%, 8% up to 26% as the concentration of leflunomide increases. This reflects an increase in the general toxicity of the drug.

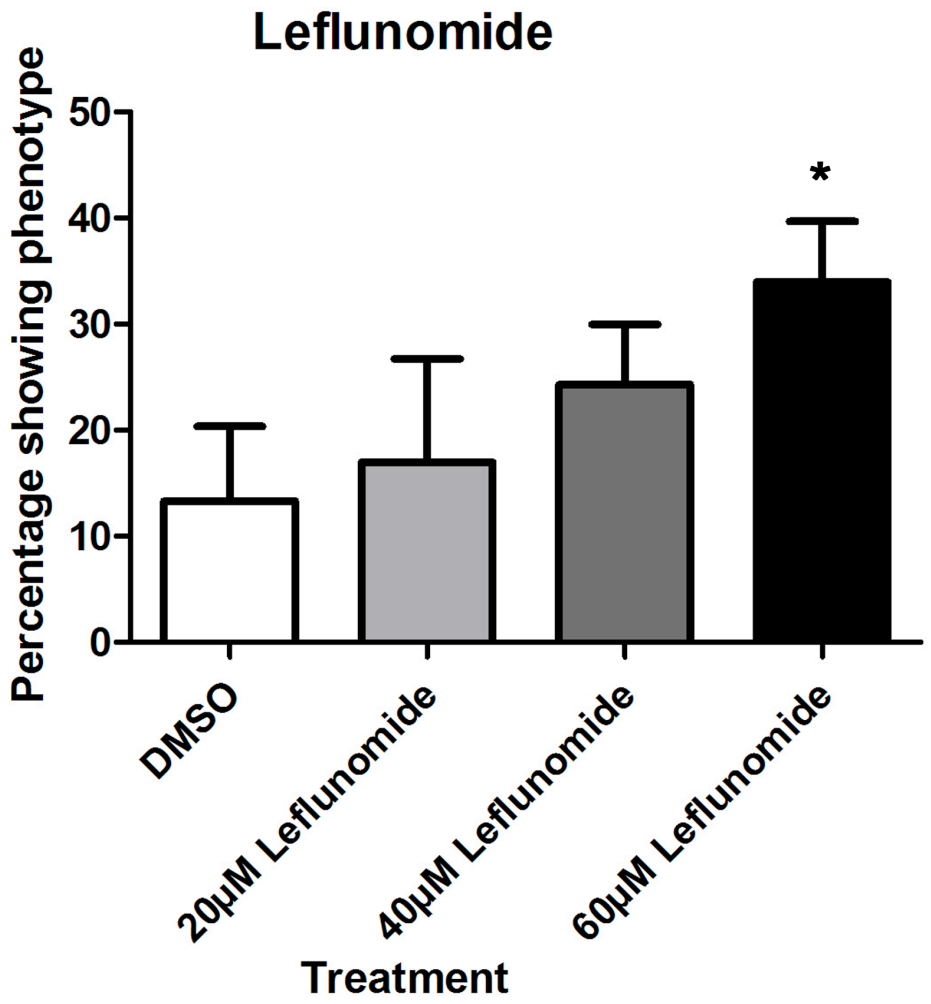

Table 3.1 *X.laevis* phenotypes seen after leflunomide treament

	Total embryos	*Wild type*	*Pigment loss*	*Developmental defects**
DMSO	*155*	*134 (86%)*	*19 (12%)*	*2 (2%)*
20μM leflunomide	*158*	*125 (79%)*	*25 (16%)*	*8 (5%)*
40μM leflunomide	*164*	*111 (68%)*	*39 (24%)*	*14 (8%)*
60μM leflunomide	*141*	*58 (41%)*	*47 (33%)*	*36 (26%)*

* Developmental defects include oedema, stunting and eye abnormalities

Figure 3.2: The percentage of X.laevis embryos showing a pigment loss phenotype after leflunomide treatment. Graph showing the percentage of embryos showing pigment loss phenotype and wild type phenotype for DMSO control (n=155), 20μM leflunomide (n=158), 40μM leflunomide (n=164) and 60μM leflunomide (n=141). *=p<0.05 by Kruskall Wallis statistical test.

3.2.2 Applying leflunomide at different stages

3.2.2.1 Phenotypic analysis

To analyse the effect of leflunomide at different stages of development, embryos were added to 60μM leflunomide or DMSO containing media at stages 1, 8 and 12. 60μM leflunomide was established as an effective dose from the previous dose response experiments. It was hypothesised that adding leflunomide earlier before neural crest cell specification starts at stage 12, would give a stronger pigment cell loss phenotype. This was seen to be the case however the drug also appeared to affect the general development of the embryos. Adding the drug before gastrulation i.e. stage 1 and 8 caused the embryos to have a stunted phenotype and display improper eye development. Adding it to the embryos at stage 12 appeared to give a similar phenotype to that seen when added at stage 15, embryos displayed fairly normal development but appeared to have less melanophores.

Embryos added to DMSO at stage 1 displayed a wild type phenotype (**figure 3.3A**). Embryos added to 60μM leflunomide at stage 1 (**figure 3.3B**) had an almost complete loss of melanophores however they appeared much shorter in length due to stunted growth. They also appeared to be much shorter and wider than the wild type embryos and displayed a loss of retinal pigment in the eye suggesting improper eye development. Embryos added to DMSO at stage 8 displayed a wild type phenotype (**figure 3.3C**). Embryos added to 60μM leflunomide at stage 8 (**figure 3.3D**) also show an almost complete loss of melanophores however these too appear stunted and display eye development defects. Embryos added to DMSO post gastrulation at stage 12 show a wild type phenotype (**figure 3.3E**). Embryos added to 60μM leflunomide at stage 12 (**figure 3.3F**) show fewer melanophores in the head lateral stripe and tail regions of the embryos. The embryos also appear normal in shape and display fewer general developmental defects. Melanophores in the tail again seem unable to migrate into the underside of the tail.

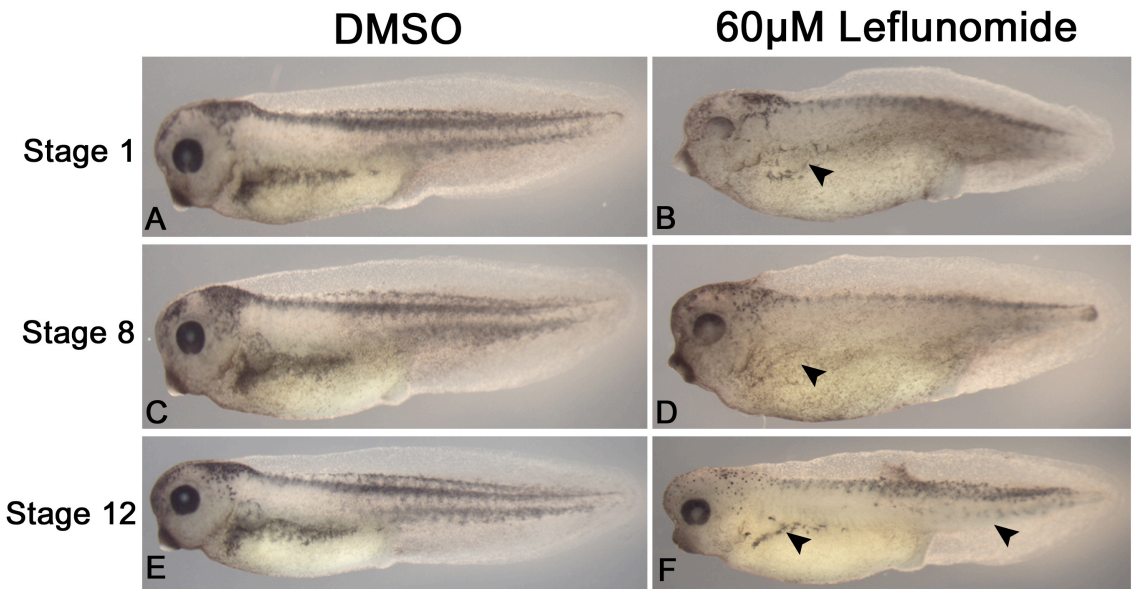

Figure 3.3: Applying leflunomide at different stages of development. (**A**) Embryos added to DMSO at stage 1 showing wild type phenotype. (**B**) Embryos added to 60µM leflunomide at stage 1 show loss of melanophores (black arrow head) and also stunting and eye defects. (**C**) Embryos added to DMSO at stage 8 show wild type phenotype. (**D**) Embryos added to 60µM at stage 8 show loss of melanophores (black arrow head) and also stunting and eye defects. (**E**) Embryos added to DMSO at stage 12 show wild type phenotype. (**F**) Embryos added to 60µM at stage 12 show a loss of melanophores in the lateral stripe and tail (black arrow heads).

3.2.2.2 Quantitative analysis

The number of embryos showing wild type and pigment loss phenotypes were counted after DMSO treatment at stage 1, 8 and 12 and also 60µM leflunomide treatment at the same stages and plotted as a graph of the percentage of embryos showing these phenotypes (**figure 3.4**). The percentage of embryos showing a pigment loss phenotype starts off very high at 51% when 60µM leflunomide is added at stage 1. This number gradually decreases as the drug is added at later stages showing 47% of embryos with pigment loss when leflunomide is added at stage 12. This is to be expected as administering the drug earlier before neural crest specification ensures that the drug is taking effect at a point which will sufficiently block neural crest development. This results in a higher frequency of the pigment cell loss phenotype.

The graph in **figure 3.4** represents the percentage of embryos showing a pigment loss phenotype. Other phenotypes commonly seen include oedemas, stunting of growth (embryos appear shorter than normal) and abnormalities to the eye such as retinal pigment loss. The results shown in **table 3.2** demonstrate that a low percentage (5-7%) of embryos have developmental defects in the DMSO control samples. This percentage was relatively high (34%) in the embryos treated with 60µM leflunomide at stage 1 however what is not reflected by this is that all of the pigment loss embryos in this category also show many other defects including stunting and eye abnormalities shown in **figure 3.3**. This is also the case for embryos added to 60µM leflunomide at stage 8, 25% of this category show developmental defects however all of the pigment loss embryos also have stunting and eye abnormalities. This may arise to due off target effects of the drug preventing the embryos undergoing normal gastrulation. This is a common effect seen in chemical screens when the compound is added before gastrulation. Pigment loss embryos added to leflunomide at stage 12 show no other developmental defects and only 18% of the total embryos in this category show such defects (**table 3.2**).

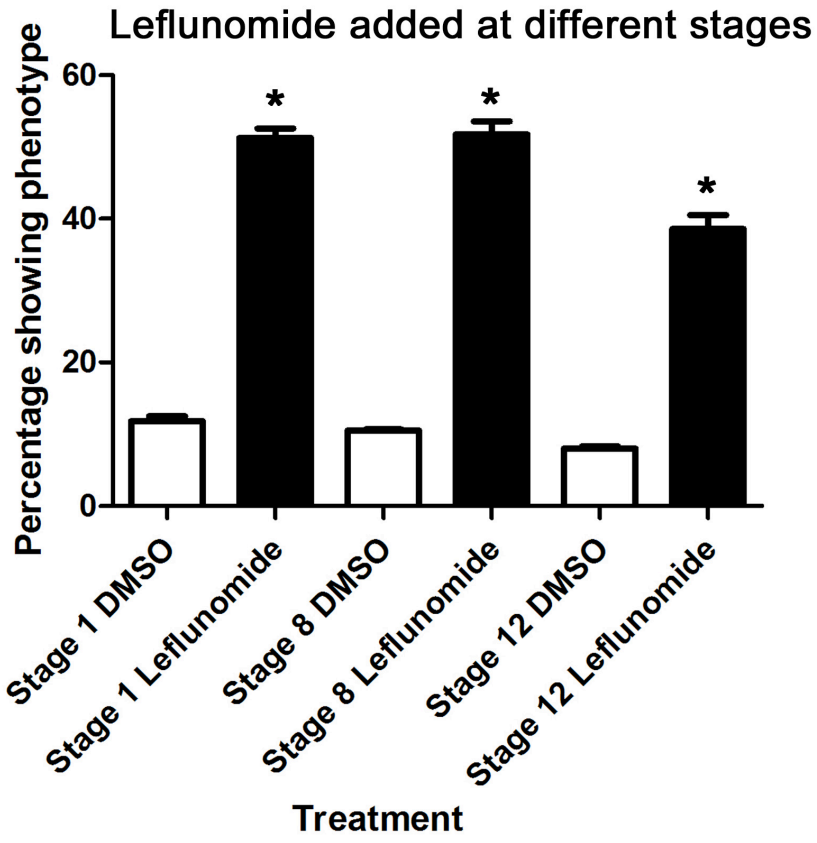

Table 3.2 Phenotypes seen when leflunomide is added at different stages

	Total embryos	*Wild type*	*Pigment loss*	*Developmental defects**
DMSO Stage 1	*60*	*50 (83%)*	*7 (12%)*	*3 (5%)*
DMSO Stage 8	*67*	*56 (83%)*	*7 (10%)*	*4 (7%)*
DMSO Stage 12	*63*	*55 (87%)*	*5 (8%)*	*3 (5%)*
60µM leflunomide Stage 1	*72*	*11 (15%)*	*37 (51%)*	*24 (34%)*
60µM leflunomide Stage 8	*73*	*17 (23%)*	*38 (52%)*	*18 (25%)*
60µM leflunomide Stage 12	*67*	*29 (43%)*	*26 (39%)*	*12 (18%)*

* Developmental defects include oedema, stunting and eye abnormalities

Figure 3.4: The percentage of embryos showing a pigment loss phenotype after leflunomide addition at different stages. Graph showing the percentage of embryos showing pigment loss phenotype and wild type phenotype for DMSO control added at stage 1 (n=60), stage 8 (n=67) , stage 12 (n=63) and 60µM leflunomide added at stage 1(n=72), stage 8 (n=73) and stage 12 (n=67). *=p<0.05 by Kruskall Wallis statistical test

3.2.3 The phenotype seen after leflunomide treatment of stage 38 Xenopus tropicalis

3.2.3.1 Phenotypic analysis

After looking at the phenotype given by leflunomide in *Xenopus laevis*, we looked at the phenotype given in *Xenopus tropicalis*. This experiment was carried out as it would be interesting to see whether the chemical genetic experiment of adding leflunomide to the embryos media, would have a stronger effect on the diploid *X.tropicalis* species over the tetraploid *X.laevis*. Being diploid it would be logical to observe a stronger phenotype as fewer copies of the same gene are present in the embryos to provide redundancy. *X.tropicalis* embryos were put into either 60µM leflunomide or DMSO as a control at stage 15. The leflunomide and DMSO are added straight to the embryos media, 0.1xMMR. These embryos were left to develop at 26^{o}C until they had reached stage 38. At this stage they were fixed and phenotypically scored for defects in their melanophore formation and migration.

Leflunomide was shown to have a much stronger effect on the *X.tropicalis* embryos then *X.laevis* embryos. Clear defects were seen in melanophore formation after 60µM leflunomide treatment compared to DMSO treated control embryos (**figure 3.5A**). The loss of melanophores seen in *X.laevis* is much less obvious. Less melanophores were seen in the head region (**figure 3.5B and C**), the lateral stripe (**figure 3.5D and E**) and the tail region (**figure 3.5F and G**) of 60µM leflunomide treated embryos when compared to DMSO treated controls. On closer examination the melanophores themselves appear to have lost their dendritic morphology and adopted a more rounded one (**figure 3.5D and E**).

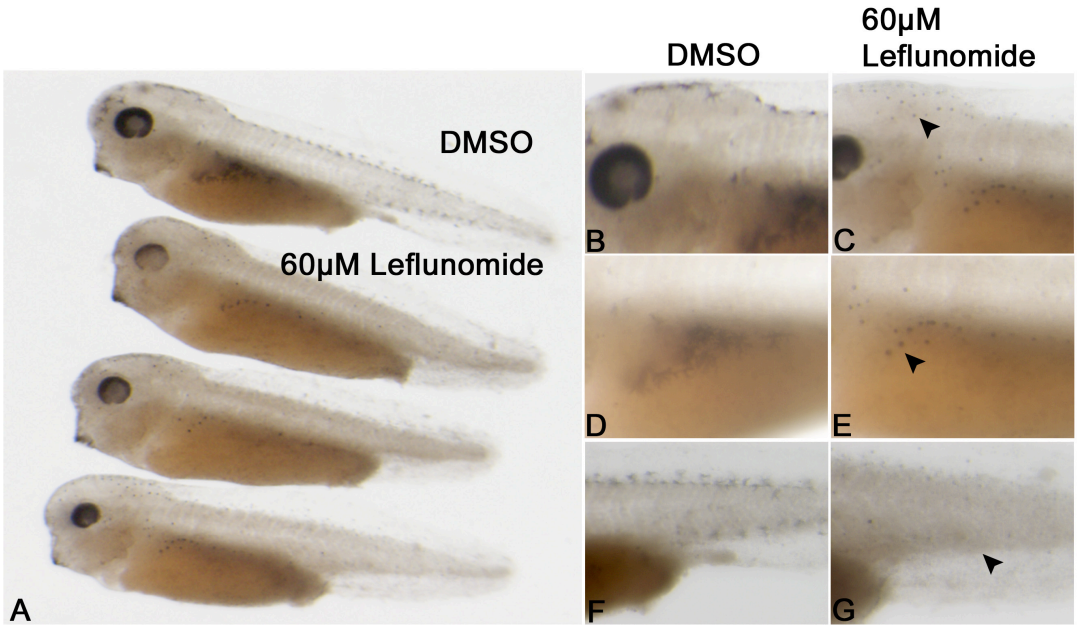

Figure 3.5: The effect of leflunomide on *Xenopus* tropicalis. (**A**) Top embryo is a wild type embryo which has undergone DMSO treatment as part of a control group. Its melanophore morphology appears normal. The three beneath this developed in 60µM leflunomide and they appear to have fewer melanophores with no dendritic morphology. (**B**) Head region of WT embryo shows normal melanophores. (**C**) Head region of leflunomide treated embryo shows less melanophores which have a rounded morphology (black arrow head). (**D**) Tail of WT embryo shows normal melanophores in the normal position. (**E**) Tail of leflunomide treated embryo has no melanophores (black arrow head). (**F**) Lateral pigment of WT embryo appears normal. (**G**) Lateral pigment of leflunomide treated embryo. Melanophores are fewer in number and appear rounded (black arrow head).

3.2.3.2 Quantitative analysis

The number of embryos showing wild type and pigment defect phenotypes were counted after both DMSO and 60µM leflunomide treatment and plotted as a graph of the percentage of embryos showing a pigment loss phenotype (**figure 3.6**). 47% of embryos after leflunomide treatment were seen to have the pigmentation defects seen in **figure 3.5** compared to only 9% of embryos showing pigmentation defects in the DMSO control (**table 3.3**). This is greater than the number of *X.laevis* showing a pigment loss (33% shown in **figure 19**). Suggesting that the tropicalis phenotype is stronger and occurs more frequently.

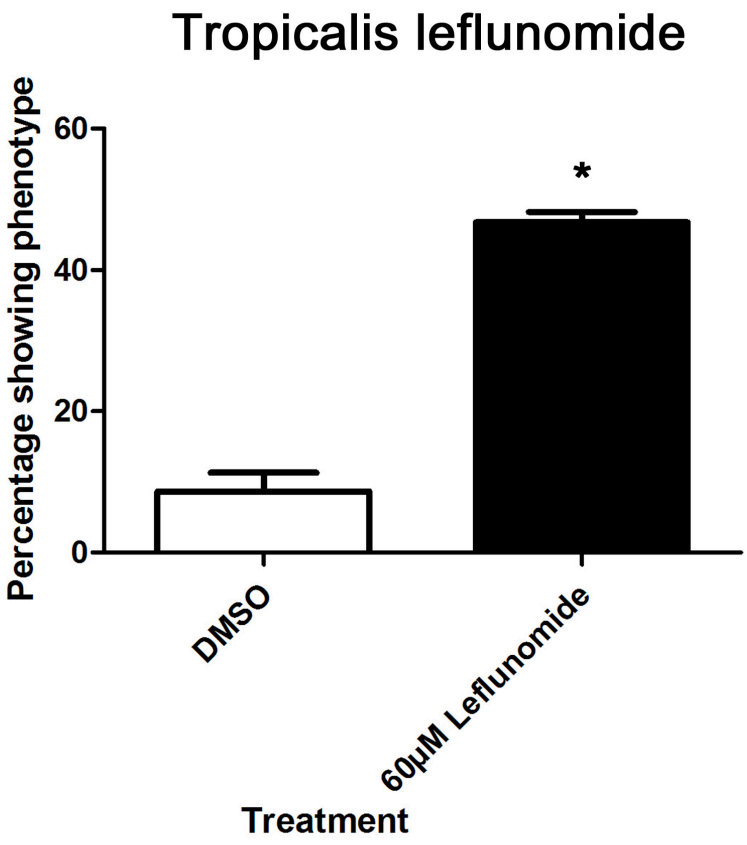

Table 3.3 X.tropicalis phenotype seen after leflunomide treament

	Total embryos	*Wild type*	*Pigment loss*
DMSO	*302*	*275 (91%)*	*27 (9%)*
60µM leflunomide	*252*	*134 (53%)*	*118 (47%)*

Figure 3.6: The percentage of X.tropicalis embryos showing a pigment loss phenotype after leflunomide treatment. Graph showing the percentage of embryos showing pigment loss phenotype and wild type phenotype for DMSO control (n=302), and 60µM leflunomide (n=252). *=p<0.05 by Mann-Whitney U statistical test

3.2.4 Affect of leflunomide treatment on craniofacial development

Craniofacial cartilage is derived from cranial neural crest cells and can easily be stained using an alcian blue stain. Alcian blue will stain glycosaminoglycans specific to cartilage leaving the cartilage of the embryo stained blue and the rest of the embryo unaffected. Observing the structure of cranio-facial cartilage is a commonly used method to analyse the development of cranial neural crest cells. Here *Xenopus laevis* embryos were added to DMSO and a gradient of leflunomide concentrations at stage 15 and left to develop until stage 45 when they were fixed and underwent alcian blue staining to visualise the development of cranio-facial cartilage. Embryos were visualised in glycerol to increase the transparency of the head region.

DMSO treated embryos (**figure 3.7A**) show normal cranio-facial cartilage development. The alcian blue stains dark blue in all of the cranio-facial cartilage present in the head region of the embryo. 20µM leflunomide treated embryos (**figure 3.7B**) also show a wild type phenotype. Their cranio-facial cartilage appears normal and stains dark blue. 40µM leflunomide treated embryos (**figure 3.7C**) show some defects in their cranio-facial cartilage development. Cartilage starts to appear disorganised and a paler blue. 60µM leflunomide treated embryos (**figure 3.7D**) show clear cranio-facial cartilage defects. Cartilage and head region is clearly not properly developed and alcian blue staining appears pale blue.

To further analyse the organisation of the embryos craniofacial cartilage it was removed by dissection. The DMSO treated cartilage (**figure 3.7E**) shows normal organisation comparable to the diagram in **figure 3.7G**. The 60µM leflunomide treated cartilage (**figure 3.7F**) has small, disorganised branchial cartilage regions compared to the DMSO control. It also appears paler in colour suggesting that less cartilage has been formed.

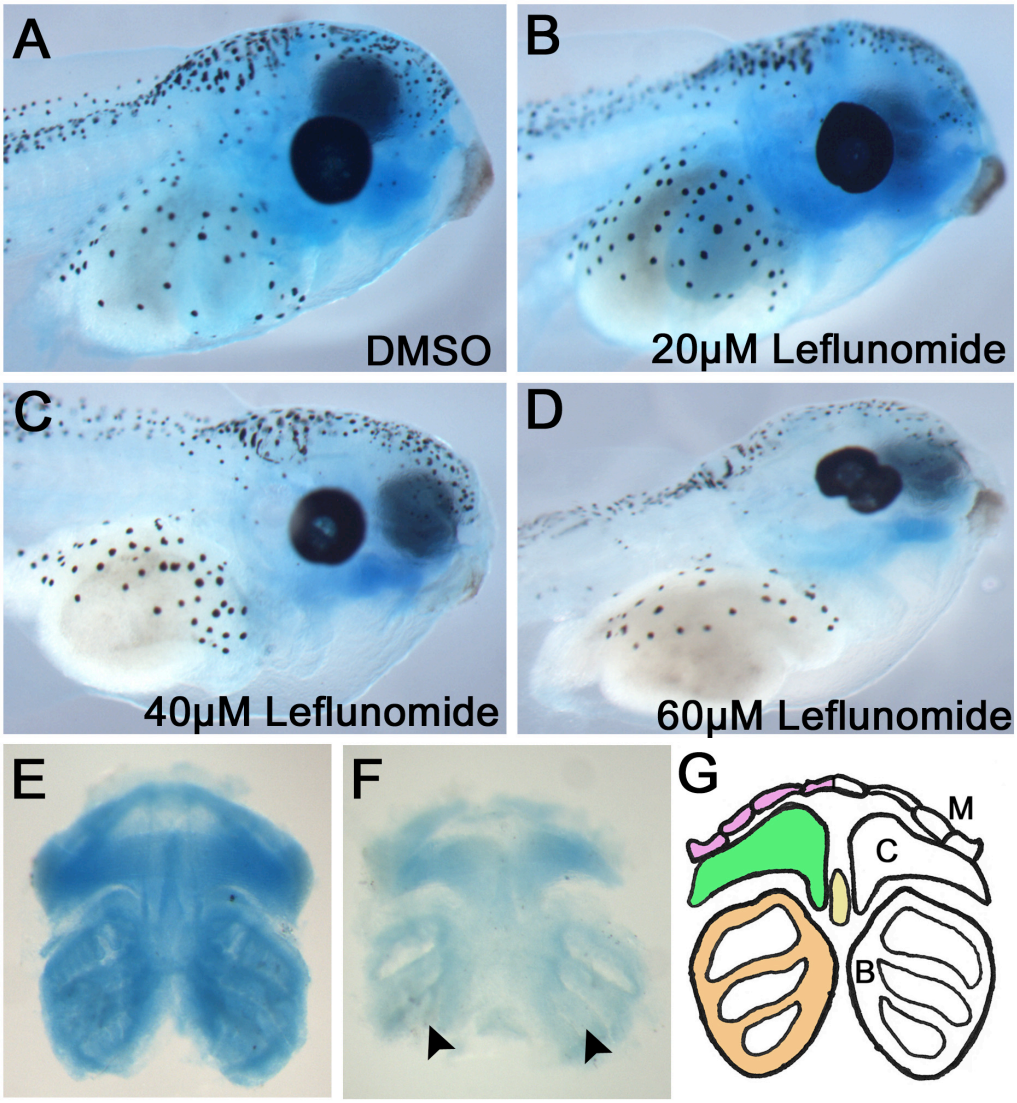

Figure 3.7: The effect of leflunomide on cranio-facial cartilage. (**A-D**) DMSO, 20μM, 40μM, and 60μM leflunomide treated embryos at stage 45 after alcian blue staining. (**E**) Dissected cranio-facial cartilage of a DMSO treated embryo. (**F**) Dissected cranio-facial cartilage of a 60μM leflunomide treated embryo. Embryos show a disorganisation in the development of the branchial cartilage (black arrow heads). (**G**) Diagram representing normal cranio-facial cartilage development. M=Meckels cartilage, C=Ceratohyal, B=Branchial cartilage.

3.2.5 Affect of leflunomide treatment on sensory neuron development

Sensory neurons are another neural crest cell derivative with simple assays used to test their development. They can be tested simply by poking the embryo with a pipette tip and observing the reaction of the embryo. Here the embryos were treated with 60µM leflunomide before and after gastrulation (at stages 8 and 12 respectively) then left to develop at 18^{o}C until reaching stage 37 when they would be taken out of leflunomide and washed overnight in clean media (0.1xMMR). These were left to develop until stage 38 when embryos have a full sensory response. Washing the embryos is important to ensure any phenotype seen is due to neural crest defects and not a side effect of the compound. Embryos then underwent a poke from a pipette tip straight to the back of the embryo or a stroke, which involves running the pipette tip from the head to the tail of the embryo. If the embryos swim away they are scored 1, if they twitch on the spot they are scored 0.5 and if they fail to react they are scored 0. For each treatment type, 30 embryos were tested in 3 rounds of 10 and the average score for these 3 lots of ten is displayed.

Embryos treated with DMSO from stage 8 and stage 12 both show a normal response from poking (**figure 3.8 top panel**) and stroking (**figure 3.8 bottom panel**). Most of these embryos responded normally and swam away in response to the external stimulus. After 60µM leflunomide treatment at stage 8, the embryos show a significant decrease in their ability to respond to both poking (**figure 3.8 top panel**) and stroking (**figure 3.8 bottom panel**) indicating a loss of sensory neuron development. Similarly, embryos treated with 60µM leflunomide at stage 12 show a significant decrease in their ability to respond to both poking (**figure 3.8 top panel**) and stroking (**figure 3.8 bottom panel**) when compared to the DMSO control. There was a slight increase seen in the response ability observed between embryos added to leflunomide at stage 12 compared to stage 8 however this difference is not statistically significant. DMSO treated and stage 12 leflunomide treated embryos were filmed undergoing a poke response. This video can been seen in **appendix 1**.

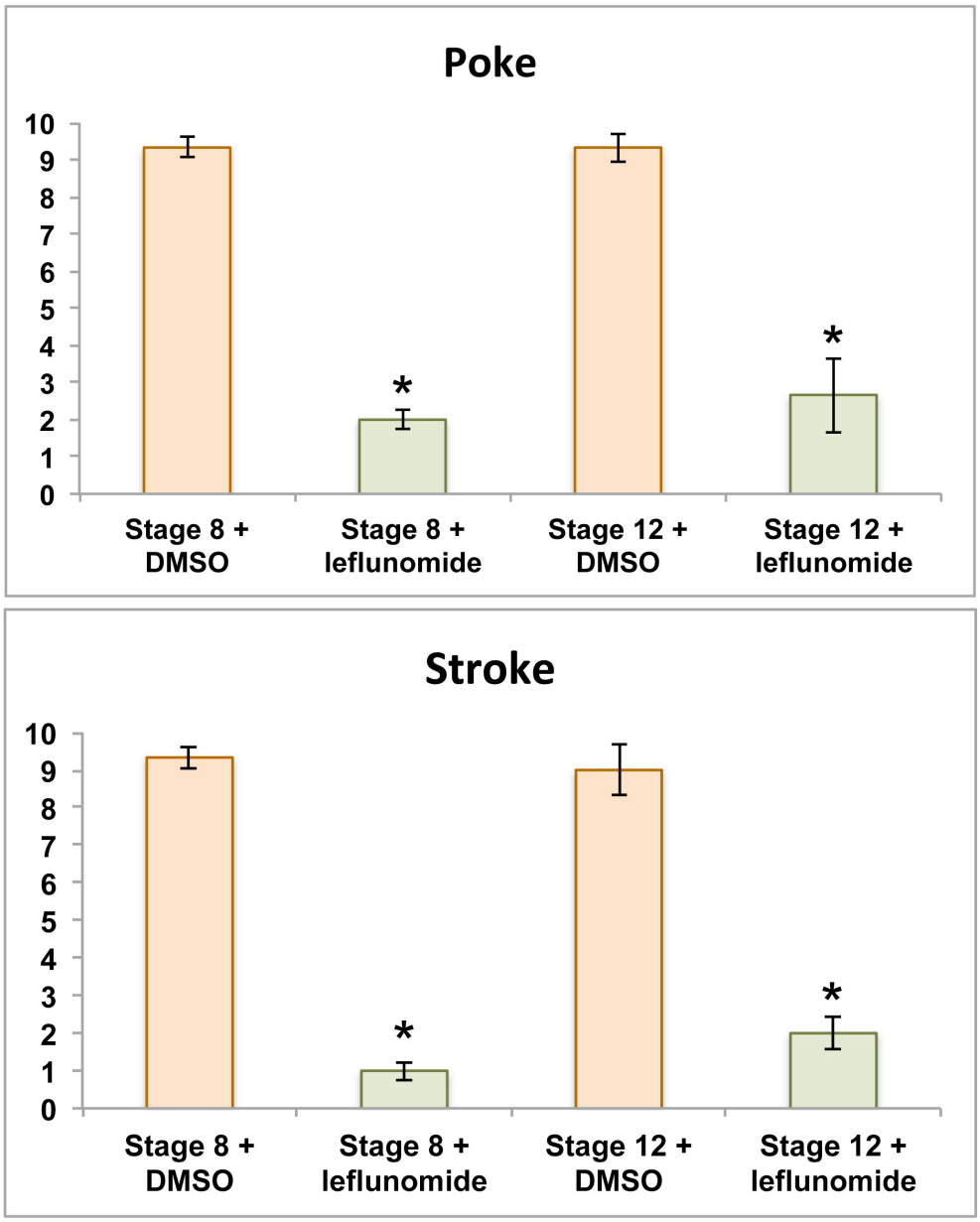

Figure 3.8: Poke and stroke analysis of senory neuron development. (Top panel) Embryos undergo poking to the dorsal side and their response is tallied as follows. Swim=1, twitch=0.5 no response=0. The average of 30 embryos (3 experiments using 10 embryos) is shown. (Bottom panel) Embryos undergo stroking of a pipette tip from the head region to the tail and their response is tallied as follows. Swim=1, twitch=0.5 no response=0. The average of 30 embryos is shown. For both conditions embryos were treated with DMSO and 60μM leflunomide from stages 8 and 12. *=$p<0.05$ by students t-test.

3.3 Other small molecule compounds affecting transcription elongation

3.3.1 5,6-dichloro-1-beta-D-ribofuranosylbenzimidazole (DRB)

3.3.1.1 Phenotypic analysis

To confirm the phenotype seen from leflunomide treatment embryos were treated with other small molecule compounds, which have the same function. 5,6-dichloro-1-beta-D-ribofuranosylbenzimidazole (DRB) has been commonly used in studies analysing the effect of inhibiting transcriptional elongation. It is from this compound that the transcriptional elongation complex component DSIF gets its name (5,6-dichloro-1-beta-D-ribofuranosylbenzimidazole sensitivity inducing factor). This experiment will also suggest whether leflunomide is an appropriate drug to carry out further experiments with or whether other compounds are able to give the same phenotype more effectively.

Embryos treated with DMSO (**figure 3.9A**) show a wild type phenotype. Embryos treated with DRB show high concentrations needed in a dose response before any phenotype is seen (**figure 3.9B-D**). 100μM DRB treated embryos (**figure 3.9B**) also appear wild type. After 140μM DRB treatment (**figure 3.9C**), a small percentage of embryos show a loss of melanophores similar to the phenotype seen from 60μM leflunomide treatment. After 170μM DRB treatment (**figure 3.9D**), embryos show a clear loss of melanophores in the head, lateral stripe and tail however many embryos also show other developmental defects such as bent tails and abnormal eye development, probably due to toxicity of the drug used at such high concentrations. Because leflunomide gives a pigment loss phenotype at lower concentrations and without general development side effects it was deemed a more effective drug to use to analyse transcriptional elongation inhibition than DRB.

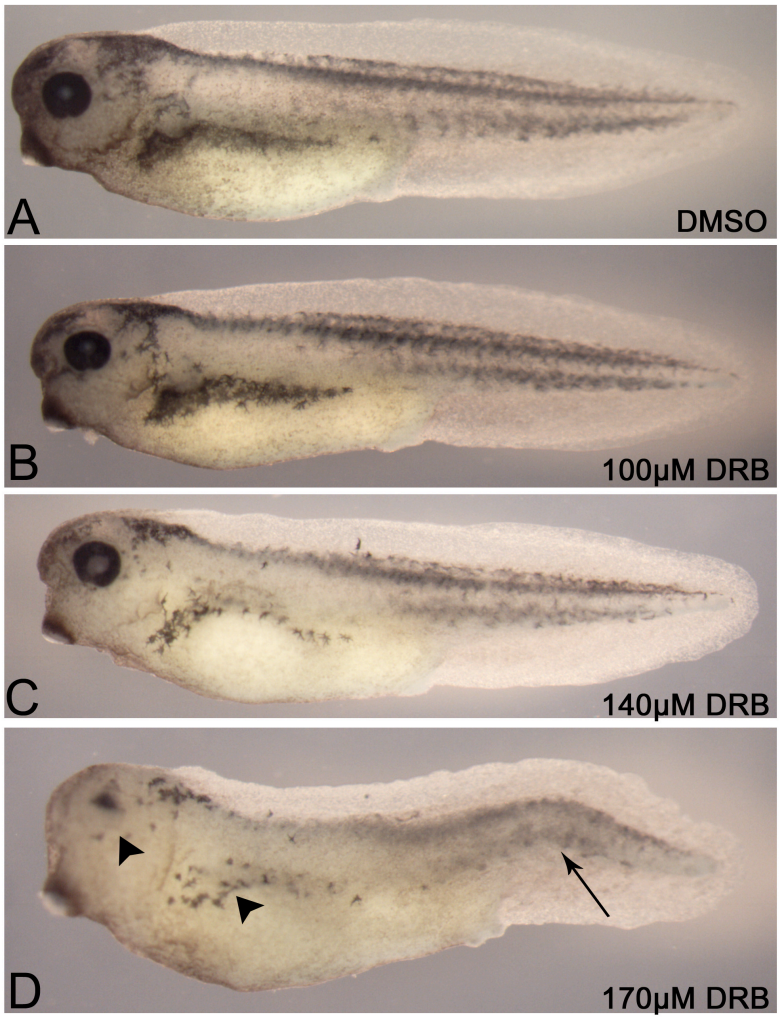

Figure 3.9: Dose response of 5,6-dichloro-1-beta-D-ribofuranosylbenzimidazole (DRB). (**A**) DMSO treated embryo showing a wild type phenotype. (**B**) 100µM DRB treated embryo shows wild type phenotype. (**C**) 140µM DRB treated embryo shows some loss of melanophores in the lateral stripe. (**D**) 170µM DRB treated embryo shows loss of pigment in the eye and lateral stripe (black arrow heads). Less melanophores in the tail however tail appears bent (arrow).

3.3.1.2 Quantitative analysis

The number of embryos showing wild type and pigment loss phenotypes were counted after DMSO, 100μM DRB, 140μM DRB and 170μM DRB treatment. These data were then plotted as a graph of the percentage of embryos showing pigment loss phenotype (**figure 3.10**). The percentage of embryos showing a pigment loss phenotype increases dose dependently from 12%, 15%, 25% up to 35% from DMSO up to 170μM DRB. This is to be expected as demonstrated in **figure 3.9**, increasing the dose of DRB resulted in a stronger phenotype and as shown by the graph in **figure 3.10** it is more commonly seen. At 170μM DRB the percentage of embryos showing a pigment loss phenotype (35%) is similar to that of 60μM leflunomide treated embryos (33%). Using leflunomide over DRB could be considered advantageous as it is more efficient and reliable to use compounds at the lowest possible concentration to avoid off target effects.

The graph in **figure 3.10** represents the percentage of embryos showing just a pigment loss phenotype. Other phenotypes seen include oedemas, stunting of growth (embryos appear shorter than normal) and abnormalities to the eye including a complete loss of the eye. The results shown in **table 3.4** demonstrate that a relatively high percentage (22%) of embryos have developmental defects in the DMSO control samples. This higher than normal percentage can be explained by the increased amount of DMSO in the embryos media. As the highest concentration of compound used in these experiments was 170μM the percentage of DMSO used in the control was increased to reflect this. 1.7% of the media was DMSO which is high considering 2% is the highest concentration a *Xenopus* embryo will tolerate [270]. It is for such reasons as this that using high drug concentrations is not good practice. The amounts of general developmental defects appear to stay constant with the equivalent DRB concentration i.e. 23% at 170μM (**table 3.4**), however this is because this does not reflect how all of the pigment loss embryos display defects including loss of eye pigment and a kinked tail (**figure 3.9**).

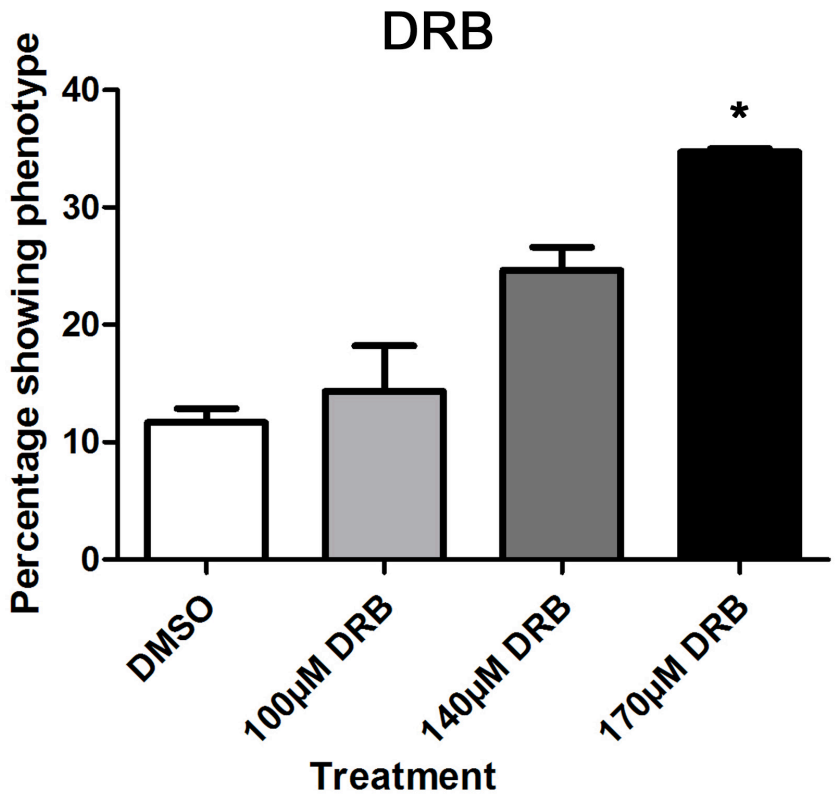

Table 3.4 Phenotypes seen after DRB treament

	Total embryos	*Wild type*	*Pigment loss*	*Developmental defects**
DMSO	*50*	*33 (66%)*	*6 (12%)*	*11 (22%)*
100μM DRB	*54*	*37 (69%)*	*8 (15%)*	*9 (16%)*
140μM DRB	*52*	*32 (62%)*	*13 (25%)*	*7 (13%)*
170μM DRB	*52*	*22 (42%)*	*18 (35%)*	*12 (23%)*

* Developmental defects include oedema, stunting and eye abnormalities

Figure 3.10: Percentage of embryos showing a pigment loss phenotype after 5,6-dichloro-1-beta-D-ribofuranosylbenzimidazole (DRB) treatment. Graph showing the percentage of embryos showing a pigment loss phenotype after DMSO (n=50), 100μM DRB (n=54), 140μM DRB (n=52) and 170μM DRB (n=52). *=$p<0.05$ by Kruskall Wallis statistical test

3.3.2 Cyclin dependent kinase 9 (CDK9) inhibitor

3.3.2.1. Phenotypic analysis

Another type of compound commonly used to inhibit transcriptional elongation are those which inhibit the enzyme CDK9, the active component of the P-TEFb complex which allows transcription elongation to occur. General CDK9 inhibitors have many off target effects such as inhibiting CDK2, an enzyme structurally similar to CDK9. The CDK9 inhibitor used in this screen claims to be specific for CDK9. Again this screen allows the efficiency of leflunomide to be compared to other compounds, which carry out the same function.

The DMSO treated embryos (**figure 3.11A**) show a wild type phenotype with normal amounts of melanophores in the head, lateral stripe and tail. Similarly to DRB, the CDK9 inhibitor required very high concentrations before a phenotype was observed (**figure 3.11B-D**). After treatment with 100μM CDK9 inhibitor (**figure 3.11B**) the embryos still appear wild type. At 140μM of CDK9 inhibitor (**figure 3.11C**) the embryos show a clear pigment cell loss phenotype. Pigment cell loss can be seen in the eye, lateral stripe and tail. At 170μM of CDK9 inhibitor (**figure 3.11D**) the embryos show a loss of pigment cells in the eye, lateral stripe and tail. At this concentration all of the embryos also displayed developmental defects such as stunting and bent tails. These are side effects often seen when compounds a added to embryos at very high concentrations and so are considered off target effects.

Similarly to DRB the CDK9 inhibitor is only effective at very high concentrations. This is not optimal as demonstrated using high concentrations of a compound tends to give off target general developmental defects. In comparison to leflunomide both DRB and the CDK9 inhibitor use very high concentrations of compound, which is not ideal for specific genetic experiments. They did however both give the same melanophore loss phenotype seen from leflunomide treatment.

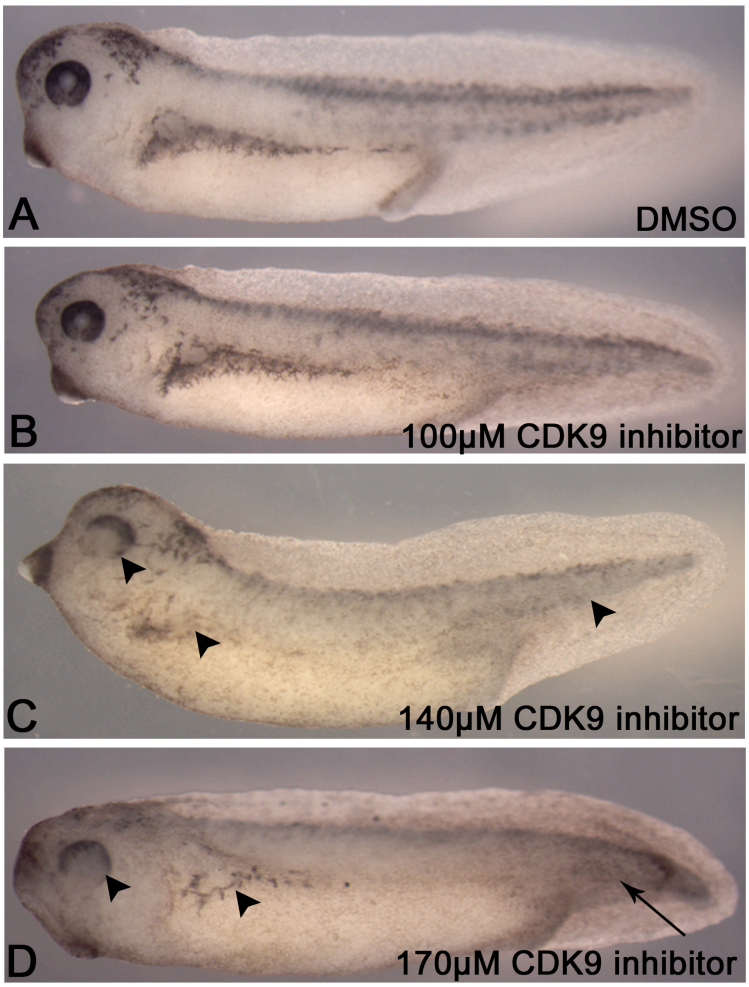

Figure 3.11: Dose response of CDK9 inhibitor. (A) DMSO treated embryo showing a wild type phenotype. (**B**) 100μM CDK9 inhibitor treated embryo shows wild type phenotype. (**C**) 140μM CDK9 inhibitor treated embryo shows loss of melanophores in the lateral stripe, eye and tail (black arrow heads). (**D**) 170μM CDK9 inhibitor treated embryo shows loss of pigment in the eye and lateral stripe (black arrow heads). Less melanophores are found in the tail however tail appears bent (arrow) and embryos are stunted.

3.3.2.2 Quantitative analysis

The number of embryos showing wild type and pigment loss phenotypes were counted for DMSO, 100μM CDK9 inhibitor, 140μM CDK9 inhibitor and 170μM CDK9 inhibitor treatment. These data were plotted as a graph of the percentage of embryos showing these phenotypes (**figure 29**). The percentage of embryos showing a pigment loss phenotype gradually increases in a dose dependent manner from 16%, 15%, 34% up to 36% from DMSO up to 170μM CDK9 inhibitor. Increasing the dose of CDK9 inhibitor results in a stronger phenotype (**figure 3.11**) and as shown by the graph in **figure 3.12**, the general phenotype is also more commonly seen. At 140μM CDK9 inhibitor the percentage of embryos showing a pigment loss phenotype (36%) is similar to that of 60μM leflunomide treated embryos (33%). This is however a similar problem to using DRB, it is inefficient and unreliable to use compounds at high concentrations as off target effects arise and so leflunomide would be a better alternative to use in further experiments.

The graph in **figure 3.12** represents the percentage of embryos showing either a pigment loss phenotype. Similarly to previous experiments, other phenotypes are seen including oedemas, stunting of growth and abnormalities to the eye. The results shown in **table 3.5** indicate that the amounts of general developmental defects appear to increase drastically with increasing CDK9 inhibitor concentration i.e. 31% of embryos have such defects at 170μM (**table 3.5**), this also does not reflect that all of the pigment loss embryos display defects including loss of eye pigment and stunting (**figure 3.9D**). Overall this compound appeared to have many off target side effects causing many developmental defects to occur and therefore would not be as efficient for further genetic experiments when compared to leflunomide.

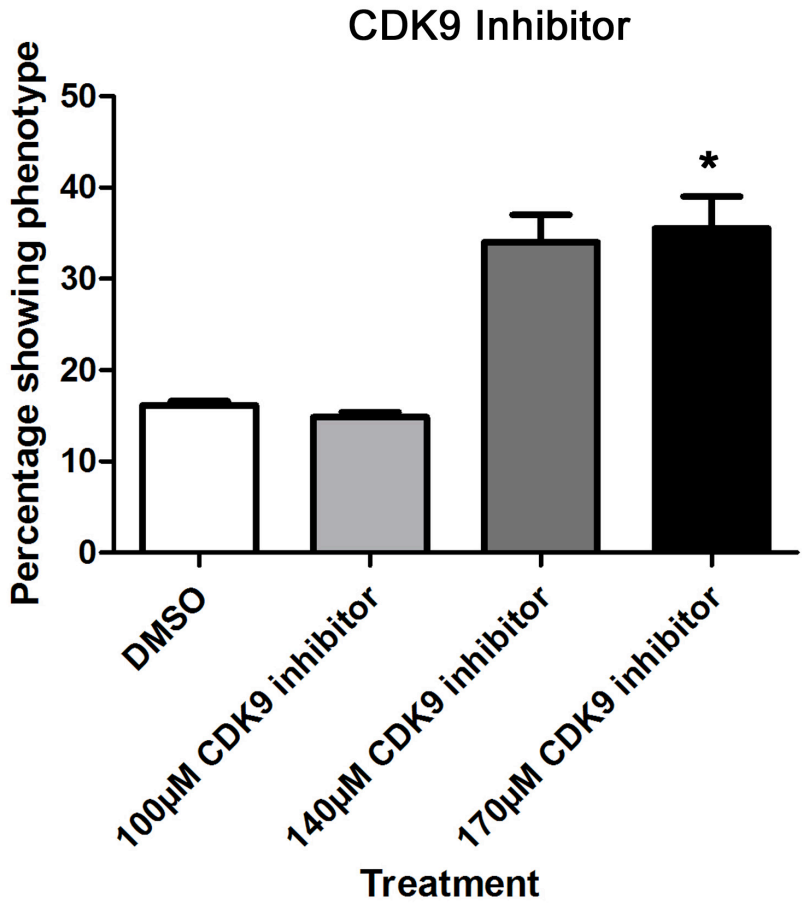

Table 3.5 Phenotypes seen after CDK9 inhibitor treatment

	Total embryos	*Wild type*	*Pigment loss*	*Developmental defects**
DMSO	*43*	*31 (72%)*	*7 (16%)*	*5 (12%)*
100μM CDK9 inhibitor	*47*	*33 (70%)*	*7 (15%)*	*7 (15%)*
140μM CDK9 inhibitor	*56*	*23 (41%)*	*19 (34%)*	*14 (25%)*
170μM CDK9 inhibitor	*69*	*23 (33%)*	*25 (36%)*	*21 (31%)*

***Developmental defects include oedema, stunting and eye abnormalities.**

Figure 3.12: Percentage of embryos showing a pigment loss phenotype after CDK9 inhibitor treatment. Graph showing the percentage of embryos showing a pigment loss phenotype after DMSO (n=43), 100μM CDK9 inhibitor (n=47), 140μM CDK9 inhibitor (n=56) and 170μM CDK9 inhibitor (n=69) *=p<0.05 by Kruskall Wallis statistical test

3.4 Analysis of genes affected by leflunomide using in situ hybridization on whole embryos

3.4.1 Neural plate and neural plate border specifiers

The previous experiments shown indicate that treatment of 60μM leflunomide causes *Xenopus* embryos to show a loss of neural crest derivatives such as melanophores, cranio-facial cartilage and sensory neurons. The reduction in this variety of derivatives suggests that the neural crest cells themselves are not forming or are not being specified into neural crest cells and therefore not undergoing differentiation into the different cell types they are able to form. Neural crest cells are initially induced at the neural plate border at stage 12 due to the upregulation of neural plate border specific genes such as Zic1, Zic3 and Pax3. To investigate the stage of neural crest development in which transcriptional elongation is important, stage 3 embryos were added to 60μM leflunomide and left to develop until stage 12 when they were fixed to undergo *in situ* hybridisation for neural plate border markers. Some were also fixed at stage 15 to investigate any possible effect leflunomide might have on general neural plate development by carrying out *in situ* hybridisation for the pan neural plate marker Sox2.

In situ hybridisation for the neural plate border markers Zic1, Zic3 and Pax3 after DMSO treatment (**figure 3.13A, C and E**) show wild type expression in the neural plate border of stage 12 embryos. After leflunomide treatment (**figure 3.13B, D and F**) there appears to be no change to the expression of these neural plate border genes and their expression resembles that of the wild type expression seen in the DMSO treated embryos. This suggests that leflunomide is not having an effect on early neural crest induction at the neural plate border. Similarly the neural plate marker Sox2 shows wild type expression in both the DMSO treated (**figure 3.13G**) and leflunomide treated embryos (**figure 3.13H**) indicating that leflunomide has no effect on general neural development.

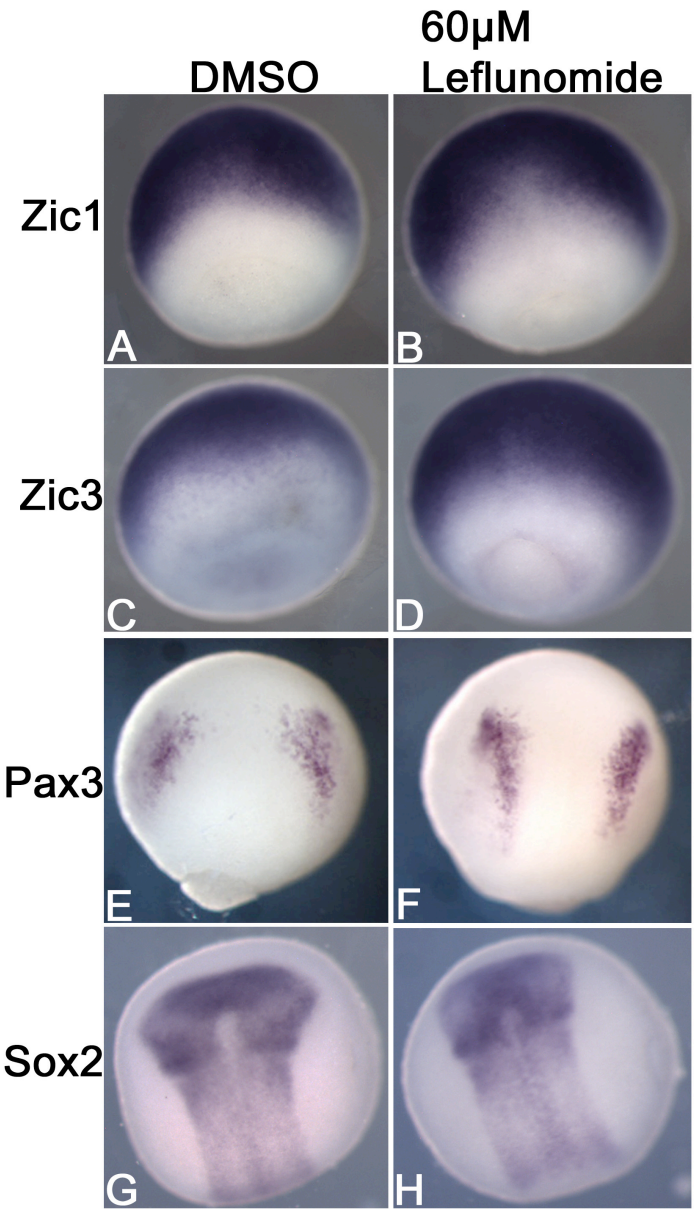

Figure 3.13: The affect of leflunomide on neural plate and neural plate border specifiers. (**A,C** and **E**) DMSO treated embryos at stage 12 showing wild type expression of Zic1, Zic3 and Pax3 respectively. (**B, D** and **F**) 60µM leflunomide treated embryos at stage 12 also showing wild type expression of neural plate border markers Zic1, Zic3 and Pax3 respectively. (**G**) DMSO treated embryo at stage 15 showing wild type Sox2 expression. (**H**) 60µM leflunomide treated embryo showing wild type Sox2 expression.

3.4.2 Neural crest specifiers

Following induction at the neural plate border the neural crest cells undergo specification. There are many genes shown to be involved in this process. To analyse the effect of leflunomide on neural crest specification in situ hybridisation experiments were carried out using a range of neural crest specifying genes. Embryos were treated with 60μM leflunomide and left to develop until stage 15 (or 13 for c-Myc) when they were fixed for in situ hybridisation of neural crest specifier genes.

The most striking downregulation for these neural crest specifiers was seen after in situ hybridisation of c-Myc and Sox10. Other neural crest specifiers showed some downregulation of expression but not as frequently as c-Myc and Sox10. c-Myc is an early neural crest specifier and starts to be expressed in the neural crest at stage 13. DMSO treated embryos showing wild type c-Myc expression (**figure 3.14A**) show expression in the early neural crest cells in the anterior of the embryo and also dorsal neural tissues. It is not specific for neural crest and plays a role in determining other tissue types. After treatment with leflunomide, the anterior patches of expression appear downregulated (**figure 3.14B**), leaving the dorsal neural expression unaffected. Sox10 wild type expression shown in **figure 3.14C** is specific for the neural crest cells at stage 15 and continues to be expressed in migrating crest cells where it plays a key role in neural crest differentiation. Along with c-Myc this neural crest specifier showed a striking downregulation of expression after leflunomide treatment (**figure 3.14D**), which was frequently detected in 47% of embryos (**figure 3.15**).

Other neural crest specifier genes tested include Slug (**figure 3.14E**), Sox9 (**figure 3.14G**) and FoxD3 (**figure 3.14I**). These all show specific expression in the neural crest cells. After leflunomide treatment these three neural crest specifiers show some downregulation of expression (**figure 3.14F, H and J**) however it is seen much less commonly, 14%, 7% and 6% of embryos displayed a loss of their expression pattern (**figure 3.15**). These results suggest that leflunomide is acting on neural crest cells during their specification and differentiation.

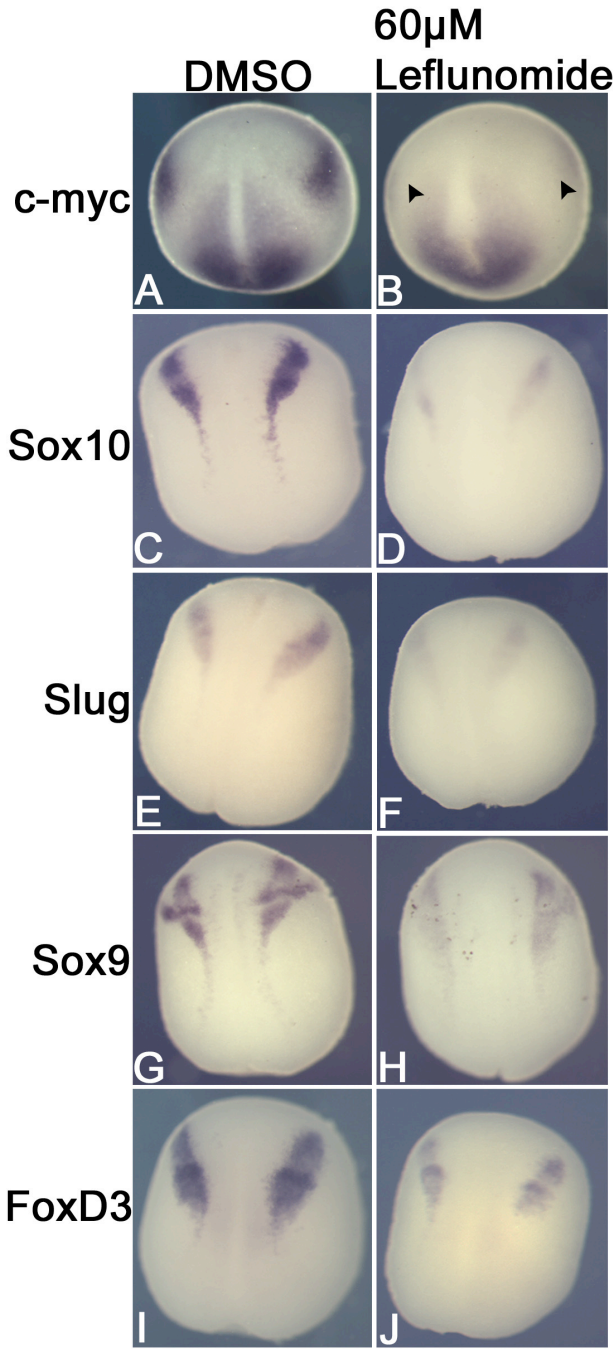

Figure 3.14: The effect of leflunomide of neural crest specifiers. (**A**) DMSO treated embryo at stage 13 showing wild type c-Myc expression. (**B**) 60µM leflunomide treated embryo showing specific downregulation of c-Myc in the neural crest cells (black arrow heads). (**C,E,G** and **I**) DMSO treated embryos at stage 15 showing expression of Sox10, Slug, Sox9 and FoxD3 respectively. (**D, F, H** and **J**) 60µM leflunomide treated embryos showing downregulation of expression of Sox10, Slug, Sox9 and FoxD3 respectively.

3.4.3 Quantitative analysis

Embryos undergoing in situ hybridisation after either DMSO (**figure 3.13** and **figure 3.14**) or 60μM leflunomide treatment (**figure 3.13** and **figure 3.14**) were scored as to whether the expression pattern seen appeared wild type, a partial loss of expression or a loss of expression. Examples of this are shown for FoxD3 expression in **figure 3.15 A**, **B** and **C**. Once all of the embryos had been counted and placed into these categories a graph can be plotted of the percentage of embryos showing these expression levels for each gene of interest (**figure 3.15**). The graph representing the results obtained after DMSO treatment (**figure 3.15 top panel**) shows that mostly the expression patterns seen are wild type. This was true for all of the genes tested. This is to be expected as this is the control group and so there is no reason for there to be any loss of expression. This is also reflected in **table 3.6**, which shows all genes to have above 90% wild type expression. Some partial loss is seen in below 10% of embryos, which is a result of embryo quality or *in situ* hybridisation efficiency.

The gene showing the highest frequency of expression loss is Sox10 (**figure 3.15 bottom panel**). Table 3.7 shows that 47% of these embryos had a loss of gene expression and 39% showed a partial loss. This is a very large proportion of these embryos. c-Myc also demonstrated a very high frequency of expression loss (**figure 3.15 bottom panel**) this gene saw a 30% loss of expression and a 37% partial loss (**table 3.7**). These two genes showed the clearest knockdown of expression. Other Neural crest specifiers (Sox9, FoxD3 and Slug) show some loss but always below a 10% frequency. Neural plate and neural plate border markers (Zic1, Zic3 and Sox2) showed 0% loss of expression (**table 3.7**) suggesting that leflunomide does not affect these areas of development. 5% of the Sox2 in situ embryos showed an expansion of expression, this is sometimes seen for neural plate markers when development of the neural plate border is disrupted. These results would suggest that leflunomide is having an effect on neural crest specifiers, predominantly c-Myc and Sox10.

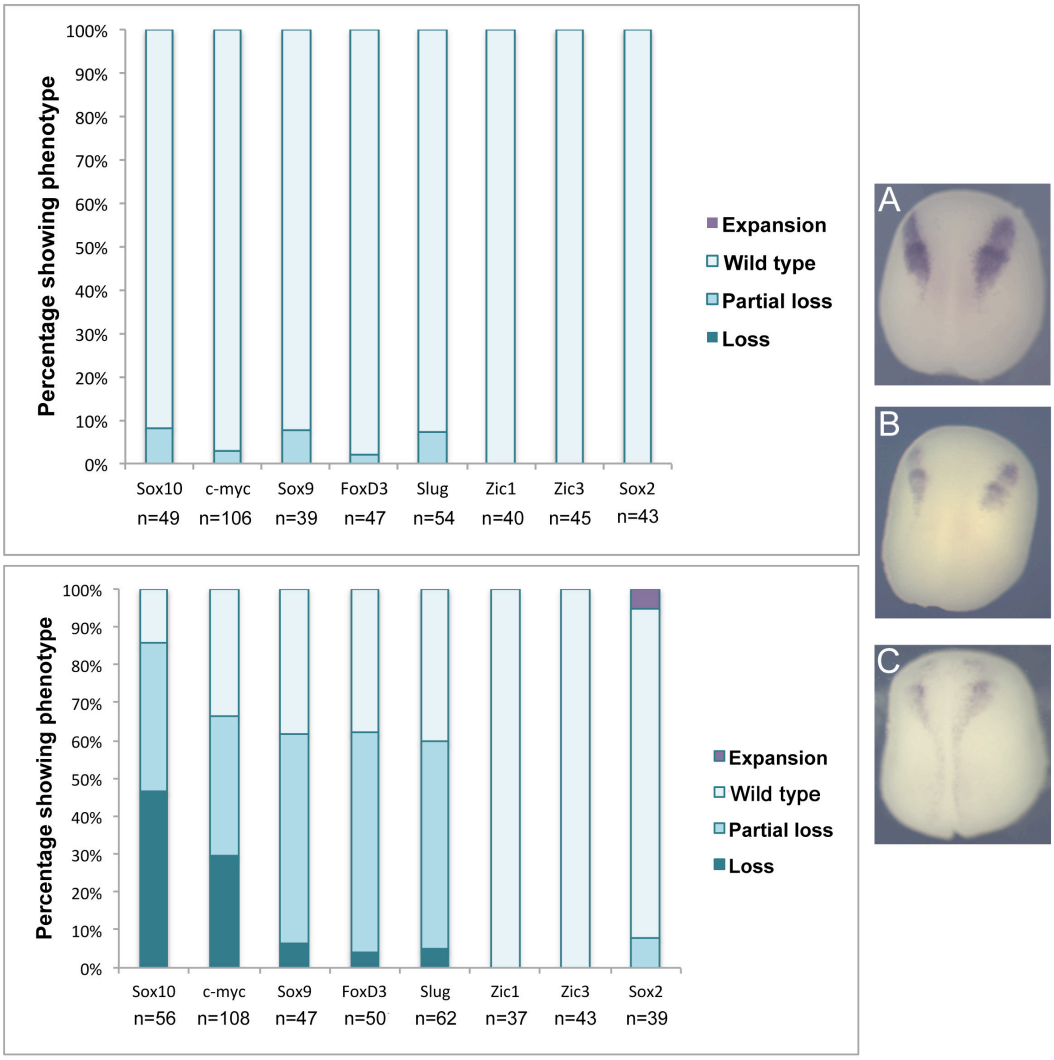

Figure 3.15: The percentage of embryos showing a loss or partial loss of neural plate, neural plate border or neural crest specifying genes. (**A**) Wild type expression. (**B**) Partial loss of expression. (**C**) Loss of expression. (Top panel) DMSO treated embryos are scored for wild type, partial loss, loss and expansion of expression after *in situ* hybridisation of Sox10 (n=49), c-Myc (n=106), Sox9 (n=39), FoxD3 (n=47), Slug (n=54), Zic1 (n=40), Zic3 (n=45) and Sox2 (n=43). (Bottom panel) 60μM leflunomide treated embryos are scored for wild type, partial loss, loss and expansion of expression after *in situ* hybridisation of Sox10 (n=56), c-Myc (n=108), Sox9 (n=47), FoxD3 (n=50), Slug (n=62), Zic1 (n=37), Zic3 (n=43) and Sox2 (n=39).

Table 3.6 Qualitative expression levels after DMSO treatment

	Total embryos	*Wild type*	*Partial loss*	*Loss*	*Expansion*
Sox10	*49*	*45 (92%)*	*4 (8%)*	*0 (0%)*	*0 (0%)*
c-Myc	*106*	*103 (97%)*	*3 (3%)*	*0 (0%)*	*0 (0%)*
Sox9	*39*	*36 (92%)*	*3 (8%)*	*0 (0%)*	*0 (0%)*
FoxD3	*47*	*46 (98%)*	*1 (2%)*	*0 (0%)*	*0 (0%)*
Slug	*54*	*50 (93%)*	*4 (7%)*	*0 (0%)*	*0 (0%)*
Zic1	*40*	*40 (100%)*	*0 (0%)*	*0 (0%)*	*0 (0%)*
Zic3	*45*	*45 (100%)*	*0 (0%)*	*0 (0%)*	*0 (0%)*
Sox2	*43*	*43 (100%)*	*0 (0%)*	*0 (0%)*	*0 (0%)*

Table 3.7 Qualitative expression levels after 60μM leflunomide treatment

	Total embryos	*Wild type*	*Partial loss*	*Loss*	*Expansion*
Sox10	*56*	*8 (14%)*	*22 (39%)*	*26 (47%)*	*0 (0%)*
c-Myc	*108*	*36 (33%)*	*40 (37%)*	*32 (30%)*	*0 (0%)*
Sox9	*47*	*18 (38%)*	*26 (55%)*	*3 (7%)*	*0 (0%)*
FoxD3	*50*	*18 (36%)*	*29 (58%)*	*2 (6%)*	*0 (0%)*
Slug	*62*	*19 (31%)*	*34 (55%)*	*3 (14%)*	*0 (0%)*
Zic1	*37*	*37 (100%)*	*0 (0%)*	*0 (0%)*	*0 (0%)*
Zic3	*43*	*43 (100%)*	*0 (0%)*	*0 (0%)*	*0 (0%)*
Sox2	*39*	*34 (87%)*	*3 (8%)*	*0 (0%)*	*2 (5%)*

3.5 Discussion

The aim of this chapter was to use leflunomide to investigate the role of transcriptional elongation in neural crest cell development. Initial experiments showed that treating *Xenopus* embryos with leflunomide reduced neural crest derivatives seen in tadpole stage *Xenopus* embryos. Embryos treated with leflunomide showed a reduction in the number of neural crest derived melanophores present in both *Xenopus laevis* and *Xenopus tropicalis*. The diploid *X.tropicalis* species demonstrated a more pronounced phenotype than the tetraploid *X.laevis* species. *X.tropicalis* showed much fewer melanophores and the ones that did form appeared rounded in shape unlike the wild type dendritic shape usually adopted by fully differentiated melanophores. This difference between species is likely to arise due to redundancy occurring in the tertraploid laevis species. If leflunomide is targeting certain neural crest specification genes, having 4 copies of each means leflunomide has twice as many to knockdown and so would therefore inherently be less efficient. Alternatively the phenotype seen in *tropicalis* may be more striking simply because this species are smaller and so the compound may penetrate easier. The phenotype seen in Zebrafish is also more very striking and these are very small diploid organisms.

To test the time at which leflunomide is having an effect, the compound was added at stage 1, stage 8 and stage 12. These time points were chosen as stage 1 gives the longest possible time in the drug. Stage 8 is just before gastrulation to highlight any general developmental issue, which may arise during gastrulation. Stage 12 is when neural crest cells start to be specified and so this is the time at which we want to target these cells. Adding the drug at stage 1 and 8 caused many general developmental defects. A very high percentage of embryos were shown to exhibit a loss of melanophores suggesting that adding at these early stages could prevent a large proportion of neural crest specification. However all of these embryos also appeared stunted and so it is difficult to assume if the loss of melanophores is due to loss of neural crest or general developmental delay or secondary effect. Adding

leflunomide at stage 12 gave a similar phenotype when added at stage 15 which would otherwise appear normal in shape and size whilst displaying few general development defects. This suggests that transcriptional elongation is important for neural crest development around the time of induction/specification.

Other experiments carried out in *X.laevis* confirmed that a reduced amount of neural crest derivatives are seen after leflunomide treatment. These included testing sensory neurons, after leflunomide treatment embryos underwent a 'poke or stroke' test to monitor their ability to respond to external stimulus. These embryos showed a statistically significant reduction in their ability to react. This could suggest that fewer sensory neurons are present in the embryo potentially due to a reduced amount of neural crest cells or an inability for them to differentiate properly. Similarly, there was seen to be a reduction in the amount of neural crest derived branchial cartilage in leflunomide treated embryos. This cartilage appeared disorganised after alcian blue staining suggesting a defect in the cranial neural crest development. It is clear from these experiments that treating with leflunomide causes a reduction in neural crest derivatives. The fact that there is a reduction seen and not a failure to migrate would suggest that the neural crest cells are not being induced, specified or differentiating properly.

Functional experiments looking at particular gene expression must be carried out in order to answer the question of how leflunomide is acting. Before these were carried out it was important to confirm the phenotype seen from leflunomide treatment with other drugs known to inhibit transcriptional elongation. This would also allow us to verify whether leflunomide was a good drug to use for further experiments in terms of its relative toxicity levels. So far leflunomide has shown not to cause excessive levels of developmental defects and the concentration at which it is used is not so high that it would be considered to be causing off target effects. To conduct these experiments chemical tests were carried out using the compound DRB, a drug used in many initial experiments characterising transcriptional elongation and pausing in various cell lines and also a CDK9 inhibitor with a high specificity for

CDK9 and not other kinases. One problem commonly seen with kinase inhibitors is that they target many different kinases inadvertently causing many unexpected off target effects. Both of these compounds demonstrated a loss of melanophores confirming the phenotype seen for leflunomide treatment and therefore provides further evidence for the action of leflunomide to be blocking transcriptional elongation rather than inhibiting DNA replication. They also however only gave a phenotype at very high concentrations and with many off target side effects. This rendered these compounds to be not as efficient as leflunomide and so leflunomide was considered appropriate to use in further experiments.

To assess the stage at which transcriptional elongation is important in neural crest development, leflunomide treated embryos were fixed and underwent in situ hybridisation for various neural plate border, neural plate and neural crest specifying genes. No effect was seen to the neural plate border genes Zic1, Zic3 and Pax3 suggesting that neural crest are induced at the neural plate border and do not require transcriptional pausing and subsequent elongation at this stage. Similarly the neural plate marker Sox2 was unaffected suggesting that regulation of transcriptional elongation is not important for general neural development. Differences in genes expression were only seen in genes involved in the specification and differentiation of neural crest cells.

Firstly c-Myc was shown to be drastically knocked down in leflunomide treated embryos but only in the specific neural crest regions at the anterior and of the embryos. c-Myc expressed in the dorsal neural tissues appeared unaffected. This could potentially make sense as discussed in the introduction, c-Myc is known to play a role in neural crest specification and is also implicated in transcriptional elongation. Studies which have knocked down Med26, the SEC component, have shown there to be a loss of c-Myc expression in embryonic stem cell lines [199]. Neural crest cells are a highly synchronous cell type and c-Myc is at the forefront of the specification of this cell type expressed very early on in neural crest specification.

Sox10 was also shown to be severely downregulated after leflunomide treatment. Sox10 is also a neural crest specifier and has

been shown to function directly downstream of c-Myc in the neural crest gene regulatory network [2]. It is also at the forefront of neural crest differentiation and continues to be expressed after specification in the differentiating crest. It is responsible for the differentiation of several cell types including melanophores and sensory neurons, which would explain the loss of these neural crest derivatives after leflunomide treatment. Other neural crest specifying genes were shown to have some downregulation or alteration to their expression pattern. These included Sox9, which is key for the differentiation of cranio-facial cartilage development. This slight knockdown and alteration of Sox9 expression could explain why the *Xenopus* craniofacial cartilage is present but appears disorganised. Partial knockdown and alteration of the expression of Slug, FoxD3 and Sox9 could be an indirect effect of the knockdown of c-Myc as these genes lie downstream of this in the neural crest gene regulatory network however there are many other signal which feed into them to regulate their expression such as BMP and FGF signals [2].

Chapter IV

RNA sequencing of animal caps treated with leflunomide

4.1 Introduction

The results obtained in chapter 3 suggests that leflunomide is acting on neural crest cells during the specification stage of their development. To analyse this further the following experiments were designed which will utilise the *Xenopus* animal cap assay to separate out neural crest tissue from neuro-ectoderm, ectoderm and mesoderm. The animal cap assay makes *Xenopus* an excellent model for neural crest development. This assay involves injecting the early one or two cell stage embryo with different RNAs into the animal pole to induce certain cell types and tissues. Injecting Noggin will induce neuro-ectoderm. Injecting Wnt and Noggin induces neural crest and leaving the embryos uninjected allows ectoderm to form. After injecting, embryos are left until stage 9 when the cells of the animal pole are removed and placed in media to grow to their desired stage, in this case stage 15 the time of neural crest specification.

In this chapter an assay has been adapted so that animal caps are placed in media containing DMSO as a control or 60μM leflunomide to dertermine by unbiased RNA sequencing which genes are affected by leflunomide treament. Animal caps first underwent PCR and *in situ* hybridisation experiments to test whether this approach would work. Firstly we wanted to insure that neural crest is sufficiently induced and secondly that leflunomide was able to knock down gene expression of neural crest specifiers. Based on these experiments working the main aim of this chapter was to send off RNA from these animal caps for RNA sequencing to enable us to analyse changes in RNA expression on a whole genome scale. From this we hoped to confirm some of the results already obtained, identify other genes involved in the process to give a better idea of the mechanism behind inhibiting transcriptional elongation, and finally to try to identify some novel genes potentially involved in neural crest specification and confirm these by *in situ* hybridisation.

4.2 Xenopus animal cap experiments

4.2.1. Determining amounts of Noggin and Wnt to inject.

Before animal cap experiments could be carried out it must first be determined how much of the neural crest inducing factors Noggin and Wnt should be injected to obtain neural crest tissue. For this an optimal amount is required which will allow the induction of neural crest and would also show the knock down of neural crest specific genes, which is to be expected after leflunomide treatment. Initially we tested 500pg of Noggin capped RNA and varying amounts of Wnt capped RNA, 50pg, 100pg and 150pg injected together into the animal pole of a one-cell stage embryo. After injection the embryos were left to reach stage 9 when an ectodermal animal cap explant was removed and placed in 60μM leflunomide or DMSO. This was also done for whole embryos and non-injected animal caps, which will go on to form default ectodermal cell types. To observe the induction of neural crest in these explants they underwent RNA extraction at stage 15 and subsequent cDNA synthesis which was used to carry out a PCR reaction with Slug, a commonly used marker for neural crest specification (**figure 4.1**).

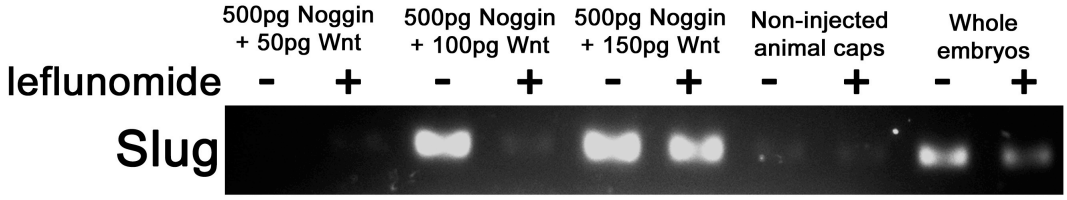

Figure 4.1: Testing the amounts of Wnt and Noggin to induce animal caps to give rise to neural crest. Animal caps were treated with or without leflunomide. cDNA made from these underwent a PCR reaction using Slug primers. When 500pg of Noggin and 50pg of Wnt were injected into one cell stage embryos the animal caps produced did not form neural crest. Using 500pg of Noggin and 100pg of Wnt induced neural crest and was knocked down by leflunomide treatment. 500pg of Noggin and 150pg of Wnt induced neural crest but no knock down was observed after leflunomide treatment. Non-injected animal caps show no slug expression. The whole embryo shows Slug expression but less than the induced caps and a small amount of knock down after leflunomide treatment.

From this result it could be determined that 500pg of Noggin and 50pg of Wnt was not sufficient to induce neural crest. 500pg of Noggin and 100pg of Wnt was sufficient to induce neural crest in the ectoderm

explants at a level that allowed the knockdown of Slug after leflunomide treatment. These amounts are therefore used for all experiments to follow. When the amount of Wnt was increased to 150pg no knockdown of Slug could be identified after leflunomide treatment suggesting that Wnt upregulation may rescue the action of leflunomide (**figure 4.1**). This is discussed further later. As expected the non-injected animal caps showed no slug expression indicating that animal caps had been cut successfully with no mesoderm contamination which would result in the formation of neuroectoderm or neural crest cell fates. After leflunomide treatment the whole embryo samples show some knockdown of Slug but not entirely indicated by the presence of a small band (**figure 4.1**). This is in keeping with the *in situ* hybridisation results obtained which suggest only a partial knockdown of Slug in the whole embryo. This form of PCR is only semi quantitative and so quantitative PCR should be carried out before conclusions are drawn about the levels of expression.

4.2.2. The effect of leflunomide on gene expression in animal caps induced to become neural crest, neuroectoderm and ectoderm

4.2.2.1. PCR results for Slug, Sox2, Keratin and Brachyury

Initial experiments were carried out using the same animal cap assay described. Embryos were injected at the one cell stage with 500pg of Noggin and 100pg of Wnt to induce neural crest, 500pg alone to induce neuroectoderm and non-injected to give default ectoderm cell fates. Whole embryos and all animal cap variants were added to either DMSO as a control or 60μM leflunomide from stage 9 when explants were removed until stage 15. cDNA synthesised from the RNA of these embryos were used to carry out PCR (**figure 4.2**) and Q-PCR (**figure 4.3**) for neural crest markers Slug and FoxD3, neuroectoderm marker Sox2, mesoderm marker Brachyury and housekeeping control gene histone H4.

The results from this showed that Slug is expressed in the animal caps induced to become neural crest after DMSO treatment however

when leflunomide is present Slug expression is seen to be knocked down (**figure 4.2)**. As expected caps induced to become neuroectoderm and ectoderm show very little Slug expression (**figure 4.2**). The whole embryo shows Slug expression with some knockdown of Slug after 60μM leflunomide treatment (**figure 4.2**). The same was seen for FoxD3 expression using Q-PCR. FoxD3 is expressed in the neural crest caps but this is significantly reduced after leflunomide treatment (**figure 4.3A**). FoxD3 expression is low in the neuroectoderm and ectoderm caps which is expected as FoxD3 is a neural crest specifying gene (**figure 4.3A**). It is highly expressed in the whole embryo and shows a reduction after leflunomide treatment (**figure 4.3A**) comparable to the partial knockdown seen using in situ hybridisation on whole embryos.

Sox2, the neuroectoderm marker predominantly showed expression in the animal caps injected with Noggin fated to become neuroectoderm (**figure 4.2 and 4.3B**). A small amount of expression is also present in the caps injected with both Noggin and Wnt. Both of these cap types showed no significant reduction in Sox2 expression after leflunomide had been administered (**figure 4.2 and 4.3B**). Sox2 was not expressed in the non-injected animal caps as was to be expected and was found to be expressed in the whole embryo with no effect after leflunomide treatment (**figure 4.2 and 4.3B**).

The mesodermal marker Brachyury was found to be expressed in none of the animal cap explants (**figure 4.2**). This is to be expected as these explants should only contain tissue from the upper ectoderm layer of the embryo and not the mesoderm layer. This lack of Brachyury expression indicated that the animal caps in this experiment were cut cleanly and therefore any expression of neural crest or neuroectoderm markers seen is due only to prior injection and not signals from contaminating mesoderm. Expression was seen in the whole embryo with no knockdown was caused by leflunomide treatment (**figure 4.2**). Finally, histone H4 was used as a positive control gene. Its expression is seen to be constant for all animal cap variant groups and the whole embryo and is not affected by the presence of leflunomide (**figure 4.2 and 4.3C**). This suggests that the same amount of RNA was used to make cDNA for each

sample and that the same amount of cDNA was loaded into each reaction making the results comparable. Water is used instead of cDNA for negative control groups and so no amplification of gene expression is seen in these PCR reactions (**figure 4.3**).

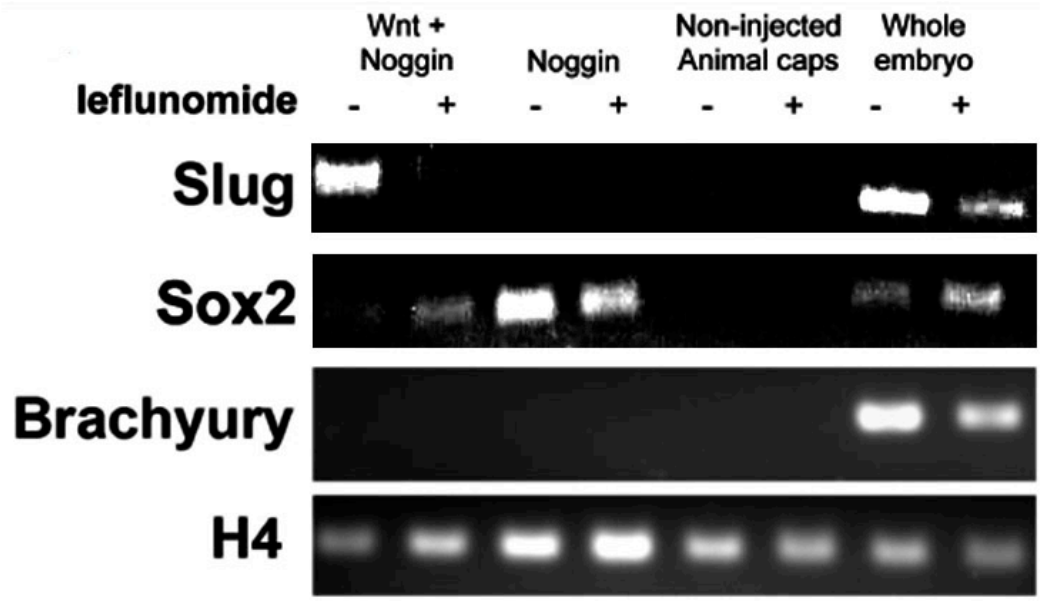

Figure 4.2: Animal cap experiments to observe the effect of leflunomide on Slug, Sox2 and Brachyury using PCR. Slug, Sox2, Brachyury and Histone H4 expression for Noggin and Wnt injected animal caps, Noggin injected animal caps, non-injected animal caps and whole embryos with DMSO (-) or leflunomide treatment (+). Histone H4 was used as a housekeeping gene. The expression of this is constant in all sample types. Concentrations used are 500pg Noggin and 100pg Wnt.

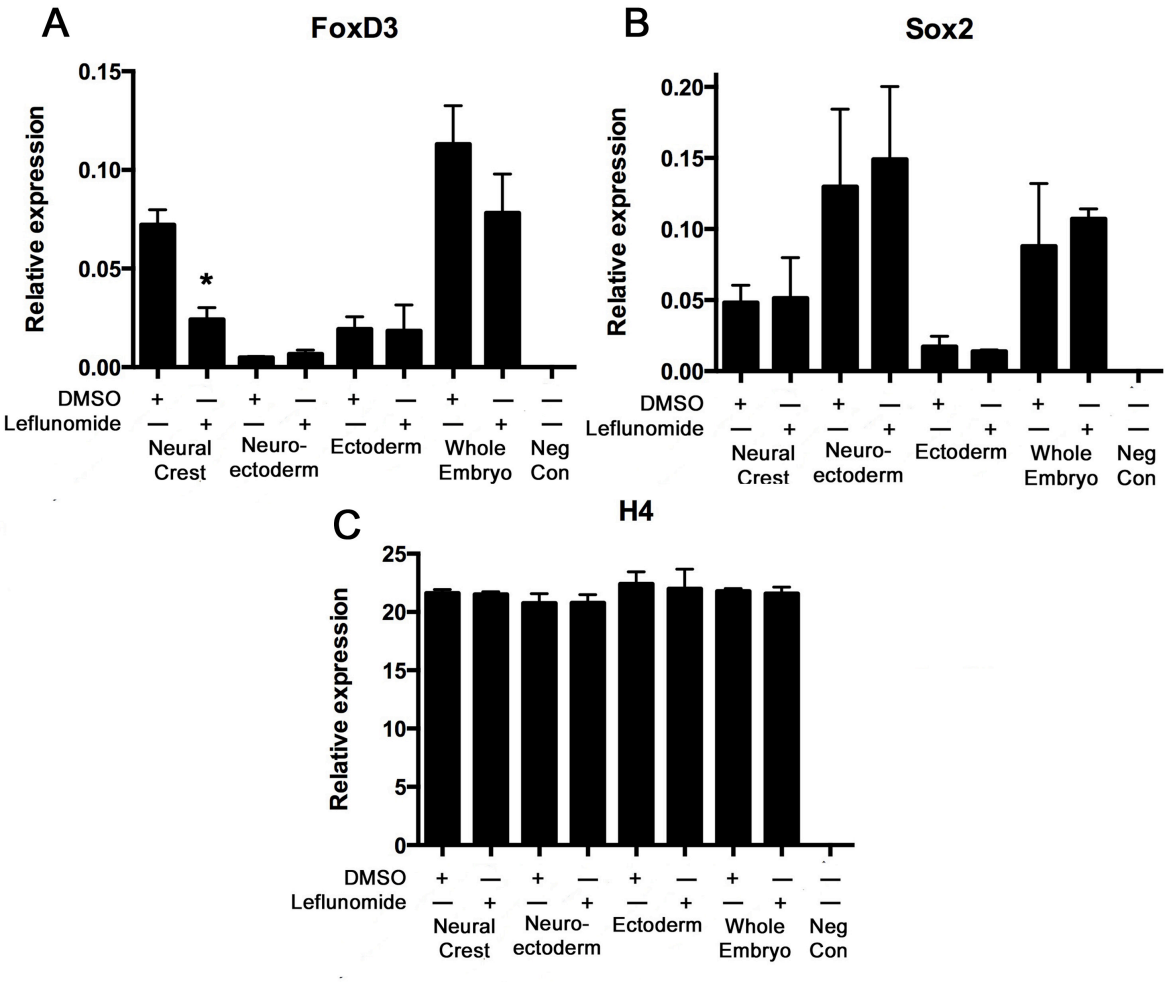

Figure 4.3: Q-PCR results showing the effect of leflunomide on FoxD3, Sox2 and Histone H4. (A) FoxD3 expression for neural crest animal caps, neuroectoderm animal caps, ectoderm animal caps and whole embryos with DMSO or leflunomide treatment. **(B)** Sox2 expression for neural crest animal caps, neuroectoderm animal caps, ectoderm animal caps and whole embryos with DMSO or leflunomide treatment **(C)** Histone H4 is used as a housekeeping gene, the expression levels for this are constant for all sample types to ensure the same amount of cDNA is present in each sample. This shows H4 expression for neural crest animal caps, neuroectoderm animal caps, ectoderm animal caps and whole embryos with DMSO or leflunomide treatment. For all genes analysed sigma water is used instead of cDNA as a negative control. Concentrations used are 500pg Noggin and 100pg Wnt. n=3 for all samples. *= $p<0.05$ using ANOVA

4.2.2.2. in situ hybridisation of leflunomide treated animal caps

Animal caps were injected and treated in the same way as the PCR experiments only once they had reached stage 15 they were fixed and underwent *in situ* hybridisation for the neural crest marker Slug. This experiment is another way of determining the effect of leflunomide on the transcription of neural crest specifying genes and can be used to back up PCR results. The result obtained was the same as that seen for the PCR experiment. Slug expression was detected in the animal caps induced to become neural crest (**figure 4.4A**) but this was abrogated due to the administration of leflunomide (**figure 4.4B**). No Slug expression was detected in the animal caps fated to become neuroectoderm or ectoderm as expected (**figure 4C-F**). Whole embryos were left to reach stage 15 to gauge the stage of the animal caps and then underwent a Slug *in situ* to show the probe used is specific for neural crest (**figure 4.4G and H**).

To verify that neural crest have been induced in the animal caps, some of the Noggin and Wnt injected caps were left to develop until the equivalent of stage 38 when neural crest derived melanophores are fully differentiated in the *Xenopus* tadpole. These animal caps should show expression of the melanophore marker dopachrome tautomerase (DCT) if they have been sufficiently induced to become neural crest. The DCT *in situ* carried out on these animal caps is shown in **figure 4.5**. The expression pattern appears speckled indicating many melanophores present on the caps (**figure 4.5A**). The melanophores may appear clumped together and densely compacted or they may appear individually as single melanophores (**figure 4.5B**). Expression of Slug and DCT in the animal caps confirms that neural crest cell fate has been sufficiently induced.

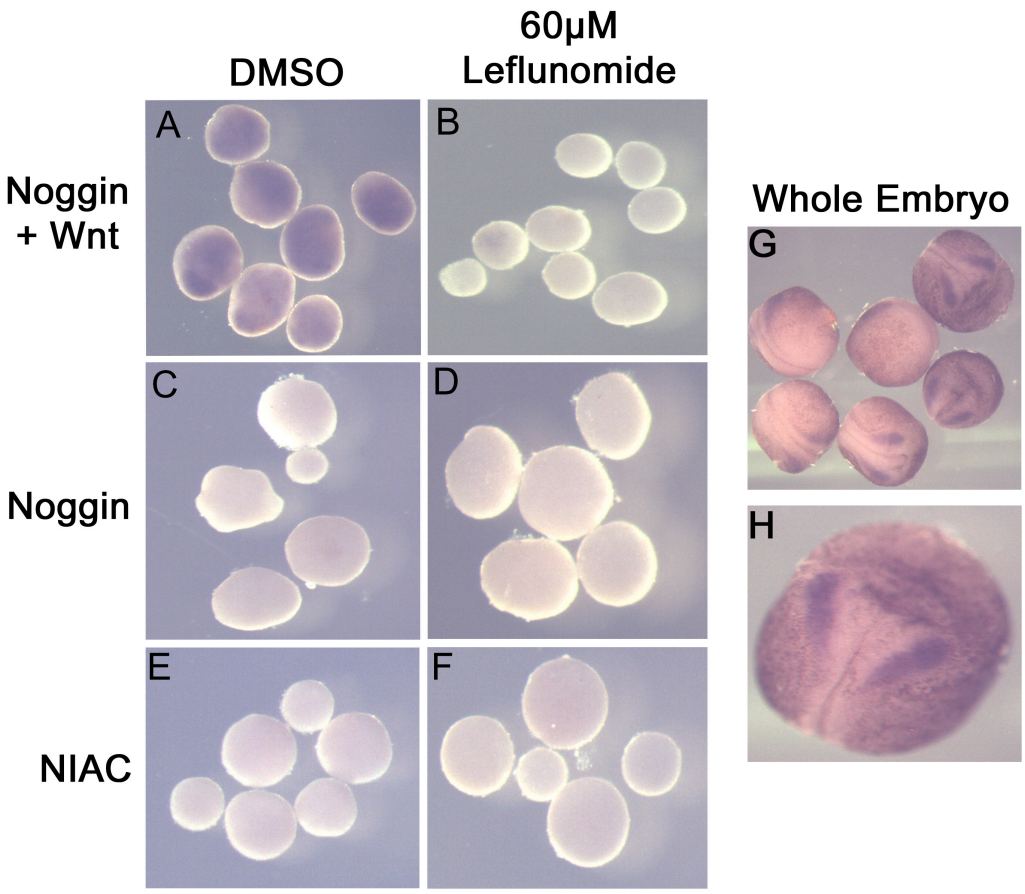

Figure 4.4: The effect of leflunomide on Slug expression detected by *in situ* hybridisation. Animal caps underwent *in situ* and were subsequently bleached to observe expression (**A**) DMSO control animal caps injected with Noggin and Wnt show Slug expression. (**B**) Leflunomide treated Noggin and Wnt injected animal caps show very little Slug expression. (**C**) DMSO control Noggin injected caps show no Slug expression. (**D**) Leflunomide treated Noggin injected caps show no Slug expression. (**E**) DMSO control non-injected animal caps show no Slug expression. (**F**) Leflunomide treated non-injected animal caps show no Slug expression. (**G**) Collective picture of whole embryo control illustrating the normal position of Slug expression and confirming the efficiency of the probe used. (**H**) Close view of one control whole embryo displaying Slug expression.

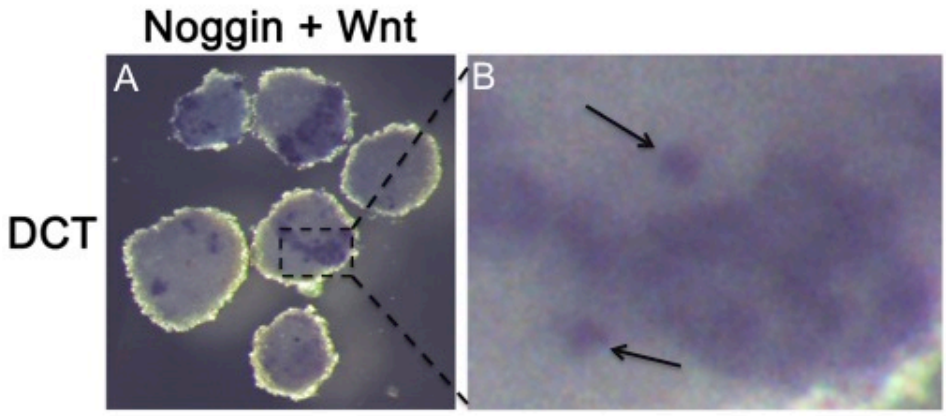

Figure 4.5: DCT expression in Noggin and Wnt injected animal caps. (A) Noggin and Wnt injected animal caps at stage 38 show DCT expression in melanophores. (**B**) An inlarged image of one animal cap shows DCT expression in individual melanophores (black arrows) and also clumps of melanophores expressing DCT.

4.3 Quality control of RNA sequencing

4.3.1 Samples sent for RNA sequencing

Once it had been established that the leflunomide experiment would work in animal cap explants it was decided that some of these samples should be sent for RNA sequencing. In order to make RNA sequencing libraries a minimum of 2µg of RNA is required. To be safe it was deemed advantageous to collect RNA in excess of this to ensure all of the libraries were made efficiently. RNA extraction of 40 animal caps on average yielded 1.5µg of RNA. 0.5µg of this was used to produce cDNA to test the samples for the correct gene expression by Q-PCR i.e. neural crest markers in the Noggin and Wnt injected samples. RNA was collected from Noggin and Wnt injected caps, Noggin injected caps and non-injected caps all with DMSO treatment or 60µM leflunomide treatment giving 6 sample types. Each experiment was carried out 3 times and the RNA remaining after confirmation by Q-PCR was pooled together to give the required amount of RNA to produce sequencing libraries. The quality of this RNA was tested by running on an agarose

gel and by nanodrop. The sample types including the amounts of RNA obtained and the nanodrop readings for each are shown in **table 4.1**.

Table 4.1 Samples sent for RNA sequencing

Sample	*Treatment*	*Total RNA/µg*	*260/280*	*260/230*
Noggin and Wnt (Neural crest)	*DMSO*	*4.6*	*1.81*	*2.10*
Noggin and Wnt (Neural crest)	*60µM leflunomide*	*2.7*	*1.86*	*1.67*
Noggin (Neuroectoderm)	*DMSO*	*3.1*	*1.77*	*2.13*
Noggin (neuroectoderm)	*60µM leflunomide*	*3.9*	*1.82*	*2.00*
Non-injected (Ectoderm)	*DMSO*	*5.2*	*1.85*	*1.89*
Non-injected (Ectoderm)	*60µM leflunomide*	*6.1*	*1.86*	*1.85*

4.3.2 Quality of cDNA libraries

RNA samples were sent to the high throughput genomics centre at the Wellcome Trust Centre for Human Genetics in the University of Oxford for library preparation and sequencing. One of the most important factors of obtaining reliable next generation sequencing data is having good quality libraries. Sequencing platforms require shearing of cDNA libraries by focused ultra-sonicators which will mechanically shear the DNA to give fragments of around 300bp which will undergo size selection and adapter ligation for use on the specific sequencing platform. For quality control the quantitiy and fragment size of these libraries was analysed using an Agilent 2100 bioanalyzer to give a smear analysis (**figure 4.6**) and an electropherogram (**figure 4.7**). These were carried

out by the Wellcome Trust Centre for Human Genetics at the University of Oxford.

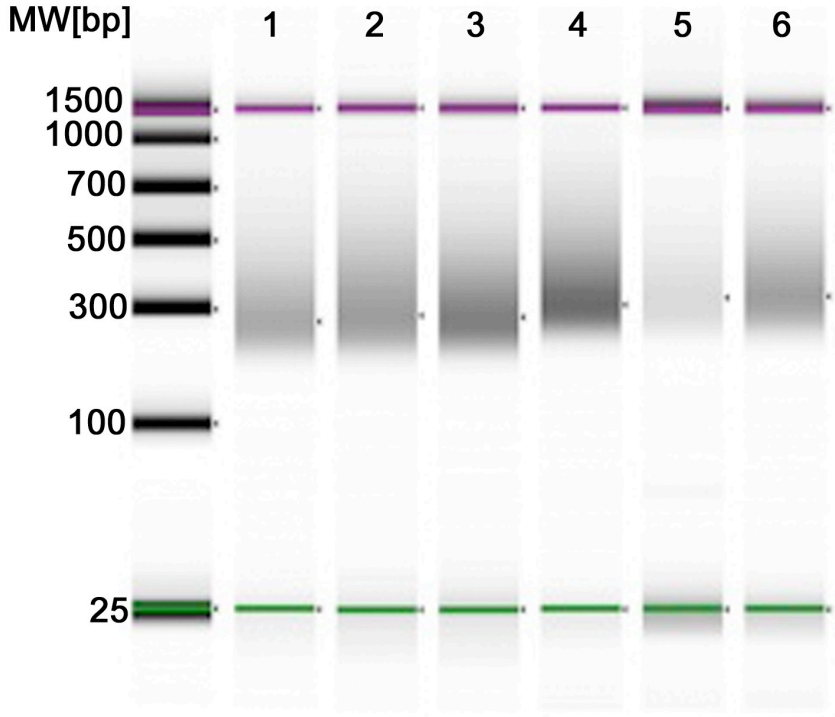

Figure 4.6 Smear analysis of sequencing libraries. Each lane represents a different cDNA library. 1 = Noggin and Wnt DMSO treated, 2 = Noggin and Wnt leflunomide treated, 3 = Noggin DMSO treated, 4 = Noggin leflunomide treated, 5 = Non-injected DMSO treated, 6 = Non-injected leflunomide treated. Purple lines show the upper marker. Green lines show the lower marker. Black arrow heads show average fragment size for each library at approximately 300bp.

Smear analysis is considered the most accurate method for analysing library quality, however it is good practice to compare smear analysis results to those obtained by electropherogram. For smear analysis 1µl of each cDNA library is run on a gel and from this the average fragment size can be determined by the darkest region of the smear. Here each library shows an average fragment size of around 300bp (**figure 4.6**), which is ideal for adapter ligation for next generation sequencing platforms. Also shown are the upper (purple line) and lower (green line) markers which are added to the samples to better gauge the library size.

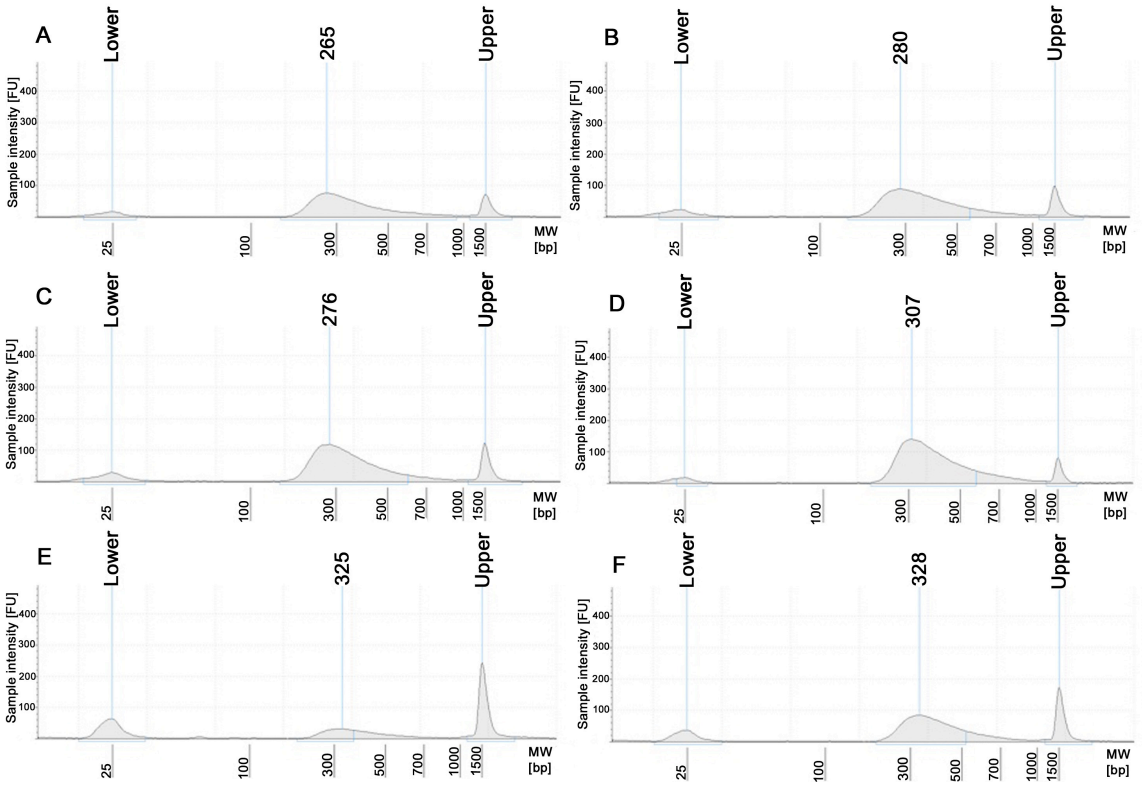

Figure 4.7 Electropherogram representing fragment sizes of sequencing libraries. (**A**) Noggin and Wnt DMSO treated average fragment size 265bp. (**B**) Noggin and Wnt leflunomide treated average fragment size 280bp. (**C**) Noggin DMSO treated average fragment size 276bp. (**D**) Noggin leflunomide treated averge fragment size 307 bp. (**E**) Non-injected DMSO treated average fragment size 325bp. (**F**) Non-injected leflunomide treated average fragment size 328bp. FU=fluorescent units. MW=molecular weight. Lower=lower marker. Upper=upper marker.

The cDNA libraries were also loaded onto a bioanalyzer chip, which gives a read out as an electropherogram (**figure 4.7**). Library samples were loaded with a fluorescent dye, which incorporates into double stranded DNA to give a readout in fluorescent units representing the size of the library fragments. Each library shows an average fragment size of approximately 300bp measured from the peak representing the library fragments (**figure 4.7A-F**). This confirms what was seen by smear analysis (**figure 4.6**). This again suggests good library quality as 300bp is an ideal size for sequencing platforms. The upper and lower markers (**figure 4.7**) were added as a control to library samples to give a relative view of library fragment sizes and to ensure the electrophoresis chip has run efficiently.

4.3.3. Quality of RNA sequencing

Analysis of the RNA sequencing results was done with Dr Simon Moxon, a bioinformatician in our lab. To assess the quality of the RNA sequencing results the amount of reads obtained for each gene in the *X.laevis* genome was plotted for the leflunomide treated samples against the untreated samples. The log of these values were plotted in a read distribution graph using R (**figure 4.8**) and assigned a colour based on the fold change found when comparing the treated against the untreated samples. Those genes showing no difference in fold change or very little difference are shown in yellow and red. Those that show differences in gene expression appear purple or blue depending on how great the fold change is. The ideal situation is to have most of your genes aligning well along the midline with a small percentage of genes deviating from this midline. If the graph displayed most of the genes deviating from the midline it would suggest that a large proportion of the expressed genes in the genome are affected by leflunomide treatment, which would not be specific or interesting.

Treated against untreated analysis was carried out for the three tissue types sent for sequencing (neural crest, neuroectoderm and ectoderm) and plotted as read distribution graphs shown in **figure 4.8A B** and **C**. All three graphs show little deviation from the midline of the plots. This is good as it indicates specific changes in gene expression across the genome and not general changes to the whole genome. The neural crest samples (**figure 4.8A**) shows the most points appearing blue in colour indicating a difference in gene expression of certain genes. This could either be genes upregulated (those appearing above the midline) or downregulated (those appearing below the midline). This was to be expected as previous experiments indicate that leflunomide treatment is mostly affecting neural crest development. A few changes in gene expression are also seen in the neuroectoderm sample (**figure 4.8B**). Interestingly there are almost no differences between the ectoderm samples, which shows very few blue points on the plot (**figure 4.8C**).

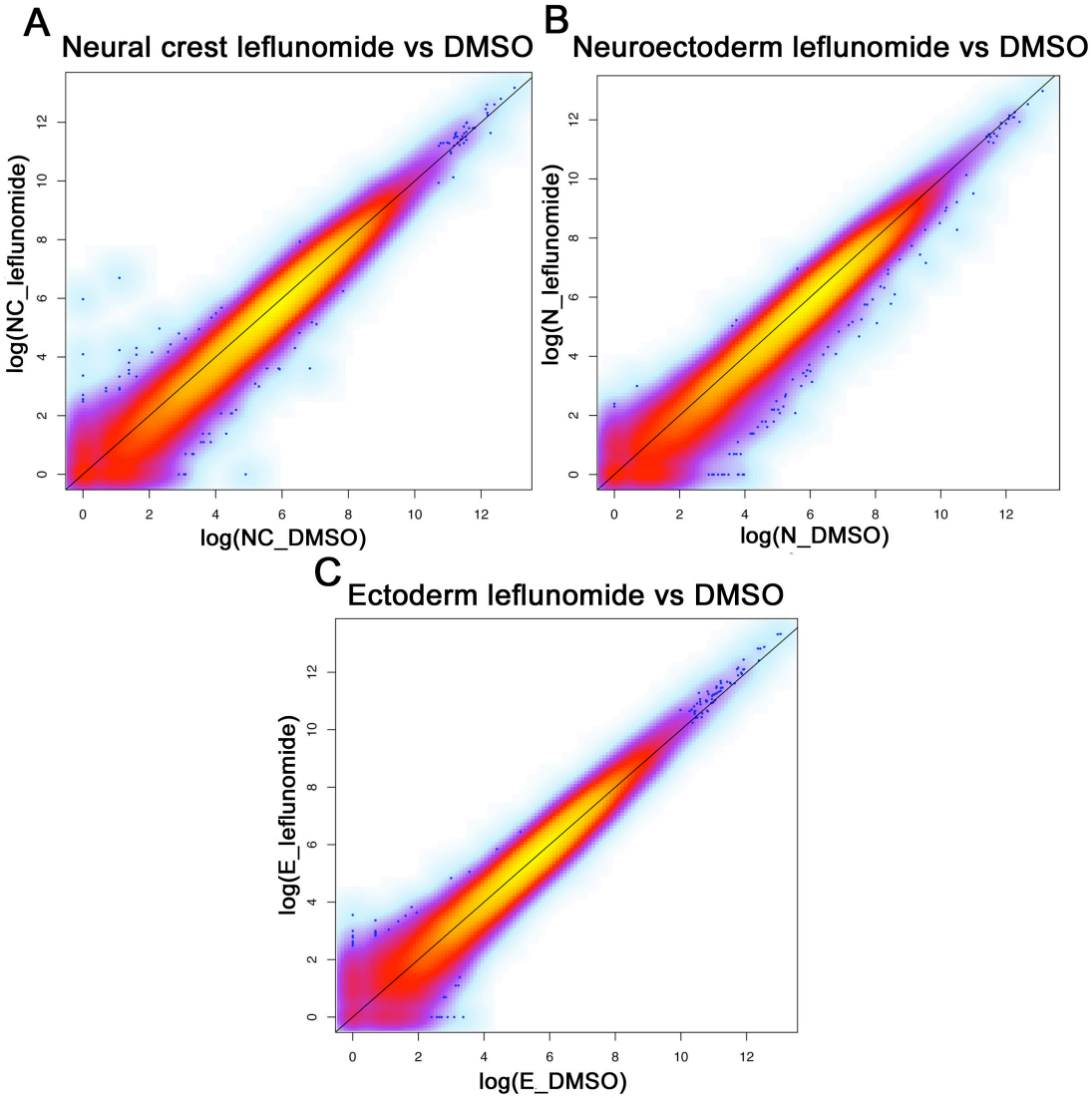

Figure 4.8 RNA sequencing read distribution plots. (**A**) Neural crest read distribution. (**B**) Neuroectoderm read distribution. (**C**) Ectoderm read distribution. The log of leflunomide treated reads are plotted against the log of DMSO treated reads. Red and Yellow indicates little to no fold change in expression. Purple and blue indicates some change and large changes in fold of gene expression.

4.4 Results of RNA sequencing

4.4.1 Genes downregulated in the neural crest samples

The RNA sequencing data were analysed and listed in order of genes showing the most significant downregulation or upregulation of expression after leflunomide treatment for each sample type. For this analysis only genes showing the most significant differences in expression based on their p value have been analysed and so the first 100 genes on the list were separated into two groups, those downregulated and those upregulated. These groups were then separated into categories based on gene function. The result of those genes found to be downregulated after leflunomide treatment are shown as a pie chart in **figure 4.9,** which shows the percentage of the overall genes analysed each category takes up. These categories are then broken down into a list of the individual genes comprising them, which can be seen in **table 4.2** and a full list in **appendix 2**.

The category which occupies the majority of genes downregulated in the neural crest animal cap samples are genes involved in neural crest development. This was to be expected as previous experiments have suggested that neural crest cells are very sensitive to leflunomide treatment and we have hypothesised that transcriptional elongation is important for neural crest development. 40% of the genes downregulated in the neural crest animal cap samples were involved in neural crest development (**figure 4.9**). Most of these were well-known neural crest specifiers such as Sox10, FoxD3 and Sox9. Some were genes shown to be involved in neural crest cell migration such as Myosin10, which very recently has been identified to promote cranial neural crest migration in the branchial arches [271].

Other migration genes downregulated include CXCR4 and Cd44 receptors. These are expressed by the neural crest cells and their ligands (Sdf1 and Hyaluronan) are expressed on the ventral ectoderm where chemotaxis promotes the movement of the neural crest cells into the branchial arches [59, 272]. Some of the genes put into the neural crest

development category are implicated to be involved in neural crest development in the literature however further investigation should be carried out to confirm this. Crisp2 has been shown to be upregulated in animal caps injected with Noggin and Wnt [273]. Riddle3/4 have been shown to be expressed in *Xenopus* stem cells so they may be present in the neural crest [274]. To further investigate these potentially novel neural crest genes, *in situ* hybridisations will be carried out to investigate the temporal and spatial expression of these.

Another category of genes seen to be downregulated in this sample type are heat shock proteins. This is interesting as previously described, the genes encoding heat shock proteins are classic examples of genes which will undergo polymerase pausing. These genes are thought to be primed in a paused state until heat shock occurs before undergoing transcriptional elongation. Many examples of paused heat shock proteins can be found in the literature and so this gives some support to the suggestion that leflunomide is predominantly targeting those genes, which are undergoing pausing and transcriptional elongation. In this sample type there are three different heat shock proteins, Hsp90aa1.1, Hsp105 and Hsp110, which are all seen to be sensitive to leflunomide.

Other genes downregulated include proteases normally expressed by neural crest cells to help them migrate through the extracellular matrix; genes such as Vimetin, which are associated with epithelial to mesenchymal transition; cell adhesion and signalling molecules which may normally allow the neural crest cells to communicate with each other; a purine synthesis enzyme is seen to be downregulated. This is potentially interesting as leflunomide is usually associated with the inhibition of pyrimidine synthesis. Finally BMP antagonists were downregulated. These are normally present to attenuate BMP signals allowing neural crest cells to form. Without such signals BMP is fully expressed which will not promote the induction of neural crest cells [12].

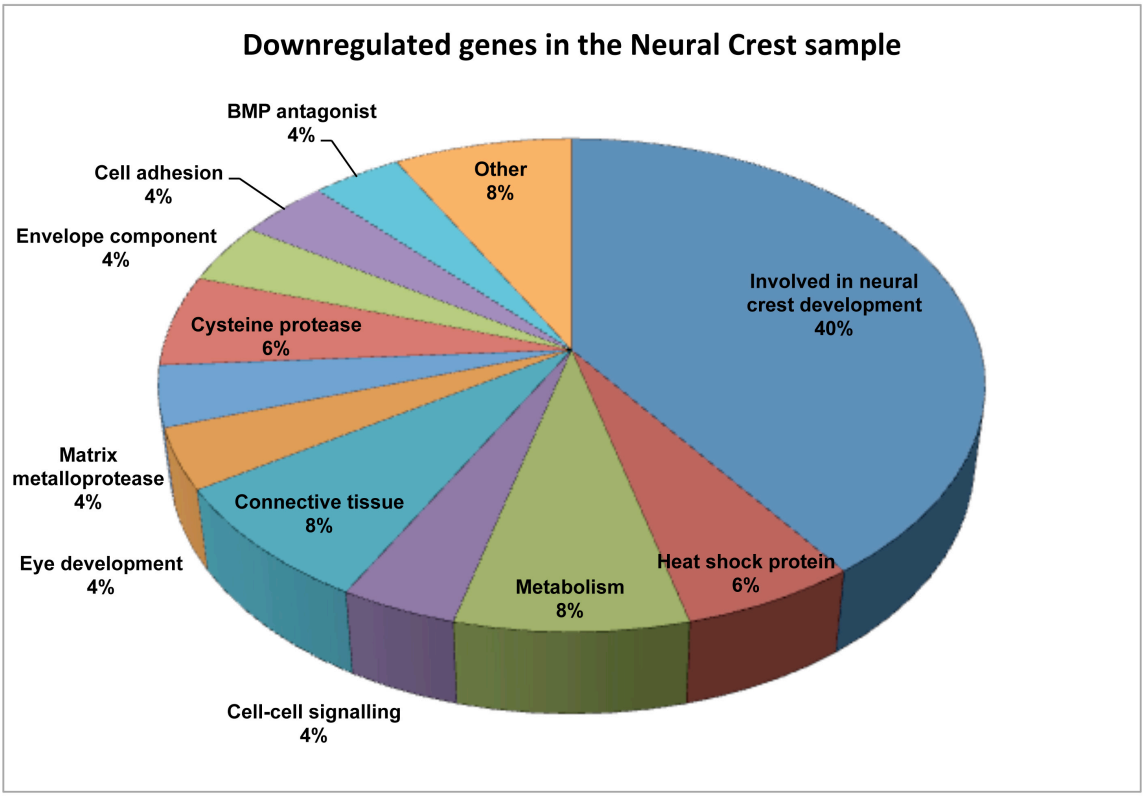

Figure 4.9 Pie chart showing the categories of genes down regulated in the neural crest animal cap sample after leflunomide treatment. Each gene downregulated in this sample type was put into a category and is displayed based on what percentage of the total genes looked at that category represents. Each slice of the pie chart represents a different category.

Table 4.2 Genes downregulated in neural crest animal cap sample after leflunomide treatment

Category	***Gene name***	***Description***	***p-value***
Involved in neural crest development	FoxD3	Neural crest specifier	2.20E-17
	Sox10	Neural crest specifier	3.48E-08
	Nr2f5	Wnt antagonist. Knockdown leads to loss of Sox9	3.39E-08
	p63	Wnt antagonist. Knockdown leads to loss of Sox9	1.22E-07
	Crisp2	Shown to be expressed in Wnt and Noggin injected animal caps. Needs further investigation.	9.81E-07
	Sox9	Neural crest specifier	0.000320735
	Sox8	Neural crest specifier	0.000417912
	Snail	Neural crest specifier	0.000501486
	Riddle4	Differentiation and migration of *Xenopus* embryonic stem	0.00064359

		cells. Needs further investigation	
	Tiarin	D-V patterning. Knockdown leads to upregulated FoxD3 and Twist	0.000713025
	Cd44	Neural crest migration	0.000710453
	CXCR4	Neural crest migration	0.000788999
	Slug	Neural crest specifier	0.001397235
	Myosin10	Neural crest migration	0.001393705
	Riddle3	Differentiation and migration of *Xenopus* embryonic stem cells. Needs further investigation	0.002592028
	Hoxa2b	Neural crest AP patterning	0.002949001
	Ap2-b	Neural crest specifier	0.003003123
	Tshirt1	Neural crest AP patterning	0.004662415
	Tshirt3	Neural crest AP patterning	0.000394662
Heat shock proteins	Hsp90aa1.1	Heat shock response gene	0.000331953

	Hsp105	Heat shock response gene	0.002679511
	Hsp110	Heat shock response gene	0.006790721
Metabolism	Rapgef2	GTP exchange factor	5.35E-05
	Cyctochrome b-245	NADPH oxidase	0.000523672
	Phosphofrucktokinase	Glycolysis	0.003049477
	glycosyltransferase-like protein	glycosylation of alpha-dystroglycan	0.006856805
Cell-cell signalling	Neuropilin 1	Membrane bound receptor	0.003447966
	Gap junction gamma 1	Diffusion from cell to cell	0.004515787
Connective tissue	Lectin	Carbohydrate binding proteins	2.98E-05
	Fibrillin	Elastic fibres	0.000220774
	Micro-fibrillar associated protein 2	Elastin associated microfibrils	0.000321755
	Versican	Proteoglycan	0.004977814
Eye development	Mafb	Lens development	1.62E-05
	Slit	Directs retinal ganglion	0.006416862
Matrix metalloprotease	Mmp28	Breakdown extracellular matrix	0.005479091
	Mmp13	Breakdown extracellular	0.001096916

		matrix	
Cysteine protease	Calpain 8	Proteolytic enzyme	0.002423052
	Cathepsin Z	Proteolytic enzyme	0.004530473
	Calpain 9	Proteolytic enzyme	0.005898228
Envelope component	Cornifilin	Component of cornified envelope	5.78E-06
	Sciellin	Component of cornified envelope	0.003969336
Cell adhesion	Neural adhesion molecule (NCAM)	Expressed on surface of neurons	0.00057836
	Claudin1	Tight junctions	6.03E-07
BMP antagonist	Jiraiya	BMP antagonist	0.000209636
	Follistatin	BMP7 antagonist	0.000908341
Other	Myocyte enchancer factor 2	Muscle development	0.0002553
	Gart	Purine synthesis	0.000837793
	Aquaporin3	Blood antigens	0.001956033
	Vimentin	Epithelial to mesenchymal transition	0.00349757

4.4.2 Genes upregulated in the neural crest samples

Perhaps the most striking thing seen in the genes upregulated after leflunomide treatment in the neural crest animal caps are the number of genes involved in cranial neural crest migration. These genes are not those usually expressed by the neural crest cells but by the surrounding ectoderm where they act as chemokines to promote the migration of the neural crest cells through the branchial arches (**figure 4.10** and **table 4.3**). Examples of these seen here to be upregulated include Sdf1 and Hyaluronan both of which are expressed in the ectoderm found ventrally to the branchial arches. These act as ligands to receptors expressed on the neural crest cells, the Cd44 and CXCR4 receptors and so promoting neural crest migration ventrally by chemotaxis [59]. Interestingly the receptors themselves usually expressed by the neural crest cells were seen in the list of genes downregulated. This might suggest that the neural crest cells have not had the chance to form neural crest and so form the surrounding ectoderm instead.

One gene we expected to see upregulated was cyctochrome p450 (**table 4.3**). This gene usually gets upregulated by cells in response to drug treatment to allow them to metabolise the drug. This is a good result as we want the drug to be metabolised by the animal cap cells in order for it to carry out its function. It is therefore expected that we see this increase in cyctochrome p450 as leflunomide is a small molecule compound which gets metabolised for its activity and so adding it to animal caps should upregulate this drug metabolism gene.

It was interesting to see that Hexim1 was in the list of upregulated genes. As described in the introduction Hexim1 is found bound to P-TEFb and in turn bound to 7SK snRNP when P-TEFb is in its inactive form. HEXIM1 is therefore acting as a kind of CDK inhibitor. Increasing the level of Hexim1 expression would suggest that more HEXIM1 is made and therefore P-TEFb is more commonly found in its inactive form implying that P-TEFb is unable to carry out its role to promote transcriptional elongation in the neural crest cells. More genes

are then held in a paused state. It was hypothesised that leflunomide was inhibiting transcriptional elongation however this gives a potential mechanism to this hypothesis.

Another interesting gene shown to be upregulated was Geminin. The Geminin protein has been previously implicated to regulate transcription through epigenetic modification. It is capable of regulating the activity of the polycomb repressive complex, which acts to trimethylate H3K27 to induce a repressive transcription state. Previous studies have shown that Geminin was able to repress neuronal differentiation through this mechanism and maintains neuronal cells in a precursor state. Overexpression of Geminin has been shown to upregulate neuroectoderm precursor markers such as Sox2 and Sox3 and downregulate genes involved in neuronal differentiation such as Neurod4 [275]. This could be interesting if this could be applied to neural crest differentiation as this RNA sequencing data has shown that genes involved in early neural crest formation are upregulated such as Wnt and BMP. Previous experiments have shown that leflunomide treatment causes a loss of neural crest derivatives and genes involved in early neural crest differentiation such as Sox10.

Many genes were seen to be upregulated which change the anterior posterior patterning of the embryos. Canonical Wnt signalling was seen to be upregulated in this neural crest sample after leflunomide treatment. Wnt signalling is known to be important for the induction of neural crest so it may seem strange that it should be upregulated when we are seeing a loss of neural crest derivatives. Recent studies have shown that Wnt signalling plays different roles in neural crest development depending on the stage at which it is expressed. Conditional β-catenin activation in mice has shown that if Wnt signalling is activated in the premigratory neural crest the number of melanophores decreases. If it is activated in migratory crest the craniofacial cartilage appears disorganised and less sensory neurons develop and the melanophores develop ectopically not appearing as they usually would [276].

This is the phenotype we see after leflunomide treatment in stage 38 embryos. Leflunomide treated embryos are seen to develop melanophores unable to migrate into the tail. These melanophores may be ectopically formed due to activation of Wnt/β-catenin signalling in the migratory neural crest. This also explains why we see a drastic loss in sensory neuron function and the abnormal craniofacial cartilage development also seen in mice with conditional activation of Wnt/β-catenin signalling in premigratory neural crest. It is probably because of this upregulation of Wnt that we see an upregulation of other genes involved in anterior posterior patterning. Some of these are known to be direct targets of Wnt such as Gbx2 and Hoxd1. Without the neural crest cells present the dynamic of the anterior embryo is completely thrown off course. Signals from the neural crest cells are responsible for inhibiting many posteriorising and placodal genes and so this could explain why these anterior posterior patterning and placodal genes are shown as being upregulated.

It is well established that intermediate levels of BMP are required for early neural crest induction along with Wnt and FGF signals from the underlying mesoderm. This attenuated BMP signalling is achieved by the secretion of BMP antagonists such as Noggin and Chordin. This same attenuated BMP gradient is also known to be important for starting neural crest cell migration as the intial signal promoting neural crest to undergo epithelial to mesenchymal transition. The upregulation of BMP may be as a result of the other neural crest migration abnormalities seen. TGFβ is associated with changing neural crest cell fate. Exposing neural crest cells to TGFβ signals will cause them to switch fate into a smooth muscle lineage [89]. It is possible that as leflunomide treatment is reducing the amount of neuron, melanophore and cartilage derivatives that these neural crest cells are moving down a different lineage such as this instead.

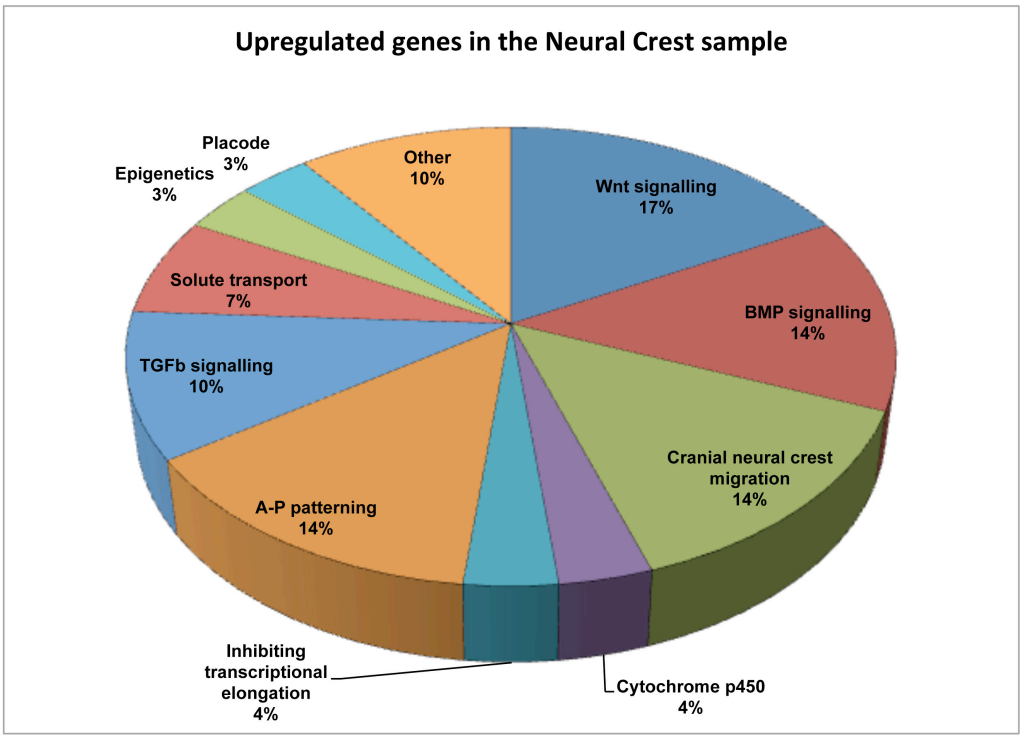

Figure 4.10 Pie chart showing the categories of genes upregulated in the neural crest animal cap sample after leflunomide treatment. Each gene upregulated in this sample type was put into a category and is displayed based on what percentage of the total genes looked at that category represents. Each segment of the pie chart represents a category.

Table 4.3 Genes upregulated in neural crest animal cap sample after leflunomide treament

Category	*Gene name*	*Description*	*p-value*
Wnt signalling	Sp5	Downstream of β-catenin	6.17E-05
	Wnt1	Canonical Wnt	0.000111897
	Frizzled 8	Canonical Wnt receptor	0.000512652
	Sp6	Downstream of β-catenin	0.006095883
BMP signalling	BMP7	BMP	1.58E-05
	Ventx2.1	Mediates BMP4 signalling	0.00027312
	Blimp1	Upregulates BMP signalling	0.000518871
	Sizzled (Frzb3)	Antagonises BMP signalling	6.47E-25
Cranial neural crest migration	Nkx3.1	Promotes correct migration of cranial neural crest cells	2.56E-05
	Sdf1	Cxcr4 ligand expressed in ectoderm surrounding NC to promote their migration	0.000150424
	Hyaluronan	Cd44 ligand expressed in ectoderm surrounding NC	0.001817622

		to promote their migration	
	GATA binding factor 3	Expressed in ventral surrounding ectoderm of branchial arches to promote NC migration	0.004069282
Cytochrome p450	Cytochrome p450	Drug metabolism	4.49E-15
Inhibiting transcriptional elongation	Hexim1	Binds to P-TEFb to keep it in an inactive state	0.003333565
Anterior posterior (AP) patterning	Anterior gradient 2	Setting up AP patterning	3.46E-05
	Hoxd1	Hox gene expressed anteriorly. Set up AP patterning	0.001101447
	Gbx2	Targetted by Wnt to pattern the anterior embryo	0.002898934
TGFβ	Pinhead	Nodal co-factor	0.000597899
	Cripto-1	Nodal co-factor	0.001215938
	Bambi	TGFβ receptor	0.004012539
Solute transport	SLC16A3	Cell surface solute transport	0.000374833
	SLC38A2	Cell surface solute transport	0.000639699
Epigenetics	Geminin	Expression of	0.000836454

		geminin antagonizes the expression of neuronal differentiation markers	
Placode	Tbx3	Expressed in lateral placodes	0.000228121
Other	CB1	Cell surface receptor	0.000182573
	Cidea	Apoptosis	0.001319887
	Stathmin	Microtubule dynamics	0.0038627

4.4.3 Genes downregulated and upregulated in the neuroectoderm samples

The neuroectoderm sample was analysed in the same way as the neural crest. Genes were listed in order of those showing the most significant downregulation or upregulation of expression after leflunomide treatment. For this analysis only genes showing the most significant differences in expression have been analysed and separated into two groups, those downregulated and those upregulated. The result of those genes found to be downregulated after leflunomide treatment are shown as a pie chart in **figure 4.11**. The categories shown in the pie chart are broken down into a list of the individual genes comprising them, which can be seen in **table 4.4**. Most of the genes affected in this sample type showed a downregulation of gene expression, only a few showed upregulation and so these are listed in **table 4.5** and have not been displayed as a pie chart.

The most striking thing seen in this sample is that the majority of genes downregulated are those which are involved in the development of the non-neural ectoderm. In early development the ectoderm is divided in two areas. Those closest to the Spemann organiser (at the dorsal side) which will receive the signals secreted from the organiser such as Noggin and Chordin and this region of ectoderm will form the neuro-ectoderm. The region of ectoderm found further from these signals will not be specialised into neuro-ectoderm and will form the non-neural ectoderm. In this sample we see many genes involved in the differentiation of the non-neural ectoderm and those expressed in the superficial ectoderm such as keratin, being downregulated.

This suggests that the neuroectoderm is expanding at the expense of the non-neural ectoderm. This is also confirmed as in the list of genes upregulated in this sample we see Sox1 which is a master regulater gene for maintaining neuro-ectoderm in a progenitor state and not a differentiated one. Also we see Xbf-2, which functions to convert ectodermal cells into a neuroectoderm lineage. This expansion of neuroecotderm is often seen when neural crest cells are not present.

Neural crest cells normally restrict the expansion of the neuroectoderm into the neural plate border regions.

Many of the results obtained for this sample are similar to those obtained for the neural crest sample. Both sample types see a downregulation of genes involved in metabolism, solute transport and cornified envelope development. The reasons for this are still unclear. Both samples show an upregulation in the expression of cytochrome p450, which occurs as a response to the addition of a drug to the sample as cyctochrome p450 is associated with drug metabolism. Both samples also show differences in anterior posterior patterning genes however where they are upregulated in the neural crest sample they appear downregulated in the neuroectoderm sample. It is well known that disrupting neural crest development and the anterior signals such as Wnt and BMP will lead to alterations in the anterior posterior pattern of the embryo. Here we seem to see a reduction in the anterior structures as there are also many genes involved in cement gland formation, which appear downregulated. Lectins are highly expressed in the cement gland so this may also explain why these are downregulated.

Also interstingly there are many genes involved in blood development such as Alpha 1,3/4 fucosyltransferase Lewis 1,2 and B3gnt1 all involved in determinging antigens on the surface of blood cells. Also genes involved in maintaining blood cell pluripotency such as Elf1 and Et3vl and also Lapl02, which is involved in blood cell migration. This is not suprising as a loss of blood circulation phenotype is seen in Spt6 (a DSIF component) mutant Zebrafish. It is now well established through the work of several studies that erythropoiesis is regulated by RNA polymerase pausing and transcriptional elongation. TIF1-Ɣ will recruit the P-TEFb complex to erythroid genes such as Gata-1 to promote erythropoiesis and so it is logical that we see this downregulation of genes involved in erythropoiesis. It should however be mentioned that it is strange that these blood genes are expressed in the neuroectoderm sample and the reason for this is unkown.

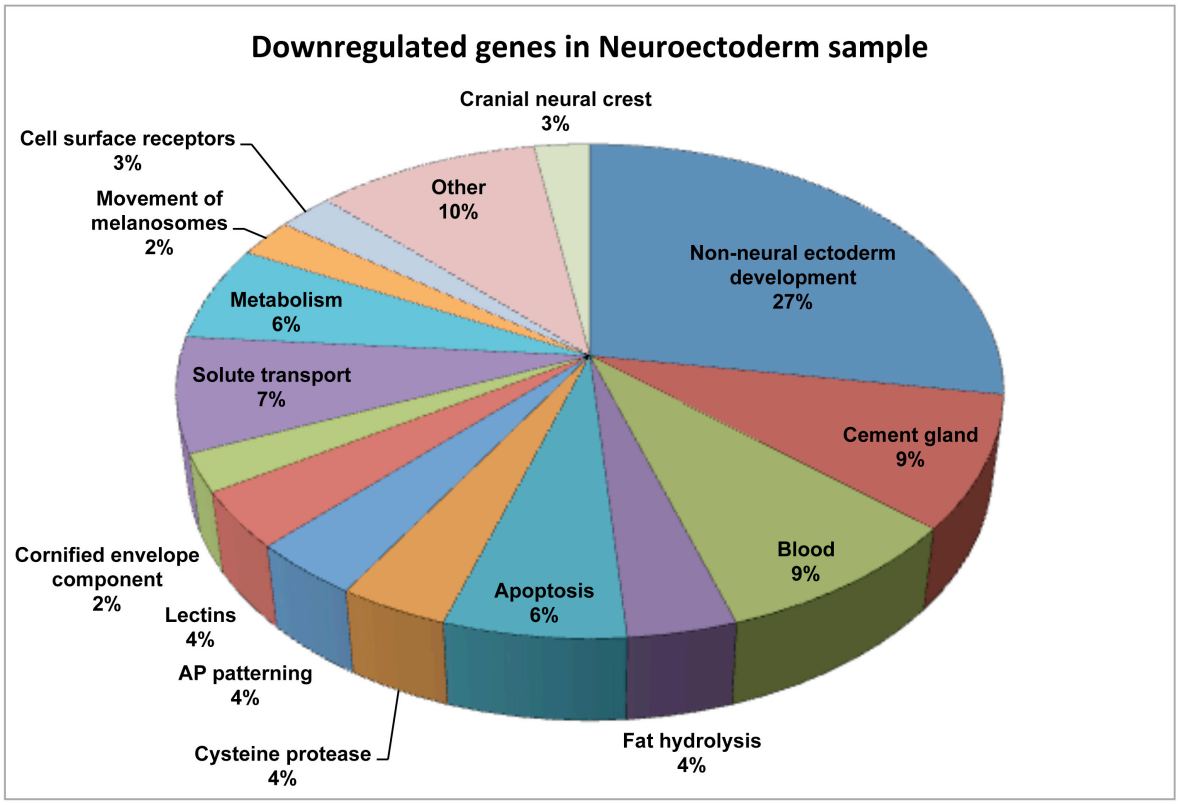

Figure 4.11 Pie chart showing the categories of genes downregulated in the neuroectoderm animal cap sample after leflunomide treatment. Each gene downregulated in this sample is sorted into categories based on the gene function. Each segment of the pie chart represents a category.

Table 4.4 Genes downregulated in neuroectoderm animal cap sample after leflunomide treament

Category	*Gene name*	*Description*	*p-value*
Non-neural ectoderm development	Otogelin	Mucociliary epithelial development	6.88E-22
	Epidermal type I cytokeratin	Protein found in outer skin	7.95E-21
	Keratin	Protein found in outer skin	2.29E-20
	B2 keratin	Protein found in outer skin	2.56E-18
	Grainyhead-like 3	Switches neuroectoderm fate to epidermal ectoderm	1.87E-13
	Ezrin	Ectodermal microvilli development	1.33E-12
	XIRG	Expressed in non-neural ectoderm	1.18E-09
	Znf750	Expressed in non-neural ectoderm	1.51E-09
	XK70 keratin	Protein found in outer skin	3.35E-09
	Kruppel like factor 4	Important for skin development	1.37E-08
	Cytokeratin type II	Protein found in outer skin	6.14E-08
	Grainyhead-like-1	Expressed in non-neural ectoderm. Gene silenced by Geminin	1.01E-07

	Type I keratin	Protein found in outer skin	2.08E-07
	Mid1ip1	Mucociliary epithelial development	2.67E-07
	Keratin 19	Protein found in outer skin	8.29E-07
	Esrp1	Epithelial cell specific splicing	1.11E-06
	Keratin 18	Protein found in outer skin	4.19E-06
	Eps8l1	Epidermal growth factor receptor	4.65E-06
	S1pr1	Endothelial differentiaition	8.71E-06
	Keratin 8	Protein found in outer skin	1.74E-05
	Tfap2c	Epidermal trancription factor	0.000197197
	Dlx3	Expressed in non-neural ectoderm	0.000400418
Cement gland	Muc2	Expressed in the cement gland	5.10E-18
	Fam3d	Expressed in the cement gland	2.07E-10
	Galnt6.2	Expressed in the cement gland	4.85E-10
	Neptune	Expressed in the cement gland	2.34E-06
	Gale	Expressed in the cement gland	3.42E-06
	Golm1	Expressed in the cement gland	5.81E-05

	Pitx1	Expressed in the cement gland	0.000213274
Blood	Alpha 1,3/4 fucosyltransferase Lewis 1	Blood cell antigens	2.09E-09
	KIT ligand	Expressed on blood cells	1.75E-07
	B3gnt1	Blood cell antigens	9.51E-05
	Elf1	Transcriptional programme of haemopoeititc stem cells	0.000216757
	Lapl02	Blood cell differentiation/migration	0.000286255
	Alpha 1,3/4 fucosyltransferase Lewis 2	Blood cell antigens	0.000405235
	Etv3l	Transcriptional programme of haemopoeititc stem cells	0.000431928
Fat hydrolysis	LipaseH	Hydrolyses fat	2.95E-09
	Lipid desaturase	Hydrolyses fat	2.42E-07
	Fa2h	Sphingolipid fatty acid hydroxylase	0.000352598
Apoptosis	Dapk2	Apoptosis	3.16E-09
	Deoxyribonuclease gamma	Apoptosis	4.29E-09
	growth arrest and DNA-damage-inducible	Causes DNA damage and	2.05E-05

		growth arrest by removing methylation marks	
	Mixed lineage kinase 2	Apoptosis	0.000327953
	Rassf6	Apoptosis	0.000335887
Cysteine protease	Calpain 1	Cysteine protease	1.06E-06
	Calpain 2	Cysteine protease	0.000176406
AP patterning	Anterior gradient 2	Anterior posterior patterning	2.81E-10
	Anterior gradient 1	Anterior posterior patterning	1.68E-06
	Np77	Anterior posterior patterning	7.53E-06
Lectins	Epidermal lectin	Carbohydrate binding protein	4.64E-23
	X-epilectin	Carbohydrate binding protein	4.18E-08
	Xgalectin-VIa	Carbohydrate binding protein	6.19E-05
Cornified envelope component	Sciellin	Cornified envelope component	3.19E-11
	Cornifelin1	Cornified envelope component	8.26E-05
Solute transport	Synaptotagmin 1	Membrane-trafficking protein	6.82E-07
	Slc7a4	Cationic amino acid transporter	1.15E-06
	Nipal4	Mg^{2+} transporter	2.07E-05
	Solute carrier family 18	Solute transport	2.52E-05

	SLC12A8	Cation-chloride cotransporter	6.09E-05
	Chloride channel ClC-5	Chloride transport	6.06E-05
Metabolism	Glutamine fructose-6-phosphate transaminase 1	Glutamate metabolism	2.02E-09
	Rab27a	GTPase	2.55E-08
	Rab25	GTPase	1.67E-05
	Arl4c	GTP exchange	8.94E-05
	Ectonucleoside triphosphate diphosphohydrolase 4	Hydrolyses nucleotide triphosphates	0.000133012
Movement of melanosomes	Rab27a	Part of a complex which moves melanosomes along actin	2.55E-08
	Melanoregulin	Moves melanosomes along actin	0.000215623
Cell surface receptors	Gpr160	G-protein coupled receptor	1.86E-06
	Tetraspanin 1	Transmembrane receptor	0.000137467
Cranial neural crest	Dlx2	Cranial neural crest migration	7.44E-05
	Nkx3.1	Cranial neural crest migration	0.000343902
Other	Cytidine monophospho-N-acetylneuraminic acid hydroxylase	Cell cell interaction	1.47E-07
	Peripheral myelin protein	Component of myelin	1.22E-05
	Annexin II	Diverse cellular functions	2.95E-05
	Rab3d	Regulates noggin secretion to inhibit	2.97E-05

		BMP	
	Calcium/calmodulin-dependent protein kinase (CaM kinase) II gamma	Calcium homeostasis	3.37E-05
	Sp7	Bone differentiation	5.53E-05
	Arginase	Urea cycle	8.31E-05
	Frrs1	Iron reduction	0.000165395

Table 4.5 Genes upregulated in neuroectoderm animal cap sample after leflunomide treament

Category	***Gene name***	***Description***	***p-value***
Neurogenesis	Xbf-2	Converts cells from epidermal to neuroectoderm	4.31E-08
	Sox1	Ectoderm differentiation into neuroectoderm	0.000598916
Muscle development	Murc	Muscle related extracellular matrix glycoprotein	0.000451026
Cytochrome p450	Cytochrome p450	Drug metabolism	0.005792073

4.4.5 Genes downregulated and upregulated in the ectoderm samples

Not many changes were seen in the ectoderm sample after leflunomide treatment. This was to be expected as leflunomide treatment appears to be relatively specific for neural crest cells and so if something as broad as the ectoderm were being significantly affected by preventing transcriptional elongation we would expect a much more severe and less specific phenotype at stage 38. The genes that are affected are listed in **table 4.6** which shows all the genes downregulated and **table 4.7** which shows all the genes upregulated after leflunomide treatment. It is immediately apparent that there are very few genes affected.

The interesting genes showing a downregulation include heat shock protein 90aa1.1. This was also seen to be downregulated in the neural crest sample. Heat shock proteins are classic examples of genes which will undergo polymerase pausing and so it is good to see these genes in the RNA sequencing data as it gives reassurance that leflunomide is in fact specifically inhibiting these genes which undergo pausing and transcriptional elongation. Also seen to be downregulated is CTP synthase 1-A, which is involved in pyrimidine synthesis. This result is expected as leflunomides main function is to inhibit pyrimidine synthesis.

When we look at the genes upregulated in this sample we see cytochrome p450 again. This is upregulated in all three samples as it is important for the metabolism of drugs. This again is good to see as it gives reassurance that the drug leflunomide as been sufficiently added to the sample. HEXIM1 is also upregulated, which again gives us evidence that leflunomide is acting to inhibit transcriptional elongation by inhibiting P-TEFb's action. Some of the other genes shown to be upregulated in this sample type were downregulated in the neural crest sample. These include MMP13, Claudin1 and lectin. This could suggest a possible cell fate switch between the neural crest cells and the non-neural ectoderm. This is possible as the neural crest cells also upregulated markers normally found in the ectoderm surrounding the crest cells. Further investigation into this is required.

Table 4.6 Genes downregulated in ectoderm animal cap sample after leflunomide treament

Category	***Gene name***	***Description***	***p-value***
Heat shock protein	Hsp90aa1.1	Heat shock protein	6.68E-07
Pyrimidine synthesis	CTP synthase 1-A	Enzyme involved in pyrimidine synthesis	1.15E-05
Actin binding	Coro1a	Actin binding protein	5.99E-05
Metabolism	Chromosome condensation 1	GTP exchange	0.000289312

Table 4.7 Genes upregulated in ectoderm animal cap sample after leflunomide treament

Category	***Gene name***	***Description***	***p-value***
Cytochrome p450	Cytochrome p450	Drug metabolism	2.79E-21
Matrix metalloprotease	Mmp13	Breakdown extracellular matrix	0.000164963
Cell adhesion	Claudin 1	Tight junctions	2.48E-07
Inhibiting transcriptional elongation	HEXIM1	Binds P-TEFb in its inactive form	3.10E-05
Anti-oxidant defence	Gstp1	Anti-oxidant defence	5.55E-05
Lectin	Lectin	Carbohydrate binding protein	0.000450621
Chitinase	Ctbs	Endoderm differentiation	0.000365471

4.7 in situ hybridisation of potential novel neural crest genes found in the RNA sequencing experiment.

4.7.1 in situ hybridisation of Crisp, Riddle3 and Riddle4

The neural crest sample of the RNA sequencing revealed some downregulated genes, which had very little information about them in the literature and only some suggestions about their potential role in neural crest development. These genes were Crisp, Riddle 3 and Riddle 4, all of which showed huge knockdown in expression after leflunomide treatment. To further characterise these genes, *in situ* hybridisations were carried out to see where and when they were expressed. These *in situs* were carried out at stages 15 and 18 when neural crest cells are specified (**figure 4.12**). In situs were also carried out at other stages but no specific expression patterns were detected and so are not shown here.

Crisp was shown to be expressed in the edges of the neural plate at the neural plate border at stages 15 (**figure 4.12A**) and 18 (**figure 4.12B**). The expression pattern is however very faint, which may reflect the level of Crisp expression or the quality of the probe used. Riddle3 and 4 were both seen to be expressed in the neural plate border of stage 15 embryos (**figure 4.12C and E**). The expression for both at stage 18 is however very interesting. Patches of very high expression appear at the neural plate border in the shape and position associated with neural crest cells (**figure 4.12D and F**). This expression appears to be very specific for neural crest. There is also expression seen in the surrounding ectoderm however not as highly expressed as in the neural crest region. It could be suggested from this *in situ* data that Crisp, Riddle 3 and Riddle 4 are all expressed in the neural crest however to confirm this further experiments should be carried out such as a double *in situ* with a known neural crest marker and functional studies using morpholinos to knock down the protein levels of these genes.

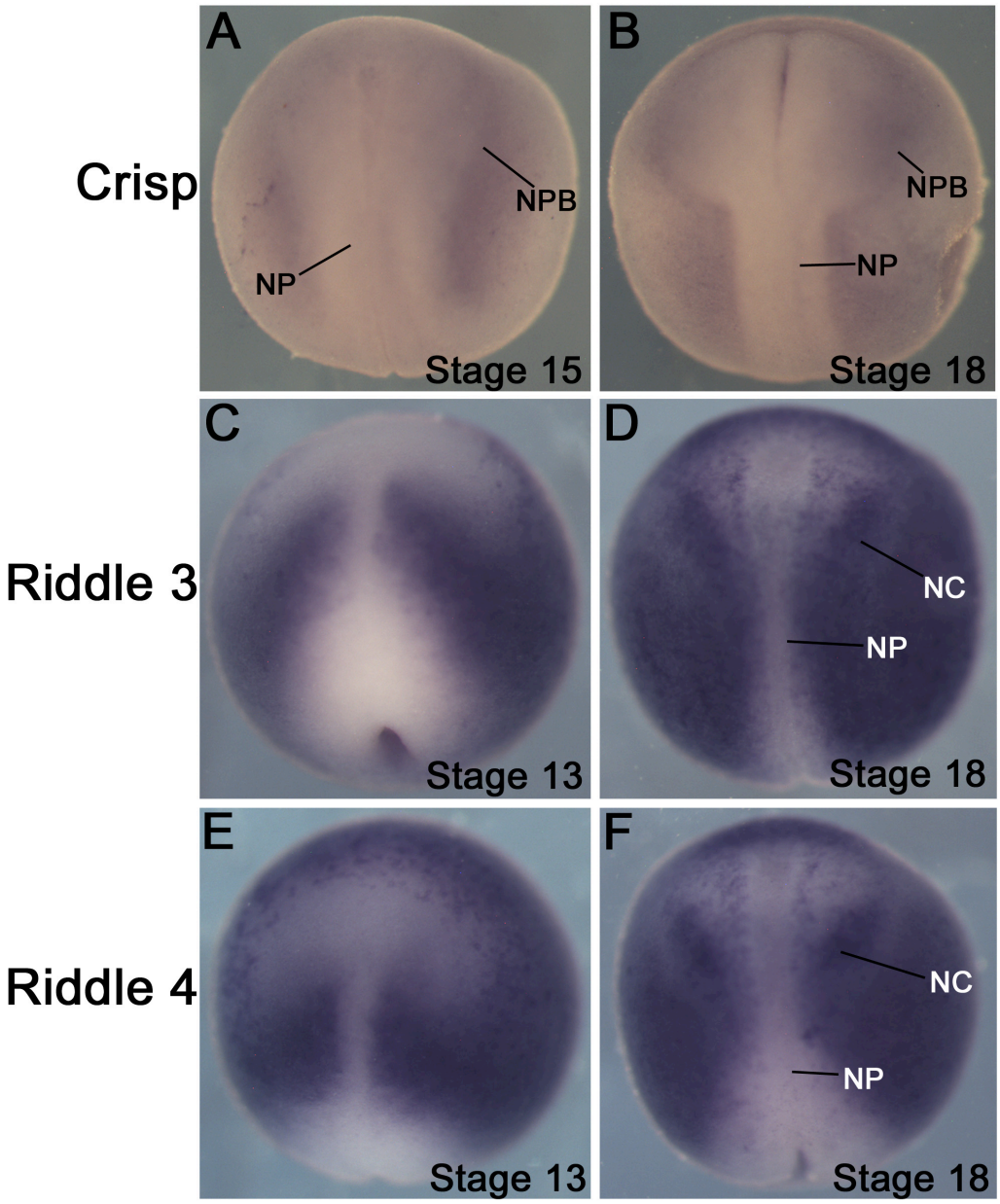

Figure 4.12 Novel neural crest genes. (A) *in situ* hybridisation for Crisp shows expression in the neural plate border at stage 15 **(B)** and at stage 18. **(C and E)** *In situ* hybridisation for Riddle 3 and 4 at stage 15 shows expression in the neural plate border. **(D and F)** *in situ* hybridisation for Riddle 3 and 4 show expression in the ectoderm and potentially in the neural crest at the neural plate border.

4.6 Discussion

The aims of this chapter were to establish an animal cap assay, which could be used to narrow down the investigation to analyse the effect of inhibiting transcriptional elongation specifically on neural crest cells. Animal cap assays are a useful tool when using *Xenopus* as an animal model as they can be induced to become a variety of different tissue types. To induce a neural crest cell fate the embryos should be injected with Wnt and a BMP antagonist, here we have used Noggin. To start it was necessary to establish a concentration of Wnt and Noggin RNA to be injected to sufficiently induce the neural crest cell fate. This was found to be 500pg of Noggin and 100pg of Wnt and so all subsequent experiments used these concentrations to induce neural crest. In addition to this, preliminary PCR and *in situ* experiments suggested that leflunomide was capable of knocking down neural crest markers in these neural crest animal caps. It would appear from these experiments that the knockdown of neural crest specifiers Slug and FoxD3 is much greater in the animal cap when compared to the experiments carried out in the whole embryos. This may be because the animal cap assay reduced the amount of signals, which would normally be received from the underlying mesoderm.

With a suitable animal cap assay designed, the main aim of this chapter was to obtain RNA sequencing from animal caps to determine genes affected by leflunomide treatment. For this 6 samples were produced; a neural crest sample, a neuroectoderm sample and a control ectoderm sample all with and without leflunomide treatment. The neuroectoderm sample was generated by the injection of Noggin alone and acts as a control to see which genes downregulated in the neural crest sample are neural crest specific and not globally expressed in neural tissue. The ectoderm sample acts similarly as a control to see whether inhibiting transcriptional elongation is specific to neural crest or whether it is a genome wide phenomenon.

The results obtained suggest that there is a lot of specificity for the inhibition of transcriptional elongation and neural crest cell

development. Many neural crest specifying genes were seen to be downregulated after leflunomide treatment. It is known that transcriptional elongation cannot be completely specific for neural crest development as many other studies have been carried out which show that it is important in a variety of other cell types. What is reassuring is that genes found to be paused in these other cell types and tissues also appeared in these RNA sequencing data. All of the samples displayed a loss of heat shock proteins, which were one of the first classes of genes to be shown to undergo RNA polymerase pausing. The neural crest sample showed two specific heat shock proteins Hsp105 and 110 which have not previously been shown to undergo pausing as they are both recently discovered and so there is not a great deal about them in the literature. Investigating the role of these and their ability to undergo pausing in neural crest cells could be interesting for follow on experiments.

Another cell type, which is often associated with the inhibition of RNA polymerase pausing is blood cells. Spt6 knockdown in Zebrafish has been shown to lead to a reduction in circulating blood cells and it is now thought that this occurs as the erythropoiesis specific transcription factor TIF1-Y is able to recruit the P-TEFb complex to genes involved in erythropoiesis such as Gata1. It was therefore not unexpected for us to see many genes involved in blood differentiation and migration appearing to be downregulated in this RNA sequencing data.

Many of the neural crest genes shown to be downregulated were those which were previously thought to be sensitive to leflunomide treatment in the whole embryo *in situ* experiments shown in chapter 3. These included Sox10, FoxD3, Slug and Sox9. c-Myc also showed a decrease by 2-fold but was not seen in the top most significant genes which seems surprising. There are possible explanations for this, firstly although the neural crest sample shows a decrease in myc expression, the neuroectoderm shows a large increase in myc expression and it is known that animal caps induced to become neural crest by Wnt and Noggin injection also show an increase amount of neuroectoderm gene expression and so it is possible that myc expression is knocked down specifically in the neural crest but upreguated in other tissue types. The

other suggestion is that myc is known to be directly downstream of Wnt and so the increase in Wnt expression seen in the neural crest sample could be increasing the myc expression. The whole embryo *in situs* of myc were carried out in embryos at stage 13 when the neural crest is pre-migratory. It is possible that something is happening between stage 13 and 15 to gradually increase Wnt expression and therefore gradually increase myc expression. I think it is possible that myc itself is undergoing pausing at stage 13 and this is causing an increase in Wnt signals as a feedback mechanism to rescue myc expression. This is just a theory and needs further investigation.

As mentioned for reasons which remain unclear the neural crest samples show an increase in Wnt expression. Wnt is known to play different roles in neural crest development depending on the time at which it is expressed. Early on in neural crest development it is required for induction. However, if it is expressed later on in neural crest development as the crest cells are beginning to migrate it almost has the reverse effect and decreases the amount of neural crest derivatives seen. Conditional mouse knock outs of Wnt activated specifically in the migratory neural crest show a loss of sensory neuron function, ectopic melanophores and disorganised cranio-facial cartilage. This matches the phenotype we see after leflunomide treatment in stage 38 *Xenopus*.

Finally, I believe it could be interesting to carry out follow on experiments to investigate the ability of the neural crest sample to downregulate receptors which they normally express (CXCR4 and Cd44) and in turn upregulate the ligands (Sdf1 and Hyaluronan) which are usually expressed by the surrounding ectoderm. This could indicate that the neural crest cells are able to switch fate into this surrounding ectoderm. It is possible that this change in ligand-receptor expression has been induced by the increase in canonical Wnt signalling in these cells. This would also co-incide with the alteration of cranio-facial cartilage seen when Wnt is upregulated in migratory neural crest cells. This again is just a theory and will require further experiments discussed later.

Chapter V

Investigating the expression and function of the P-TEFb complex in neural crest development

5.1 Introduction

The results obtained using leflunomide so far suggest that transcriptional elongation is a process important in the development of neural crest cells specifically at the point of their specification. To further investigate this, known components of the transcriptional elongation machinery were investigated with respect to *Xenopus* neural crest. The complex known to be responsible for promoting transcriptional elongation is the P-TEFb complex so it made sense to investigate where and when the expression of P-TEFb components occurred in *Xenopus* development. The components of this complex are Cdk9, the kinase responsible for phosphorylating the negative transcriptional elongation complexes and an associated cyclin. The cyclin most associated with Cdk9 is CyclinT1 however, there is also mention in the literature of Cdk9 forming a complex with CyclinT2 and CyclinK so these were also investigated [277-279]. Cdk9 has different alleles present in the tetrapoid *Xenopus* genome, known as Cdk9a and Cdk9b. Both of these alleles were investigated in these experiments.

To investigate the expression of these components *in situ* hybridisation was carried out to visualise the temporal and spatial expression patterns. Double *in situs* were also carried out to observe overlap in the expression of the P-TEFb components with a known neural crest marker. This would allow us to determine whether this complex is expressed in neural crest cells. Following on from this functional studies were carried out using morpholinos designed to prevent the translation of the P-TEFb components. Experiments were carried out to analyse the effect of inhibiting the translation of this complex on neural crest by assaying the development of neural crest derivatives such as melanophores, cranial facial cartilage and sensory neurons. In addition, the expression of genes involved in neural crest induction and specification were analysed after P-TEFb knockdown by *in situ* hybridisation.

5.2 The expression pattern of P-TEFb complex components

5.2.1 Cdk9a expression

Cdk9a is one of two Cdk9 alleles found in the *Xenopus* genome. To start off the investigation into the temporal and spatial expression of the P-TEFb complex, an *in situ* hybridisation of Cdk9a was carried out at different stages of *Xenopus* development from stage 10.5 up to stage 38 (**figure 5.1**). This experiment will allow us to see where Cdk9a mRNA is expressed at these stages as we predict that it would be expressed in the neural crest cells and potentially their migrating derivatives. During gastrulation at stage 10.5 Cdk9a was seen to be expressed in the surrounding ectoderm of the embryo but not in the involuting mesoderm and endoderm (**figure 5.1A**). The expression pattern appeared darker in the dorsal side at the dorsal blastopore lip. These dorsal regions will eventually give rise to dorsal structures such as neural crest and neural tube.

At neurula stages the expression pattern appears specific for the neural plate and neural plate border regions. This is first seen in embryos at stage 12.5 (**figure 5.1B**) and the expression pattern continues to be neural specific at stages 15 and 18 (**figure 5.1C** and **D**). At stages 15 and 18 the expression pattern appears to be in the edges of the neural plate at the neural plate border, which is the region in which the neural crest cells will form. In order to be certain if this expression is expressed in these regions a double in situ should be carried out with a known neural crest marker (see below). At stage 22 the expression of Cdk9a can be seen in the migrating neural crest of the branchial arches (**figure 5.1E**). This expression in the branchial arches also persists in the migrating crest in tailbud stages 26 and 32 (**figure 5.1F** and **G**). It is also seen to be expressed in the differentiated branchial arches at stage 38 once the embryos reach tadpole stage (**figure 5.1H**). This suggests that Cdk9a is potentially expressed in the neural crest cells during their specification and also in the migrating neural crest derivatives.

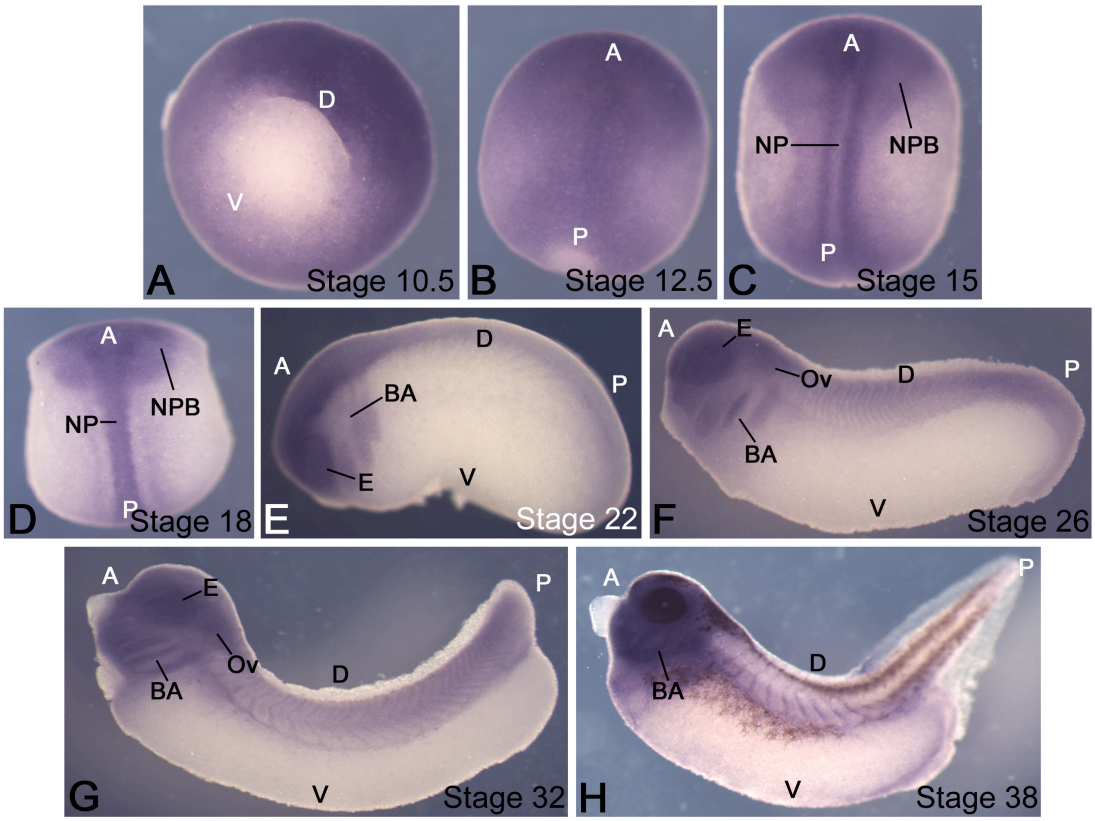

Figure 5.1 The expression pattern of Cdk9a. **(A)** Expression in the dorsal ectoderm at stage 10.5. **(B)** Expression in the early neural plate at stage 12.5. **(C,D)** Expression in the neural plate (NP) and neural plate border (NPB) at stage 15 and 18. **(E, F, G)** Expression in the branchial arches (BA), otic vesicle (Ov) and eye **(E)** at stages 22, 26 and 32. **(H)** Expression in the branchial arches at stage 38. A=anterior, P=posterior, D=dorsal and V=ventral.

5.2.2 Cdk9b expression

Cdk9b is the second Cdk9 allele in the *Xenopus laevis* genome and so an *in situ* hybridisation was also carried out on this allele. Similar to Cdk9a, Cdk9b acts as the kinase enzyme in the P-TEFb complex, which promotes positive transcriptional elongation [154]. This *in situ* was also carried out to gauge the spatial and temporal expression of the P-TEFb complex in *Xenopus* embryos from gastrula all the way up to tadpole stages (**figure 5.2**). At gastrula stage 10.5 the expression of Cdk9b can be seen in the dorsal ectoderm at the dorsal blastopore lip (**figure 5.2A**), which was also the case for Cdk9a. No expression is seen in the involuting mesoderm and endoderm. At neurula stages 13, 15 and 18 the expression of Cdk9b is seen in the neural plate and neural plate border where neural crest cells will form (**figure 5.2B, C** and **D**).

In tailbud stage embryos the expression of Cdk9b is seen in the neural crest derived branchial arches and also the eye and otic vesicle. This is shown in a stage 25 and 30 embryo (**figure 5.2E** and **F**). This expression pattern is the same as that seen for Cdk9a. Finally in a tadpole embryo at stage 38 the expression is seen in the migrated crest of the branchial arches (**figure 5.2G**). All of the expression patterns obtained for Cdk9b (**figure 5.2**) are comparable to those obtained for Cdk9a (**figure 5.1**). The expression seems to be in the neural plate border regions where the neural crest are formed and then it is still expressed in the neural crest derivatives as they migrate. To ensure that this expression does overlap with the neural plate border at neurula stages, a double *in situ* hybridisation should be carried out with a known neural crest marker (see below).

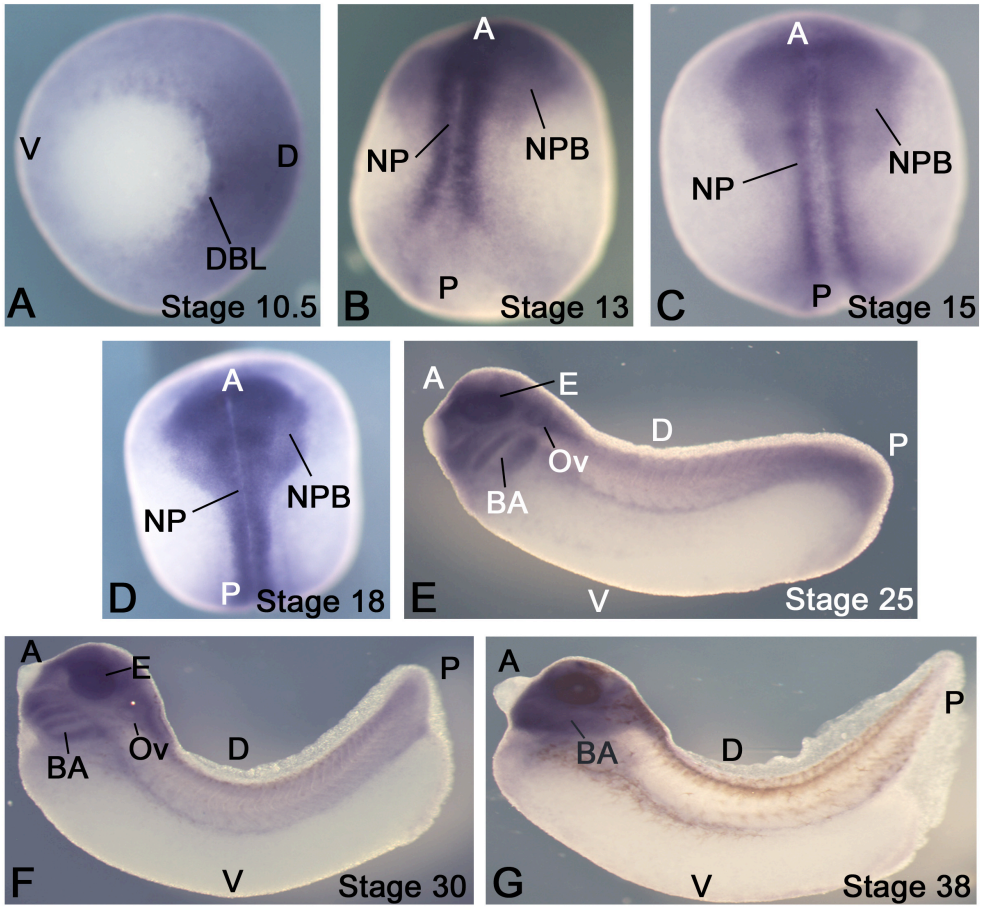

Figure 5.2 The expression pattern of Cdk9b. **(A)** Expression in the dorsal ectoderm at the dorsal blastopore lip (DBL) at stage 10.5. **(B)** Expression in the early neural plate (NP) and neural plate border (NPB) at stage 13. **(C,D)** Expression in the neural plate and neural plate border at stage 15 and 18. **(E, F)** Expression in the branchial arches (BA), otic vesicle (Ov) and eye **(E)** at stages 25 and 30. **(G)** Expression in the branchial arches at stage 38. A=anterior, P=posterior, D=dorsal and V=ventral.

5.2.3 CyclinT1 expression

CyclinT1 is the cyclin component most commonly found to be associated with Cdk9 in the P-TEFb complex. CyclinT1 is responsible for receiving developmental signals, which promote the activity of the P-TEFb complex, driving it to the correct gene to release RNA Pol ll from pausing. It also allows the connection of the P-TEFb complex to the super elongation complex. As CyclinT1 is also a component of P-TEFb it was thought to be important to carry out this *in situ* to compare the expression pattern obtained to that of Cdk9. This *in situ* was also carried out on *Xenopus* embryos ranging from gastrula stage 10 up to tadpole stage 38 (**figure 5.3**). The expression pattern obtained for CyclinT1 at gastrula stage 11 appears only in the ectoderm and not the mesoderm or endoderm (**figure 5.3A**). This should be confirmed by sectioning stage 10.5 embryos. This was the same expression seen for Cdk9a and b. At neurula stages 15 and 18 the expression pattern is confined to the neural plate and neural plate border (**figure 5.3B** and **C**).

In tailbud stage embryos at stage 26 and 32 the expression pattern is found in the branchial arches, otic vesicle and the eye (**figure 5.3D** and **E**). At tadpole stage 38 the expression still appears in the neural crest derived branchial arches (**figure 5.3F**). These expression patterns obtained for CyclinT1 match those obtained for Cdk9a and b at all stages of *Xenopus* development. Expression appears to reside in the neural plate border of neurula stage embryos, the region in which neural crest will form. This again must be confirmed using a double *in situ* of CyclinT1 with a known neural crest marker. Later on at tailbud stages 26 and 32 and tadpole stage 38, the expression is seen in the neural crest derived branchial arches. These results would suggest that the P-TEFb complex and therefore transcriptional elongation is important in the development of neural crest cells.

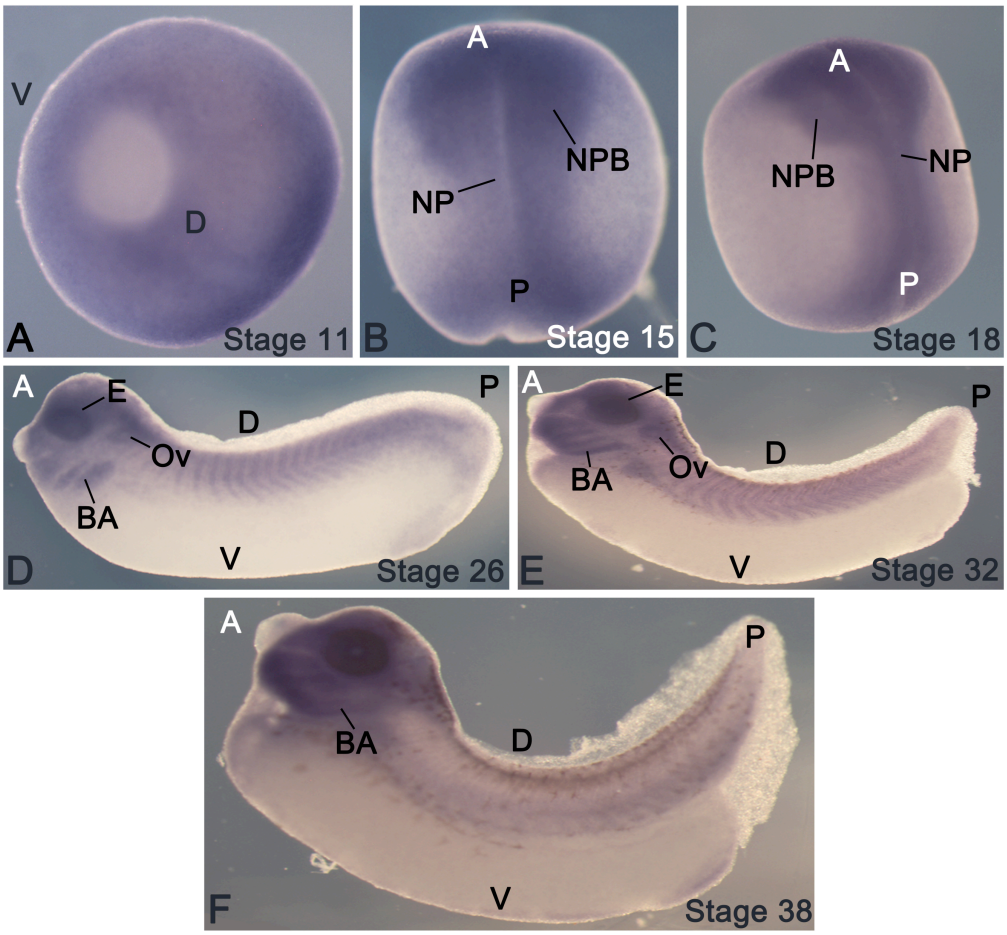

Figure 5.3 The expression pattern of CyclinT1. **(A)** Expression in the dorsal ectoderm at stage 11. **(B,C)** Expression in the neural plate (NP) and neural plate border (NPB) at stage 15 and 18. **(D,E)** Expression in the branchial arches (BA), otic vesicle (Ov) and eye **(E)** at stages 26 and 32. **(F)** Expression in the branchial arches at stage 38. A=anterior, P=posterior, D=dorsal and V=ventral.

5.2.4 CyclinT2 expression

CyclinT2 acts in the same way as CyclinT1. It has been shown to associate with Cdk9 acting as the cyclin associated with the enzymatic Cdk. CyclinT2 is however less commonly refered to in the literature as being in a complex with Cdk9. It is thought to be CyclinT1 which is predominantly associated with Cdk9 in the P-TEFb complex. This aside it was still deemed important for this study to investigate the temporal and spatial expression of CyclinT2 so that it could be compared to that of CyclinT1. An *in situ* hybridisation was carried out for CyclinT2 on Xenopus embryos ranging from gastrula stage 10.5 up to tadpole stage 38 (figure 5.4). The expression pattern obtained was the same as those obtained for the two Cdk9 alleles and CyclinT1. At gastrula stage 10.5 the expression was mostly seen in the dorsal ectoderm (**figure 5.4A**), the region of ectoderm fated to become neural structures. At the early neurula stage 12.5, the expression is still seen in the ectoderm but starts to be confined to the neural plate (**figure 5.4B**).

At neurula stages 15 and 17 the *in situ* expression pattern for CyclinT2 is seen in the neural plate and the neural plate border, the region in which neural crest cells will form (**figure 5.4C** and **D**). At tailbud stages 25 and 30 the expression is seen in the branchial arches formed from the migrating neural crest (**figure 5.4D** and **E**). Finally at stage 38 in tadpole embryos the expression can still be seen in the branchial arches as the crest have fully migrated and differentiated. The result obtained for CyclinT2 is comparable to the expression pattern of Cdk9 and CyclinT1. Much like these expression patterns, CyclinT2 appears to be expressed in the regions where the early neural crest cells are specified. This must be confirmed by double *in situ* hybridisation. The expression pattern is again seen in the migrating crest of the branchial arches much like Cdk9 and CyclinT1.

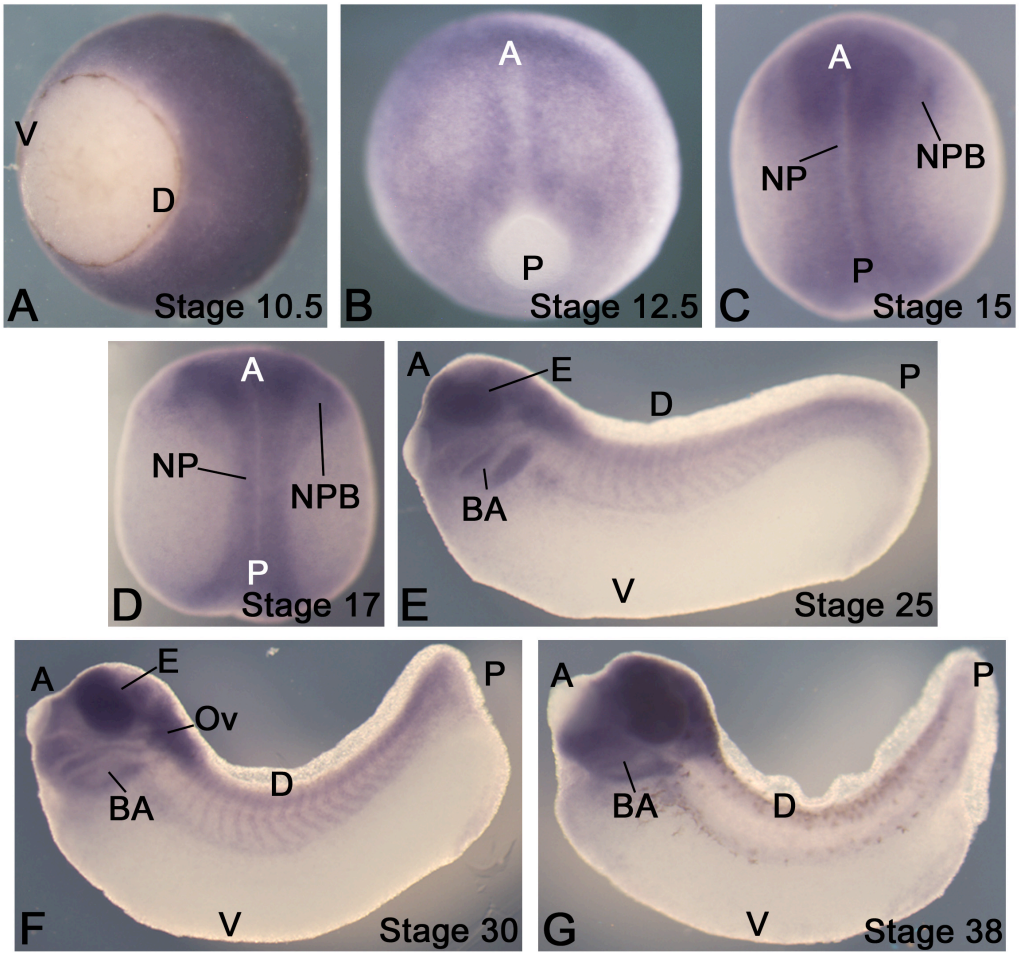

Figure 5.4 The expression pattern of CyclinT2. **(A)** Expression in the dorsal ectoderm at stage 10.5. **(B)** Expression in the early neural plate at stage 12.5. **(C,D)** Expression in the neural plate (NP) and neural plate border (NPB) at stage 15 and 18. **(E, F)** Expression in the branchial arches (BA), otic vesicle (Ov) and eye **(E)** at stages 25 and 30. **(H)** Expression in the branchial arches at stage 38. A=anterior, P=posterior, D=dorsal and V=ventral.

5.3 Double in situ hybridisation of P-TEFb components and neural crest marker Sox10

5.3.1 Whole embryo P-TEFb and Sox10 in situ hybridisation

In situ hybridisation experiments of the P-TEFb complex components, Cdk9a, Cdk9b, CyclinT1 and CyclinT2 demonstrated an expression pattern in the neural plate border region of neurula stage embryos. This region is where the neural crest cells form and become specified. As we are interested in whether P-TEFb and transcriptional elongation is important for neural crest development it is important to see if the expression of these P-TEFb components overlaps with the expression of neural crest cell markers. For this next experiment the P-TEFb components underwent an *in situ* hybridisation using NBT (nitro blue tetrazolium) to detect alkaline phosphatase activity. This gives the blue precipitate wherever the P-TEFb component is expressed. Immediately after this a second *in situ* is carried out for the known neural crest marker Sox10. Sox10 is visualised using fast red to detect alkaline phosphatase activity and so the neural crest regions are labelled on the embryo in red. This was carried out in stage 17 embryos for Cdk9a, Cdk9b, CyclinT1 and CyclinT2 (shown in blue) in combination with Sox10 (shown in red).

The results obtained suggest that each of the P-TEFb comonents are co-expressed in the same regions as the neural crest marker Sox10 (**figure 5.5**). This was seen to be true for Cdk9a (**figure 5.5A**), Cdk9b (**figure 5.5B**), CyclinT1 (**figure 5.5C**) and CyclinT2 (**figure 5.5D**). In the whole embryo the expression patterns appear to overlap however it is difficult to be certain, as it is unclear if the expression is found at the same depth into the embryo. When the red and blue precipitates overlap the colour seen is a darker brown/red. To be able to be sure of whether the expression seen is in the same plane in terms of depth and therefore within the same cells, these double *in situ* embryos were sectioned and the fast red detected by fluorescence making the colour difference easier to judge.

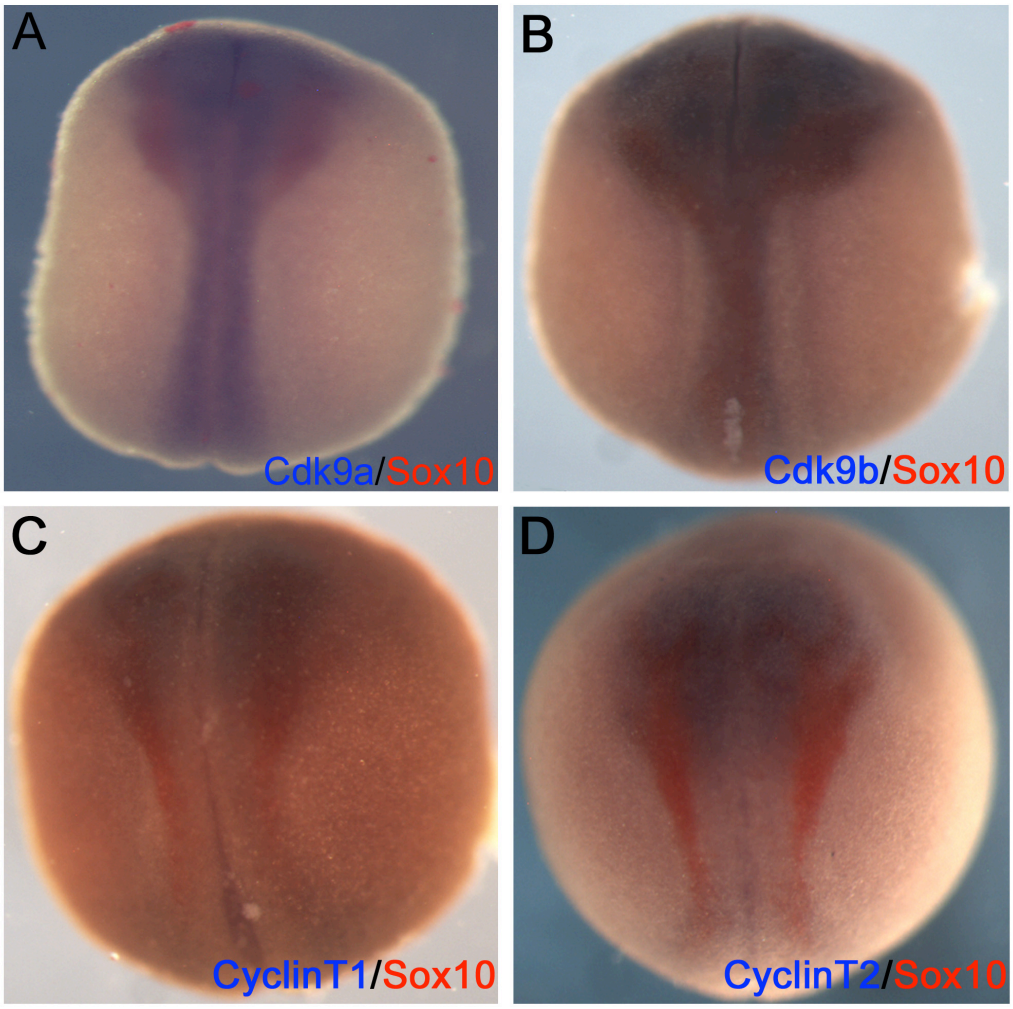

Figure 5.5: Double *in situ* hybridisation of P-TEFb component and neural crest marker Sox10. (A) Stage 17 embryo showing Cdk9a expression (blue) and Sox10 expression (red). **(B)** Stage 17 embryo showing Cdk9b expression (blue) and Sox10 expression (red). **(C)** Stage 17 embryo showing CyclinT1 expression (blue) and Sox10 expression (red). **(D)** Stage 17 embryo showing CyclinT2 expression (blue) and Sox10 expression (red).

5.3.2 Sectioned P-TEFb and Sox10 in situ hybridisation

Embryos which had undergone a double *in situ* for a P-TEFb component (blue) and Sox10 (red) were sectioned to more clearly see if there is an overlap in the two expression patterns. After sectioning, the blue expression pattern obtained after a Cdk9a *in situ* appears to be in the neural plate and at the edges of the neural plate, in the neural plate border (**figure 5.6A**). The expression for Sox10 in seen as two patches either side of the neural plate as Sox10 is only expressed in the neural plate border in the developing neural crest cells (**figure 5.6B**). When this is magnified further in the areas, which express Sox10 can be outlined (**figure 5.6Bi**) and seen to correspond with an area of blue expression representing Cdk9a (**figure 5.6Ai**). This would suggest that Cdk9a and Sox10 are co-expressed at the neural plate border within the neural crest cells.

This was also seen for the other P-TEFb components investigated here. Cdk9b expression appears the same as Cdk9a expression in the sectioned embryos. The expression is seen in the neural plate and neural plate border (**figure 5.6C**). The outlined region of Sox10 expression represents the area in which neural crest cells are found (**figure 5.6Di**). This region clearly overlaps with the blue Cdk9b expression outlined in **figure 5.6Ci**. The CyclinT1 expression (**figure 5.6E**) and the CyclinT2 expression (**figure 5.6G**) after sectioning can be seen in the neural plate and neural plate border. The expression of Sox10 in these sectioned embryos is seen in the neural plate border (**figure 5.6F and H**). When this region of Sox10 expression is outlined (**figure 5.6Fi and Hi**) and can be seen to overlap with the expression of CyclinT1 and T2 in the neural plate border (**figure 5.6Ei and Gi**). This suggests that components of the P-TEFb complex are co-expressed in with Sox10 within neural crest cells at the time of neural crest cell specification and may therefore be playing a role in the development of these cells at this time.

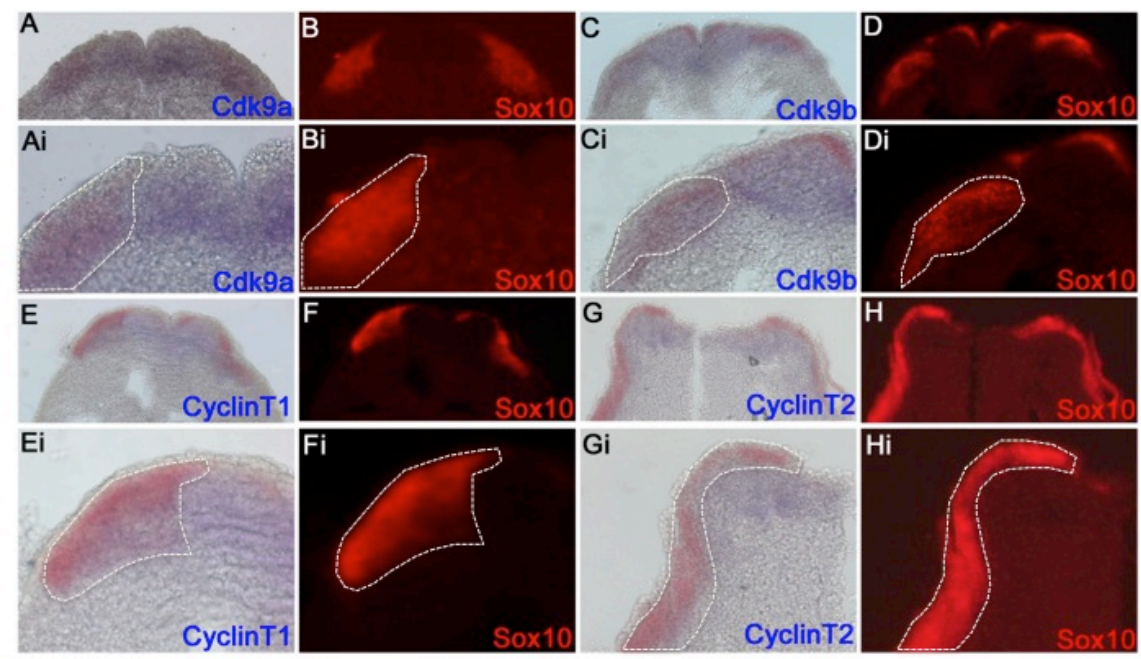

Figure 5.6: Sectioned embryos after a double in situ for P-TEFb components (blue) and Sox10 (red). (A) 5x magnification Cdk9a expression (blue) in the neural plate and neural plate border. **(Ai)** 20x magnification Cdk9a expression outlined in the neural plate border. **(B)** 5x magnification Sox10 expression. **(Bi)** 20x Sox10 expression outlined in the neural plate border. **(C)** 5x magnification Cdk9b expression (blue) in the neural plate and neural plate border. **(Ci)** 20x magnification Cdk9b expression outlined in the neural plate border. **(D)** 5x magnification Sox10 expression. **(Di)** 20x Sox10 expression outlined in the neural plate border. **(E)** 5x magnification CyclinT1 expression (blue) in the neural plate and neural plate border. **(Ei)** 20x magnification CyclinT1 expression outlined in the neural plate border. **(F)** 5x magnification Sox10 expression. **(Fi)** 20x Sox10 expression outlined in the neural plate border. **(G)** 5x magnification CyclinT2 expression (blue) in the neural plate and neural plate border. (**Gi)** 20x magnification CyclinT2 expression outlined in the neural plate border. **(H)** 5x magnification Sox10 expression. **(Hi)** 20x Sox10 expression outlined in the neural plate border.

5.4 Morpholino knockdown of P-TEFb components

5.4.1 in vitro translation

Once the expression of the P-TEFb compex components had been established the next step was to carry out functional experiments using morpholinos to block the translation of the P-TEFb components. This would prevent the activity of the P-TEFb complex therefore preventing transcriptional elongation from occurring. Morpholinos were designed for Cdk9a, Cdk9b and CyclinT1 refer to chapter 2 materials and methods for morpholino sequences. Before a morpholino can be used its activity must be established *in vitro* using an *in vitro* translation method. For this experiment an *in vitro* translation is set up using the translation machinery of rabbit reticulocytes and a plasmid containing the gene of interest in this case a P-TEFb component. The gene of interest will be transcribed and translated in an eppedorf tube by the rabbit reticulocyte machinery. To be able to detect the protein made, the methionine added to the reaction is radioactively labelled and so the levels of protein present can then be seen by imaging on a phosphorimager. When a translation blocking morpholino is added to the reaction you would expect to see less protein produced compared to your control.

Cdk9a, Cdk9b and CyclinT1 proteins were successfully translated from their plasmids using the *in vitro* translation method (**figure 5.7**). To the same amount of plasmid an increasing amount of corresponding morpholino was added at concentrations of 40ng, 80ng and 100ng. All three P-TEFb components saw a dose dependent decrease in protein levels due adding increasing concentrations of morpholino. This suggests that the morpholinos are capable of efficiently preventing translation and can be used in further experiments. Luciferase comes with the in vitro translation kit to be used as a positive control to ensure translation is taking place. As an extra control the highest concentration of morpholino was added to luciferase to prove that each morpholino is specific for its target gene and cannot block luciferase protein translation (**figure 5.7**)

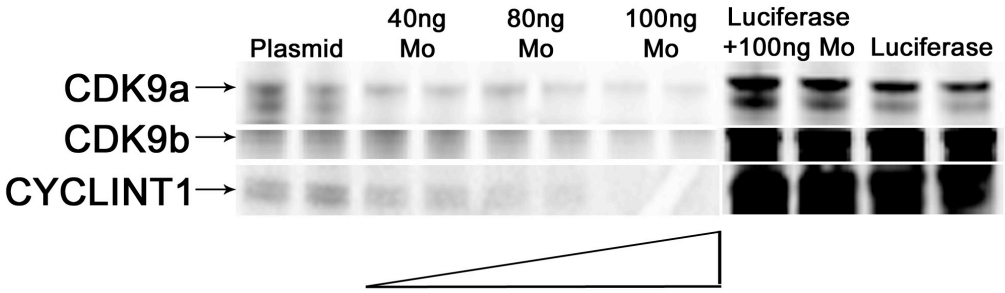

Figure 5.7 *in vitro* translation of Cdk9a, Cdk9b and CyclinT1. Each sample was loaded in duplicate as a loading control. The lanes labelled plasmid show the amount of protein produced by the plasmid alone. Subsequent lanes show protein produced after increasing morpholino concentrations at 40ng, 80ng and 100mg. Control lanes show expression of a luciferase control plasmid and adding 100ng of each morpholino to this luciferase control plasmid.

5.4.2. Phenotype seen after Cdk9a morpholino knockdown

To study the function of Cdk9a in *Xenopus* development, a morpholino was designed to block the transcription of the Cdk9a protein. This would prevent the enzymatic activity of the P-TEFb complex and therefore prevent transcriptional elongation. Cdk9a morpholino was injected into both cells of a two-cell stage embryo at varying concentrations to determine a concentration, which would give a consistant phenotype. From the *in vitro* translation it could be estimated that somewhere between 80ng and 100ng would be most effective. At the same time a standard control morpholino is injected in the same way corresponding to the highest concentration of Cdk9a morpholino used.

This experiment demonstrated that most of the control morpholino injected embryos displayed a wild type phenotype with a normal number of melanophores (**figure 5.8A**). This wild type phenotype was seen at a high frequency in most of the injected embryos (**figure 5.8E**). Injection of 40ng of morpholino appeared to have little affect on the development of the embryos again; most appeared wild type (**figure 5.8B**). A small number of embryos started to display some loss of pigmentation after injection of 80ng of Cdk9a morpholino (**figure 5.8C**). This pigment loss is seen in the eye and lateral stripe. After 100ng of morpholino injection embryos display a clear loss of pigmentation in the eye, lateral stripe head and tail (**figure 5.8D**). This is seen in 28% of the injected embryos as demonstrated in a group image (**figure 5.8F**). These data have been quantified based on whether the injected embryos displayed a wild type or pigment loss phenotype and are shown in **figure 5.9** and **table 5.1**. Melanophores are neural crest derived which indicates that Cdk9a may be functioning in the development of the neural crest. This phenotype obtained also mimics that which was seen after leflunomide treatment. It could be suggested from this result that blocking P-TEFb activity results in defects of neural crest derived melanophores. Following this other neural crest derivatives should be investigated.

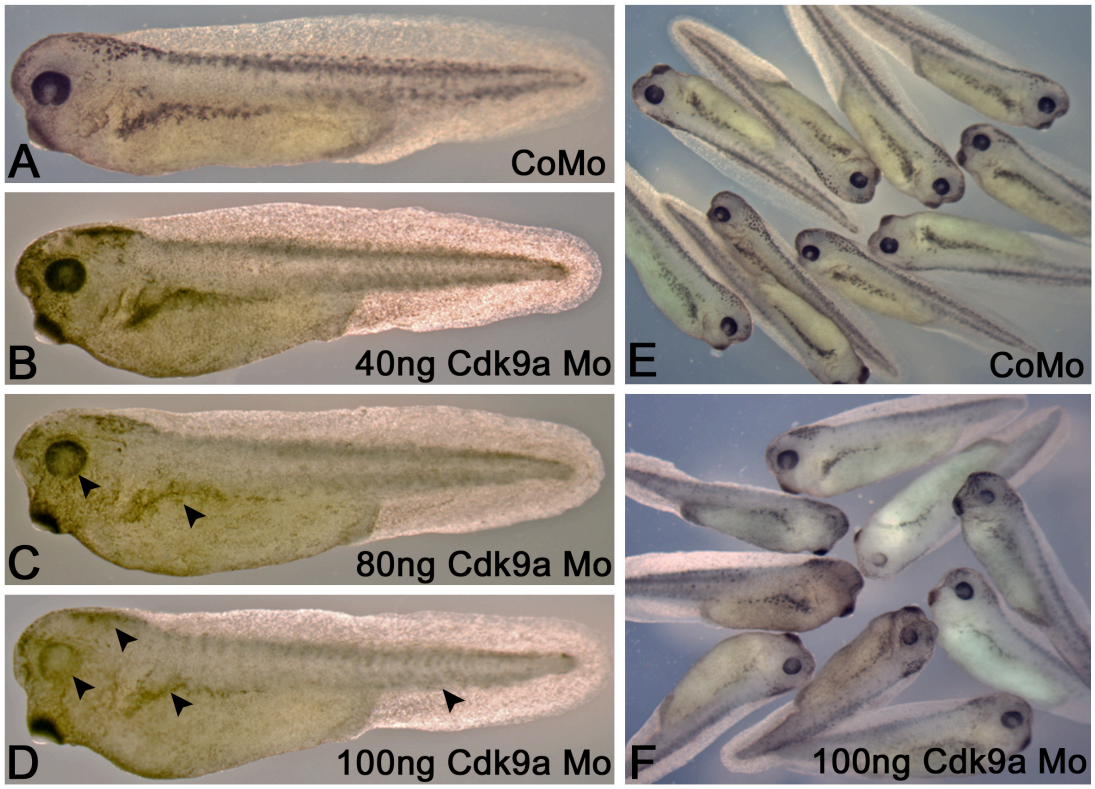

Figure 5.8 The phenotype obtained after Cdk9a knockdown. All embryos were injected into both cells at the 2 cell stage **(A)** 100ng standard control morpholino (CoMo). **(B)** 40ng Cdk9a morpholino **(C)** 80ng Cdk9a morpholino showing pigment loss in the eye and lateral stripe (black arrow heads). **(D)** 100ng Cdk9a morpholino showing pigment loss in the eye, lateral stripe, head and tail (black arrow heads). **(E)** Group of control morpholino injected embryos. **(F)** Group of 100ng Cdk9a morpholino injected embryos. Mo=morpholino.

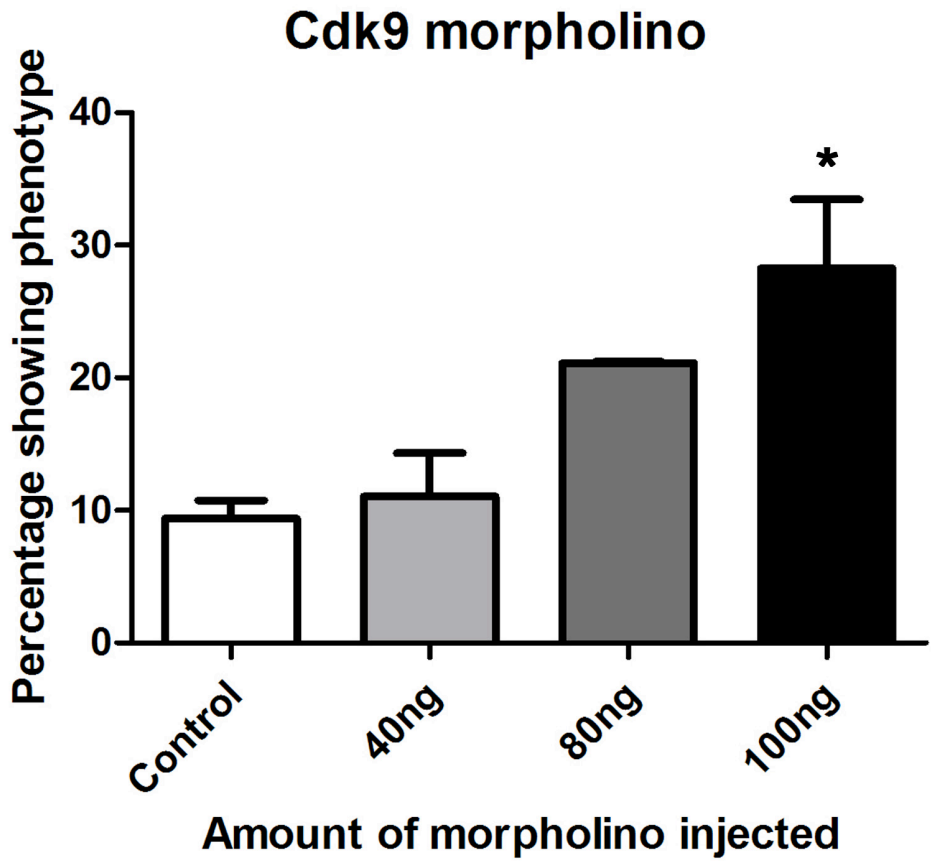

Table 5.1 Quantification of Cdk9a knockdown

Morpholino	*Total embryos*	*Wild type*	*Pigment loss*	*Developmental defects**
100ng Control	*119*	*93 (78%)*	*11 (9%)*	*15 (13%)*
40ng Cdk9a	*73*	*61 (84%)*	*8 (11%)*	*4 (5%)*
80ng Cdk9a	*76*	*52 (68%)*	*16 (21%)*	*8 (11%)*
100ng Cdk9a	*138*	*71 (51%)*	*38 (28%)*	*29 (21%)*

*Developmental defects include eye defects, oedema and stunting

Figure 5.9 Graph showing the percentage of embryos showing a pigment loss phenotype after Cdk9a morpholino injection. From left to right 100ng control morpholino (n=119), 40ng Cdk9a morpholino (n=73) 80ng Cdk9a morpholino (n=76) and 100ng Cdk9a morpholino (n=138). *=p<0.05 by Kruskall Wallis statistical test

5.4.3 Phenotype seen after CyclinT1 knockdown

Along with Cdk9a it was important to investigate the function of CyclinT1. CyclinT1 is another component of P-TEFb and so it was hypothesised that the phenotype seen after CyclinT1 knockdown would be similar to that obtained after Cdk9a knockdown. CyclinT1 is not responsible for the enzymatic activity of P-TEFb however it responsible for receiving signals to activate the complex and connect the complex to the super elongation complex to allow it to carry out its role in transcriptional elongation. It is therefore a key regulator of transcriptional elongation and it could therefore be assumed that the knockdown of this protein would prevent transcriptional elongation from occurring. Similarly to the knockdown of Cdk9a, CyclinT1 morpholino was injected into both cells of a two-cell stage embryo at a range of concentrations. These injected embryos were left to develop until stage 38 when they were fixed and their phenotype observed. It could be estimated from the *in vitro* translation that the most effective concentration would be between 40ng and 80ng.

Embryos injected with the standard control morpholino demonstrated a wild type phenotype (**figure 5.10A**). This was seen in most of the embryos injected as demonstrated in the group image (**figure 5.10E**). After 20ng of morpholino injected the embryos mostly displayed a wild type phenotype (**figure 5.10B**). A small percentage of embryos injected with 40ng of morpholino started to display a pigment loss phenotype with some embryos displaying a loss of melanophores in the lateral stripe (**figure 5.10C**). After 60ng injections of morpholino a large percentage of embryos displayed a pigment loss phenotype (**figure 5.10D** and **F**). This pigment loss is seen in the lateral stripe, eye, head and tail. These data were quantified based on whether the embryos displayed a wild type or pigment loss phenotype and are shown as a graph in **figure 5.11** and in **table 5.2**. This mimics the phenotype seen after Cdk9a knockdown and that obtained after leflunomide treatment giving further evidence for a role of transcriptional elongation in the development of neural crest cells.

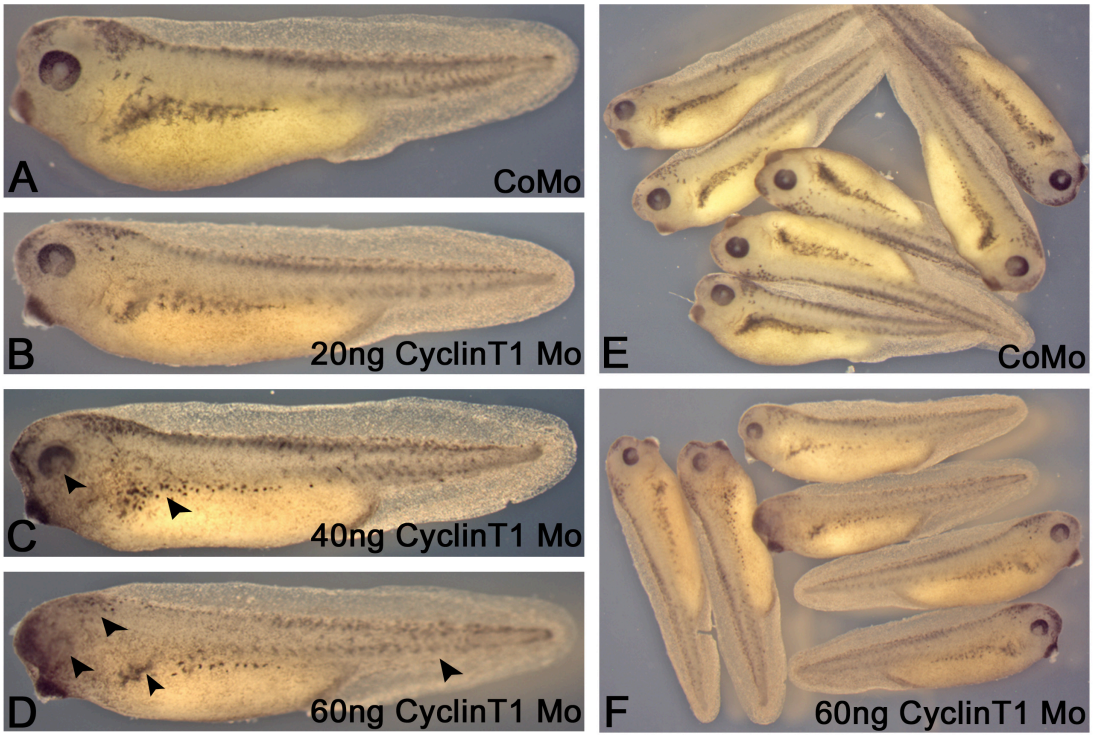

Figure 5.10 The phenotype obtained after CyclinT1 knockdown. All embryos were injected into both cells at the 2 cell stage **(A)** 60ng standard control morpholino (CoMo). **(B)** 20ng CyclinT1 morpholino **(C)** 40ng CyclinT1 morpholino showing pigment loss in the eye and lateral stripe (black arrow heads). **(D)** 60ng CyclinT1 morpholino showing pigment loss in the eye, lateral stripe, head and tail (black arrow heads). **(E)** Group of control morpholino injected embryos. **(F)** Group of 60ng CyclinT1 morpholino injected embryos. Mo=morpholino.

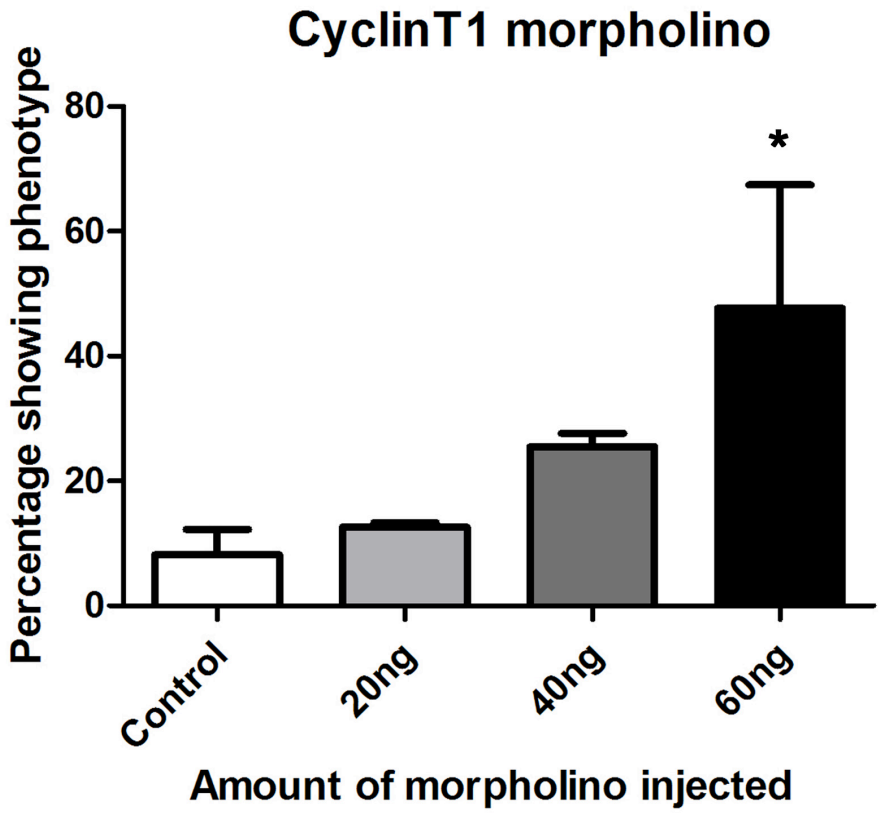

Table 5.2 Quantification of CyclinT1 knockdown

Morpholino	*Total embryos*	*Wild type*	*Pigment loss*	*Developmental defects**
60ng Control	*105*	*87 (83%)*	*8 (8%)*	*10 (9%)*
20ng CyclinT1	*87*	*71 (82%)*	*11 (13%)*	*5 (5%)*
40ng CyclinT1	*94*	*60 (64%)*	*24 (26%)*	*10 (10%)*
60ng CyclinT1	*95*	*39 (41%)*	*32 (34%)*	*24 (25%)*

*Developmental defects include eye abnormalities, oedema and stunting

Figure 5.11 Graph showing the percentage of embryos showing a pigment loss phenotype after CyclinT1 morpholino injection. From left to right 60ng control morpholino (n=105), 20ng CyclinT1 morpholino (n=87) 40ng CyclinT1 morpholino (n=94) and 60ng CyclinT1 morpholino (n=95). *=$p<0.05$ by Kruskall Wallis statistical test.

5.4.4 Phenotype seen after Cdk9b morpholino knockdown and Cdk9a/b combined morpholino knockdown

To follow on from the knockdown of Cdk9a and CyclinT1 it was important to knockdown the other Cdk9 allele in the Xenopus genome, Cdk9b. Knocking out this allele should give the same phenotype seen when Cdk9a was knocked down. Following on from this a double knockdown of both alleles was achieved by co-injecting both the a and b allele morpholinos. Cdk9b morpholino was injected at increasing concentrations in both cells of a two-cell stage embryo. These were left to develop until stage 38 to analyse the phenotype. At the same time increasing concentrations of a mixture of Cdk9a and Cdk9b morpholino were co-injected in the same way and fixed at the same stage.

Injection of a standard control morpholino showed a wild type phenotype in 84% of the embryos injected (**figure 5.12A, E** and **I**). Injection of 40ng of Cdk9b morpholino also demonstrated a mostly wild type phenotype (**figure 5.12B**). Injection of 80ng of Cdk9b morpholino gave 11% of embryos with some pigment loss in the lateral stripe but the phenotype was not very strong (**figure 5.12C**). Injection of 100ng of the Cdk9b morpholino gave 17% of embryos with pigment loss in the lateral stripe, head, eye and tail (**figure 5.12D**) however this phenotype is not as strong as that obtained after Cdk9a or CyclinT1 knockdown. It also did not occur as frequently. This may reflect the efficiency of the morpholino. Morpholino efficiency greatly varies between genes depending on their design. Co-injection of 20ng of Cdk9a and b morpholino gave a mostly wild type phenotype (**figure 5.12F**). Some pigment loss is seen after injection of 40ng of a and 20ng of b (**figure 5.12G**). Injection of 60ng of Cdk9a and 40ng of Cdk9b morpholino gives a stronger pigment loss phenotype in 29% of the embryos (**figure 5.12H and J**). These data were quantified and are displayed in a graph showing the percentage of embryos with wild type or pigment loss phenotypes in **figure 5.13** and **table 5.3**.

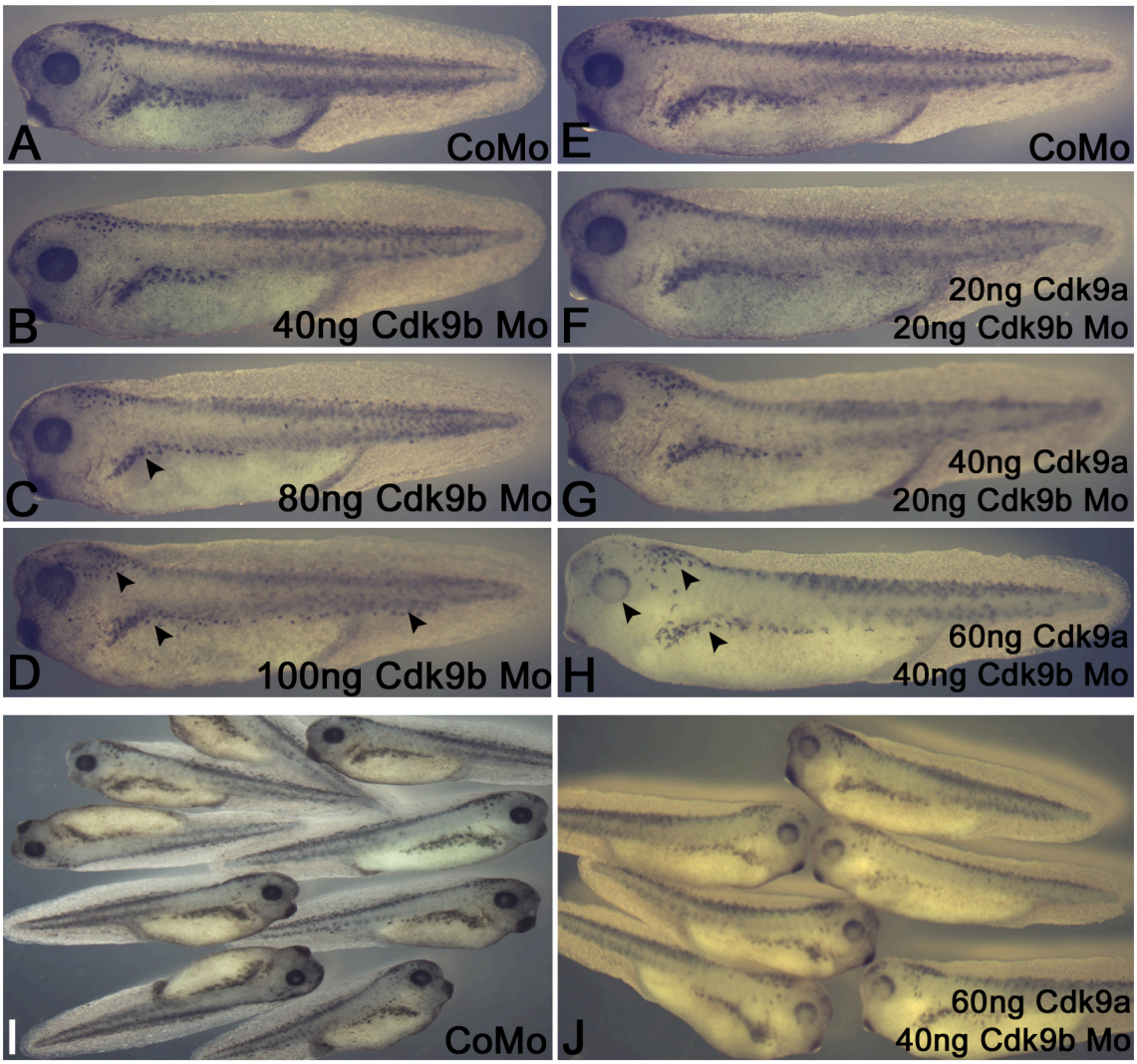

Figure 5.12 The phenotype obtained after Cdk9b knockdown and both Cdk9a and b knockdown. All embryos were injected into both cells at the 2 cell stage **(A)** 100ng standard control morpholino (CoMo). **(B)** 40ng Cdk9b morpholino **(C)** 60ng Cdk9b morpholino showing pigment loss in the lateral stripe (black arrow heads). **(D)** 100ng Cdk9b morpholino showing pigment loss in the lateral stripe, head and tail (black arrow heads). **(E)** 100ng standard control morpholino (CoMo). **(F)** 20ng of Cdk9a and 20ng Cdk9b morpholino co-injected **(G)** 40ng of Cdk9a and 20ng Cdk9b morpholino. **(H)** 60ng Cdk9a and 40ng Cdk9b morpholino showing pigment loss in the lateral stripe and head (black arrow heads). **(I)** Group of control morpholino injected embryos. **(J)** Group of 60ng Cdk9a and 40ng of Cdk9b morpholino injected embryos. Mo=morpholino.

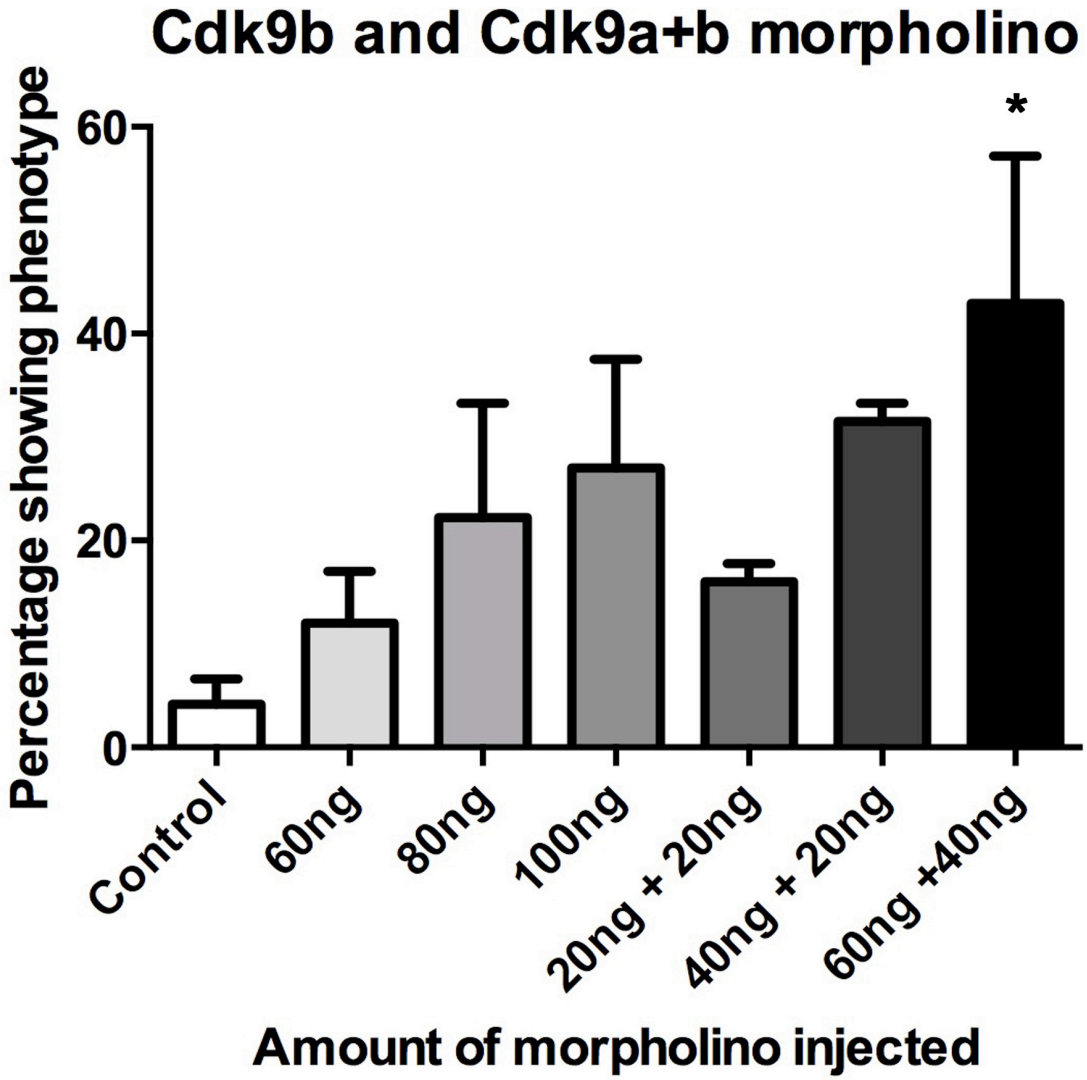

Table 5.3 Quantification of Cdk9b and Cdk9a + Cdk9b knockdown

Morpholino	*Total embryos*	*Wild type*	*Pigment loss*	*Developmental defects**
Control	*77*	*65 (85%)*	*5 (6%)*	*7 (9%)*
60ng Cdk9b	*77*	*60 (77%)*	*9 (11%)*	*8 (12%)*
80ng Cdk9b	*51*	*35 (68%)*	*7 (14%)*	*9 (18%)*
100ng Cdk9b	*62*	*38 (61%)*	*12 (19%)*	*12 (20%)*
20ng Cdk9a 20ng Cdk9b	*70*	*41 (59%)*	*12 (17%)*	*17 (24%)*
20ng Cdk9a 40ng Cdk9b	*81*	*37 (46%)*	*25 (30%)*	*19 (24%)*
40ng Cdk9a 60ng Cdk9b	*73*	*16 (22%)*	*25 (34%)*	*32 (44%)*

***Developmental defects include oedema, stunting and eye abnormalities**

Figure 5.13 Graph showing the percentage of embryos showing a pigment loss phenotype after CyclinT1 morpholino injection. From left to right 100ng control morpholino (n=77), 60ng Cdk9b morpholino (n=77) 80ng Cdk9b morpholino (n=62) and 100ng Cdk9b morpholino (n=62), 20ng Cdk9a 20ng Cdk9b morpholino (n=70) 40ng Cdk9a 20ng Cdk9b morpholino (n=81) and 60ng Cdk9a 40ng Cdk9b morpholino (n=103). *=$p<0.05$ by Kruskall Wallis statistical test.

5.4.5 The effect of Cdk9 and CyclinT1 knockdown on craniofacial development

To investigate the role of the P-TEFb in neural crest development other neural crest derivatives were observed. Craniofacial cartilage is derived from cranial neural crest cells and can be stained for using an alcian blue stain. This experiment was previously carried out after leflunomide treatment, which showed a disorganisation in branchial cartilage. Alcian blue will stain glycosaminoglycans specific to cartilage and so the blue stain observed can be assumed to be only cartilage. Here embryos were injected in one cell of two at the two cell stage with either standard control morpholino, Cdk9a morpholino or CyclinT1 morpholino and left to develop until stage 45 when they were fixed and underwent alcian blue staining to visualise the development of cranio-facial cartilage. This cartilage was then dissected and imaged.

Injection of the standard control morpholino into one half of the embryo had no effect on the development of the cranio-facial cartilage (**figure 5.14A**). Both sides appeared the same demonstrating the wild type development represented in the schematic diagram in **figure 5.14B**. After injection of the Cdk9a morpholino into half of the embryo, the injected half (on the right hand side) appeared to display defects in cartilage development (**figure 5.14C**). The branchial cartilage appears smaller and disorganised compared to the control side of the embryo. The Meckel's and Ceratohyal cartilage appears relatively unaffected. After injection of the CyclinT1 morpholino into half of the embryo, the injected half (on the right hand side) also appeared to display defects in cartilage development (**figure 5.14D**). The branchial cartilage again appears smaller and very disorganised compared to the control side of the embryo. Similarly to Cdk9a knockdown, the Meckel's and Ceratohyal cartilage appeared mostly unaffected. This would suggest that knockdown of the P-TEFb complex affects the development of cranial neural crest cells.

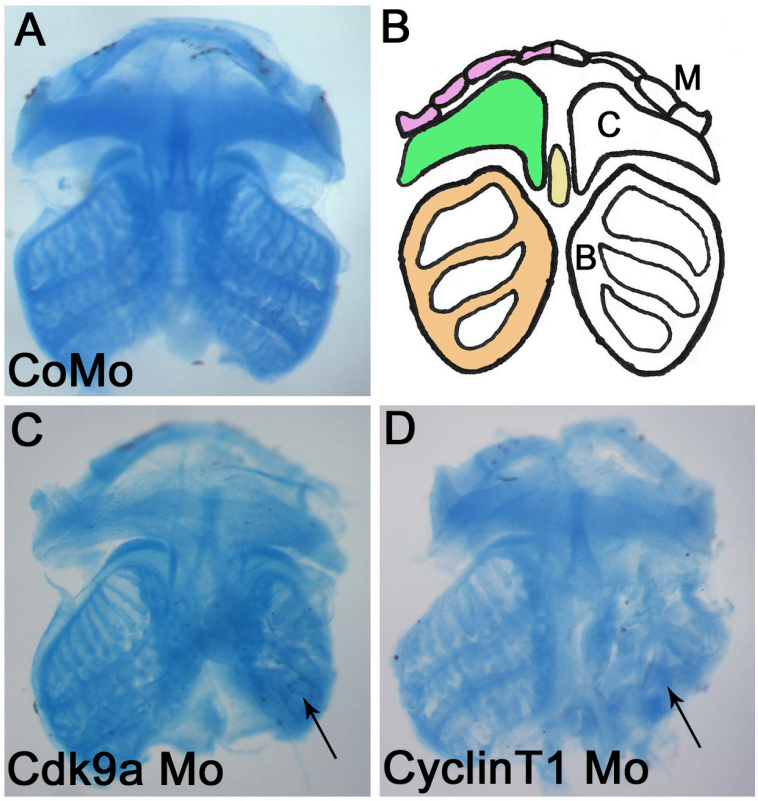

Figure 5.14: The effect of P-TEFb knockdown on cranio-facial cartilage. (A) Dissected 100ng control morpholino (CoMo) injected embryos at stage 45 after alcian blue staining. **(B)** Diagram representing normal cranio-facial cartilage development. M=Meckels cartilage, C=Ceratohyal, B=Branchial cartilage. **(C)** Dissected cranio-facial cartilage of a 100ng Cdk9a morpholino injected embryo at stage 45. Embryos show a disorganisation in the development of the branchial cartilage (black arrow). **(D)** Dissected cranio-facial cartilage of a 60ng CyclinT1 morpholino injected embryo at stage 45. Embryos show a disorganisation in the development of the branchial cartilage

5.4.6 The effect of Cdk9a and CyclinT1 knockdown on sensory neuron development

Sensory neurons are a neural crest cell derivative and as demonstrated previously after leflunomide treatment their development can be tested simply by poking the embryo and observing the reaction. Here the embryos were injected in both cells at the two cell stage with either a control morpholino, a Cdk9a morpholino or a CyclinT1 morpholino. These embryos were left to develop at 18^{o}C until reaching stage 38 when the embryos have a full sensory response. Embryos then underwent a poke from a pipette tip straight to the back of the embryo or a stroke i.e. running the pipette tip from the head to the tail of the embryo. If the embryos swim away they were scored 1, if they twitched they were scored 0.5 and if they failed to react they were scored 0. For each injection type, 30 embryos were tested in 3 rounds of 10 and the average of these experiments is displayed in **figure 5.15**.

Injection of the control morpholino had no effect on the development of the embryo's sensory neurons. Almost 100% of embryos gave a full reaction and swam away from both a poke and a stroke (**figure 5.15**). Injection of Cdk9a morpholino saw a significant decrease in the embryo's ability to react (**figure 5.15**). Most embryos either did not react or merely twitched after both a poke (**figure 5.15 top panel**) or stroke (**figure 5.15 bottom panel**). Similarly knockdown of CyclinT1 also significantly reduced the reaction capability of the embryos after a poke (**figure 5.15 top panel**) and a stroke (**figure 5.15 bottom panel**). Videos of these embryos displaying these phenotypes can be seen in **appendix 3**. These embryos mostly did not respond or a few displayed a twitch. This suggests that knockdown of P-TEFb complex components leads to a disruption in the development of sensory neurons in *Xenopus* embryos further suggesting that transcriptional elongation is important to the development of neural crest cells. This also confirms the sensory neuron phenotype seen after leflunomide treatment in chapter three.

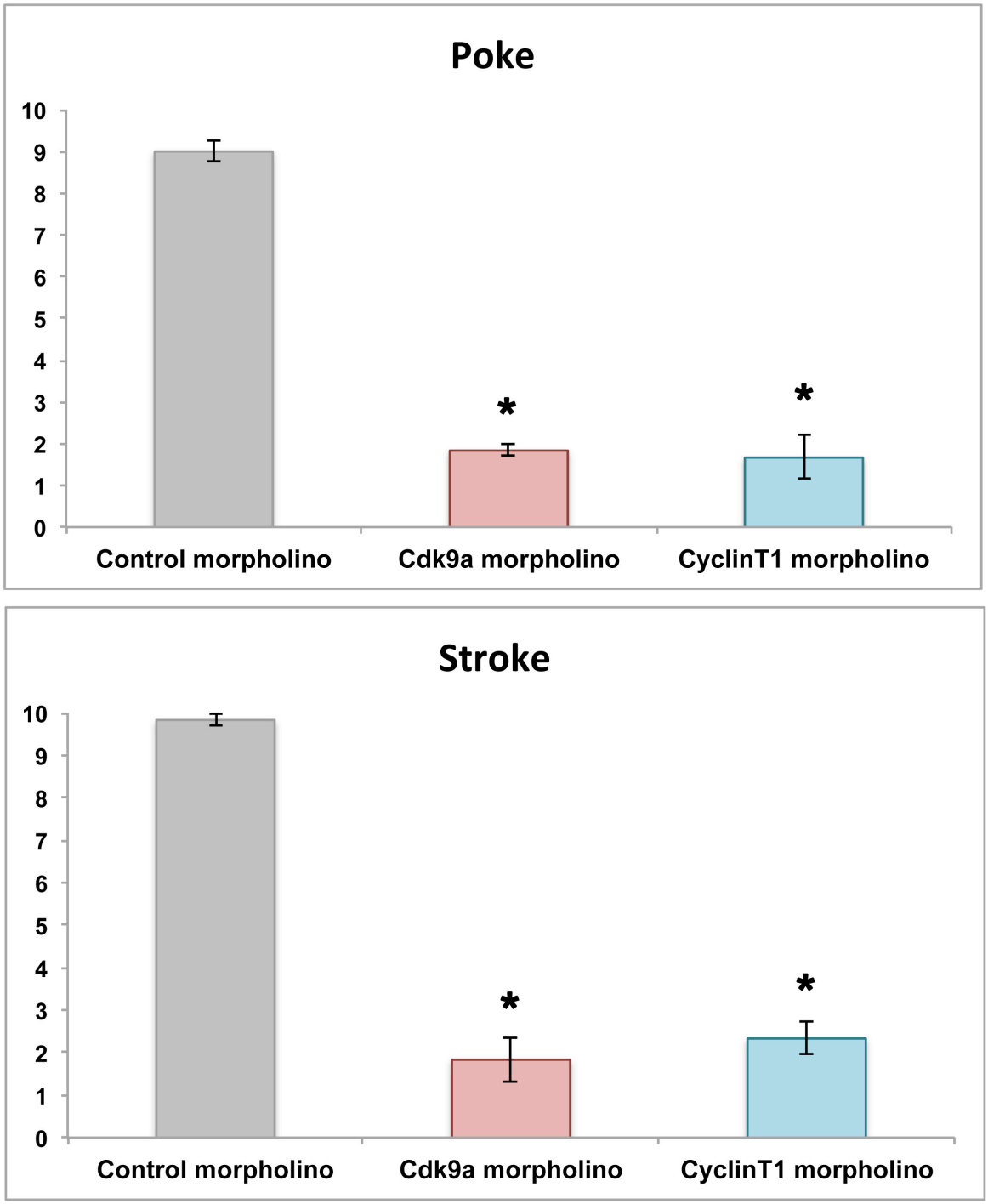

Figure 5.15: Poke and stroke analysis of senory neuron development after morpholino injection. (Top panel) Embryos undergo poking to the dorsal side and their response is tallied as follows. Swim=1, twitch=0.5 no response=0. The average of 30 embryos is shown taken from 3 sperate experiments using 10 embryos for each. (Bottom panel) Embryos undergo stroking of a pipette tip from the head region to the tail and their response is tallied as follows. Swim=1, twitch=0.5 no response=0. The average of 30 embryos is shown. For both conditions embryos were injected with 100ng control morpholino, 100ng Cdk9a morpholino or 60ng of CyclinT1 morpholino. *=$p<0.05$ by students t-test.

5.5 in situ hybridisation after knockdown of P-TEFb components

5.5.1 Neural plate and neural plate border genes

The experiments shown so far in this chapter indicate that knockdown of Cdk9 and CyclinT1 in *Xenopus* embryos results in a loss of neural crest derivatives such as melanophores, cranio-facial cartilage and sensory neurons. To investigate the stage at which transcriptional elongation is important in neural crest development, *in situs* were carried out for neural plate border and neural crest specifying genes. Neural crest cells are initially induced at stage 12 at the neural plate border. This occurs because of the upregulation of neural plate border genes such as Zic1, Zic3 and Pax3. To investigate the effect of knocking down P-TEFb components on these genes, embryos were injected with morpholinos for Cdk9a, Cdk9b and CyclinT1 in one cell of a two-cell stage embryo. These were left to develop until stage 12 when they were fixed to undergo *in situ* hybridisation for neural plate border markers. Embryos were also fixed at stage 15 to investigate P-TEFb knockdown on general neural plate development by carrying out *in situ* hybridisation for neural plate marker Sox2. Morpholinos were co-injected with LacZ capped RNA and after fixing a β-gal stain was carried out causing the injected half of the embryo to appear red.

The results of this *in situ* showed that knockdown of all three P-TEF-b components, Cdk9a, Cdk9b, CyclinT1 and a combination of both Cdk9a and b cause no change in the expression of neural plate border markers Zic1, Zic3 and Pax3 (**figure 5.16B-E, G-J** and **L-O**) compared to the control morpholino injection (**figure 5.16A, F** and **K**). There was also no change seen to the expression of neural plate marker Sox2 (**figure 5.16Q-T**) when compared to the control morpholino injected embryos (**figure 5.16P**). These results suggest that transcriptional elongation is not important at these early induction stages of neural crest development. These results are also comparable to the results obtained after leflunomide treatment and subsequent *in situ* for neural plate border markers.

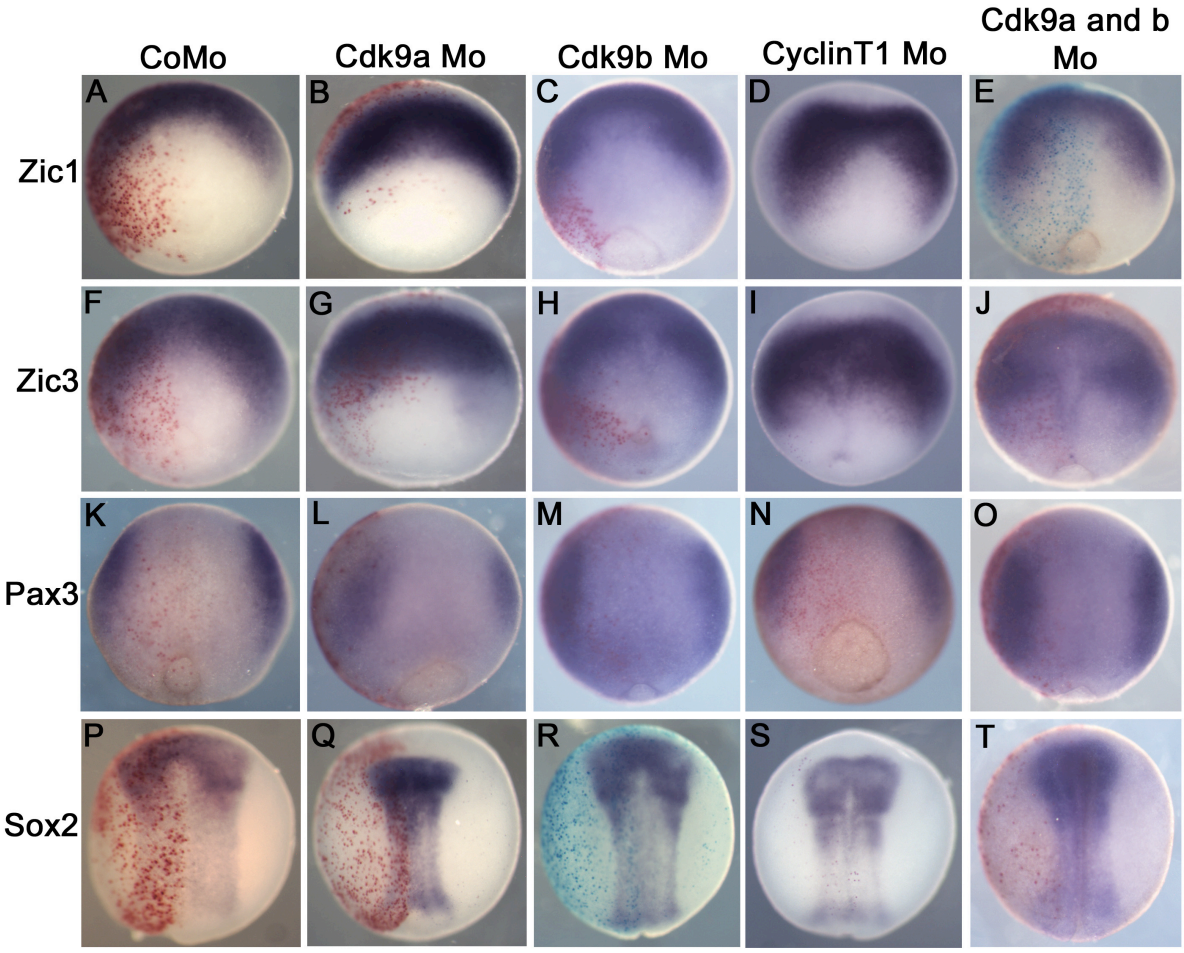

Figure 5.16 *in situ* of neural plate border markers after P-TEFb knockdown. (A,F,K,P) Standard control morpholino injected embryos showing wild type expression of Zic1, Zic3, Pax3 and Sox2 respectively. **(B,G,L,Q)** 100ng Cdk9a morpholino injected embryos showing no change in expression of Zic1, Zic3, Pax3 and Sox2 respectively. **(C,H,M,R)** 100ng Cdk9b morpholino injected embryos showing no change in expression of Zic1, Zic3, Pax3 and Sox2 respectively**. (D,I,N,S)** 60ng CyclinT1 morpholino injected embryos showing no change in expression of Zic1, Zic3, Pax3 and Sox2 respectively**. (E,J,O,T)** 60ng Cdk9a and 40ng Cdk9b morpholino injected embryos showing no change in expression of Zic1, Zic3, Pax3 and Sox2 respectively. Injected side is always on the left and is marked by β-gal stain. Zic1, Zic3 and Pax3 *in situ* hybridisations are carried out on stage 12 embryos. Sox2 *in situ* hybridisation is carried out on stage 15 embryos.

5.5.2 Neural crest specifier genes

Following on from neural crest induction, the cells undergo specification due to the upregulation of neural crest specifier genes. To investigate the effect of inhibiting transcriptional elongation on neural crest specification, the P-TEFb components Cdk9a, Cdk9b, CyclinT1 and a combination of both Cdk9a and Cdk9b were knocked down using morpholinos injected into one cell of a two-cell stage embryo. This left half of the embryo unaffected acting as an internal control. These embryos were fixed at stage 15 (or stage 13 for c-Myc an early neural crest specifier) to undergo *in situ* for various neural crest specifying genes. Morpholinos were co-injected with LacZ capped RNA so the injected side appears red after β-gal stain.

The most strikingly obvious knock down of gene expression is seen after *in situ* for c-Myc (**figure 5.17B-E**) and Sox10 (**figure 5.17G-J**) when compared to the control morpholino injected embryos after the same *in situs* (**figure 5.17A** and **F**). The knock down of c-Myc expression was seen specifically in the anterior regions, which give rise to the neural crest cells. c-Myc expression appeared unaffected in other areas such as the posterior region where c-Myc expression is present in presumptive neural tissue. Sox10 expression is seen to be completely lost in a large percentage of the injected embryos. Sox10 is thought to reside directly downstream of c-Myc in the neural crest gene regulatory network and so it is logical to see a downregulation of this gene [2]. Some knockdown or alteration in expression is seen in other neural crest specifying genes Sox9, Slug and FoxD3 (**Figure 5.17L-O, Q-T** and **V-Y**) when compared to the control morpholino injected controls (**figure 5.17K, P** and **U**). These genes reside downstream of c-Myc but have many other signalling pathways feeding into them and so it is very likely that we would not see a complete knockdown of these genes. These results suggest that transcriptional elongation is important for neural crest development at the stage of specification and is particularly important for c-Myc expression. These results are also comparable to those obtained after leflunomide treatment.

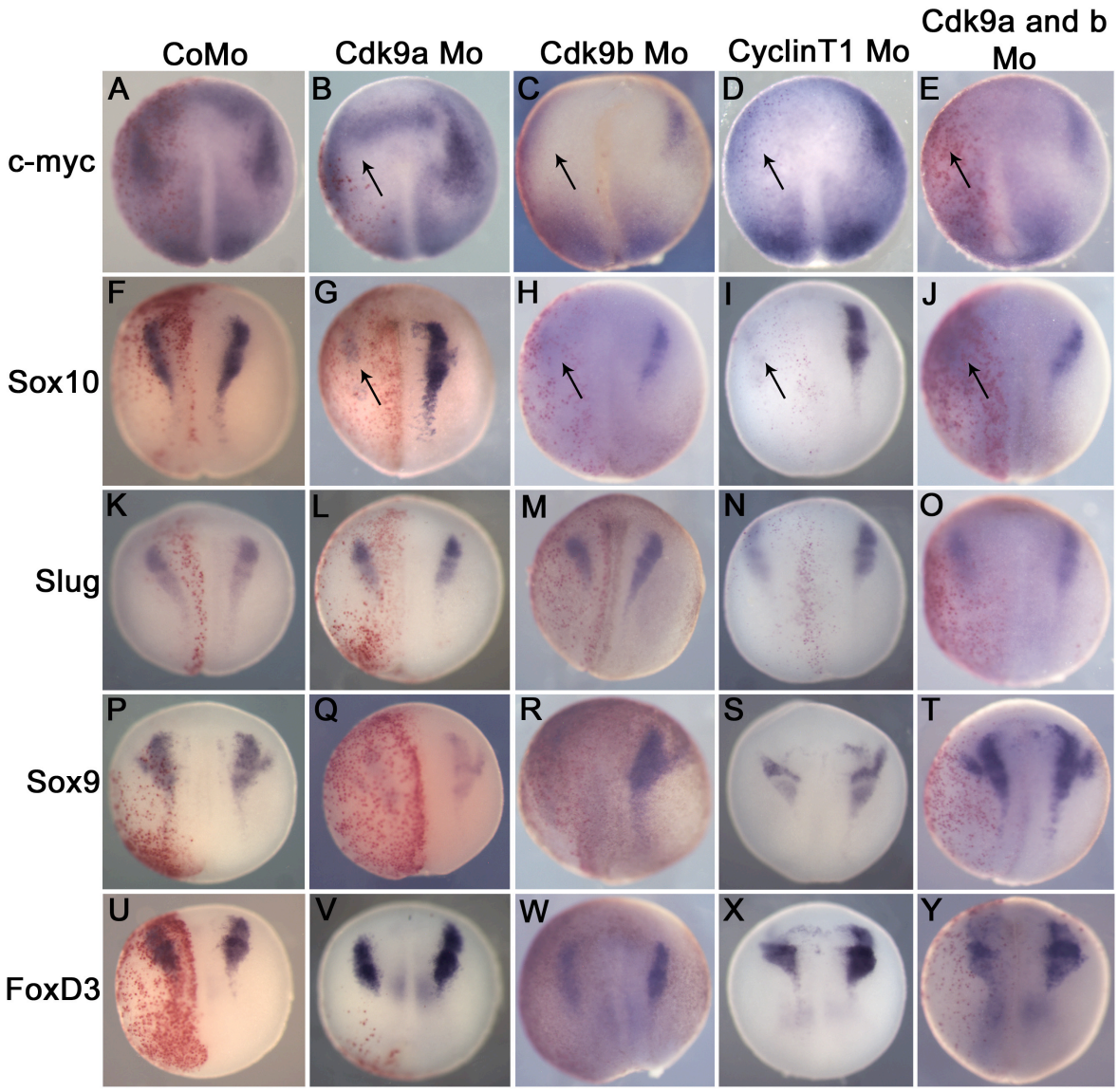

Figure 5.17 *in situ* of neural crest specifier markers after P-TEFb knockdown. (A,F,K,P,U) Standard control morpholino injected embryos showing wild type expression of c-Myc, Sox10, Slug, Sox9 and FoxD3. **(B,G,L,Q,V)** 100ng Cdk9a morpholino injected embryos showing knockdown of c-Myc and Sox10 (black arrows) and some alteration to the expression of Slug, Sox9 and FoxD3. **(C,H,M,R,W)** 100ng Cdk9b morpholino injected embryos showing knockdown of c-Myc and Sox10 (black arrows) and some alteration to the expression of Slug, Sox9 and FoxD3. **(D,I,N,S,X)** 60ng CyclinT1 morpholino injected embryos showing knockdown of c-Myc and Sox10 (black arrows) and some alteration to the expression of Slug, Sox9 and FoxD3. **(E,J,O,T,Y)** 60ng Cdk9a and 40ng Cdk9b morpholino injected embryos showing knockdown of c-Myc and Sox10 (black arrows) and some alteration to the expression of Slug, Sox9 and FoxD3. Injected side is always on the left and is marked by β-gal stain. c-Myc *in situ* hybridisation is carried out on stage 13 embryos and all other *in situ* hybridisations are carried out on stage 15 embryos

5.5.3 Quantification of neural crest specifier, neural plate and neural plate border in situs

Embryos which had undergone *in situ* hybridisation for neural plate, neural plate border and neural crest specifying genes (**figure 5.16** and **5.17**) were scored based on whether they displayed a wild type, partial loss or loss phenotype. Examples of these are shown in **figure 5.18A**. The *in situ*s carried out were for neural plate border genes Zic1, Zic3 and Pax3. Neural plate marker Sox2, and neural crest specifiers, c-Myc, Sox10, Slug, Sox9 and FoxD3. After injection of standard control morpholino most of the embryos showed wild type expression for all of these genes (**figure 5.18B** and **table 5.4**). A very small percentage, below 10% for each gene displayed a partial loss. After Cdk9a and CyclinT1 morpholino injection a large percentage of embryos at around 40%, displayed a loss of c-Myc and Sox10 expression (**figure 5.18C,D**, **table 5.5** and **5.6**). Many of these embryos at aound 40% again displayed a partial loss leaving around 80% of injected embryos displaying some level of expression loss. The other neural crest specifiers displayed around 20% partial loss but not much complete loss is seen (**figure 5.18C,D, table 5.5** and **5.6**). Zic1, Zic3, Pax3 and Sox2 all mostly display the wild type phenotype.

The percentage of embryos displaying a loss phenotype after Cdk9b morpholino injection is considerably smaller than those injected with Cdk9a or CyclinT1 morpholino (**figure 5.18E** and **table 5.7**). Only around 10% of embryos displayed a loss of c-Myc and Sox10 expression and around 30% displaying a partial loss. This gives approximately 40% of embryos displaying a knockdown phenotype after Cdk9b morpholino injection which is half that seen after Cdk9a or CyclinT1 injection. It could be suggested that the Cdk9b morpholino is not as efficient. Injecting a combination of Cdk9a and Cdk9b at lower concentrations shows levels of knockdown phenotype similar to that of Cdk9a and CyclinT1 morpholino injection alone (**figure 5.18F** and **table 5.8**).

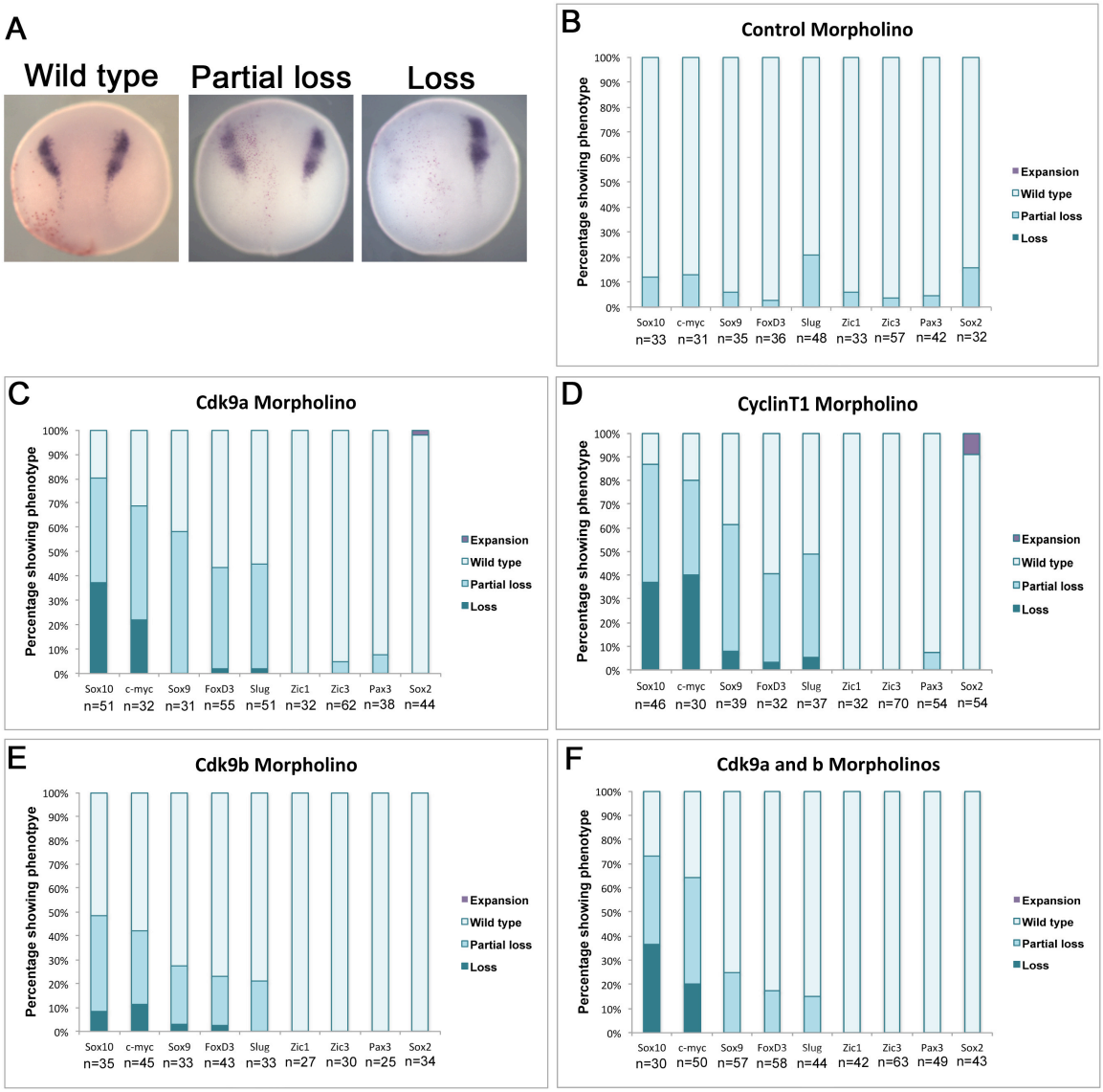

Figure 5.18 Quantification of gene knockdown after morpholino injection. (A) Examples of wild type, partial loss and loss phenotypes using Sox10 expression. **(B)** The percentage of embryos showing a wild type, partial loss, loss or expansion phenotype after injection of a standard control morpholino. **(C)** The percentage of embryos showing a wild type, partial loss, loss or expansion phenotype after injection of 100ng Cdk9a morpholino. **(D)** The percentage of embryos showing a wild type, partial loss, loss or expansion phenotype after injection of 60ng CyclinT1 morpholino. **(E)** The percentage of embryos showing a wild type, partial loss, loss or expansion phenotype after injection of 100ng Cdk9b morpholino.**(F)** The percentage of embryos showing a wild type, partial loss, loss or expansion phenotype after injection of 60ng Cdk9a morpholino and 40ng Cdk9b morpholino.Embryos underwent in situ for Sox10, c-Myc, Sox9, FoxD3, Slug, Zic1, Zic3, Pax3 and Sox2. N numbers are shown at the bottom of each graph. Zic1, Zic3 and Pax3 *in situ* hybridisations were carried out on stage 12 embryos. c-Myc *in situ* hybridisations were carried out on stage 13 embryos. Sox10, Slug, Sox9, FoxD3 and Sox2 *in situ* hybridisations were carried out on stage 15 embryos.

Table 5.4 Quantification of expression after control morpholino injection

	Total embryos	*Wild type*	*Partial loss*	*Loss*	*Expansion*
Sox10	*33*	*29 (89%)*	*4 (11%)*	*0 (0%)*	*0 (0%)*
c-Myc	*31*	*27 (87%)*	*4 (13%)*	*0 (0%)*	*0 (0%)*
Sox9	*35*	*33 (94%)*	*2 (6%)*	*0 (0%)*	*0 (0%)*
FoxD3	*36*	*35 (97%)*	*1 (3%)*	*0 (0%)*	*0 (0%)*
Slug	*48*	*38 (79%)*	*10 (21%)*	*0 (0%)*	*0 (0%)*
Zic1	*33*	*31 (93%)*	*2 (7%)*	*0 (0%)*	*0 (0%)*
Zic3	*57*	*55 (93%)*	*2 (7%)*	*0 (0%)*	*0 (0%)*
Pax3	*42*	*40 (95%)*	*2 (5%)*	*0 (0%)*	*0 (0%)*
Sox2	*32*	*27 (84%)*	*5 (16%)*	*0 (0%)*	*0 (0%)*

Table 5.5 Quantification of expression after Cdk9a morpholino injection

	Total embryos	*Wild type*	*Partial loss*	*Loss*	*Expansion*
Sox10	*51*	*10 (20%)*	*22 (43%)*	*19 (37%)*	*0 (0%)*
c-Myc	*32*	*10 (31%)*	*15 (47%)*	*7 (22%)*	*0 (0%)*
Sox9	*31*	*13 (42%)*	*18 (58%)*	*0 (0%)*	*0 (0%)*
FoxD3	*55*	*31 (56%)*	*23 (42%)*	*1 (2%)*	*0 (0%)*
Slug	*51*	*28 (55%)*	*22 (43%)*	*1 (2%)*	*0 (0%)*
Zic1	*32*	*32 (100%)*	*0 (0%)*	*0 (0%)*	*0 (0%)*
Zic3	*62*	*59 (95%)*	*3 (5%)*	*0 (0%)*	*0 (0%)*
Pax3	*38*	*35 (92%)*	*3 (8%)*	*0 (0%)*	*0 (0%)*
Sox2	*44*	*43 (98%)*	*0 (0%)*	*0 (0%)*	*1 (2%)*

Table 5.6 Quantification of expression after CyclinT1 morpholino injection

	Total embryos	*Wild type*	*Partial loss*	*Loss*	*Expansion*
Sox10	*46*	*6 (13%)*	*23 (50%)*	*17 (37%)*	*0 (0%)*
c-Myc	*30*	*6 (20%)*	*12 (40%)*	*12 (40%)*	*0 (0%)*
Sox9	*39*	*15 (38%)*	*21 (54%)*	*3 (8%)*	*0 (0%)*
FoxD3	*32*	*19 (59%)*	*12 (38%)*	*1 (3%)*	*0 (0%)*
Slug	*37*	*19 (51%)*	*16 (43%)*	*2 (6%)*	*0 (0%)*
Zic1	*32*	*32 (100%)*	*0 (0%)*	*0 (0%)*	*0 (0%)*
Zic3	*70*	*70 (100%)*	*0 (0%)*	*0 (0%)*	*0 (0%)*
Pax3	*54*	*50 (93%)*	*4 (7%)*	*0 (0%)*	*0 (0%)*
Sox2	*54*	*49 (91%)*	*0 (0%)*	*0 (0%)*	*5 (9%)*

Table 5.7 Quantification of expression after Cdk9b morpholino injection

	Total embryos	*Wild type*	*Partial loss*	*Loss*	*Expansion*
Sox10	*35*	*18 (51%)*	*14 (40%)*	*3 (9%)*	*0 (0%)*
c-Myc	*45*	*26 (58%)*	*14 (31%)*	*5 (11%)*	*0 (0%)*
Sox9	*33*	*24 (73%)*	*8 (24%)*	*1 (3%)*	*0 (0%)*
FoxD3	*43*	*33 (77%)*	*9 (21%)*	*1 (2%)*	*0 (0%)*
Slug	*33*	*26 (79%)*	*7 (21%)*	*0 (0%)*	*0 (0%)*
Zic1	*27*	*27 (100%)*	*0 (0%)*	*0 (0%)*	*0 (0%)*
Zic3	*30*	*30 (100%)*	*0 (0%)*	*0 (0%)*	*0 (0%)*
Pax3	*25*	*25 (100%)*	*0 (0%)*	*0 (0%)*	*0 (0%)*
Sox2	*34*	*34 (100%)*	*0 (0%)*	*0 (0%)*	*0 (0%)*

Table 5.8 Quantification of expression after Cdk9a and Cdk9b morpholino injection

	Total embryos	*Wild type*	*Partial loss*	*Loss*	*Expansion*
Sox10	*30*	*8 (26%)*	*11 (37%)*	*11 (37%)*	*0 (0%)*
c-Myc	*50*	*18 (36%)*	*22 (44%)*	*10 (20%)*	*0 (0%)*
Sox9	*57*	*36 (63%)*	*12 (37%)*	*0 (0%)*	*0 (0%)*
FoxD3	*58*	*48 (83%)*	*10 (17%)*	*0 (0%)*	*0 (0%)*
Slug	*53*	*45 (85%)*	*8 (15%)*	*0 (0%)*	*0 (0%)*
Zic1	*42*	*42 (100%)*	*0 (0%)*	*0 (0%)*	*0 (0%)*
Zic3	*63*	*63 (100%)*	*0 (0%)*	*0 (0%)*	*0 (0%)*
Pax3	*49*	*49 (100%)*	*0 (0%)*	*0 (0%)*	*0 (0%)*
Sox2	*43*	*43 (100%)*	*0 (0%)*	*0 (0%)*	*0 (0%)*

5.5.4 In situ of sensory neuron genes after P-TEFb knockdown

Knocking down the P-TEFb components was shown to reduce the embryo's ability to respond to mechanical stimulus suggesting a defect in sensory neurons. To further investigate this *in situs* were carried out post morpholino injection to look at the expression of various genes known to be downstream in the neural crest gene regulatory network, which lead to neural crest differentiation into sensory neurons. Runx1 and Islet1 are both genes which reside downstream of Sox10 in the neural crest gene regulatory network to promote sensory neuron differentiation [280]. Ngnr is involved in sensory neuron differentiation however these sensory neurons are not neural crest derived [280]. These neurons develop in parallel to those derived from neural crest. For this experiment embryos were injected with a standard control morpholino, Cdk9a morpholino or a CyclinT1 morpholino in one cell of a two-cell stage embryo. Morpholinos were co-injected with lacZ and so the injected half of the embryo appeared red after β-gal stain.

Injection of the Cdk9a and CyclinT1 morpholino resulted in a downregulation of Runx1 and Islet1 expression on the injected side of the embryo with 30-40% of embryos displaying a complete loss of expression (**figure 5.19B,C,E** and **F**) when compared to the control morpholino injected embryos (**figure 5.19A** and **D**). No downregulation was seen in Ngnr expression after Cdk9a or CyclinT1 morpholino injection (**figure 5.19H** and **I**). These embryos appeared the same as the control morpholino injected embryos (**figure 5.19G**). These data have been quantified based on embryos displaying a wild type, partial loss or loss phenotype and the data are shown in **figure 5.20** and **table 5.9**. These results show that genes involved in neural crest differentiation into sensory neurons are downregulated after knockdown of P-TEFb. These genes reside downsteam of Sox10 and so it is logical to see a downregulation in these. It also confirms the loss of sensory neuron function seen in the stage 38 embryos by the poke and stroke assay. No change was seen in Ngnr expression suggesting that P-TEFb is relatively specific for neural crest development in this situation.

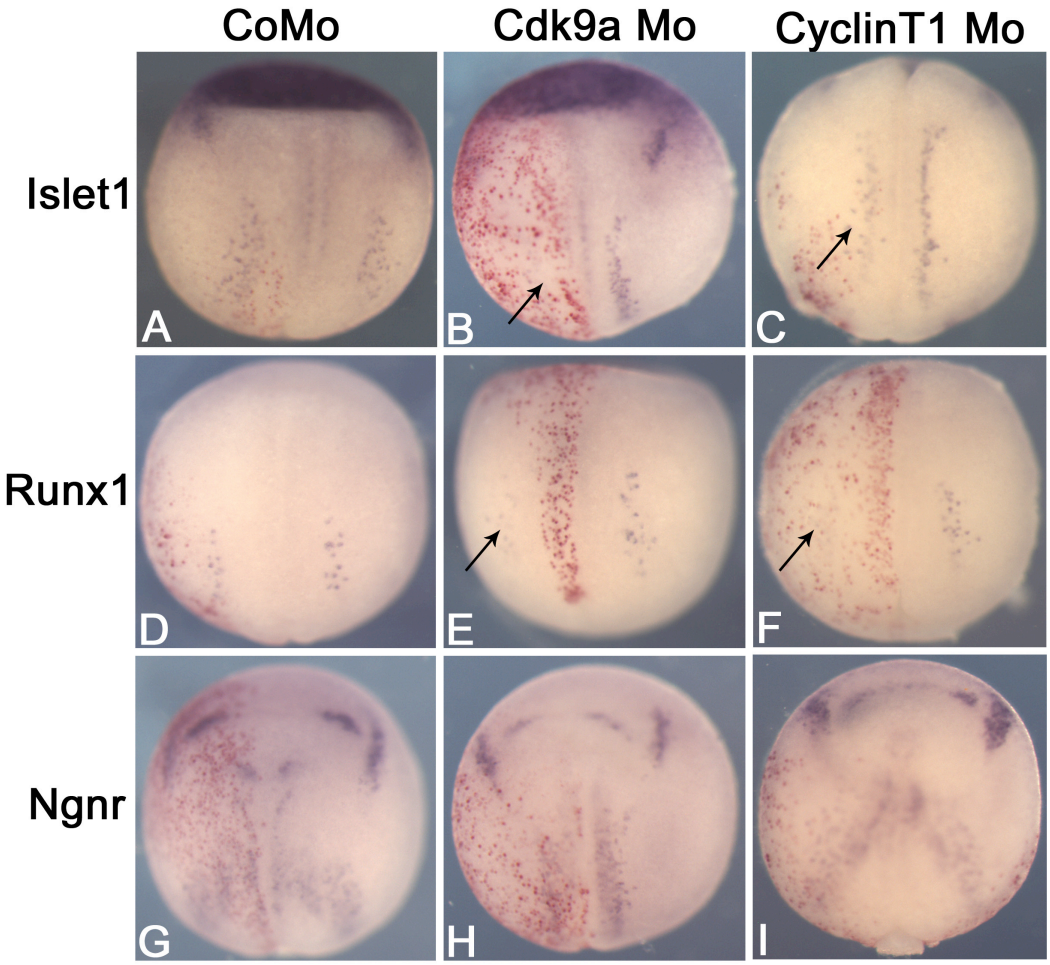

Figure 5.19 *in situ* of sensory neuron markers after P-TEFb knockdown. (A,D,G) Standard control morpholino injected embryos showing wild type expression of Islet1, Runx1 and Ngnr. **(B,E,H)** 100ng Cdk9a morpholino injected embryos showing knockdown of expression of Islet1 and Runx1 (black arrows) and wild type Ngnr expression. **(C,F,I)** 60ng CyclinT1 morpholino injected embryos showing knockdown of expression of Islet1 and Runx1 (black arrows) and wild type Ngnr expression. Injected side is shown on the left and stained red by β-gal stain. All embryos are fixed at stage 18.

5.5.5 Quantification of sensory neuron markers after P-TEFb knockdown

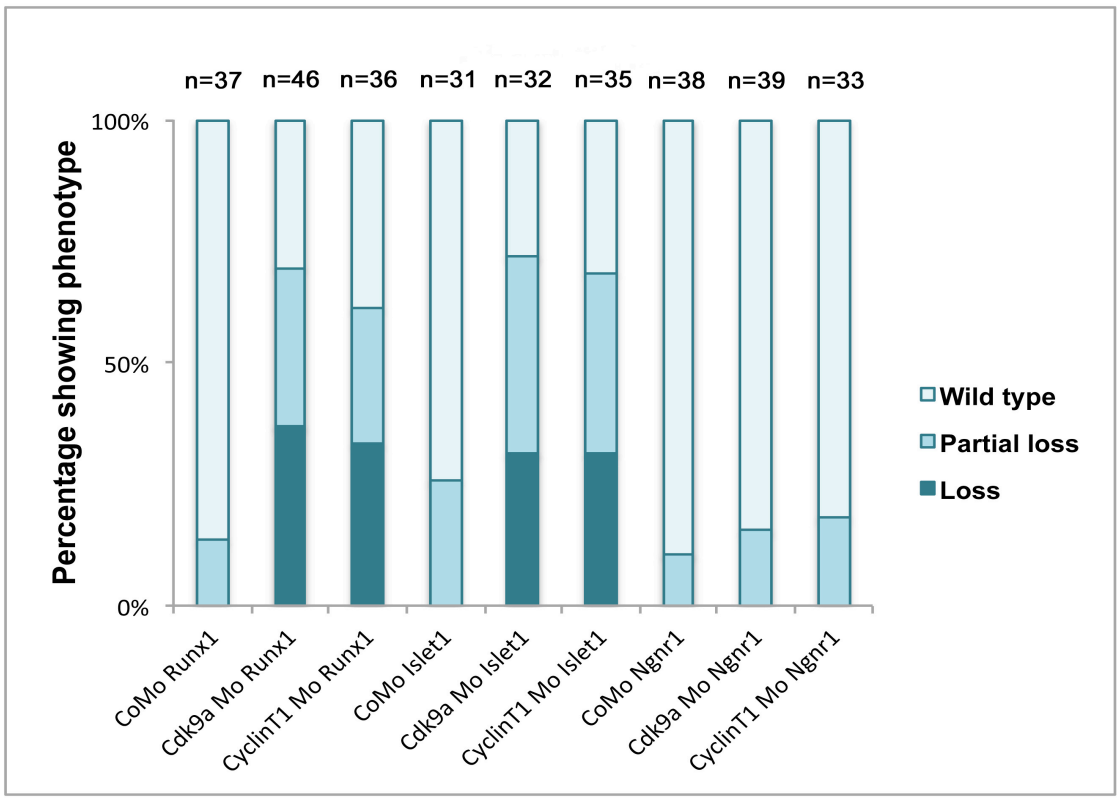

Figure 5.20 Graph showing quantification of sensory neuron markers after P-TEFb knockdown. From left to right shows the percentage of embryos showing a wild type, partial loss or loss phenotype for Runx1, Islet1 and Ngnr1 after standard control morpholino (CoMo), 100ng Cdk9a morpholino or 60ng CyclinT1 morpholino. N numbers are shown at the top of the graph.

Table 5.9 Quantification of sensory neuron markers after P-TEFb knockdown

	Morpholino	*Total embryos*	*Wild type*	*Partial loss*	*Loss*
Runx1	*Control*	*37*	*32 (86%)*	*5 (14%)*	*0 (0%)*
	Cdk9a	*46*	*14 (30%)*	*15 (32%)*	*17 (38%)*
	CyclinT1	*36*	*14 (39%)*	*10 (28%)*	*12 (33%)*
Islet1	*Control*	*31*	*23 (74%)*	*8 (26%)*	*0 (0%)*
	Cdk9a	*32*	*9 (28%)*	*13 (40%)*	*10 (32%)*
	CyclinT1	*35*	*11 (31%)*	*13 (37%)*	*11 (32%)*
Ngnr1	*Control*	*38*	*34 (89%)*	*4 (11%)*	*0 (0%)*
	Cdk9a	*39*	*33 (85%)*	*6 (15%)*	*0 (0%)*
	CyclinT1	*33*	*27 (81%)*	*6 (19%)*	*0 (0%)*

5.5.6 in situ hybridisation of trigeminal placode markers after P-TEFb knockdown

The data collected so far suggest that transcriptional elongation is important for neural crest specification by regulating the expression of c-Myc. To further confirm this other genes known to reside downstream of c-Myc were investigated. Studies using c-Myc morpholinos in *Xenopus* have shown that knockdown of c-Myc also affects the development of trigeminal placodes along with neural crest. Trigeminal placodes and neural crest are often found to develop alongside each other giving rise to similar cell types [141]. Trigeminal placodes are though to give rise to the cranial sensory neurons. To investigate the effect of P-TEFb knockdown on trigeminal placode development, *in situ* hybridisation was carried out for trigeminal markers, Tbx2, NeuroD and Elrd after morpholino injection [104, 281, 282]. These embryos were injected in one cell of a two-cell stage embryo. The injected side was detected by β-gal stain.

All three of these trigeminal markers Tbx2, NeuroD and Elrd showed a loss of expression after injection of Cdk9a morpholino or CyclinT1 morpholino (**figure 5.21B,C,E,F,H** and **I**) when compared to the control morpholino injected embryos (**figure 5.21A,C** and **F**). The trigeminal placode expression can be seen as a small patch at the anterior end on both sides of the embryo. Loss of these patches are indicated by black arrows on **figure 5.21**. It can be seen on these embryos that other placodes marked by the *in situ* are unaffected. These include the lateral placodes, which arise directly underneath the trigeminal placodes and can be seen after Tbx2 *in situ* (**figure 5.21A,B** and **C**). This suggests that P-TEFb knockdown specifically affected placodes, which have c-Myc upstream in their gene regulatory network giving further evidence for the regulation of c-Myc by transcriptional elongation. The embryos in this experiment were quantified based on whether thay displayed a wild type, partial loss or loss phenotype and the data are shown in **figure 5.22** and **table 5.10.**

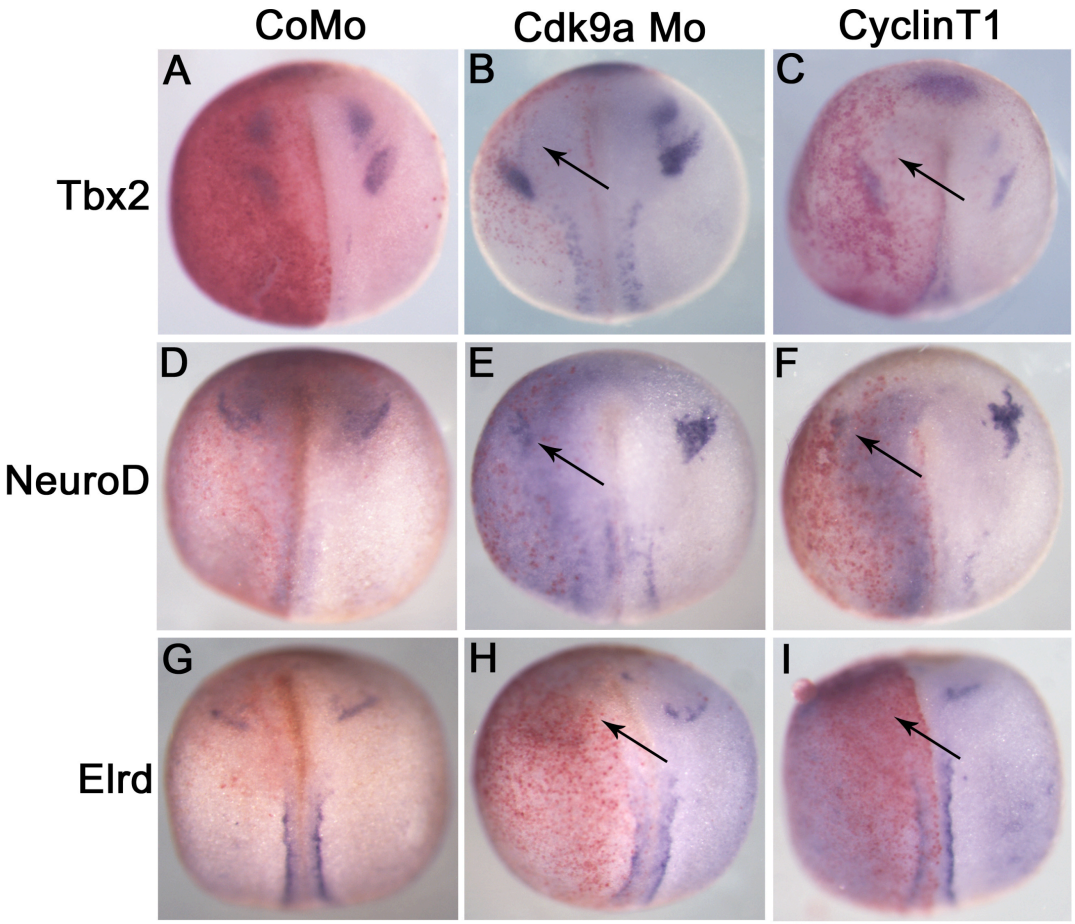

Figure 5.21 *in situ* of trigeminal placode markers after P-TEFb knockdown. (A,D,G) Standard control morpholino injected embryos showing wild type expression of Tbx2, NeuroD and Elrd. **(B,E,H)** 100ng Cdk9a morpholino injected embryos showing knockdown of expression of Tbx2, NeuroD and Elrd (black arrows). **(C,F,I)** 60ng CyclinT1 morpholino injected embryos showing knockdown of expression of Tbx2, NeuroD and Elrd (black arrows). Injected side is shown on the left and stained red by β-gal stain. All embryos are at stage 18.

5.5.7 Quantification of trigeminal marker in situs after P-TEFb knockdown

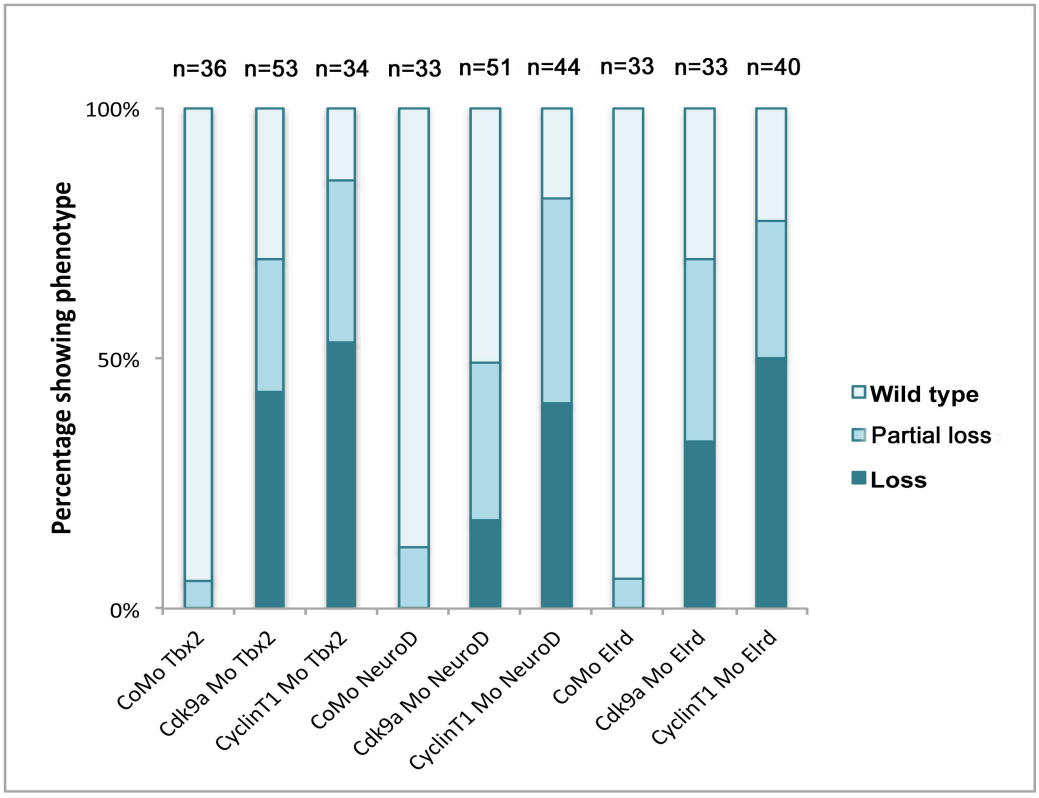

Figure 5.22 Graph showing quantification of trigeminal placode markers after P-TEFb knockdown. From left to right shows the percentage of embryos showing a wild type, partial loss or loss phenotype for Tbx2, NeuroD and Elrd after standard control morpholino (CoMo), 100ng Cdk9a morpholino or 60ng CyclinT1 morpholino. N numbers are shown at the top of the graph.

Table 5.10 Quantification of trigeminal placode markers after P-TEFb knockdown

	Morpholino	***Total embryos***	***Wild type***	***Partial loss***	***Loss***
Tbx2	*Control*	*36*	*34 (94%)*	*2 (6%)*	*0 (0%)*
	Cdk9a	*53*	*16 (30%)*	*14 (26%)*	*23 (44%)*
	CyclinT1	*34*	*5 (15%)*	*11 (32%)*	*18 (53%)*
NeuroD	*Control*	*33*	*29 (88%)*	*4 (12%)*	*0 (0%)*
	Cdk9a	*51*	*26 (51%)*	*16 (31%)*	*9 (18%)*
	CyclinT1	*44*	*8 (18%)*	*18 (41%)*	*18 (41%)*
Elrd	*Control*	*33*	*31 (94%)*	*2 (6%)*	*0 (0%)*
	Cdk9a	*33*	*10 (30%)*	*12 (36%)*	*11 (34%)*
	CyclinT1	*40*	*9 (22%)*	*11 (28%)*	*20 (50%)*

5.6 Rescue experiments

5.6.1 Mutagenesis expression construct rescue experiments

In order to prove that the loss of gene expression we see is specifically due to the loss of Cdk9 or CyclinT1 by morpholino knockdown, it is important to carry out rescue experiments. For these experiments rescue constructs are made using site directed mutagenesis to alter the morpholino binding site within Cdk9a, Cdk9b and CyclinT1. These mutated versions of the genes of interest are cloned into a vector containing a poly-A linker at the 3' end of the gene so that cRNA can be transcribed from it and used to inject into the Xenopus embryo as a rescue construct. Here we use Sox10 expression as a readout of the level of rescue resulting when these rescue constructs were co-injected with the morpholinos of Cdk9a and Cdk9b. CyclinT1 has not been done yet as there have been some problems with the cloning process which have still not been resolved.

Embryos injected with the Cdk9a morpholino (**figure 5.23A**) or Cdk9b morpholino (**figure 5.23B**) show 73% and 42% of embryos with a loss of Sox10 expression in the injected side. Embryos were co-injected with 100pg of rescue construct along with the same dose of morpholino and (**figure 5.23C** and **D**) fewer of these embryos displayed loss of Sox10 expression. 54% of Cdk9a and 100pg of rescue construct injected embryos and 11% of Cdk9b and 100pg of rescue construct injected embryos showed loss of expression. This suggests that the rescue construct partially rescued the knockdown of Sox10 seen from morpholino injection. Embryos injected with Cdk9a morpholino and 500pg of rescue construct (**figure 5.23E**) display greater levels of rescue. Only 26% of these embryos showed a loss of Sox10 expression, which is much less compared to the 73% showing loss after morpholino injection alone. Injection of 500pg of rescue construct after Cdk9b morpholino injection also shows a degree of rescue similar to that of 100pg (**figure 5.23 F**). These data are shown as a graph (**top panel figure 5.23**) and in **table 5.11.**

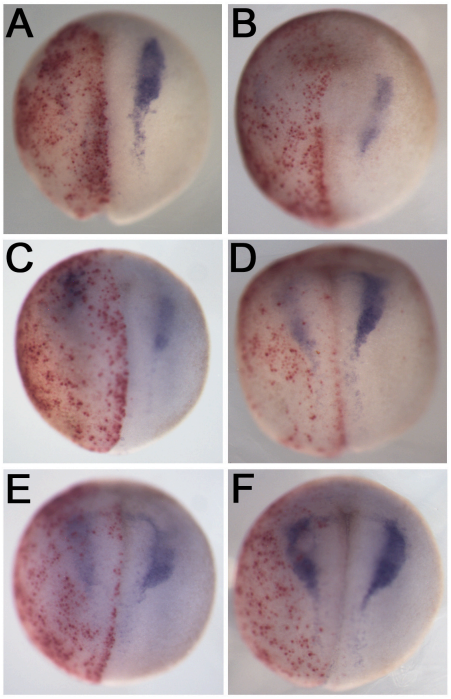

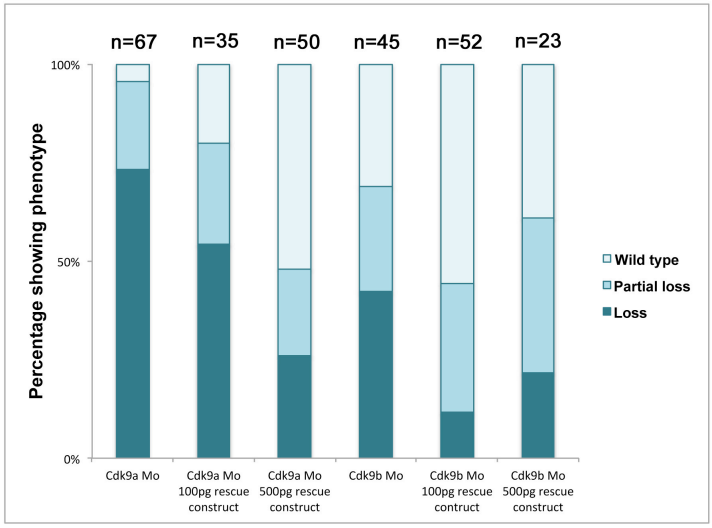

Table 5.11 Mutagenesis rescues

Morpholino	*Rescue construct/pg*	*Total embryos*	*Wild type*	*Partial loss*	*Loss*
Cdk9a	*0*	*67*	*3 (5%)*	*15 (22%)*	*49 (73%)*
Cdk9a	*100*	*35*	*7 (21%)*	*9 (25%)*	*19 (54%)*
Cdk9a	*500*	*50*	*26 (52%)*	*11 (22%)*	*13 (26%)*
Cdk9b	*0*	*45*	*14 (32%)*	*12 (26%)*	*19 (42%)*
Cdk9b	*100*	*52*	*29 (57%)*	*17 (32%)*	*6 (11%)*
Cdk9b	*500*	*23*	*9 (40%)*	*9 (39%)*	*5 (21%)*

Figure 5.23 Mutagenesis rescues. (A) 100ng Cdk9a morpholino showing loss of Sox10 expression. **(B)** 100ng Cdk9b morpholino showing loss of Sox10 expression. **(C)** 100ng Cdk9a morpholino co-injected with 100pg mutant Cdk9a RNA showing a partial loss of Sox10. **(D)** 100ng Cdk9b morpholino co-injected with 100pg mutant Cdk9b RNA showing a partial loss of Sox10. **(E)** 100ng Cdk9a morpholino co-injected with 500pg mtant Cdk9a RNA showing rescue of Sox10 expression. **(F)** 100ng Cdk9b morpholino co-injected with 500pg Cdk9b RNA showing rescue of Sox10 expression. Injected side is always on the left as indicated by a red β-gal stain. The panel on the right shows a quantification of the wild type, partial loss, loss phenotypes counted displayed as a graph of the percentage of embryos showing these phenotypes and also in table 5.11. n numbers are shown at the top of the graph.

5.6.2 c-Myc rescues

Transcriptional elongation may regulate neural crest development by regulating the expression of neural crest specifier c-Myc. To test this theory a rescue experiment was carried out in which Cdk9 and CyclinT1 morpholinos were co-injected with c-Myc capped RNA. This capped RNA should replace the c-Myc expression lost due to P-TEFb knockdown allowing neural crest cells to develop normally again. The level of the rescue was measured by using a Sox10 *in situ* as Sox10 is known to be expressed downstream of c-Myc in the neural crest gene regulatory network. If Sox10 transcription is also regulated by P-TEFb we would not expect c-Myc to rescue. Embryos were injected in one cell of a two cell stage embryo with the morpholino and a dose range of c-Myc RNA.

Injection of Cdk9a or CyclinT1 morpholinos resulted in a loss of Sox10 expression (**figure 5.24A** and **B**) when compared to a control morpholino injected embryo (**figure 5.24G**). When embryos were co-injected with 100pg of c-Myc capped RNA there was seen to be a decrease in the number of embryos showing a complete loss of Sox10 expression and some rescue was apparent (**figure 5.24C** and **D**). After injection of 500pg of c-Myc RNA even fewer embryos displayed a loss of Sox10 expression and expression was almost completely restored (**figure 5.24E** and **F**). Injection of 500pg of c-Myc alone showed little change to Sox10 expression, however a small percentage of embryos displayed an upregulation phenotype (**figure 5.24H**). These embryos were quantified based on whether they displayed a wild type, partial loss, loss or expansion phenotype and these data are displayed in **figure 5.24** as a graph and in **table 5.12**. These data show a shift from a large percentage embryos displaying a loss phenotype to embryos displaying predominantly a partial loss or wild type phenotype after myc RNA injection. The percentage of loss seen goes from 38% to 8% after 100pg of myc injection rescuing Cdk9a morpholino injection. This goes down further to 3% after injection of 500pg of myc. A similar trend is seen when rescuing CyclinT1 knockdown. This suggests that myc is capable of partially rescuing the effects of P-TEFb knockdown.

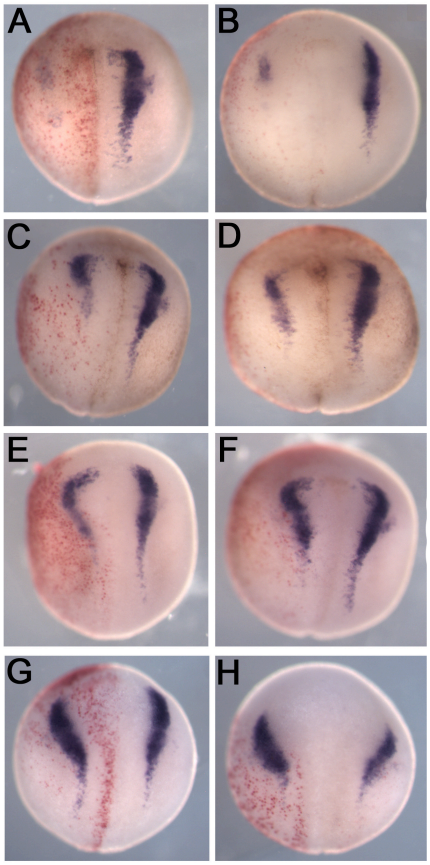

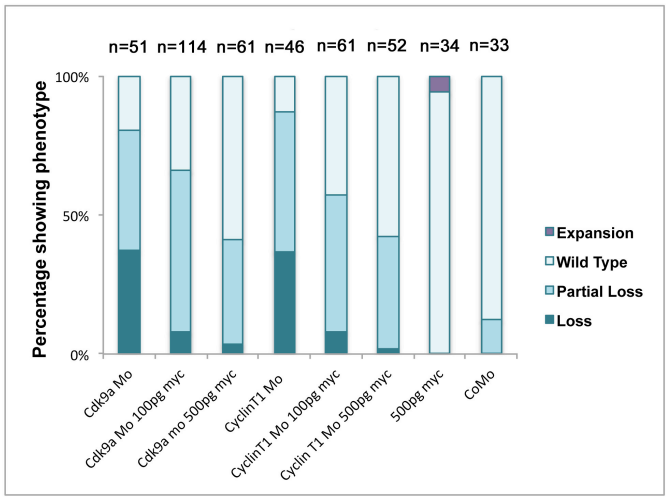

Table 5.11 Quantification of c-myc rescue

Morpholino	*c-myc RNA/pg*	*Total embryos*	*Wild type*	*Partial loss*	*Loss*	*Expansion*
Cdk9a	*0*	*51*	*10 (19%)*	*22 (43%)*	*19 (38%)*	*0 (0%)*
Cdk9a	*100*	*114*	*39 (34%)*	*66 (58%)*	*9 (8%)*	*0 (0%)*
Cdk9a	*500*	*61*	*36 (59%)*	*23 (38%)*	*2 (3%)*	*0 (0%)*
CyclinT1	*0*	*46*	*6 (13%)*	*23 (50%)*	*17 (37%)*	*0 (0%)*
CyclinT1	*100*	*61*	*26 (43%)*	*30 (49%)*	*5 (8%)*	*0 (0%)*
CyclinT1	*500*	*52*	*30 (58%)*	*21 (37%)*	*1 (5%)*	*0 (0%)*
	500	*34*	*32 (94%)*	*0 (0%)*	*0 (0%)*	*2 (6%)*
Control	*0*	*33*	*29 (88%)*	*4 (12%)*	*0 (0%)*	*0 (0%)*

Figure 5.24 Rescuing P-TEFb knockdown with c-Myc. (A) 100ng Cdk9a morpholino showing loss of Sox10 expression. **(B)** 60ng CyclinT1 morpholino showing loss of Sox10 expression. **(C)** 100ng Cdk9a morpholino co-injected with 100pg c-Myc RNA showing a partial loss of Sox10. **(D)** 60ng CyclinT1 morpholino co-injected with 100pg c-Myc RNA showing a partial loss of Sox10. **(E)** 100ng Cdk9a morpholino co-injected with 500pg c-Myc RNA showing rescue of Sox10 expression. **(F)** 60ng CyclinT1 morpholino co-injected with 500pg c-Myc RNA showing rescue of Sox10 expression. **(G)** Control morpholino injected embryos showing wild type Sox10 expression. **(H)** 500pg of c-Myc RNA injection showing expansion of Sox10 expression. Injected side is always on the left as indicated by a red β-gal stain. The panel on the right shows a quantification of the wild type, partial loss, loss and expansion phenotypes counted displayed as a graph of the percentage of embryos showing these phenotypes and also in table 5.11. n numbers are shown at the top of the graph.

5.7 Discussion

The aims of this chapter were to test the hypothesis suggested from results obtained using leflunomide treatment that regulation of transcriptional elongation is important for neural crest development. To do this we investigated the expression of the P-TEFb complex and observed the effects on neural crest development caused by knocking it down. Knocking down the P-TEFb complex prevents transcriptional elongation from occurring and leaves genes in a paused state unable to be fully transcribed. Based on the results obtained using leflunomide it was hypothesised that the P-TEFb complex would be expressed in the neural crest cells and knocking down this complex would result in a reduced amount of neural crest derivatives. Initially, *in situ* hybridisation experiments were carried out for the P-TEFb components Cdk9a, Cdk9b, CyclinT1 and CyclinT2. This revealed that the P-TEFb components were expressed in the ectoderm of gastrula stage embryos, the neural plate and neural plate border of neurula stage embryos and the branchial arches of tailbud and tadpole stage embryos. This suggested that the P-TEFb components were expressed in the neural crest cells at the neural plate border and in the migrating neural crest of the branchial arches. Double *in situ* hybridisation of the P-TEFb components with Sox10 a known neural crest marker confirmed that these components were expressed in the neural crest cells at the neural plate border.

These *in situ* results suggest that P-TEFb plays a role in the development of neural crest cells. To confirm this morpholinos were designed for Cdk9a, Cdk9b and CyclinT1 to knock down the protein levels of the P-TEFb proteins. Initially morpholino efficiency was tested using an in vitro translation system. This combines a plasmid containing Cdk9a, Cdk9b and CyclinT1 and the corresponding morpholino in an in vitro translation. The aim of this is to block the translation of the plasmid using varying concentrations of the morpholino. This was achieved and all of the morpholinos obtained were shown to be capable of knocking down their specific protein. It could be suggested from this experiment that CyclinT1 was the most efficient morpholino being capable of

complete knockdown at using 60ng of morpholino. Cdk9a was able to knockdown protein at around 80ng. Cdk9b however was not very efficient as some protein was still detected after 100ng of morpholino was added. This is likely due to the design of the morpholino. Morpholino efficiency is known to vary greatly based on the position at which they bind and the surrounding nucleotides increasing or decreasing binding efficiency similar to the binding of a primer.

Initial experiments knocking down the P-TEFb components showed that the development of neural crest derivatives was impaired. The first neural crest derivatives to be investigated were melanophores. Knockdown of Cdk9a and CyclinT1 resulted in a large percentage of embryos displaying a pigment loss phenotype. Knockdown of Cdk9b resulted in a similar phenotype however occurring much less frequently probably because this morpholino is not as efficient as the Cdk9a or CyclinT1 morpholino. Knockdown of both the Cdk9a and Cdk9b allele resulted in a large percentage of embryos showing a pigment loss phenotype. The frequency to which this occurred was similar to that of Cdk9a or CyclinT1 alone showing that lower morpholino concentrations could be used if both alleles were knocked down reducing the redundancy. Due to the inefficiency of the Cdk9b morpholino it was not used for all subsequent experiments.

Knockdown of Cdk9a and CyclinT1 also resulted in defects of other neural crest derivatives including cranial facial cartilage. An alcian blue stain of morpholino injected embryos revealed a disorganisation in the branchial cartilage of the injected side. This result is comparable to that obtained after leflunomide treatment. There was also seen to be a loss of sensory neuron function as assayed by the poke and stroke method. Embryos injected with morpholino show a reduced response to external stimulus. This phenotype was also seen in the leflunomide treated embryos and further suggests that P-TEFb is playing an important role in neural crest development. Following on from this *in situ* hybridisation was carried out for genes involved in neural crest differentiation into sensory neurons such as Runx1 and Islet1. Both of these show a loss of expression after P-TEFb knockdown.

To investigate when P-TEFb and transcriptional elongation is playing a role in neural crest development, *in situ* hybridisation was carried out for markers at various stages of neural crest development. Firstly neural plate border markers which are expressed during early neural crest induction. *In situs* for these showed no change in expression suggesting that P-TEFb is not important for the transcription of these early genes. Following on from this a broad range of neural crest specifiers were investigated. This showed that the genes predominantly effacted by P-TEFb knockdown were c-Myc and Sox10. This was also shown to be the case for leflunomide treatment. c-Myc is an early neural crest specifier which has been implicated in other studies to be regulated by RNA polymerase pausing and transcriptional elongation. Sox10 is a neural crest specifier thought to be expressed directly downstream of c-Myc. Other neural crest specifiers show some alteration of their expression not commonly a total loss of expression probably due to a number of other gene networks feeding into these to maintain their expression.

To confirm the importance of c-Myc expression regulation by P-TEFb and transcriptional elongation, other genes downstream of c-Myc were investigated by *in situ* hybridisation. It is known that c-Myc lies upstream in the gene regulatory network governing the expression of trigeminal placodes. Knockdown of c-Myc in *Xenopus* leads to a loss of trigeminal placode markers. Here we show that similarly knockdown of P-TEFb also results in a knockdown of trigeminal placode markers Tbx2, NeuroD and Elrd. This gives strong evidence for the regulation of c-Myc expression by P-TEFb. Following on from this rescue experiments were carried out aiming to rescue the loss of Sox10 expression following morpholino injection by co-injecting with c-Myc RNA. These experiments suggest that injection of myc RNA is capable of rescuing the loss of Sox10 expression seen resulting from a loss of P-TEFb suggesting that c-Myc is a target of the P-TEFb complex. This suggests that c-Myc itself undergoes RNA polymerase pausing and that P-TEFb is able to promote the transcriptional elongation of c-Myc.

Chapter VI

Discussion

6.1 Discussion

6.1.1 The phenotype seen after inhibiting transcriptional elongation

The molecular mechanisms controlling neural crest cell specification and differentiation are complex and consist of many layers of regulation to ensure the cells move down the correct lineage and form the correct cell types. Here we provide evidence for an additional layer of regulation at the transcriptional elongation level. Other cell types, which have been described in other studies to undergo regulation at the level of transcriptional elongation are multipotent in nature. These include embryonic stem cells and haematopoietic stem cells. Based on this it seems logical that a multipotent cell population such as neural crest cells would also require this regulation. The aim of this work was to investigate the precise time at which transcriptional elongation is important for neural crest development and if it is important in the development of these cells to determine what genes are primarily affected and which are secondary targets.

The methods in which transcriptional elongation have been investigated in this study involved the use of the small molecule compound leflunomide as an inhibitor of transcriptional elongation. Secondly through the use of morpholino knockdowns against components of the P-TEFb complex to prevent positive transcriptional elongation from occurring. Both of these methods gave comparable results. Both demonstrate a disruption in the development of neural crest derivatives including melanophores, sensory neurons and cranio-facial cartilage. Melanophores develop incorrectly appearing rounded rather than dendritic in many cases and not migrating to the positions they are usually found in structures such as the underside of the tail (**figure 3.1**). Interestingly during the leflunomide study it was demonstrated that *X.tropicalis*, the diploid relative of *X.laevis* displayed a more striking phenotype (**figure 3.3**). This is likely due to the decreased number of alleles present in the diploid embryos, which require knock down before a

phenotype is seen. This suggests that this diploid species may be better suited for this type of chemical screen in future. A similar result has been seen in other studies, which have used Spt5 (a component of DSIF) mutant lines of *Xenopus tropicalis* and Zebrafish. The *Xenopus* Spt5 mutant known as *cyd vicious* has only a thin line of melanophores running along its neural tube. It is also paralysed suggesting a loss of sensory neuron function [283]. The zebrafish Spt5 mutant embryos appeared to have a complete loss of melanophores and reduced blood circulation [148].

The phenotype we see at stage 38 after inhibition of transcriptional elongation is one associated with the disruption of normal neural crest development. As well as abnormal melanophore development we also see what can be suggested as a complete loss of sensory neuron development. The embryos treated with leflunomide and those which had undergone morpholino injection displayed almost no response to external stimulation by poking. To confirm this loss of sensory neuron development an *in situ* hybridisation was carried out for known senory neuron markers downstream of Sox10, Runx1 and Islet1 [280]. Both of these markers showed a loss of expression after morpholino knockdown of Cdk9 and CyclinT1, the components of P-TEFb (**figure 5.19**). It was also seen in this study that inhibiting transcriptional elongation resulted in defects in the development of the neural crest derived cranio-facial cartilage. The cartilage was never completely missing but appeared disorganised in its structure (**figure 5.14**).

This phenotype we are seeing suggests that transcriptional elongation is playing a role in neural crest development. There are different possibilities as to why the different neural crest lineages investigated display varying levels of irregularity. Firstly we see a complete loss of sensory neurons, a large loss of melanophores and a disorganisation of cranio-facial development. This could be explained by the fact that according to the *in situ* and RNA sequencing data, we see the most significant loss in Sox10 expression. Sox10 is known to be important in the differentiation of neural crest cells into melanophores and sensory neurons but not cranio-facial cartilage. This requires another

member of the SoxE family, Sox9, which showed a moderate knockdown by *in situ* after leflunomide treatment and morpholino injection.

6.1.2. Wnt upregulation and neural crest development

It is also possible that the neural crest defects we see are due to changes in Wnt signalling during neural crest development. The RNA sequencing carried out in chapter 4 shows that Wnt signalling components are upregulated after leflunomide treatment at stage 15 in *Xenopus* animal caps. Recent studies using conditional activation of β-catenin have shown that upregulation of Wnt signalling during early induction of neural crest cells leads to increased numbers of neural crest derivatives mostly melanophores [276]. However if Wnt signalling is

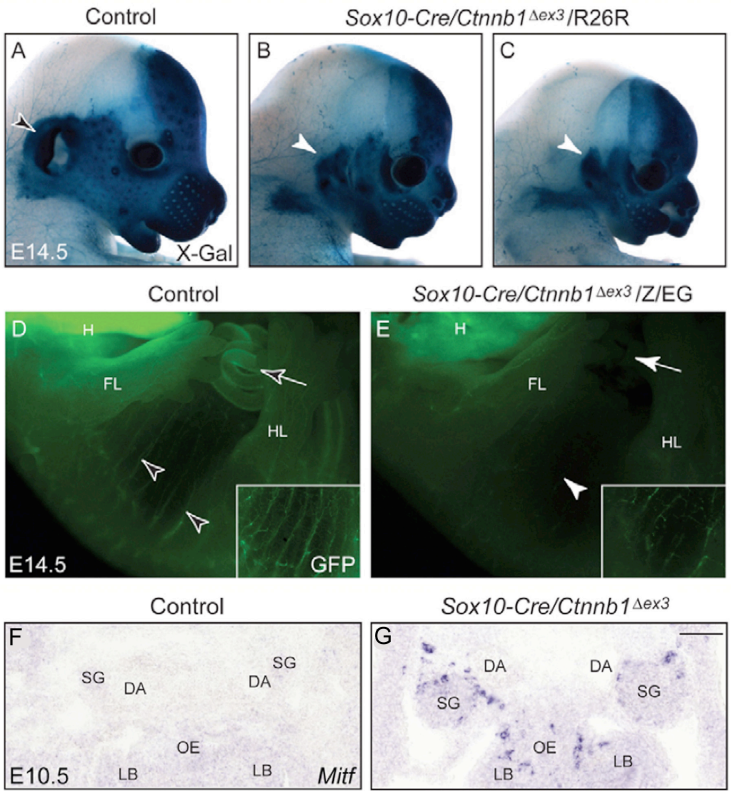

Figure 6.1 β-catenin activation in migratory neural crest leads to craniofacial malformation, loss of peripheral neurons and ectopic Mitf expression. **(A)** Control X-GAL stain shows normal neural crest in the face. **(B,C)** Malformations of the snout and ear after β-catenin activation**. (D)** normal peripheral neuron development in control embryo. **(E)** Loss of peripheral neurons after β-catenin activation. **(F)** No Mitf expression in control embryo. **(G)** Ectopic Mitf expression after β-catenin activation. Retrieved from [276]

upregulated later in neural crest development when the neural crest cells are specified, there is a loss of neural crest derivatives such as sensory neurons resulting in what are described as 'malformations' of the cranio-facial cartilage and ectopic expression of melanophores (**figure 6.1**) [276]. This same study found that although melanophores appear reduced in their normal positions, a Mitf and DCT *in situ* revealed melanophores to be located in unusual places including the kidney, spleen and diaphragm [276]. This phenotype could match the phenotype seen in the *Xenopus* embryos in this study. To confirm this it would be interesting to carry out a Mitf or DCT *in situ* on the leflunomide treated or morpholino injected embryos and section them to look for ectopic expression.

6.1.3. c-Myc is important for transcriptional elongation in neural crest cells

To identify where and when transcriptional elongation is important for neural crest development, *in situ* hybridisation experiments were carried out after leflunomide treatment and morpholino knockdown for various markers of neural crest development. To confirm these findings RNA sequencing was carried out on animal caps induced to become neural crest. These experiments showed that inhibiting transcriptional elongation has no effect on the development of early neural plate border markers such as Zic1, Zic3 and Pax3. The first changes in gene expression were seen when looking at genes involved in neural crest specification and differentiation. The two genes demonstrating the greatest level of knockdown by *in situ* were c-Myc an early neural crest specifier and Sox10 a neural crest specifier also expressed in the migrating neural crest. What is most likely is that c-Myc is the direct target of transcriptional elongation inhibition and Sox10 is a secondary target as it is thought to lie directly downstream of c-Myc [2].

c-Myc is known to be an early neural crest specifier; previous knock down studies in *Xenopus* have shown that myc is important for the expression of downstream neural crest specifiers such as Sox10 and the development of neural crest derivatives such as melanophores and craniofacial cartilage [33]. It was also shown in this same study that knock down of c-Myc also knocks down the expression of trigeminal placode markers such as Six1 and there is a loss of Sox10 expression in the trigeminal, seventh (VII), ninth (IX), and tenth (X) cranial ganglia (**figure 6.2**). This would suggest that if c-Myc is the primary target of inhibiting transcriptional elongation in neural crest cells than we should see a loss of trigeminal placode markers after morpholino knockdown of P-TEFb components. *In situ* hybridization for trigeminal placode markers Tbx2, NeuroD and Elrd showed precisely this after knockdown of both Cdk9 and CyclinT1 giving strong evidence that myc undergoes polymerase pausing and transcriptional elongation (**figure 5.21**).

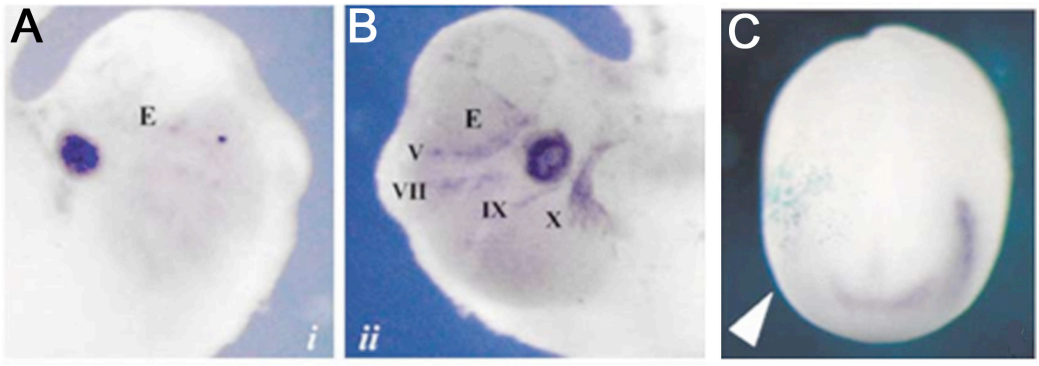

Figure 6.2 Myc knockdown leads to a loss of trigeminal placodes. (A) myc morpholino injected side of an embryo showing loss of Sox10 expression in the trigeminal, seventh (VII), ninth (IX), and tenth (X) cranial ganglia. **(B)** Control side showing normal expression. **(C)** Loss of Six1 expression after myc morpholino injection (white arrow head). Adapted from [33]

It makes sense for myc to be the primary target for regulation by transcriptional elongation and RNA polymerase pausing in neural crest cells. Previous studies using stem cell lines have shown that c-Myc undergoes pausing by knocking out a component of the SEC, Med26 [199]. That combined with its known role in neural crest specification makes it a clear candidate. To ensure that Sox10 was not a direct target and that its downregulation is a secondary effect of myc knockdown, rescue experiments were carried out using a myc expression construct after morpholino knockdown of Cdk9 and CyclinT1. This experiment

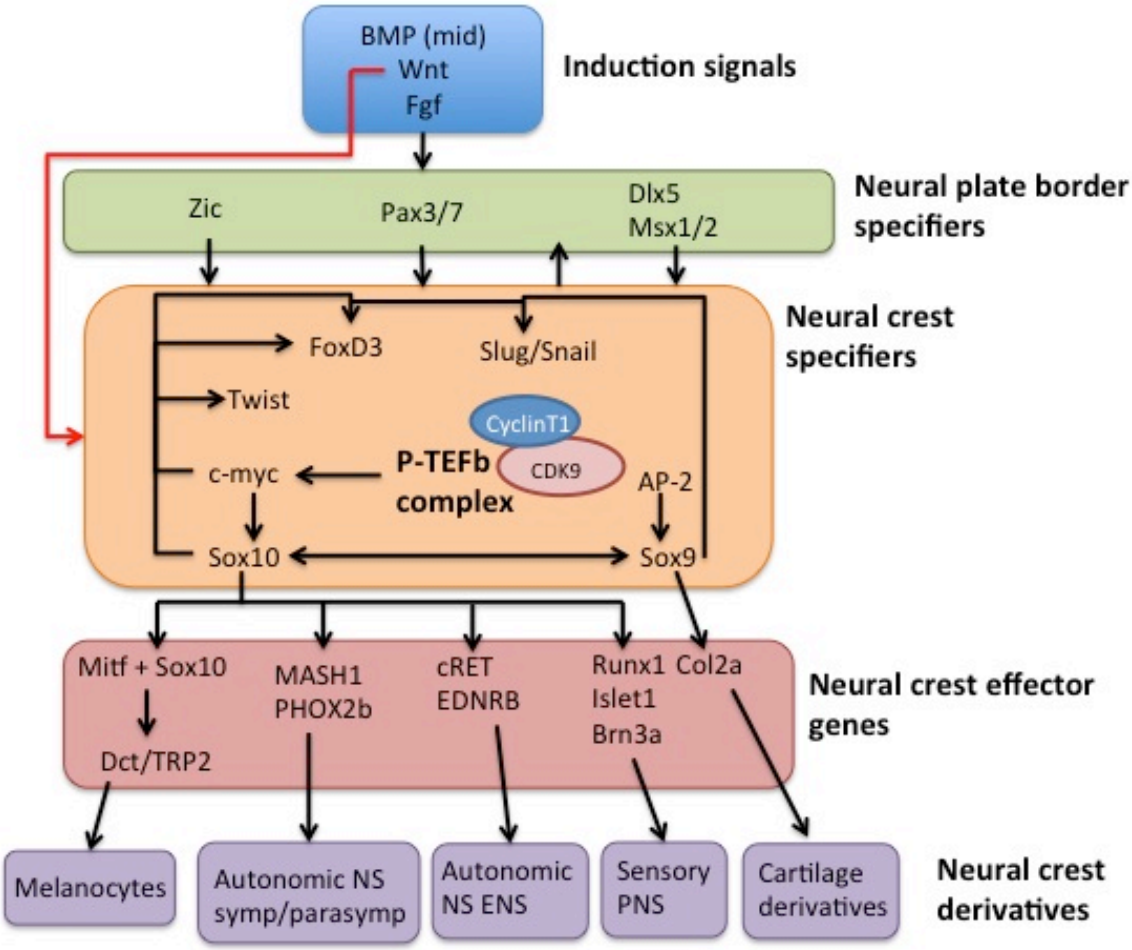

Figure 6.3 A model for the position of P-TEFb in neural crest development. P-TEFb seems to be targeting c-Myc directly. Loss of P-TEFb leads to a downregulation of c-Myc, Sox10 and alterations in the expression of the other transcriptional factors shown on this model. This could suggest that c-Myc is directly feeding into Sox10 and that the other changes seen are downstream alterations found due to this Sox10 knockdown. This model is a very simplified diagram of the neural crest gene regulatory network as not all genes involved in this network are shown here. To keep the model simple only a few examples from each level are shown. These levels are induction signals, neural plate border specifiers, neural crest specifiers, neural crest effector genes and neural crest derivatives.

succeeded in rescuing Sox10 expression suggesting that Sox10 is not itself a target of P-TEFb but must be knocked down due to the loss of upstream c-Myc signals (**figure 5.23**). This is shown as a model demonstrating the position P-TEFb plays a role in neural crest development in **figure 6.3**.

What remains unclear is the dynamic in this scenario between c-Myc, BMP and Wnt signalling. It is well known from studies in colon cancer that myc lies downstream of Wnt signalling [284]. However we see a downregulation of c-Myc and an upregulation of Wnt. The downregulation of myc that we see in the RNA sequencing is not as drastic as we would have expected from our *in situ* data. My hypothesis is that Wnt has upregulated in an attempt to maintain an equilibrium with myc, after myc was downregulated by inhibition of transcriptional elongation at stage 12 during early neural crest specification. Wnt has upregulated in response to bring the myc levels back up. This is just a hypothesis and needs further investigation. It is also unclear why BMP appears upregulated after leflunomide treatment in neural crest animal caps at stage 15 and BMP antagonist follistatin appears downregulated (**table 4.2** and **4.3**). Different types of crosstalk between BMP and Wnt may occur in a tissue dependent fashion. It is possible for Wnt and BMP to have a common target in the same tissue or cell [285]. An example of this was found in the developing mouse kidney. In this specific tissue high levels of BMP signals resulted in increased canonical Wnt signalling. This resulted in a phospho-Smad1/Tcf4/β-catenin complex, which was identified to upregulate c-Myc expression giving evidence for both Wnt and BMP synergistically upregulating c-Myc [286].

It would be interesting to see if upregulation of BMP Smad1 signalling can increase c-Myc expression in neural crest cells. For future work we also want to try to show that Wnt signalling is able to stabilize the c-Myc protein in neural crest cells. This has been implicated in Drosophila as inhibition of GSK3β leads to an accumulation of the myc protein [287]. What seems strange is that both BMP and Wnt are so clearly upregulated when there is no clear explanation why. Studies in other cancer cell types have shown that myc and Wnt are in a feedback

loop with each other. This occurs because myc can inhibit Wnt antagonists such as secreted frizzled receptor proteins (SFRPs) [288]. The only SFRP, which appears upregulated in the RNA sequencing data is Sizzled (Frzb3) which after recent studies has been identified not to inhibit Wnt at all but instead engages in a feedback loop with BMP by inhibiting tolloid enzymes which usually inhibit Chordin, which downregulates BMP. So Sizzled will inhibit BMP but BMP upregulates Sizzled [289].

Interestingly Sizzled is known to be inhibited in neural crest development by Slug. It could be possible that by reducing myc expression by inhibiting transcriptional elongation there is a reduction in downstream transcription factors like Slug [290]. Less myc means less Slug which means more Sizzled. All of these patterns are seen in the RNA sequencing. It is also suggested in the literature that Sizzled is capable of upregulating c-Myc however there is little evidence to back this up [291]. This still begs the question of how Wnt is upregulated. One possiblilty is through the feedback loop it is thought to undergo with c-Myc. c-Myc upregulates Wnt by inhibiting Wnt inhibitors and Wnt upregulates c-Myc [288]. This is still unclear and needs further investigation.

6.1.4 A fate switch for neural crest cells

Another interesting result, which came out of the RNA sequencing data was the changes in the expression of chemokine receptors and ligands normally found on neural crest cells. Neural crest cells normally express the receptors such as Cxcr4 and CD44 on their cell surface [41]. The underlying ectoderm found ventrally to the migrating neural crest cells will express the corresponding ligands, stromal cell derived factor (Sdf1) and Hyaluronan. *In situ* hybridisation experiments in *Xenopus laevis* have shown that Cxcr4 is expressed in both the premigratory and migratory NCCs (**figure 6.4A-D**) [41]. Sdf1 is expressed in the ectoderm always ahead of the neural crest cells (**figure 6.1E-I**). The cells find themselves attracted to the ligand expressing

ectoderm by chemotaxis. Sdf1 is known to be a strong chemoattractant and is known to be required for normal cranial neural crest migration and misexpression can lead to a loss in the organisation of the cranial neural crest [292].

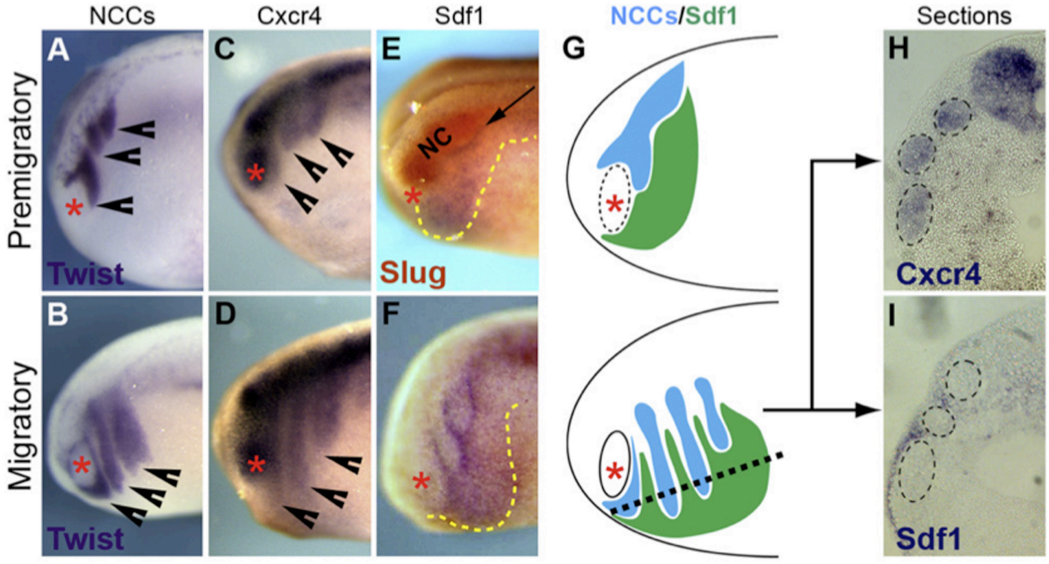

Figure 6.4 Sdf1 and Cxcr4 expression in Xenopus laevis. (**A**) Twist expression shows the position of premigratory and (**B**) migratory neural crest cells (arrow heads) (**C**) Cxcr4 is expressed in the premigratory NCCs (**D**) Cxcr4 is expressed in the migrating NCCs (**E**) Sdf1 is expressed in the ventral ectoderm (**F**) Sdf1 expression moves ventrally with the NCCs. (**G**) A schematic of the migrating NCCs in relation to the position of Sdf1. (**H**) Section showing the expression of Cxcr4 in the NCCs (**I**) Section showing expression of Sdf1 in the surrounding ectoderm. Retrieved from referece [59]

Sdf1 and Cxcr4 chemotaxis is known to function by promoting Rac1 activity, a Rho-GTPase responsible for creating the migratory shape of the cells. Rac1 causes the cells to protrude forward lamellipodia, which are stabilized allowing the cell to migrate towards the Sdf1 chemoattractant signal. In the case of neural crest cells, there will be a large number of cells all migrating at once. These cells will bump into each other and upon doing so the lamellipodia retract allowing the cell to control its direction based on what the other neural crest cells are doing. When one neural crest cell comes into contact with another it will draw in its lamellipodia and form new ones on the adjacent side of the cells. This process is known as contact inhibition locomotion (CIL). This

occurs as the contacting cells will express N-cadherins on their surface which will promote the non-canonical Wnt pathway which upregulates RhoA and downregulates Rac1 allowing cells to repolarise (**figure 6.5**). CIL between neural crest cells has been shown to be essential for chemotaxis to occur [59].

This role of Sdf1 and Cxcr4 in neural crest development helps to identify an explanation for the results obtained in the RNA sequencing data shown in chapter four. This data suggests that Sdf1 normally expressed by the surrounding ectoderm is upregulated in the neural crest sample and the receptor Cxcr4 normally expressed by the cells is downregulated after leflunomide treatment. This further backs up the

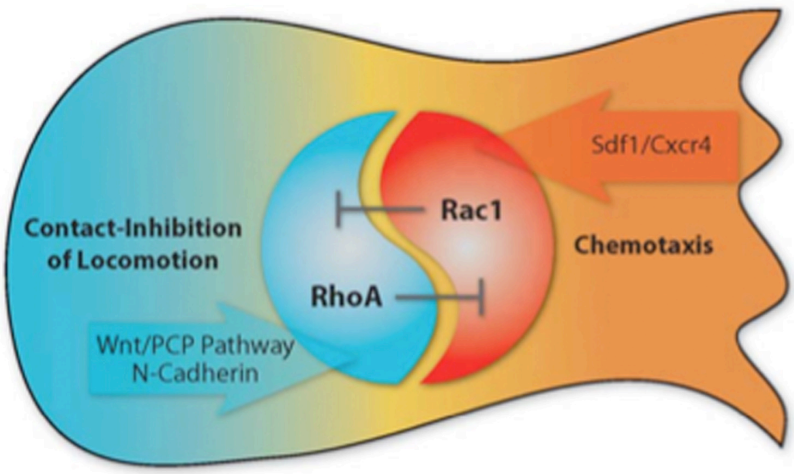

Figure 6.5 Contact inhibition locomotion and chemotaxis of neural crest cells. The right half of the figure (red) shows how Sdf1 and Cxcr4 promote chemotaxis by upregulating Rac1 allowing cell protrusions. This is balanced to direct the cells by non-canonical Wnt signalling which will upregulate Rho after contact with other cells to cause protrusions to withdraw by inhibiting Rac1 shown on the left half of the figure (blue). Retrieved from reference [285]

hypothesis that transcriptional elongation is important for neural crest development. It also gives a suggestion as to what these neural crest cells are becoming. If they are no longer becoming neural crest cells then it is likely that they have undergone a fate switch potentially into surrounding ectodermal cells. This is possible as the neural crest cell sample treated with leflunomide was seen to be upregulating several

markers normally found in the surrounding ectoderm such as Sdf1, Nkx3.1, Hyaluronan and Gata binding factor 3. This also gives a possible suggestion as to why the *Xenopus* embryos treated with leflunomide and injected with P-TEFb morpholinos are seen to have disorganised cranial facial cartilage at tadpole stages. It is likely that the cells are not migrating properly due to this receptor/ligand switch.

The only question here that remains to be answered is what is causing Sdf1 to be upregulated. Very little is known as to what causes Sdf1 expression. It is possible, based on the RNA sequencing data, that the Sdf1 expression is caused by canonical Wnt signalling as Wnt signalling was seen to be greatly upregulated after leflunomide treatment. This could potentially explain why other studies in which Wnt has been upregulated later on in neural crest development have seen a disorganisation of the cranio-facial cartilage. This is just a hypothesis and requires further work to verify. Further experiments, which could be carried out include in-situ hybridisation of Sdf1 and Cxcr4 on whole embryos to see if the expression pattern of these is altered after leflunomide treatment or knockdown of P-TEFb. It would also be good to confirm the result seen in the RNA sequencing using animal caps. PCR could be carried out for both Sdf1 and Cxcr4 to observe a switch in their expression levels. To further investigate the possibility of Wnt upregulation promoting Sdf1 expression a small molecule compound activating Wnt signalling could be applied at different stages of neural crest development and the expression of both Sdf1 and Cxcr4 could be observed. Compounds used to activate Wnt are usually those, which inhibit GSK3 responsible for the degradation of β-catenin. An example of one often used is 6-bromoindirubin-3'-oxime (BIO), a GSK3 inhibitor [293].

6.1.5 HEXIM1 upregulation after leflunomide treatment

There are three possible forms of the P-TEFb complex, two active forms (when P-TEFb is bound to the SEC and Brd4) and one inactive form (when P-TEFb is bound to HEXIM1), which are all present in the cell nucleus. This type of regulation of the P-TEFb complex is important to ensure that transcriptional elongation occurs at the correct time in development. P-TEFb is held in an inactive state by reversible binding with the 7SK small nuclear ribonucleoprotein particle (snRNP) and the inhibitory domain of HEXIM1. When transcriptional elongation is required this binding is reversible and the P-TEFb complex binds with the SEC in response to developmental cues. These activating signals provide specificity for P-TEFb to its target genes [157].

After leflunomide treatment it was seen that HEXIM1 was upregulated in the neural crest, neuroectoderm and ectoderm samples. This gives evidence that leflunomide is inhibiting transcriptional elongation as an increase in HEXIM1 would suggest that more P-TEFb is being held in its inactive form. It is thought that leflunomide is able to do this due to its known mechanism as an inhibitor of DHODH. This mechanism involves the metabolism of leflunomide into A771726. This metabolite will inhibit de novo synthesis of pyrimidines and therefore RNA transcription and DNA replication [294]. Leflunomide is a good candidate for our experiments as it is already FDA approved for rheumatoid arthritis treatment where it is thought to inhibit DHODH in lymphocytes to have an anti-inflammatory effect [295].

This study shows that leflunomide is inhibiting transcriptional elongation through P-TEFb inhibition and suggests that it is not altering the methylation patterns on the genes. The fact that all three cell types show an increase in this indicate that this is an effect of leflunomide addition. What is interesting is that although all three cell types have increased HEXIM1 levels the neural crest sample is the only one that shows decreases in its specific gene expression i.e. neural crest specific genes. No neuroectoderm specific genes such as Sox2 were downregulated in the neuroectoderm sample and no ectoderm specific

genes were downregulated in the ectoderm sample. This suggests that regulation of transcriptional elongation is relatively specific for neural crest development. It may be involved in other cell types not investigated here but this data does suggest that it is not required for all genes and all cells types.

6.1.6 Geminin upregulation

Geminin regulates the polycomb repressive complex (PRC) which carries out histone modifications to silence specific genes. Through this mechanism, Geminin has been shown in *Xenopus* to be involved in maintaining the pluripotent state of cells and maintaining the neural precursor cell fate [275]. Geminin expression is downregulated after neural differentiation [275]. This was one of the genes, which was seen to be highly upregulated in the RNA sequencing data. This seemed interesting because of the links made between geminin, epigenetics and transcription regulation and so it could help us to explain some of the results that we see after inhibiting transcriptional elongation in *Xenopus*.

Recent studies investigating the role of Geminin in *Xenopus* development have used microarrays to analyse a wide spread of genes affected by upregulating the expression of Geminin and so it was interesting to compare these results to those obtained in the RNA sequencing data obtained here. There were many cross overs between the two data sets. For example both the microarray after Geminin overexpression and the RNA sequencing shown in chapter four see a downregulation of c-Myc, Cxcr4 and Tiarin. Also the microarray shows downregulation of Tbx2, the trigeminal placode marker downregulated after P-TEFb knockdown shown by *in situ* in chapter five. The microarray data also demonstrates an upregulation of neuroprogenitor genes such as Sox1, which seems to be the trend seen in the neuroectoderm sample after RNA sequencing. The microarray data is mostly focused on genes involved in neurogenesis and so it is hard to make a full comparison but it is good to see some cross over between these similar studies.

6.1.7 Heat shock proteins

The transcription of heat shock proteins is rapidly induced upon stress or heat to cells. Their function is to prevent cells apoptosing in response to these stresses. Missexpression of these are associated with cancer and ageing [242, 245]. It is well charatersied that heat shock proteins will undergo transcriptional pausing at their promoter region and subsequent transcriptional elongation [220, 246, 247]. P-TEFb is recruited by these heat signals to allow transcriptional elongation to occur [250]. It was good to see that all three of the samples sent for RNA sequencing had a decrease in heat shock protein expression. This gives us confidence that leflunomide is acting to inhibit transcriptional elongation.

What appears interesting is that some heat shock proteins have been associated with aspects of neural crest development. Upregulation of hsp70 leads to c-Myc upregulation in cancer cells [243]. Hsp105/110 expression pattern studies have identified these to potentially be expressed in the neural crest along with some other neural tissue types such as the brain [296]. Interestingly Hsp105/110 expression was relatively specific to the neural crest animal cap sample. It was also one of the genes identified to be downregulated by leflunomide treatment. For future work it would be interesting to further investigate the role of these heat shock proteins in neural crest development. It could be possible that these are a primary target of inhibiting transcriptional elongation, which might lead to defects in neural crest development.

6.1.8. Conclusions and future work

The work shown in this thesis suggests that regulation of transcriptional elongation is important for the development of neural crest cells. Inhibiting transcriptional elongation results in a decrease in the expression of c-Myc and Sox10 and other neural crest markers leading to defects in the normal development of neural crest derivatives such as

melanophores, sensory neurons and cranio-facial cartilage. c-Myc has been shown here to be particularly sensitive to inhibition of transcriptional elongation and so it is possible that c-Myc is a primary target of RNA polymerase pausing and this results in the neural crest defects seen here. Other studies have shown that c-Myc is sensitive to polymerase pausing. The loss of Sox10 expression can be rescued by injection of c-Myc RNA suggesting that Sox10 is not a primary target of RNA polymerase pausing.

To further confirm that c-Myc is a primary target it would be good to rescue the loss of Sox10 expression with c-Myc but still see a loss of endogenous c-Myc. This could be done perhaps by rescuing with human c-Myc RNA but carrying out an in-situ for *Xenopus* c-Myc. In this situation the probes must be carefully designed not to cross react. Alternatively a probe could be made for the c-Myc 3'UTR which would only recognise endogenous c-Myc and not the c-Myc injected. Although c-Myc has been shown to be paused in other cell types it would also be a good experiment to show this in the *Xenopus* whole embryo and animal cap. This could be done using ChIP PCR or sequencing with antibodies against RNA polymerase II to see where along the gene body the polymerase is most commonly found. After inhibiting transcriptional elongation we would hypothesise that RNA polymerase II will be most commonly found at the promoter region of c-Myc indicating a that the gene is held in a paused state.

Although RNA polymerase pausing is known to be important in other cell types such as blood cells and stem cells, it could be suggested that it is also specific for neural crest cells. There has been a debate in the literature recently as to whether pausing is seen to some extent in all cell types or whether it is a phenomena specific to certain cells. The results obtained here show that when the three cells types neural crest, neuroectoderm and ectoderm have transcriptional elongation inhibited the only cell type to show specific changes was the neural crest sample. All three samples displayed an increase in HEXIM1 expression suggesting that P-TEFb is held in an inactive state, however the neural crest sample was the only sample to also display a loss in its orginal fate.

The neural crest specifier genes such as Sox10 and Slug were seen to be downregulated and genes expressed in the surrounding ectoderm were upregulated in their place. The neuroectoderm did not lose its orginal cell fate. Genes expressed in neuroprogenitor cells such as Sox1 were seen to be upregulated and genes involved in ectoderm formation were downregulated. This would suggest that more neuroectoderm is present irrespective of ectoderm and that the neuroectoderm cell fate is not lost upon inhibiting transcriptional elongation. The ectoderm cell type showed no changes in any ectoderm specific genes and so it can be suggested that this cell type was not afftected by inhibiting transcriptional elongation. These data indicate that transcriptional elongation is not important for the development of all cell types but could be considered relatively specific for neural crest cells.

1. Schneider, M., A. Schambony, and D. Wedlich, *Prohibitin1 acts as a neural crest specifier in Xenopus development by repressing the transcription factor E2F1.* Development, 2010. **137**(23): p. 4073-81.

2. Sauka-Spengler, T. and M. Bronner-Fraser, *A gene regulatory network orchestrates neural crest formation.* Nat Rev Mol Cell Biol, 2008. **9**(7): p. 557-68.

3. White, R.M., et al., *DHODH modulates transcriptional elongation in the neural crest and melanoma.* Nature, 2011. **471**(7339): p. 518-22.

4. Loffler, M., et al., *Dihydroorotat-ubiquinone oxidoreductase links mitochondria in the biosynthesis of pyrimidine nucleotides.* Mol Cell Biochem, 1997. **174**(1-2): p. 125-9.

5. Wu, J.Q. and M. Snyder, *RNA polymerase II stalling: loading at the start prepares genes for a sprint.* Genome Biol, 2008. **9**(5): p. 220.

6. Rahl, P.B., et al., *c-Myc regulates transcriptional pause release.* Cell, 2010. **141**(3): p. 432-45.

7. Harland, R.M. and R.M. Grainger, *Xenopus research: metamorphosed by genetics and genomics.* Trends in genetics : TIG, 2011. **27**(12): p. 507-15.

8. Tickle, L.W.a.C., *Principles of Development*. 4th ed2010: Oxford University Press. 720.

9. Huang, X. and J.P. Saint-Jeannet, *Induction of the neural crest and the opportunities of life on the edge.* Dev Biol, 2004. **275**(1): p. 1-11.

10. Bonstein, L., S. Elias, and D. Frank, *Paraxial-fated mesoderm is required for neural crest induction in Xenopus embryos.* Dev Biol, 1998. **193**(2): p. 156-68.

11. Marchant, L., et al., *The inductive properties of mesoderm suggest that the neural crest cells are specified by a BMP gradient.* Dev Biol, 1998. **198**(2): p. 319-29.

12. LaBonne, C. and M. Bronner-Fraser, *Neural crest induction in Xenopus: evidence for a two-signal model.* Development, 1998. **125**(13): p. 2403-14.

13. Mayor, R., R. Morgan, and M.G. Sargent, *Induction of the prospective neural crest of Xenopus.* Development, 1995. **121**(3): p. 767-77.

14. Mayor, R., N. Guerrero, and C. Martinez, *Role of FGF and noggin in neural crest induction.* Dev Biol, 1997. **189**(1): p. 1-12.

15. Monsoro-Burq, A.H., R.B. Fletcher, and R.M. Harland, *Neural crest induction by paraxial mesoderm in Xenopus embryos requires FGF signals.* Development, 2003. **130**(14): p. 3111-24.

16. Endo, Y., N. Osumi, and Y. Wakamatsu, *Bimodal functions of Notch-mediated signaling are involved in neural crest formation during avian ectoderm development.* Development, 2002. **129**(4): p. 863-73.

17. Glavic, A., et al., *Interplay between Notch signaling and the homeoprotein Xiro1 is required for neural crest induction in Xenopus embryos.* Development, 2004. **131**(2): p. 347-59.

18. Steventon, B., et al., *Differential requirements of BMP and Wnt signalling during gastrulation and neurulation define two steps in neural crest induction.* Development, 2009. **136**(5): p. 771-9.

19. Meulemans, D. and M. Bronner-Fraser, *Gene-regulatory interactions in neural crest evolution and development.* Developmental cell, 2004. **7**(3): p. 291-9.

20. Lewis, J.L., et al., *Reiterated Wnt signaling during zebrafish neural crest development.* Development, 2004. **131**(6): p. 1299-308.

21. Wu, J., J. Yang, and P.S. Klein, *Neural crest induction by the canonical Wnt pathway can be dissociated from anterior-posterior neural patterning in Xenopus.* Dev Biol, 2005. **279**(1): p. 220-32.

22. Garcia-Castro, M.I., C. Marcelle, and M. Bronner-Fraser, *Ectodermal Wnt function as a neural crest inducer.* Science, 2002. **297**(5582): p. 848-51.

23. Chang, C. and A. Hemmati-Brivanlou, *Neural crest induction by Xwnt7B in Xenopus.* Dev Biol, 1998. **194**(1): p. 129-34.

24. Saint-Jeannet, J.P., et al., *Regulation of dorsal fate in the neuraxis by Wnt-1 and Wnt-3a.* Proc Natl Acad Sci U S A, 1997. **94**(25): p. 13713-8.

25. Deardorff, M.A., et al., *A role for frizzled 3 in neural crest development.* Development, 2001. **128**(19): p. 3655-63.

26. Abu-Elmagd, M., C. Garcia-Morales, and G.N. Wheeler, *Frizzled7 mediates canonical Wnt signaling in neural crest induction.* Dev Biol, 2006. **298**(1): p. 285-98.

27. Monsoro-Burq, A.H., E. Wang, and R. Harland, *Msx1 and Pax3 cooperate to mediate FGF8 and WNT signals during Xenopus neural crest induction.* Dev Cell, 2005. **8**(2): p. 167-78.

28. Sato, T., N. Sasai, and Y. Sasai, *Neural crest determination by co-activation of Pax3 and Zic1 genes in Xenopus ectoderm.* Development, 2005. **132**(10): p. 2355-63.

29. Honore, S.M., M.J. Aybar, and R. Mayor, *Sox10 is required for the early development of the prospective neural crest in Xenopus embryos.* Dev Biol, 2003. **260**(1): p. 79-96.

30. Li, B., et al., *The posteriorizing gene Gbx2 is a direct target of Wnt signalling and the earliest factor in neural crest induction.* Development, 2009. **136**(19): p. 3267-78.

31. Bajpai, R., et al., *CHD7 cooperates with PBAF to control multipotent neural crest formation.* Nature, 2010. **463**(7283): p. 958-62.

32. Sauka-Spengler, T., et al., *Ancient evolutionary origin of the neural crest gene regulatory network.* Dev Cell, 2007. **13**(3): p. 405-20.

33. Bellmeyer, A., et al., *The protooncogene c-myc is an essential regulator of neural crest formation in xenopus.* Dev Cell, 2003. **4**(6): p. 827-39.

34. Kee, Y. and M. Bronner-Fraser, *To proliferate or to die: role of Id3 in cell cycle progression and survival of neural crest progenitors.* Genes Dev, 2005. **19**(6): p. 744-55.

35. Light, W., et al., *Xenopus Id3 is required downstream of Myc for the formation of multipotent neural crest progenitor cells.* Development, 2005. **132**(8): p. 1831-41.

36. Hong, S.K., M. Tsang, and I.B. Dawid, *The mych gene is required for neural crest survival during zebrafish development.* PLoS One, 2008. **3**(4): p. e2029.

37. Strobl-Mazzulla, P.H., T. Sauka-Spengler, and M. Bronner-Fraser, *Histone demethylase JmjD2A regulates neural crest specification.* Dev Cell, 2010. **19**(3): p. 460-8.

38. Pasini, D., et al., *JARID2 regulates binding of the Polycomb repressive complex 2 to target genes in ES cells.* Nature, 2010. **464**(7286): p. 306-10.

39. Nunes, M., et al., *NSPc1, a novel mammalian Polycomb gene, is expressed in neural crest-derived structures of the peripheral nervous system.* Mech Dev, 2001. **102**(1-2): p. 219-22.

40. Rouleau, M., et al., *A key role for poly(ADP-ribose) polymerase 3 in ectodermal specification and neural crest development.* PLoS One, 2011. **6**(1): p. e15834.

41. Mayor, R. and E. Theveneau, *The neural crest.* Development, 2013. **140**(11): p. 2247-51.

42. Krispin, S., et al., *Evidence for a dynamic spatiotemporal fate map and early fate restrictions of premigratory avian neural crest.* Development, 2010. **137**(4): p. 585-95.

43. McKinney, M.C., et al., *Evidence for dynamic rearrangements but lack of fate or position restrictions in premigratory avian trunk neural crest.* Development, 2013. **140**(4): p. 820-30.

44. Thiery, J.P. and J.P. Sleeman, *Complex networks orchestrate epithelial-mesenchymal transitions.* Nat Rev Mol Cell Biol, 2006. **7**(2): p. 131-42.

45. Nieto, M.A., *The snail superfamily of zinc-finger transcription factors.* Nat Rev Mol Cell Biol, 2002. **3**(3): p. 155-66.

46. Taneyhill, L.A., E.G. Coles, and M. Bronner-Fraser, *Snail2 directly represses cadherin6B during epithelial-to-mesenchymal transitions of the neural crest.* Development, 2007. **134**(8): p. 1481-90.

47. Chu, Y.S., et al., *Prototypical type I E-cadherin and type II cadherin-7 mediate very distinct adhesiveness through their extracellular domains.* J Biol Chem, 2006. **281**(5): p. 2901-10.

48. Cano, A., et al., *The transcription factor snail controls epithelial-mesenchymal transitions by repressing E-cadherin expression.* Nat Cell Biol, 2000. **2**(2): p. 76-83.

49. Ikenouchi, J., et al., *Regulation of tight junctions during the epithelium-mesenchyme transition: direct repression of the gene expression of claudins/occludin by Snail.* J Cell Sci, 2003. **116**(Pt 10): p. 1959-67.

50. Shook, D. and R. Keller, *Mechanisms, mechanics and function of epithelial-mesenchymal transitions in early development.* Mech Dev, 2003. **120**(11): p. 1351-83.

51. Chang, C. and Z. Werb, *The many faces of metalloproteases: cell growth, invasion, angiogenesis and metastasis.* Trends Cell Biol, 2001. **11**(11): p. S37-43.

52. Cai, D.H., et al., *MMP-2 expression during early avian cardiac and neural crest morphogenesis.* Anat Rec, 2000. **259**(2): p. 168-79.

53. Huh, M.I., et al., *Roles of MMP/TIMP in regulating matrix swelling and cell migration during chick corneal development.* J Cell Biochem, 2007. **101**(5): p. 1222-37.

54. Alfandari, D., et al., *Xenopus ADAM 13 is a metalloprotease required for cranial neural crest-cell migration.* Curr Biol, 2001. **11**(12): p. 918-30.

55. Harrison, M., et al., *Matrix metalloproteinase genes in Xenopus development.* Dev Dyn, 2004. **231**(1): p. 214-20.

56. Burstyn-Cohen, T. and C. Kalcheim, *Association between the cell cycle and neural crest delamination through specific regulation of G1/S transition.* Dev Cell, 2002. **3**(3): p. 383-95.

57. Vega, S., et al., *Snail blocks the cell cycle and confers resistance to cell death.* Genes Dev, 2004. **18**(10): p. 1131-43.

58. Mayor, R. and C. Carmona-Fontaine, *Keeping in touch with contact inhibition of locomotion.* Trends in cell biology, 2010. **20**(6): p. 319-28.

59. Theveneau, E., et al., *Collective chemotaxis requires contact-dependent cell polarity.* Developmental cell, 2010. **19**(1): p. 39-53.

60. Theveneau, E. and R. Mayor, *Collective cell migration of epithelial and mesenchymal cells.* Cellular and molecular life sciences : CMLS, 2013.

61. Potterf, S.B., et al., *Analysis of SOX10 function in neural crest-derived melanocyte development: SOX10-dependent transcriptional control of dopachrome tautomerase.* Dev Biol, 2001. **237**(2): p. 245-57.

62. Elworthy, S., et al., *Transcriptional regulation of mitfa accounts for the sox10 requirement in zebrafish melanophore development.* Development, 2003. **130**(12): p. 2809-18.

63. Thomas, A.J. and C.A. Erickson, *FOXD3 regulates the lineage switch between neural crest-derived glial cells and pigment cells by repressing MITF through a non-canonical mechanism.* Development, 2009. **136**(11): p. 1849-58.

64. Tachibana, M., *MITF: a stream flowing for pigment cells.* Pigment Cell Res, 2000. **13**(4): p. 230-40.

65. Schwarz, Q., et al., *Neuropilin 1 signaling guides neural crest cells to coordinate pathway choice with cell specification.* Proc Natl Acad Sci U S A, 2009. **106**(15): p. 6164-9.

66. Cooper, C.D. and D.W. Raible, *Mechanisms for reaching the differentiated state: Insights from neural crest-derived melanocytes.* Semin Cell Dev Biol, 2009. **20**(1): p. 105-10.

67. Dupin, E. and N.M. Le Douarin, *Development of melanocyte precursors from the vertebrate neural crest.* Oncogene, 2003. **22**(20): p. 3016-23.

68. Thomas, A.J. and C.A. Erickson, *The making of a melanocyte: the specification of melanoblasts from the neural crest.* Pigment Cell Melanoma Res, 2008. **21**(6): p. 598-610.

69. Lecoin, L., et al., *Cloning and characterization of a novel endothelin receptor subtype in the avian class.* Proc Natl Acad Sci U S A, 1998. **95**(6): p. 3024-9.

70. Kelsh, R.N., et al., *Stripes and belly-spots -- a review of pigment cell morphogenesis in vertebrates.* Semin Cell Dev Biol, 2009. **20**(1): p. 90-104.

71. Shin, M.K., et al., *The temporal requirement for endothelin receptor-B signalling during neural crest development.* Nature, 1999. **402**(6761): p. 496-501.

72. Uong, A. and L.I. Zon, *Melanocytes in development and cancer.* J Cell Physiol, 2010. **222**(1): p. 38-41.

73. Iyengar, B. and A.V. Singh, *Patterns of neural differentiation in melanomas.* J Biomed Sci, 2010. **17**: p. 87.

74. Patton, E.E., et al., *BRAF mutations are sufficient to promote nevi formation and cooperate with p53 in the genesis of melanoma.* Curr Biol, 2005. **15**(3): p. 249-54.

75. Garraway, L.A., et al., *Integrative genomic analyses identify MITF as a lineage survival oncogene amplified in malignant melanoma.* Nature, 2005. **436**(7047): p. 117-22.

76. Curtin, J.A., et al., *Somatic activation of KIT in distinct subtypes of melanoma.* J Clin Oncol, 2006. **24**(26): p. 4340-6.

77. Gupta, P.B., et al., *The melanocyte differentiation program predisposes to metastasis after neoplastic transformation.* Nat Genet, 2005. **37**(10): p. 1047-54.

78. Bagnato, A., et al., *Endothelin B receptor blockade inhibits dynamics of cell interactions and communications in melanoma cell progression.* Cancer Res, 2004. **64**(4): p. 1436-43.

79. Bakos, R.M., et al., *Nestin and SOX9 and SOX10 transcription factors are coexpressed in melanoma.* Exp Dermatol, 2010. **19**(8): p. e89-94.

80. Serbedzija, G.N., M. Bronner-Fraser, and S.E. Fraser, *Vital dye analysis of cranial neural crest cell migration in the mouse embryo.* Development, 1992. **116**(2): p. 297-307.

81. Baltzinger, M., et al., *Hoxa2 knockdown in Xenopus results in hyoid to mandibular homeosis.* Developmental dynamics : an official publication of the American Association of Anatomists, 2005. **234**(4): p. 858-67.

82. Cerny, R., et al., *Developmental origins and evolution of jaws: new interpretation of "maxillary" and "mandibular".* Developmental biology, 2004. **276**(1): p. 225-36.

83. Trainor, P.A. and R. Krumlauf, *Hox genes, neural crest cells and branchial arch patterning.* Current opinion in cell biology, 2001. **13**(6): p. 698-705.

84. Spokony, R.F., et al., *The transcription factor Sox9 is required for cranial neural crest development in Xenopus.* Development, 2002. **129**(2): p. 421-32.

85. Flores, M.V., et al., *A hierarchy of Runx transcription factors modulate the onset of chondrogenesis in craniofacial endochondral bones in zebrafish.* Developmental dynamics : an official publication of the American Association of Anatomists, 2006. **235**(11): p. 3166-76.

86. Bonano, M., et al., *A new role for the Endothelin-1/Endothelin-A receptor signaling during early neural crest specification.* Developmental biology, 2008. **323**(1): p. 114-29.

87. Nair, S., et al., *Requirements for Endothelin type-A receptors and Endothelin-1 signaling in the facial ectoderm for the patterning of skeletogenic neural crest cells in zebrafish.* Development, 2007. **134**(2): p. 335-45.

88. Pavan, W.J. and D.W. Raible, *Specification of neural crest into sensory neuron and melanocyte lineages.* Developmental biology, 2012. **366**(1): p. 55-63.

89. Lee, H.Y., et al., *Instructive role of Wnt/beta-catenin in sensory fate specification in neural crest stem cells.* Science, 2004. **303**(5660): p. 1020-3.

90. Greenwood, A.L., E.E. Turner, and D.J. Anderson, *Identification of dividing, determined sensory neuron precursors in the mammalian neural crest.* Development, 1999. **126**(16): p. 3545-59.

91. Ma, Q., et al., *Neurogenin1 and neurogenin2 control two distinct waves of neurogenesis in developing dorsal root ganglia.* Genes & development, 1999. **13**(13): p. 1717-28.

92. Fode, C., et al., *The bHLH protein NEUROGENIN 2 is a determination factor for epibranchial placode-derived sensory neurons.* Neuron, 1998. **20**(3): p. 483-94.

93. Eng, S.R., et al., *Defects in sensory axon growth precede neuronal death in Brn3a-deficient mice.* The Journal of neuroscience : the official journal of the Society for Neuroscience, 2001. **21**(2): p. 541-9.

94. Sun, Y., et al., *A central role for Islet1 in sensory neuron development linking sensory and spinal gene regulatory programs.* Nature neuroscience, 2008. **11**(11): p. 1283-93.

95. Dykes, I.M., et al., *Brn3a regulates neuronal subtype specification in the trigeminal ganglion by promoting Runx expression during sensory differentiation.* Neural development, 2010. **5**: p. 3.

96. Inoue, K., et al., *Runx3 controls the axonal projection of proprioceptive dorsal root ganglion neurons.* Nature neuroscience, 2002. **5**(10): p. 946-54.

97. Levanon, D., et al., *Spatial and temporal expression pattern of Runx3 (Aml2) and Runx1 (Aml1) indicates non-redundant functions during mouse embryogenesis.* Mechanisms of development, 2001. **109**(2): p. 413-7.

98. Pieper, M., et al., *Origin and segregation of cranial placodes in Xenopus laevis.* Developmental biology, 2011. **360**(2): p. 257-75.

99. Schlosser, G., *Induction and specification of cranial placodes.* Developmental biology, 2006. **294**(2): p. 303-51.

100. Brugmann, S.A. and S.A. Moody, *Induction and specification of the vertebrate ectodermal placodes: precursors of the cranial sensory organs.* Biology of the cell / under the auspices of the European Cell Biology Organization, 2005. **97**(5): p. 303-19.

101. McCabe, K.L. and M. Bronner-Fraser, *Molecular and tissue interactions governing induction of cranial ectodermal placodes.* Developmental biology, 2009. **332**(2): p. 189-95.

102. Streit, A., *The preplacodal region: an ectodermal domain with multipotential progenitors that contribute to sense organs and cranial sensory ganglia.* The International journal of developmental biology, 2007. **51**(6-7): p. 447-61.

103. Grocott, T., M. Tambalo, and A. Streit, *The peripheral sensory nervous system in the vertebrate head: a gene regulatory perspective.* Developmental biology, 2012. **370**(1): p. 3-23.

104. Schlosser, G. and K. Ahrens, *Molecular anatomy of placode development in Xenopus laevis.* Developmental biology, 2004. **271**(2): p. 439-66.

105. Schlosser, G. and R.G. Northcutt, *Development of neurogenic placodes in Xenopus laevis.* The Journal of comparative neurology, 2000. **418**(2): p. 121-46.

106. Sasaki, F., et al., *Embryonic development of the pituitary gland in the chick.* Cells, tissues, organs, 2003. **173**(2): p. 65-74.

107. Chapman, S.C., et al., *A three-dimensional atlas of pituitary gland development in the zebrafish.* The Journal of comparative neurology, 2005. **487**(4): p. 428-40.

108. Graham, A. and S.M. Shimeld, *The origin and evolution of the ectodermal placodes.* Journal of anatomy, 2013. **222**(1): p. 32-40.

109. Herzog, W., et al., *Adenohypophysis formation in the zebrafish and its dependence on sonic hedgehog.* Developmental biology, 2003. **254**(1): p. 36-49.

110. Buck, L.B., *Olfactory receptors and odor coding in mammals.* Nutrition reviews, 2004. **62**(11 Pt 2): p. S184-8; discussion S224-41.

111. Reiss, J.O. and G.D. Burd, *Cellular and molecular interactions in the development of the Xenopus olfactory system.* Seminars in cell & developmental biology, 1997. **8**(2): p. 171-9.

112. Lovicu, F.J. and J.W. McAvoy, *Growth factor regulation of lens development.* Developmental biology, 2005. **280**(1): p. 1-14.

113. Chow, R.L. and R.A. Lang, *Early eye development in vertebrates.* Annual review of cell and developmental biology, 2001. **17**: p. 255-96.

114. Ogino, H. and K. Yasuda, *Sequential activation of transcription factors in lens induction.* Development, growth & differentiation, 2000. **42**(5): p. 437-48.

115. Artinger, K.B., et al., *Placodal origin of Brn-3-expressing cranial sensory neurons.* Journal of neurobiology, 1998. **36**(4): p. 572-85.

116. Andermann, P., J. Ungos, and D.W. Raible, *Neurogenin1 defines zebrafish cranial sensory ganglia precursors.* Developmental biology, 2002. **251**(1): p. 45-58.

117. D'Amico-Martel, A. and D.M. Noden, *Contributions of placodal and neural crest cells to avian cranial peripheral ganglia.* The American journal of anatomy, 1983. **166**(4): p. 445-68.

118. Barald, K.F. and M.W. Kelley, *From placode to polarization: new tunes in inner ear development.* Development, 2004. **131**(17): p. 4119-30.

119. Noramly, S. and R.M. Grainger, *Determination of the embryonic inner ear.* Journal of neurobiology, 2002. **53**(2): p. 100-28.

120. Northcutt, R.G., K.C. Catania, and B.B. Criley, *Development of lateral line organs in the axolotl.* The Journal of comparative neurology, 1994. **340**(4): p. 480-514.

121. Smith, S.C., *Pattern formation in the urodele mechanoreceptive lateral line: what features can be exploited for the study of development and evolution?* The International journal of developmental biology, 1996. **40**(4): p. 727-33.

122. Ghysen, A. and C. Dambly-Chaudiere, *Development of the zebrafish lateral line.* Current opinion in neurobiology, 2004. **14**(1): p. 67-73.

123. Couly, G.F. and N.M. Le Douarin, *Mapping of the early neural primordium in quail-chick chimeras. I. Developmental relationships between placodes, facial ectoderm, and prosencephalon.* Developmental biology, 1985. **110**(2): p. 422-39.

124. Northcutt, R.G., *Taste buds: development and evolution.* Brain, behavior and evolution, 2004. **64**(3): p. 198-206.

125. Epstein, J.A. and B.G. Neel, *Signal transduction: an eye on organ development.* Nature, 2003. **426**(6964): p. 238-9.

126. Pannese, M., et al., *The Xenopus homologue of Otx2 is a maternal homeobox gene that demarcates and specifies anterior body regions.* Development, 1995. **121**(3): p. 707-20.

127. Simeone, A., E. Puelles, and D. Acampora, *The Otx family.* Current opinion in genetics & development, 2002. **12**(4): p. 409-15.

128. Kawahara, A. and I.B. Dawid, *Developmental expression of zebrafish emx1 during early embryogenesis.* Gene expression patterns : GEP, 2002. **2**(3-4): p. 201-6.

129. Morita, T., et al., *Differential expression of two zebrafish emx homeoprotein mRNAs in the developing brain.* Neuroscience letters, 1995. **198**(2): p. 131-4.

130. Zhou, X., et al., *Cloning and expression of xSix3, the Xenopus homologue of murine Six3.* Mechanisms of development, 2000. **91**(1-2): p. 327-30.

131. Bernier, G., et al., *Expanded retina territory by midbrain transformation upon overexpression of Six6 (Optx2) in Xenopus embryos.* Mechanisms of development, 2000. **93**(1-2): p. 59-69.

132. Lagutin, O.V., et al., *Six3 repression of Wnt signaling in the anterior neuroectoderm is essential for vertebrate forebrain development.* Genes & development, 2003. **17**(3): p. 368-79.

133. Gestri, G., et al., *Six3 functions in anterior neural plate specification by promoting cell proliferation and inhibiting Bmp4 expression.* Development, 2005. **132**(10): p. 2401-13.

134. Dutta, S., et al., *pitx3 defines an equivalence domain for lens and anterior pituitary placode.* Development, 2005. **132**(7): p. 1579-90.

135. Zilinski, C.A., et al., *Modulation of zebrafish pitx3 expression in the primordia of the pituitary, lens, olfactory epithelium and cranial ganglia by hedgehog and nodal signaling.* Genesis, 2005. **41**(1): p. 33-40.

136. Gong, S.G. and A. Kiba, *The role of Xmsx-2 in the anterior-posterior patterning of the mesoderm in Xenopus laevis.* Differentiation; research in biological diversity, 1999. **65**(3): p. 131-40.

137. Feledy, J.A., et al., *Inhibitory patterning of the anterior neural plate in Xenopus by homeodomain factors Dlx3 and Msx1.* Developmental biology, 1999. **212**(2): p. 455-64.

138. Tremblay, P., M. Kessel, and P. Gruss, *A transgenic neuroanatomical marker identifies cranial neural crest deficiencies associated with the Pax3 mutant Splotch.* Developmental biology, 1995. **171**(2): p. 317-29.

139. Murphy, M.J., A. Wilson, and A. Trumpp, *More than just proliferation: Myc function in stem cells.* Trends in cell biology, 2005. **15**(3): p. 128-37.

140. Li, X., et al., *Eya protein phosphatase activity regulates Six1-Dach-Eya transcriptional effects in mammalian organogenesis.* Nature, 2003. **426**(6964): p. 247-54.

141. Schlosser, G., *Do vertebrate neural crest and cranial placodes have a common evolutionary origin?* BioEssays : news and reviews in molecular, cellular and developmental biology, 2008. **30**(7): p. 659-72.

142. Ahrens, K. and G. Schlosser, *Tissues and signals involved in the induction of placodal Six1 expression in Xenopus laevis.* Developmental biology, 2005. **288**(1): p. 40-59.

143. Mancilla, A. and R. Mayor, *Neural crest formation in Xenopus laevis: mechanisms of Xslug induction.* Developmental biology, 1996. **177**(2): p. 580-9.

144. Litsiou, A., S. Hanson, and A. Streit, *A balance of FGF, BMP and WNT signalling positions the future placode territory in the head.* Development, 2005. **132**(18): p. 4051-62.

145. Wheeler, G.N. and A.W. Brandli, *Simple vertebrate models for chemical genetics and drug discovery screens: lessons from zebrafish and Xenopus.* Dev Dyn, 2009. **238**(6): p. 1287-308.

146. Zon, L.I. and R.T. Peterson, *In vivo drug discovery in the zebrafish.* Nat Rev Drug Discov, 2005. **4**(1): p. 35-44.

147. Tomlinson, M.L., R.A. Field, and G.N. Wheeler, *Xenopus as a model organism in developmental chemical genetic screens.* Mol Biosyst, 2005. **1**(3): p. 223-8.

148. Keegan, B.R., et al., *The elongation factors Pandora/Spt6 and Foggy/Spt5 promote transcription in the zebrafish embryo.* Development, 2002. **129**(7): p. 1623-32.

149. Hochheimer, A. and R. Tjian, *Diversified transcription initiation complexes expand promoter selectivity and tissue-specific gene expression.* Genes Dev, 2003. **17**(11): p. 1309-20.

150. Core, L.J. and J.T. Lis, *Transcription regulation through promoter-proximal pausing of RNA polymerase II.* Science, 2008. **319**(5871): p. 1791-2.

151. Wada, T., et al., *DSIF, a novel transcription elongation factor that regulates RNA polymerase II processivity, is composed of human Spt4 and Spt5 homologs.* Genes Dev, 1998. **12**(3): p. 343-56.

152. Yamaguchi, Y., et al., *NELF, a multisubunit complex containing RD, cooperates with DSIF to repress RNA polymerase II elongation.* Cell, 1999. **97**(1): p. 41-51.

153. Missra, A. and D.S. Gilmour, *Interactions between DSIF (DRB sensitivity inducing factor), NELF (negative elongation factor), and the Drosophila RNA polymerase II transcription elongation complex.* Proc Natl Acad Sci U S A, 2010. **107**(25): p. 11301-6.

154. Bres, V., S.M. Yoh, and K.A. Jones, *The multi-tasking P-TEFb complex.* Curr Opin Cell Biol, 2008. **20**(3): p. 334-40.

155. Fujita, T., I. Piuz, and W. Schlegel, *The transcription elongation factors NELF, DSIF and P-TEFb control constitutive transcription in a gene-specific manner.* FEBS Lett, 2009. **583**(17): p. 2893-8.

156. Kohoutek, J., *P-TEFb- the final frontier.* Cell Div, 2009. **4**: p. 19.

157. Luo, Z., C. Lin, and A. Shilatifard, *The super elongation complex (SEC) family in transcriptional control.* Nature reviews. Molecular cell biology, 2012. **13**(9): p. 543-7.

158. Guo, S., et al., *A regulator of transcriptional elongation controls vertebrate neuronal development.* Nature, 2000. **408**(6810): p. 366-9.

159. Bai, X., et al., *TIF1gamma controls erythroid cell fate by regulating transcription elongation.* Cell, 2010. **142**(1): p. 133-43.

160. Mueller, D., et al., *Misguided transcriptional elongation causes mixed lineage leukemia.* PLoS Biol, 2009. **7**(11): p. e1000249.

161. Seila, A.C., et al., *Divergent transcription from active promoters.* Science, 2008. **322**(5909): p. 1849-51.

162. Zhou, Q., T. Li, and D.H. Price, *RNA polymerase II elongation control.* Annual review of biochemistry, 2012. **81**: p. 119-43.

163. Li, Q.T., et al., *Analysis of the large inactive P-TEFb complex indicates that it contains one 7SK molecule, a dimer of HEXIM1 or HEXIM2, and two P-TEFb molecules containing Cdk9 phosphorylated*

at threonine 186. Journal of Biological Chemistry, 2005. **280**(31): p. 28819-28826.

164. Peterlin, B.M. and D.H. Price, *Controlling the elongation phase of transcription with P-TEFb.* Molecular cell, 2006. **23**(3): p. 297-305.

165. Michels, A.A., et al., *Binding of the 7SK snRNA turns the HEXIM1 protein into a P-TEFb (CDK9/cyclin T) inhibitor.* Embo Journal, 2004. **23**(13): p. 2608-2619.

166. Nguyen, V.T., et al., *7SK small nuclear RNA binds to and inhibits the activity of CDK9/cyclin T complexes.* Nature, 2001. **414**(6861): p. 322-5.

167. Yang, Z., et al., *The 7SK small nuclear RNA inhibits the CDK9/cyclin T1 kinase to control transcription.* Nature, 2001. **414**(6861): p. 317-22.

168. Byers, S.A., et al., *HEXIM2, a HEXIM1-related protein, regulates positive transcription elongation factor b through association with 7SK.* Journal of Biological Chemistry, 2005. **280**(16): p. 16360-16367.

169. Yik, J.H., et al., *Compensatory contributions of HEXIM1 and HEXIM2 in maintaining the balance of active and inactive positive transcription elongation factor b complexes for control of transcription.* The Journal of biological chemistry, 2005. **280**(16): p. 16368-76.

170. Barboric, M., et al., *Interplay between 7SK snRNA and oppositely charged regions in HEXIM1 direct the inhibition of P-TEFb.* Embo Journal, 2005. **24**(24): p. 4291-4303.

171. He, N., et al., *A La-related protein modulates 7SK snRNP integrity to suppress P-TEFb-dependent transcriptional elongation and tumorigenesis.* Molecular cell, 2008. **29**(5): p. 588-99.

172. Krueger, B.J., et al., *LARP7 is a stable component of the 7SK snRNP while P-TEFb, HEXIM1 and hnRNP A1 are reversibly associated.* Nucleic Acids Research, 2008. **36**(7): p. 2219-2229.

173. Xue, Y., et al., *A capping-independent function of MePCE in stabilizing 7SK snRNA and facilitating the assembly of 7SK snRNP.* Nucleic Acids Research, 2010. **38**(2): p. 360-9.

174. Luo, Z., et al., *The super elongation complex family of RNA polymerase II elongation factors: gene target specificity and transcriptional output.* Molecular and cellular biology, 2012. **32**(13): p. 2608-17.

175. Fish, R.N. and C.M. Kane, *Promoting elongation with transcript cleavage stimulatory factors.* Biochimica et biophysica acta, 2002. **1577**(2): p. 287-307.

176. Gu, W. and D. Reines, *Identification of a decay in transcription potential that results in elongation factor dependence of RNA polymerase II.* The Journal of biological chemistry, 1995. **270**(19): p. 11238-44.

177. Nechaev, S., et al., *Global analysis of short RNAs reveals widespread promoter-proximal stalling and arrest of Pol II in Drosophila.* Science, 2010. **327**(5963): p. 335-8.

178. Adelman, K., et al., *Efficient release from promoter-proximal stall sites requires transcript cleavage factor TFIIS.* Molecular cell, 2005. **17**(1): p. 103-12.

179. Flores, O., E. Maldonado, and D. Reinberg, *Factors involved in specific transcription by mammalian RNA polymerase II. Factors IIE and IIF independently interact with RNA polymerase II.* The Journal of biological chemistry, 1989. **264**(15): p. 8913-21.

180. Cojocaru, M., et al., *Genomic location of the human RNA polymerase II general machinery: evidence for a role of TFIIF and Rpb7 at both early and late stages of transcription.* The Biochemical journal, 2008. **409**(1): p. 139-47.

181. Sims, R.J., 3rd, R. Belotserkovskaya, and D. Reinberg, *Elongation by RNA polymerase II: the short and long of it.* Genes & development, 2004. **18**(20): p. 2437-68.

182. Krogan, N.J., et al., *RNA polymerase II elongation factors of Saccharomyces cerevisiae: a targeted proteomics approach.* Molecular and cellular biology, 2002. **22**(20): p. 6979-92.

183. Krogan, N.J., et al., *The Paf1 complex is required for histone H3 methylation by COMPASS and Dot1p: linking transcriptional elongation to histone methylation.* Molecular cell, 2003. **11**(3): p. 721-9.

184. Krogan, N.J., et al., *Methylation of histone H3 by Set2 in Saccharomyces cerevisiae is linked to transcriptional elongation by RNA polymerase II.* Molecular and cellular biology, 2003. **23**(12): p. 4207-18.

185. Briggs, S.D., et al., *Gene silencing: trans-histone regulatory pathway in chromatin.* Nature, 2002. **418**(6897): p. 498.

186. Dover, J., et al., *Methylation of histone H3 by COMPASS requires ubiquitination of histone H2B by Rad6.* The Journal of biological chemistry, 2002. **277**(32): p. 28368-71.

187. Wood, A., et al., *The Paf1 complex is essential for histone monoubiquitination by the Rad6-Bre1 complex, which signals for histone methylation by COMPASS and Dot1p.* The Journal of biological chemistry, 2003. **278**(37): p. 34739-42.

188. Chen, Y., et al., *DSIF, the Paf1 complex, and Tat-SF1 have nonredundant, cooperative roles in RNA polymerase II elongation.* Genes & development, 2009. **23**(23): p. 2765-77.

189. Kim, J., M. Guermah, and R.G. Roeder, *The human PAF1 complex acts in chromatin transcription elongation both independently and cooperatively with SII/TFIIS.* Cell, 2010. **140**(4): p. 491-503.

190. He, N., et al., *Human Polymerase-Associated Factor complex (PAFc) connects the Super Elongation Complex (SEC) to RNA polymerase II on chromatin.* Proceedings of the National Academy of Sciences of the United States of America, 2011. **108**(36): p. E636-45.

191. Pokholok, D.K., N.M. Hannett, and R.A. Young, *Exchange of RNA polymerase II initiation and elongation factors during gene expression in vivo.* Molecular cell, 2002. **9**(4): p. 799-809.

192. Lin, C., et al., *AFF4, a component of the ELL/P-TEFb elongation complex and a shared subunit of MLL chimeras, can link transcription elongation to leukemia.* Molecular cell, 2010. **37**(3): p. 429-37.

193. Yokoyama, A., et al., *A higher-order complex containing AF4 and ENL family proteins with P-TEFb facilitates oncogenic and physiologic MLL-dependent transcription.* Cancer cell, 2010. **17**(2): p. 198-212.

194. Biswas, D., et al., *Function of leukemogenic mixed lineage leukemia 1 (MLL) fusion proteins through distinct partner protein complexes.* Proceedings of the National Academy of Sciences of the United States of America, 2011. **108**(38): p. 15751-6.

195. Fuda, N.J., M.B. Ardehali, and J.T. Lis, *Defining mechanisms that regulate RNA polymerase II transcription in vivo.* Nature, 2009. **461**(7261): p. 186-92.

196. Lin, C., et al., *Dynamic transcriptional events in embryonic stem cells mediated by the super elongation complex (SEC).* Genes & development, 2011. **25**(14): p. 1486-98.

197. Boettiger, A.N. and M. Levine, *Synchronous and stochastic patterns of gene activation in the Drosophila embryo.* Science, 2009. **325**(5939): p. 471-3.

198. Gilchrist, D.A., et al., *Regulating the regulators: the pervasive effects of Pol II pausing on stimulus-responsive gene networks.* Genes & development, 2012. **26**(9): p. 933-44.

199. Takahashi, H., et al., *Human mediator subunit MED26 functions as a docking site for transcription elongation factors.* Cell, 2011. **146**(1): p. 92-104.

200. Jang, M.K., et al., *The bromodomain protein Brd4 is a positive regulatory component of P-TEFb and stimulates RNA polymerase II-dependent transcription.* Molecular cell, 2005. **19**(4): p. 523-34.

201. Yang, Z., et al., *Recruitment of P-TEFb for stimulation of transcriptional elongation by the bromodomain protein Brd4.* Molecular cell, 2005. **19**(4): p. 535-45.

202. Dey, A., et al., *The double bromodomain protein Brd4 binds to acetylated chromatin during interphase and mitosis.* Proceedings of the National Academy of Sciences of the United States of America, 2003. **100**(15): p. 8758-63.

203. Yang, Z., N. He, and Q. Zhou, *Brd4 recruits P-TEFb to chromosomes at late mitosis to promote G1 gene expression and cell cycle progression.* Molecular and cellular biology, 2008. **28**(3): p. 967-76.

204. Smith, E., C. Lin, and A. Shilatifard, *The super elongation complex (SEC) and MLL in development and disease.* Genes & development, 2011. **25**(7): p. 661-72.

205. Cheng, B., et al., *Functional association of Gdown1 with RNA polymerase II poised on human genes.* Molecular cell, 2012. **45**(1): p. 38-50.

206. Brannan, K., et al., *mRNA decapping factors and the exonuclease Xrn2 function in widespread premature termination of RNA polymerase II transcription.* Molecular cell, 2012. **46**(3): p. 311-24.

207. Mohan, M., et al., *Licensed to elongate: a molecular mechanism for MLL-based leukaemogenesis.* Nature reviews. Cancer, 2010. **10**(10): p. 721-8.

208. Thirman, M.J., et al., *Cloning of ELL, a gene that fuses to MLL in a t(11;19)(q23;p13.1) in acute myeloid leukemia.* Proceedings of the National Academy of Sciences of the United States of America, 1994. **91**(25): p. 12110-4.

209. Stone, B., et al., *Serologic analysis of ovarian tumor antigens reveals a bias toward antigens encoded on 17q.* International journal of cancer. Journal international du cancer, 2003. **104**(1): p. 73-84.

210. Wittmann, B.M., N. Wang, and M.M. Montano, *Identification of a novel inhibitor of breast cell growth that is down-regulated by estrogens and decreased in breast tumors.* Cancer research, 2003. **63**(16): p. 5151-8.

211. Wittmann, B.M., et al., *The breast cell growth inhibitor, estrogen down regulated gene 1, modulates a novel functional interaction between estrogen receptor alpha and transcriptional elongation factor cyclin T1.* Oncogene, 2005. **24**(36): p. 5576-88.

212. He, N. and Q. Zhou, *New insights into the control of HIV-1 transcription: when Tat meets the 7SK snRNP and super elongation complex (SEC).* Journal of neuroimmune pharmacology : the official journal of the Society on NeuroImmune Pharmacology, 2011. **6**(2): p. 260-8.

213. Kao, S.Y., et al., *Anti-termination of transcription within the long terminal repeat of HIV-1 by tat gene product.* Nature, 1987. **330**(6147): p. 489-93.

214. Zhu, Y., et al., *Transcription elongation factor P-TEFb is required for HIV-1 tat transactivation in vitro.* Genes & development, 1997. **11**(20): p. 2622-32.

215. Wei, P., et al., *A novel CDK9-associated C-type cyclin interacts directly with HIV-1 Tat and mediates its high-affinity, loop-specific binding to TAR RNA.* Cell, 1998. **92**(4): p. 451-62.

216. Zhou, Q. and J.H. Yik, *The Yin and Yang of P-TEFb regulation: implications for human immunodeficiency virus gene expression and global control of cell growth and differentiation.* Microbiology and molecular biology reviews : MMBR, 2006. **70**(3): p. 646-59.

217. Bisgrove, D.A., et al., *Conserved P-TEFb-interacting domain of BRD4 inhibits HIV transcription.* Proceedings of the National Academy of Sciences of the United States of America, 2007. **104**(34): p. 13690-5.

218. He, N., et al., *HIV-1 Tat and host AFF4 recruit two transcription elongation factors into a bifunctional complex for coordinated activation of HIV-1 transcription.* Molecular cell, 2010. **38**(3): p. 428-38.

219. Sobhian, B., et al., *HIV-1 Tat assembles a multifunctional transcription elongation complex and stably associates with the 7SK snRNP.* Molecular cell, 2010. **38**(3): p. 439-51.

220. Andrulis, E.D., et al., *High-resolution localization of Drosophila Spt5 and Spt6 at heat shock genes in vivo: roles in promoter proximal pausing and transcription elongation.* Genes & development, 2000. **14**(20): p. 2635-49.

221. Gavalas, A., et al., *Synergy between Hoxa1 and Hoxb1: the relationship between arch patterning and the generation of cranial neural crest.* Development, 2001. **128**(15): p. 3017-27.

222. Alexander, T., C. Nolte, and R. Krumlauf, *Hox genes and segmentation of the hindbrain and axial skeleton.* Annual review of cell and developmental biology, 2009. **25**: p. 431-56.

223. Studer, M., et al., *Genetic interactions between Hoxa1 and Hoxb1 reveal new roles in regulation of early hindbrain patterning.* Development, 1998. **125**(6): p. 1025-36.

224. Popperl, H., et al., *Segmental expression of Hoxb-1 is controlled by a highly conserved autoregulatory loop dependent upon exd/pbx.* Cell, 1995. **81**(7): p. 1031-42.

225. Donner, A.J., et al., *CDK8 is a positive regulator of transcriptional elongation within the serum response network.* Nature structural & molecular biology, 2010. **17**(2): p. 194-201.

226. Fivaz, J., et al., *RNA polymerase II promoter-proximal pausing upregulates c-fos gene expression.* Gene, 2000. **255**(2): p. 185-94.

227. Aida, M., et al., *Transcriptional pausing caused by NELF plays a dual role in regulating immediate-early expression of the junB gene.* Molecular and cellular biology, 2006. **26**(16): p. 6094-104.

228. Chiu, R., et al., *The c-Fos protein interacts with c-Jun/AP-1 to stimulate transcription of AP-1 responsive genes.* Cell, 1988. **54**(4): p. 541-52.

229. Lee, S.Y., et al., *The function of heterodimeric AP-1 comprised of c-Jun and c-Fos in activin mediated Spemann organizer gene expression.* PloS one, 2011. **6**(7): p. e21796.

230. Lee, S.Y., et al., *The role of heterodimeric AP-1 protein comprised of JunD and c-Fos proteins in hematopoiesis.* The Journal of biological chemistry, 2012. **287**(37): p. 31342-8.

231. Wagner, E.F., *Functions of AP1 (Fos/Jun) in bone development.* Annals of the rheumatic diseases, 2002. **61 Suppl 2**: p. ii40-2.

232. Wagner, E.F., *Bone development and inflammatory disease is regulated by AP-1 (Fos/Jun).* Annals of the rheumatic diseases, 2010. **69 Suppl 1**: p. i86-88.

233. Carleton, M., et al., *Early growth response transcription factors are required for development of CD4(-)CD8(-) thymocytes to the CD4(+)CD8(+) stage.* Journal of immunology, 2002. **168**(4): p. 1649-58.

234. Krishnaraju, K., B. Hoffman, and D.A. Liebermann, *Early growth response gene 1 stimulates development of hematopoietic progenitor cells along the macrophage lineage at the expense of the granulocyte and erythroid lineages.* Blood, 2001. **97**(5): p. 1298-305.

235. Fowler, T., R. Sen, and A.L. Roy, *Regulation of primary response genes.* Molecular cell, 2011. **44**(3): p. 348-60.

236. Herschman, H.R., *Primary response genes induced by growth factors and tumor promoters.* Annual review of biochemistry, 1991. **60**: p. 281-319.

237. Chiariello, M., M.J. Marinissen, and J.S. Gutkind, *Regulation of c-myc expression by PDGF through Rho GTPases.* Nature cell biology, 2001. **3**(6): p. 580-6.

238. Komuro, I., et al., *Endothelin stimulates c-fos and c-myc expression and proliferation of vascular smooth muscle cells.* FEBS letters, 1988. **238**(2): p. 249-52.

239. Calderwood, S.K. and D.R. Ciocca, *Heat shock proteins: stress proteins with Janus-like properties in cancer.* International journal of hyperthermia : the official journal of European Society for Hyperthermic Oncology, North American Hyperthermia Group, 2008. **24**(1): p. 31-9.

240. Schlesinger, M.J., *How the cell copes with stress and the function of heat shock proteins.* Pediatric research, 1994. **36**(1 Pt 1): p. 1-6.

241. Lindquist, S. and E.A. Craig, *The heat-shock proteins.* Annual review of genetics, 1988. **22**: p. 631-77.

242. Garrido, C., et al., *Heat shock proteins 27 and 70: anti-apoptotic proteins with tumorigenic properties.* Cell cycle, 2006. **5**(22): p. 2592-601.

243. Calderwood, S.K., et al., *Heat shock proteins in cancer: chaperones of tumorigenesis.* Trends in biochemical sciences, 2006. **31**(3): p. 164-72.

244. Ciocca, D.R. and S.K. Calderwood, *Heat shock proteins in cancer: diagnostic, prognostic, predictive, and treatment implications.* Cell stress & chaperones, 2005. **10**(2): p. 86-103.

245. Calderwood, S.K., A. Murshid, and T. Prince, *The shock of aging: molecular chaperones and the heat shock response in longevity and aging--a mini-review.* Gerontology, 2009. **55**(5): p. 550-8.

246. Rasmussen, E.B. and J.T. Lis, *In vivo transcriptional pausing and cap formation on three Drosophila heat shock genes.* Proceedings of the National Academy of Sciences of the United States of America, 1993. **90**(17): p. 7923-7.

247. Lis, J. and C. Wu, *Protein traffic on the heat shock promoter: parking, stalling, and trucking along.* Cell, 1993. **74**(1): p. 1-4.

248. Calderwood, S.K., et al., *Signal Transduction Pathways Leading to Heat Shock Transcription.* Signal transduction insights, 2010. **2**: p. 13-24.

249. Lis, J.T., et al., *P-TEFb kinase recruitment and function at heat shock loci.* Genes & development, 2000. **14**(7): p. 792-803.

250. Park, J.M., et al., *Mediator, not holoenzyme, is directly recruited to the heat shock promoter by HSF upon heat shock.* Molecular cell, 2001. **8**(1): p. 9-19.

251. Bensaude, O., *Inhibiting eukaryotic transcription: Which compound to choose? How to evaluate its activity?* Transcription, 2011. **2**(3): p. 103-108.

252. Mosner, J., et al., *Negative feedback regulation of wild-type p53 biosynthesis.* The EMBO journal, 1995. **14**(18): p. 4442-9.

253. An, W.G., et al., *Inhibitors of transcription, proteasome inhibitors, and DNA-damaging drugs differentially affect feedback of p53 degradation.* Experimental cell research, 1998. **244**(1): p. 54-60.

254. Demidenko, Z.N. and M.V. Blagosklonny, *Flavopiridol induces p53 via initial inhibition of Mdm2 and p21 and, independently of p53, sensitizes apoptosis-reluctant cells to tumor necrosis factor.* Cancer research, 2004. **64**(10): p. 3653-60.

255. Holzel, M., et al., *Defects in 18 S or 28 S rRNA processing activate the p53 pathway.* The Journal of biological chemistry, 2010. **285**(9): p. 6364-70.

256. Kanazawa, S., et al., *c-Myc recruits P-TEFb for transcription, cellular proliferation and apoptosis.* Oncogene, 2003. **22**(36): p. 5707-11.

257. Gargano, B., et al., *P-TEFb is a crucial co-factor for Myc transactivation.* Cell Cycle, 2007. **6**(16): p. 2031-7.

258. Zuber, J., et al., *RNAi screen identifies Brd4 as a therapeutic target in acute myeloid leukaemia.* Nature, 2011. **478**(7370): p. 524-8.

259. Fischer, P.M. and A. Gianella-Borradori, *Recent progress in the discovery and development of cyclin-dependent kinase inhibitors.* Expert opinion on investigational drugs, 2005. **14**(4): p. 457-77.

260. MacCallum, D.E., et al., *Seliciclib (CYC202, R-Roscovitine) induces cell death in multiple myeloma cells by inhibition of RNA polymerase II-dependent transcription and down-regulation of Mcl-1.* Cancer research, 2005. **65**(12): p. 5399-407.

261. Raje, N., et al., *Seliciclib (CYC202 or R-roscovitine), a small-molecule cyclin-dependent kinase inhibitor, mediates activity via down-regulation of Mcl-1 in multiple myeloma.* Blood, 2005. **106**(3): p. 1042-7.

262. Chao, S.H. and D.H. Price, *Flavopiridol inactivates P-TEFb and blocks most RNA polymerase II transcription in vivo.* The Journal of biological chemistry, 2001. **276**(34): p. 31793-9.

263. Holkova, B., et al., *Phase I trial of bortezomib (PS-341; NSC 681239) and alvocidib (flavopiridol; NSC 649890) in patients with recurrent or refractory B-cell neoplasms.* Clinical cancer research : an official journal of the American Association for Cancer Research, 2011. **17**(10): p. 3388-97.

264. Bible, K.C., et al., *A phase 2 trial of flavopiridol (Alvocidib) and cisplatin in platin-resistant ovarian and primary peritoneal carcinoma: MC0261.* Gynecologic oncology, 2012. **127**(1): p. 55-62.

265. Liu, X., et al., *CDKI-71, a novel CDK9 inhibitor, is preferentially cytotoxic to cancer cells compared to flavopiridol.* International journal of cancer. Journal international du cancer, 2012. **130**(5): p. 1216-26.

266. Nowicki, M.W. and M.D. Walkinshaw, *CDK9 inhibitors push cancer cells over the edge.* Chemistry & biology, 2010. **17**(10): p. 1047-8.

267. Wang, S., et al., *Discovery and characterization of 2-anilino-4-(thiazol-5-yl)pyrimidine transcriptional CDK inhibitors as anticancer agents.* Chemistry & biology, 2010. **17**(10): p. 1111-21.

268. O'Donnell, E.F., et al., *The aryl hydrocarbon receptor mediates leflunomide-induced growth inhibition of melanoma cells.* PloS one, 2012. **7**(7): p. e40926.

269. Alhefdhi, A., et al., *Leflunomide suppresses growth in human medullary thyroid cancer cells.* The Journal of surgical research, 2013.

270. Dresser, T.H., et al., *Teratogenic assessment of four solvents using the Frog Embryo Teratogenesis Assay--Xenopus (FETAX).* Journal of applied toxicology : JAT, 1992. **12**(1): p. 49-56.

271. Nie, S., Y. Kee, and M. Bronner-Fraser, *Myosin-X is critical for migratory ability of Xenopus cranial neural crest cells.* Developmental biology, 2009. **335**(1): p. 132-42.

272. Casini, P., I. Nardi, and M. Ori, *Hyaluronan is required for cranial neural crest cells migration and craniofacial development.* Developmental dynamics : an official publication of the American Association of Anatomists, 2012. **241**(2): p. 294-302.

273. McGrew, L.L., et al., *Direct regulation of the Xenopus engrailed-2 promoter by the Wnt signaling pathway, and a molecular screen for Wnt-responsive genes, confirm a role for Wnt signaling during neural patterning in Xenopus.* Mechanisms of development, 1999. **87**(1-2): p. 21-32.

274. Shibata, T., et al., *A role of D domain-related proteins in differentiation and migration of embryonic cells in Xenopus laevis.* Mechanisms of development, 2008. **125**(3-4): p. 284-98.

275. Yellajoshyula, D., et al., *Geminin regulates the transcriptional and epigenetic status of neuronal fate-promoting genes during mammalian neurogenesis.* Molecular and cellular biology, 2012. **32**(22): p. 4549-60.

276. Hari, L., et al., *Temporal control of neural crest lineage generation by Wnt/beta-catenin signaling.* Development, 2012. **139**(12): p. 2107-17.

277. Fu, T.J., et al., *Cyclin K functions as a CDK9 regulatory subunit and participates in RNA polymerase II transcription.* Journal of Biological Chemistry, 1999. **274**(49): p. 34527-34530.

278. Edwards, M.C., C. Wong, and S.J. Elledge, *Human cyclin K, a novel RNA polymerase II-associated cyclin possessing both carboxy-terminal domain kinase and Cdk-activating kinase activity.* Molecular and Cellular Biology, 1998. **18**(7): p. 4291-4300.

279. Kurosu, T., F. Zhang, and B.M. Peterlin, *Transcriptional activity and substrate recognition of cyclin T2 from P-TEFb.* Gene, 2004. **343**(1): p. 173-9.

280. Park, B.Y., et al., *Xaml1/Runx1 is required for the specification of Rohon-Beard sensory neurons in Xenopus.* Developmental biology, 2012. **362**(1): p. 65-75.

281. Green, Y.S. and M.L. Vetter, *EBF factors drive expression of multiple classes of target genes governing neuronal development.* Neural development, 2011. **6**: p. 19.

282. Perron, M., et al., *Xenopus elav-like genes are differentially expressed during neurogenesis.* Mechanisms of development, 1999. **84**(1-2): p. 139-42.

283. Goda, T., et al., *Genetic screens for mutations affecting development of Xenopus tropicalis.* PLoS genetics, 2006. **2**(6): p. e91.

284. Myant, K. and O.J. Sansom, *Wnt/Myc interactions in intestinal cancer: partners in crime.* Experimental cell research, 2011. **317**(19): p. 2725-31.

285. Itasaki, N. and S. Hoppler, *Crosstalk between Wnt and bone morphogenic protein signaling: a turbulent relationship.* Developmental dynamics : an official publication of the American Association of Anatomists, 2010. **239**(1): p. 16-33.

286. Hu, M.C. and N.D. Rosenblum, *Smad1, beta-catenin and Tcf4 associate in a molecular complex with the Myc promoter in dysplastic renal tissue and cooperate to control Myc transcription.* Development, 2005. **132**(1): p. 215-25.

287. Parisi, F., et al., *Drosophila insulin and target of rapamycin (TOR) pathways regulate GSK3 beta activity to control Myc stability and determine Myc expression in vivo.* BMC biology, 2011. **9**: p. 65.

288. Cowling, V.H. and M.D. Cole, *Turning the tables: Myc activates Wnt in breast cancer.* Cell cycle, 2007. **6**(21): p. 2625-7.

289. Mullins, M.C., *Tolloid gets Sizzled competing with Chordin.* Developmental cell, 2006. **10**(2): p. 154-6.

290. Shi, J., et al., *Snail2 controls mesodermal BMP/Wnt induction of neural crest.* Development, 2011. **138**(15): p. 3135-45.

291. Shi, J., et al., *sizzled function and secreted factor network dynamics.* Biology open, 2012. **1**(3): p. 286-94.

292. Theveneau, E. and R. Mayor, *Collective cell migration of the cephalic neural crest: the art of integrating information.* Genesis, 2011. **49**(4): p. 164-76.

293. Sato, N., et al., *Maintenance of pluripotency in human and mouse embryonic stem cells through activation of Wnt signaling by a pharmacological GSK-3-specific inhibitor.* Nature medicine, 2004. **10**(1): p. 55-63.

294. O'Donnell, E.F., et al., *The anti-inflammatory drug leflunomide is an agonist of the aryl hydrocarbon receptor.* PLoS One, 2010. **5**(10).

295. Silva, H.T., Jr., et al., *In vitro and in vivo effects of leflunomide, brequinar, and cyclosporine on pyrimidine biosynthesis.* Transplant Proc, 1997. **29**(1-2): p. 1292-3.

296. Gauley, J. and J.J. Heikkila, *Examination of the expression of the heat shock protein gene, hsp110, in Xenopus laevis cultured cells and embryos.* Comparative biochemistry and physiology. Part A, Molecular & integrative physiology, 2006. **145**(2): p. 225-34.